Coastal Hazard Risk Assessment
For
The Kapiti Coast

Dr Willem de Lange
Honorary Research Associate
Waikato University

EXECUTIVE SUMMARY

Management of natural coastal hazards is mandated through three main statutes: the Resource Management Act (RMA) 1991, the Building Act 2004, and the Civil Defence Emergency Management Act 2002. Each defines natural hazards slightly differently, reflecting their legislative aims. This report follows the RMA's definition of hazards, which includes a broad range of events impacting human life, property, or the environment; risk assessment as a combination of the probability and consequences of hazards; and climate change as human-induced alterations to the Earth's radiation balance since ~1750 CE. This report focuses on the requirements of Policy 24 of the New Zealand Coastal Policy Statement, which requires identifying high-risk areas, including considering the likely effects of climate change.

The Kāpiti Coast District Council (KCDC) identifies earthquakes, tsunamis, floods, and climate change as significant hazards. However, the district plan manages erosion and marine inundation separately without explicit hazard designation. Historically, extreme weather has been the most likely hazard associated with death, injury and property damage for the Kāpiti Coast. This report assesses extreme weather events affecting coastal erosion and inundation, alongside relative sea level rise and altered sediment dynamics, and considers climate change impacts on these hazards.

Extreme weather, particularly very low atmospheric pressure, strong to extreme winds, and intense or long-duration rainfall, contributes to coastal erosion through the combination of increased wave heights and wave steepness and increased water levels due to storm surge and wave set-up. It also contributes to inundation through increased water levels at the coast, accumulation of rainfall in low-lying areas, and increased freshwater discharge. Climate change may change the frequency and/or magnitude of extreme weather and contribute to relative sea level trends through changes in the volume and density of water in the oceans (which determines absolute or eustatic sea level). Relative sea level trends are also dependent on vertical land movement.

Historically, the Kāpiti Coast:

- Experiences predominantly locally generated waves due to north-westerly winds, with lesser influence from swell waves generated in the Tasman Sea and the southern Indian Ocean.
    - Wave heights are typically moderate, with significant wave heights usually below 3 m, although storm events can produce higher waves up to 4.5 m.
    - Available wave energy and the occurrence of extreme wave events varies in response to climate oscillations, including the El Niño-Southern Oscillation (ENSO) and the Southern Annular Mode (SAM).
    - There has been a trend towards fewer extreme wave events over recent decades, potentially related to changes in local wind patterns.

- Experiences relatively small storm surges, with only a few events exceeding 0.3 m in height.
    - Storm surge characteristics vary with wind direction for the Kāpiti Coast.
    - Extreme water levels (combining storm surge, tide and waves) increase northwards along the coast, primarily due to increasing tidal range.

- There is a strong correlation between extreme wave heights and extreme water levels (storm surges).
- Extreme water levels are predominantly associated with blocking weather patterns, particularly with low-pressure systems west of the Kāpiti Coast blocked by a high-pressure system north of the Chatham Islands.
- There is no significant historical trend for the magnitude or frequency of storm surges; natural variability in wave patterns and storm surges currently dominates climate change trends for the Southwest Pacific region, including New Zealand.

- Has recorded coastal erosion since at least the early 20th century, with formal documentation of protective structures built since the 1940s and 1950s.

- There is no evidence that elevated groundwater levels contribute to coastal erosion.

- It is predominantly exposed to tsunami hazards from local sources rather than distant Pacific Rim events, owing to the shielding effect of New Zealand's landmass against most Pacific-generated tsunamis.
  - The shallow South Taranaki Bight and the Norfolk Ridge and Lord Howe Rise wave guides attenuate Tsunami energy from northern Southwest Pacific sources (e.g., Vanuatu, Solomon Islands, Samoa).
  - Known faults (e.g. Fisherman Fault and Manaota Fault) pose significant local tsunami risks, potentially with limited warning time and high inundation potential.
    - This assessment may need updating in light of revised seismic risk probabilities, particularly for events associated with the Alpine Fault and Hikurangi subduction zone.
    - Tsunami hazards for the Kāpiti Coast due to local earthquakes include potential inundation heights of 0-5 m, with an Annual Exceedance Probability (AEP) estimated around 4%.
  - Palaeotsunami deposits, archaeological evidence, and geomorphology suggest a major local tsunami event in the late 15th century (1470-1510 CE) affecting the Kāpiti Coast. The source of this event is not well-constrained.

The Kāpiti Coast is affected by vertical land movement (VLM) due to tectonic activity, including both seismic and aseismic deformation, which results in temporal and spatial variations for the coast:

- Significant seismic events like the 2016 Kaikoura Earthquake have caused substantial VLM for the Kāpiti Coast, with initial subsidence followed by uplift due to post-event seismic relaxation.
- Continuous GPS (cGPS) data indicate complex interactions of subduction-driven subsidence, seismic rebound, and slow slip events (SSEs). The data time series are too short to predict future VLM reliably.
- InSAR (Interferometric Synthetic Aperture Radar) estimates of VLM are available but cover a very short time period and show discrepancies with cGPS data for Kāpiti Coast District, indicating they are not suitable for reliably predicting long-term trends.

- Multiple lines of evidence (cGPS, InSAR, geological data) can be used to assess VLM. These data indicate that southern parts of the Kāpiti Coast are experiencing uplift while northern areas are subsiding.

Estimating coastal inundation is relatively straightforward, assuming no changes to the coastal topography, but estimation of coastal erosion is more difficult. While there is a growing understanding of the complexities in predicting coastal erosion and its response to climate change, significant challenges remain in accurately forecasting long-term impacts.

- The Bruun Rule is a simple inundation model that does not include any parameters related to sediment processes. It assumes a linear relationship between sea level rise and inundation (shoreline retreat), which is solely dependent on a scale factor defined by the nearshore slope gradient. It lacks forecasting skills for the Kāpiti Coast, performing worse than random chance in predicting advance or retreat in response to sea level changes.
- Equilibrium models that include sediment processes, like SBeach, have been critiqued for their inability to simulate shoreline behaviour for dynamic coastlines with significant longshore sediment transport. This is evident in SBeach modelling of the Kāpiti Coast.
- Recent evaluations of shoreline erosion models suggest that machine learning models and ensemble approaches offer more reliable short-term predictions compared to empirical and process-based methods like the Bruun Rule and SBeach:
    - Ensembles of machine learning models are better equipped to handle the dynamic sediment transport scenarios present along the Kāpiti Coast.
    - Long-term projections (multi-decadal to centennial) remain highly uncertain due to the challenges of accurately forecasting future climate and forcing conditions.

This report discusses the methodology and findings of Jacobs' reports from 2021 and 2022 regarding coastal hazard vulnerability for the Kāpiti Coast. While Jacobs' reports provide insights into potential future shoreline positions under sea level rise scenarios, their reliance on the Bruun Rule and the use of "conservative" assumptions raises questions about the accuracy and applicability of their predictions, particularly in dynamic coastal environments like the Kāpiti Coast, whether they provide an assessment of the *likely* impacts of climate change, and what the probabilities of their projected outcomes are. Specific issues discussed include:

- Long-term erosion rates are projected using a methodology dominated by the sea level response factor determined by the Bruun Rule. The Bruun Rule predicts the extent of inundation (passive flooding) caused by a sea level rise, assuming a constant planar slope. A comparison of the projections determined by Jacobs with measured shoreline trends shows that the projected long-term erosion rates are greatly overestimated.
    - The remaining terms for the overall "coastal erosion" calculation are too small to significantly affect the projections beyond a few decades of projected sea level rise.
    - Time series observations of shoreline movement are available for the Kāpiti Coast that provide more useful long-term shoreline erosion rates. Restricting the analysis to the most recent higher-quality data provides reliable

estimates of the historical long-term rate, which is easily provided by the Digital Shoreline Analysis System (DSAS). These data should have been used instead of the Bruun Rule, especially to identify areas of high risk as required by Policy 24.

- The short-term erosion rate is determined using the SBeach numerical model, even though shoreline monitoring undertaken for the Kāpiti Coast District Council provides very good predictions of erosion rate distributions at the monitored sites.
    - Comparison between the SBeach predictions and observed storm responses as measured in 1976 shows that the SBeach model was a poor predictor of shoreline change. Comparison between predictions and the envelope of beach profile changes for a highly variable site also shows that the SBeach model is a poor predictor of short-term erosion rates.

- The inclusion of a dune stability factor for the Kāpiti Coast is problematic for two main reasons:
    - Dune morphology varies between spinifex-dominated dunes in the north and marram-dominated dunes in the south, and these dunes respond differently to wave erosion.
    - There is the possibility of double-dipping, as the short-term erosion rate often includes any adjustment of the scarped dune face (associated with spinifex dunes) post-storm.

- No effective methodology was used to incorporate sediment availability to account for the ongoing Holocene trend of accretion of the Kāpiti cuspate foreland. Jacobs merely assumed that accretion would cease at some point in the future without providing a credible explanation as to why this would occur.

- The assumption of constant values for Long-Term Trends, Short-Term Erosion, and Dune Stability across all periods is problematic. These factors will likely vary due to VLM, climate change and climate oscillations, anthropogenic influences, and natural variations in dune morphology and stability over time.

- Jacobs used a Monte Carlo approach to generate probability distributions for Projected Future Shoreline Positions (PFSP), which was a complicated method for estimating the error distribution for their calculations (epistemic uncertainty). Their approach does not predict the probability of input values occurring in the future (aleatoric uncertainty), which is required to assess the likelihood.

- The assumption of uniform sea level rise impacts across the Kāpiti Coast disregards variations in VLM, local storm exposure, and sediment dynamics, which can significantly influence shoreline evolution. Note that the DSAS approach does reflect site-specific differences automatically.

- Jacobs combined sea level rise projections from different sources without clear justification or consistency in selecting intermediate values. Their approach lacks

robustness in addressing the range of possible sea level rise scenarios. It tends to focus on implausible extreme events (RCP 8.5), which have a probability of exceedance of less than 1% over 100 years, instead of *likely* scenarios.

- Jacobs focused on vulnerability rather than defining high-risk areas as mandated by the NZ Coastal Policy Statement. The dominance of the Bruun Rule long-term "erosion" factor results in areas appearing to be high-risk when they are not likely to be at risk. The report's approach does not integrate likelihood assessments with vulnerability, which is essential for robust coastal hazard management and policy compliance.

This report discusses sedimentation responses to sea level changes with respect to observed shoreline changes and past responses determined from the geological record within the framework of sequence stratigraphy. This indicates that the shoreline response is predominantly dependent on sediment availability, not sea level:

- Global reviews and observations have found that most sandy shorelines are accreting despite sea level rise. This was particularly pronounced in areas with a high sediment supply, like the Kāpiti Coast.
    - The concept of accommodation space in sequence stratigraphy illustrates how sea level rise creates opportunities for sediment deposition (accretion) when sediment supply matches or exceeds accommodation space and erosion when it does not.

- The Kāpiti Coast displays different responses depending on local sediment availability and relative sea level changes. North of Paraparaumu, where sediment supply has consistently exceeded accommodation space, accretion has been observed despite subsidence (higher rate of relative sea level rise). South of Paraparaumu, a reduction in sediment supply has led to more variable responses from accretion to erosion, with most areas subject to erosion having seawalls.

This report summarises shoreline change analyses along the Kāpiti Coast using survey data and Google Earth images. The results highlight the complex interactions between sediment dynamics, local geomorphology, and sea level rise. Several key conclusions and considerations emerged:

- The primary drivers identified for shoreline changes on the Kāpiti Coast are sediment supply, extreme weather events (including flooding and spit breaching), and relative sea level changes. Sediment supply appears to be crucial for the evolution of the cuspate foreland (long-term trends), and shoreline morphology, extreme weather events, and relative sea level (i.e. storm surge) significantly influence short-term erosion.
- Extreme weather events, particularly those contributing to spit breaching, exacerbate the local coastal hazard risks.

This report analysed available relative sea level data, reviewed historic climate change assessments, analysed trends for indicators of extreme weather events, and projected future climate and absolute sea levels. Considering prehistoric and historic trends:

- Absolute sea level has varied in response to climate oscillations, long-period tidal constituents, and climate change. A record longer than 60 years is the minimum to

estimate a trend. There is no evidence of an acceleration in the long-term absolute sea level rise rate around NZ since the 1890s.

- While absolute sea level has risen since at least 1870, the relative sea level rate varies regionally due to factors like VLM. For the Kāpiti Coast, relative sea level trends from tide gauge data at Wellington suggest a historical rise of approximately 2.18 $mm.y^{-1}$, but the rate is likely to vary along the coast.
    - VLM significantly affects the relative sea level of the Kāpiti Coast. Longer time-series data from cGPS and InSAR are required to characterise the changes occurring in VLM.
    - There is a limited record of relative sea level for the Kāpiti Coast at Kāpiti Island.

- Future projections suggest continuing sea level rise due to climate change, although the observed rates do not align with the projections' upper ranges (SSP5-8.5 & SSP5-8.5 H+ scenarios). Observed data from Wellington show less acceleration than required for the projections by models like SeaRise, indicating a need for cautious interpretation of future projections.

- There is no meaningful trend for any extreme weather phenomenon associated with coastal hazards affecting the Kāpiti Coast:
    - There is no significant trend in extreme winds. Data from StatsNZ and other studies suggest variability but no consistent upward or downward trend in wind intensity or frequency.
    - There are varying trends for extreme rainfall depending on location and duration. However, the trends are small relative to the variability.
    - There is no significant trend in mean sea level (MSL) pressure, although there is a weak trend towards decreasing maximum MSL pressures and increasing minimum MSL pressures. This could imply slightly less intense storms over time, but the trends are not statistically robust.

- Prehistoric proxy data indicate that there are decadal-scale and longer fluctuations in the frequency and magnitude of extreme weather events. Still, there is no clear trend or correlation with climate change.

While there are methods for producing robust predictions of relative sea level and extreme weather up to a couple of decades into the future, these are unable to achieve the requirements of Policy 24 for consideration up to 100 years into the future.

- Sea level models cannot account for unpredictable events such as seismic activities and non-linear processes.
    - The Ministry for the Environment (MfE) provides guidance about incorporating VLM and absolute sea level projections, emphasising the need for multiple lines of evidence and cautious interpretation of model outputs.

- Climate and sea level models require information about future conditions that cannot be provided as they are yet to be discovered.

- General Circulation Models (GCMs) struggle to accurately simulate key atmospheric features (e.g., ITCZ, SPCZ) that affect New Zealand's climate. This limitation reduces the reliability of long-term climate projections beyond a few months.

- Scenarios and projections are used to indicate the spread of possible outcomes, but do not have probabilities associated with them by definition.
    - Scenarios are continually reviewed and periodically replaced. They are expected to be replaced for the next round of climate modelling (CMIP7) before the 7th Assessment Report is prepared. One driver for the change is the recognition that the higher forcing scenarios produce too much warming and/or are implausible due to invalid assumptions. New scenarios are likely to produce different projections of future climate.

The AR6 WGI report (Chapter 12) reviewed available literature on the projected global impacts of climate change, including the drivers of coastal erosion and inundation in New Zealand. This review found that the projected changes for extreme weather over the next century are smaller than present-day variability. This means that the impact of climate oscillations will dominate for the purposes of considering future climate change (Policy 24).

- The El Niño-Southern Oscillation (ENSO) and Indian Ocean Dipole (IOD) cycles operate at shorter timescales (3-7 years) and exhibit variability that can influence New Zealand's climate. Periods of consecutive phases (e.g., consecutive La Niña events from 2020-2022) can result in significant climate shifts within shorter timescales, affecting local weather patterns.

- Pacific Decadal Oscillation (PDO) and Southern Annular Mode (SAM) operate at longer timescales (centennial and millennial, respectively). These oscillations modulate shorter-term cycles like ENSO and IOD, potentially influencing the frequency and intensity of extreme weather events over more extended periods.

Climate projections for the Greater Wellington region have been produced for different radiative forcings by downscaling global climate model projections using various techniques for different climate parameters. The parameters relevant to coastal hazards on the Kāpiti are discussed and summarised in this report:

- Rare, large, extreme rainfall events are assumed to increase in intensity due to a warmer atmosphere holding more moisture.

- Changes in mean sea level pressure may result in more northeasterly winds in summer and stronger westerly winds in winter, suggesting a potential reduction in storms affecting the Kāpiti Coast District.

- Modest increases in extreme wind speeds are projected for parts of the Wellington Region. Still, there is uncertainty regarding changes in storm intensity and frequency, including tropical and extra-tropical storms.

MfE (2024) recommends dynamic adaptive pathways planning (DAPP) as a suitable approach for managing coastal hazards. It emphasises iterative planning and adaptation based on evolving knowledge and conditions.

- Effective coastal hazard management requires community-led responses and social, cultural, and economic considerations. Community involvement ensures that management strategies are accepted and sustainable over the long term.

To develop an effective approach for managing coastal erosion hazards on the Kāpiti Coast, this report recommends shifting from overly predictive models towards a scenario-neutral framework emphasising adaptive management and community involvement. This approach aligns with current best practices and recommendations outlined by MfE (2024) and other relevant studies in coastal hazard management. The key components are

1. *Vulnerability Assessment*

- Separate the risk assessment into components of vulnerability (impact severity) and likelihood (probability of occurrence). Focus on the type of hazard impact and define scenario-neutral "trigger thresholds" for risk assessment.
    - Assess vulnerabilities at specified elevations for inundation, encompassing scenarios such as storm surges, high tides, tsunamis, and relative sea-level rise. Use GIS to map vulnerable areas and evaluate potential impacts.
    - For erosion, assess vulnerabilities at specific erosion distances, possibly including scenarios for accretion. Use GIS to map vulnerable areas and assess impacts on infrastructure and communities.

2. *Likelihood Assessment*

- Given the uncertainties in long-term predictions, focus on shorter time frames (e.g., 10-20 years) where statistical methods can provide more reliable projections.
- Update hazard assessments and response plans regularly (say, every 10-15 years) to account for new data and changing risk factors, including climate change impacts.
- Activate response plans if trigger points are reached (or are likely to be reached before the next review). Implement responses incrementally based on cost-effectiveness and community acceptance.

3. Data and Tools

- Establish tide gauge stations with cGPS (e.g., Kapiti Island) for accurate local relative and absolute sea level trend monitoring.
- Consider additional cGPS stations to assess local vertical land movement.
- Employ tools like DSAS for short-term erosion predictions and consider recent historical trends for longer-term planning under plausible scenarios rather than extreme projections based on scenarios.

STRUCTURE OF REPORT

EXECUTIVE SUMMARY 1
STRUCTURE OF REPORT 9
BIOGRAPHY 10
1. Introduction 11
2. Natural Hazards and Risk 11
2.1 What are the Coastal Hazards for the Kāpiti Coast District? 15
2.2 Previous Studies of Coastal Hazards 16
2.2.1 Storm Waves 16
2.2.2 Storm Surge and Tide 19
2.2.3 Groundwater Hazards 23
2.2.4 Tsunami 25
2.2.5 Vertical Land Movement 27
2.2.6 Coastal Erosion 32
2.2.7 Effects of Changing Climate 33
2.3 Jacobs (2022) Coastal Hazard Assessment 34
2.3.1 September 1976 Storm 35
2.3.2 Sea Level Rise Response (SL) 37
2.3.3 Short-Term Erosion (ST) 41
2.3.4 Dune stability factor (DS) 44
2.3.5 Long-term Shoreline Trend (LT) 45
2.3.6 Probabilistic Approach 46
2.3.7 Is the Coastal Hazard Susceptibility and Vulnerability Analysis Fit for Purpose? 51
3. Sequence Stratigraphy (shoreline response to relative sea level changes) 52
4. Observations of Shoreline Change for the Kāpiti Coast District 55
5. Future Shoreline Responses Changing Relative Sea Level and Climate. 63
5.1 Historic Sea Level Change 65
5.2 Future Sea Level Change 70
5.2.1 Future Vertical Land Movement 72
5.2.2 Future Absolute Sea Level 75
5.3 Historic Climate Change and Projected Future Climate 83
5.3.1 Historic Climate Change 83
5.3.2 Prehistoric Climate Change 88
5.3.3 Future Climate Change 91
6. Implications for Managing Coastal Erosion Hazard. 94
6.1 Alternative Scenario Neutral Approach 95
6.1.2 Vulnerability Assessment 95
6.1.3 Likelihood Assessment 97
6.1.4 Monitoring 97
6.1.5 Prediction 97
7. References 98

8. Appendix 1: Technical Terms 107
9. Appendix 2: Kāpiti Coast: Example DSAS Analysis of Future Shoreline Locations 110
9.1. Introduction 110
9.2. DSAS Analysis 110
9.3. DSAS Analysis Results 113
9.4. Prediction of Future Shoreline Positions 116
9.5. Shoreline Maps 126
9.6. References 126
10. Appendix 3: Predicted Future Shoreline Maps 127

BIOGRAPHY

Dr Willem de Lange recently retired as a senior lecturer in Earth Sciences at Waikato University, specialising in physical oceanography, natural hazards, seismic exploration and environmental geoscience. He is a numerical modeller with expertise in simulating the impacts of coastal hazards, including erosion, tsunamis, and extreme currents and water levels. He has published more than 200 academic papers over the past 40 years (since 1985) on land and sea issues around New Zealand. He was on the Tsunami Experts Panel, which advises the government on tsunami warnings.

Dr de Lange has been awarded the Honorary Research Associate position at Waikato University.

Dr de Lange came to New Zealand from the Netherlands as a toddler in 1960. He says that since then, he has stayed in Hamilton.

1. Introduction

de Lange (2013) undertook a review of a coastal hazard assessment by Coastal System Limited (CSL) commissioned by the Kapiti Coast District Council (KCDC). The de Lange (2013) report included a review of the coastal geomorphology, processes, and sediment transport along the Kapiti Coast. It also raised some concerns about the methodology used to predict future shoreline changes, which were then used for planning purposes, including a proposal to mitigate the hazard of shoreline erosion by "managed" retreat.

Coastal Ratepayers United have requested a further analysis of changes since 2013 in terms of the shoreline positions, scientific understanding of the hazards affecting the Kapiti Coast, and a coastal hazard vulnerability undertaken for KCDC by Jacobs New Zealand Ltd (Jacobs, 2021, 2022).

2. Natural Hazards and Risk

The three New Zealand statutes - Resource Management Act (RMA) 1991, Building Act 2004, and Civil Defence Emergency Management (CDEM) Act 2002 - have different definitions of natural hazards reflecting their different purposes (Saunders et al., 2013). For this report, the definition from the RMA (1991) will be used:

> *"Any atmospheric or earth or water-related occurrence (including earthquake, tsunami, erosion, volcanic and geothermal activity, landslip, subsidence, sedimentation, wind, drought, fire, or flooding), the action of which adversely affects or may adversely affect human life, property, or other aspects of the environment."*

This definition allows adverse ecological impacts to be a criterion for identifying exposure to natural hazards, although this is not normally included in the definition of a natural hazard.

The definition of risk in relation to natural hazards is a little problematic, even though most New Zealand approaches to natural hazards claim to adopt ISO 31000:2018 (AS/NZS 4360/2004), as discussed by Saunders and Beban (2012), Saunders et al. (2013) and de Vilder et al. (2024). This standard has been superseded by AS/NZ ISO 31000:2009, which defines risk as:

> *"Effect of uncertainty on objectives.*
> *Note 1 – An effect is a deviation from the expected – positive and/or negative.*
> *Note 2 – Objectives can have different aspects (such as financial, health and safety, and environmental goals) and can apply at different levels (such as strategic, organisation-wide, project, product and process).*
> *Note 3 – Risk is often characterised by reference to potential events and consequences, or a combination of these.*
> *Note 4 – Risk is often expressed in terms of a combination of the consequences of an event (including changes in circumstances) and the associated likelihood of the occurrence.*
> *Note 5 – Uncertainty is a state, even partial, of deficiency of information related to, understand of knowledge of an event, its consequence, or likelihood."*

District Councils appear to predominantly treat risk as the combination of the likelihood of an event and the consequences of that event (Beban & Saunders, 2013). The Kāpiti Coast District Plan 2021 defines risk as (Part 1 – Definitions):

"... a combination of the probability of a natural hazard and the consequences that would result from an event of a given magnitude. Commonly expressed by the formula: risk = hazard x vulnerability."

The district plan doesn't define hazards, although it adopts the RMA 1991 (Section 2) definition of natural hazards, which is

"Any atmospheric or earth or water related occurrence (including earthquake, tsunami, erosion, volcanic and geothermal activity, landslip, subsidence, sedimentation, wind, drought, fire, or flooding) the action of which adversely affects or may adversely affect human life, property, or other aspects of the environment."

The district plan also defines vulnerability as:

"... the exposure or susceptibility of a development, building, business or community to the effects from a natural hazard event."

For this report, risk is defined following international literature as a combination of potential hazard, exposure, vulnerability, and probability of occurrence (likelihood). A hazard is defined as a natural event that potentially endangers human life or property. It is assumed that the magnitude of the event characterises hazard in some way.

The New Zealand Coastal Policy Statement (NZCPS) 2010 is a National Policy Statement resulting from the RMA 1991, and it is intended to guide councils in their day-to-day management of the coastal environment (MfE website). Policies 24-27 of NZCPS 2010 guide Local Authorities to manage risks created by coastal hazards, including climate change. This report considers explicitly the requirements of Policy 24, which is:

"Identify areas in the coastal environment that are potentially affected by coastal hazards (including tsunami), giving priority to the identification of areas at high risk of being affected.

Hazard risks, over at least 100 years, are to be assessed having regard to:

a. physical drivers and processes that cause coastal change including sea level rise;
b. short-term and long-term natural dynamic fluctuations of erosion and accretion;
c. geomorphological character;
d. the potential for inundation of the coastal environment, taking into account potential sources, inundation pathways and overland extent;
e. cumulative effects of sea level rise, storm surge and wave height under storm conditions;
f. influences that humans have had or are having on the coast;
g. the extent and permanence of built development; and
h. the effects of climate change on:
    i. matters (a) to (g) above;
    ii. storm frequency, intensity and surges; and
    iii. coastal sediment dynamics;

taking into account national guidance and the best available information on the likely effects of climate change on the region or district."

Confidence Terminology	Degree of confidence in being correct
Very high confidence	At least 9 out of 10 chance
High confidence	About 8 out of 10 chance
Medium confidence	About 5 out of 10 chance
Low confidence	About 2 out of 10 chance
Very low confidence	Less than 1 out of 10 chance

Likelihood Terminology	Likelihood of the occurrence/ outcome
Virtually certain	> 99% probability
Extremely likely	> 95% probability
Very likely	> 90% probability
Likely	> 66% probability
More likely than not	> 50% probability
About as likely as not	33 to 66% probability
Unlikely	< 33% probability
Very unlikely	< 10% probability
Extremely unlikely	< 5% probability
Exceptionally unlikely	< 1% probability

Figure 1. Quantitative terminology for likelihood defined by the IPCC (Bodecker et al, 2022).

Policy 24 states that the hazard assessment should *take into account* the *likely* effects of climate. Figure 1 shows the definitions of confidence and likelihood terminology for climate assessment reports as summarised by Bodecker et al. (2022). The Likelihood Terminology was also included in MfE guidance (Appendix F, MfE, 2017) and adopted by Jacobs (2021). The terms and equivalent probabilities do not correspond to fixed time periods, as occurs for annual exceedance probabilities (AEP), which are commonly used to define hazard probabilities in New Zealand.

Since the NCPS is an NPS under RMA 1991, climate change is defined as:

> *"a change of climate that is attributed directly or indirectly to human activity that alters the composition of the global atmosphere and that is in addition to natural climate variability observed over comparable time periods."*

According to the IPCC AR6 WG1 report, human activity has altered the greenhouse gas composition of the atmosphere since ~1750 CE (Arias et al., 2021), before Captain James Cook's first voyage to New Zealand in 1769-1770 CE. Therefore, all available historical observations of weather and sea level for Kāpiti Coast District have been obtained during a period of climate change as defined by RMA 1991.

The NZCPS 2010 document does not define hazard and takes the RMA (1991) definition given above. There does not appear to be a definition of high risk. The Natural Hazard Risk Communication Toolbox developed by the Auckland Regional Council and GNS (Auckland Council, 2014) defines high risk qualitatively as *intolerable* risk, which recognises that hazards can affect members of the community differently, and there should be community

agreement as to what levels of risk are tolerable and intolerable. The toolbox also sets out methodologies for quantifying the risk for a range of different hazards within the RMA (1991) definition, with the threshold for high risk generally being intolerable risk. All methodologies require the likelihood expressed as a probability. An aspect highlighted by the Toolbox is that high-frequency, low-consequence events may be high risk – high risk is not restricted to low-frequency, high-consequence events (Figure 2). Coastal hazard assessments generally tend to focus on "worst case" scenarios that are low frequency and presumed to possibly have high consequences (as suggested by MfE, 2017).

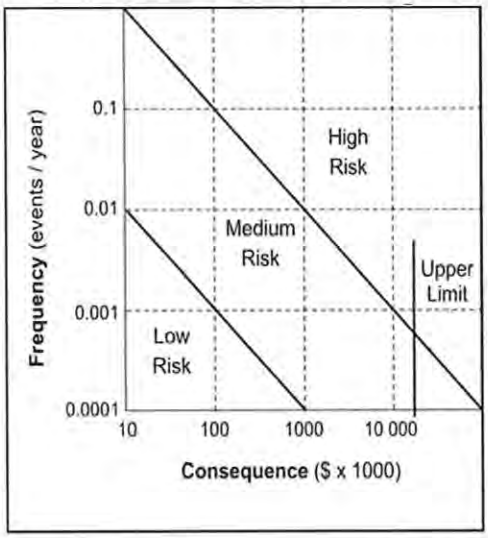

Figure 2. Qualitative assessment of risk based on frequency and magnitude of the consequences of a hazard.

NZCPS 2010 Policy 24 requires that areas potentially affected by hazards within at least 100 years into the future be identified. This requirement is modified by prioritising identifying areas of high risk and then specifying specific aspects related to *hazard risk* to give regard to in the list from (a) to (h). Overall, this is a rather difficult policy to meet since it requires predicting not only future climatic conditions and the effect on coastal processes and sediment dynamics but also the future geomorphology, effects of anthropic activities, and extent and permanence of built development. This report does not set out to achieve all the requirements of Policy 24, as it is not possible to predict the future with sufficient certainty to be able to achieve a robust, defensible assessment.

For planning purposes, a risk-based approach is considered the best method for addressing the effects of specific natural hazards by providing a framework to ensure that the economic, environmental, social, and cultural consequences of development are examined and quantified to inform planning decisions (Saunders et al., 2013). A risk-based approach to land-use planning involves five steps (Saunders et al., 2013; de Vilder et al., 2024):

1. Know your hazard.
2. Determine the severity of the consequences.
3. Evaluate the likelihood of an event.
4. Address the risk, which includes determining the tolerable risk.
5. Monitor and evaluate.

Traditionally, hazard assessments have solely or primarily focussed on steps 1 and 3 and have yet to address the consequences.

As discussed by Saunders et al. (2013), each of these steps has limitations and uncertainties. These should be quantified to inform the planning process.

2.1 What are the Coastal Hazards for the Kāpiti Coast District?

Steele et al. (2019) assessed the vulnerability of coastal communities in the Wellington Region to natural hazards, climate change and sea level rise. The natural hazards they considered were:

- Coastal inundation due to storm surge (1% Annual Exceedance Probability - AEP), including an assumed 1 m relative sea level rise.
- Tsunami inundation (no AEP specified).
- Coastal erosion (no AEP specified).

It was noted that the most damaging natural hazards in the Greater Wellington Region were earthquakes, flooding (freshwater), and tsunamis, while landslides were important locally.

Jacobs (2021, 2022) considered the coastal hazards for the Kāpiti coast to be coastal erosion and inundation hazards for the Kāpiti coast, with climate change and sea level rise modifying the risk associated with these hazards.

The focus on coastal erosion follows a long history of community concerns about erosion, primarily south of Tikotu Stream near the apex of the prominent cuspate foreland of the Kāpiti Coast. Coastal inundation has been a minor concern, particularly relative to the greater hazard of flooding associated with intense and/or prolonged rainfall events, which has the most impact on the floodplains and little impact on the higher dune areas along the coast.

After consideration of hazards affecting Kāpiti Coast District, KCDC identified the following hazards (as summarised on their website - https://www.kapiticoast.govt.nz/our-district/cdem/kapitis-natural-hazards/):

- Earthquakes and associated hazards include rupture, liquefaction, and slope failure (mass movement).
- Tsunami, with local sources recognised as a potential hazard.
- Floods are identified as the most common natural hazard in the Wellington Region and Kāpiti Coast District. They are only linked to rainfall and not marine inundation.
- Other hazards, which only identify climate change as a hazard modifier, result in more intense storms and rising sea levels.

The 2021 KCDC District plan (https://eplan.kapiticoast.govt.nz/eplan/rules/0/186/0/0/0/205) provides guidance for three hazards:

- Floods due to rainfall.
- Earthquakes and associated hazards include distant but not local tsunamis.
- Fire.

The district plan is based on a precautionary and risk-based approach and states that the effects of climate change are accounted for. There does not appear to be a consistent definition of what level of risk is acceptable or how uncertainties about future climate

effects are quantified. Despite tsunami hazards being recognised, no development restrictions are imposed in relation to tsunami risk. Erosion and marine inundation are not identified as natural hazards but are incorporated in the coastal environment section of the District Plan (https://eplan.kapiticoast.govt.nz/eplan/rules/0/201/0/0/0/205).

There appear to be two types of natural hazards omitted from consideration that are included in the RMA (1991) definition:

- Mass movement, including landslides and debris flows. The recent Landslide Planning Guidance released by GNS (de Vilder et al., 2024) states that since 1760, more than 1500 fatalities have resulted from landslides, exceeding the combined fatalities from earthquakes (501), volcanic eruptions (179) and tsunamis (1) during this period. Kāpiti District appears to experience a significant mass movement event associated with heavy rainfall affecting roads, railway lines, and other infrastructure every 4-5 years.
- Extreme weather events, excluding heavy rainfall (considered in relation to flooding). These include storm waves and surges and strong wind events, including tornadoes and waterspouts. Cyclone Gita in February 2018 is an example of an extreme weather event that affected the Kāpiti Coast. The presence of Kāpiti Island offshore, combined with the predominant wind direction, means that waterspouts are relatively common and some transition to land to become tornadoes. Recent examples of damaging tornadoes in the Kāpiti Coast District occurred in February 2008, June 2022, and April 2023.

Mass movement affects the southern Kāpiti coast from Paekākāriki towards Pukerua Bay, primarily as shallow translational landslides and debris flows during or following intense rainfall events. Debris flows following the stream channels to the coast represent the greatest coastal hazard but are limited to a small area.

This report will consider extreme weather events associated with coastal erosion and/or inundation and the impacts of changing climate (including relative sea level changes and changes in sediment supply).

2.2 Previous Studies of Coastal Hazards

2.2.1 Storm Waves

The Greater Wellington Regional Council has routinely undertaken analyses summarising the characteristics and effects of storms in the Wellington Region, including Kāpiti Coast District (*viz*. Watt, 2003, 2005). These analyses highlight the effects of localised intense and slow-moving, longer-duration regional rain and wind events.

Several studies have modelled extreme water levels, storm surges and tides, and extreme waves for the Kāpiti Coast, particularly the section from Paraparaumu to Pukerua Bay (Laing et al., 2000; Johnson et al., 2007; & Hannah, 2012; Stephens et al., 2012; Lane et al., 2012).

Laing et al. (2000) synthesised a 20-year record of wave conditions for the Kāpiti Coast using wind data estimated from wind observations at Cape Egmont, Farewell Spit, Stephens Island, and the Maui gas platform, and pressure data from New Plymouth, Farewell Spit and Paraparaumu. The estimated winds were compared with the results of the RAMS numerical model to define the characteristics of the north-westerly fetch for waves reaching the Kāpiti Coast. Single windspeed, fetch and duration estimates were then used with the JONSWAP

relationships to predict wave height and period. The approach was validated against a set of wave measurements offshore from Wanganui. Significant wave heights were less than 3 m for 99.7% of the time, and peak periods were relatively short (<10-11 s). This is unsurprising as the approach is solely based on local wind generation and ignores any swell wave energy propagating into the area from other sources. External swell waves were estimated to add <15% to the wave energy. The largest significant wave heights were 4.5 m in early November 1995 and 4.1 m in March 1995, and the 11-13 September 1976 storm had significant wave heights up to 3.6 m with a peak period of 9.4 s. These results indicate that the waves are relatively small but steep during storms. The modelled waves were used to estimate the nearshore conditions after shoaling. The results were considered uncertain as no local validation data was available to assess them.

Gorman et al. (2003a, b) undertook hindcasting of the New Zealand wave climate for 1979-1998 using the WAM wave model and winds from the European Centre for Medium-Range Weather Forecasts (ECMWF), which was validated against limited deep-water and nearshore wave data. This indicates that the Kāpiti coast has lower overall wave conditions than most of the west and east coasts of New Zealand but higher than the more sheltered northeast coast of the North Island.

Johnson et al. (2007) analysed sea level data from Kāpiti Island (23 July 1997 to 18 December 2006) and corresponding weather data from Kāpiti Island and Paraparaumu Airport. The data were used to calculate storm surges and provided input into a numerical model to hindcast the wave conditions. The wave model was calibrated and validated with data obtained from offshore gas production platforms in the South Taranaki Bight. There was no verification with coastal wave data for the Kāpiti Coast. The data were used to determine the wave height distributions at specific locations along the coast, the 95th and 99th percentile, and the maximum statistics calculated and reported. The maximum wave heights for return periods of 1 month, 3 months, 6 months, 1 year, 2 years, 10 years, 50 years and 100 years were also reported.

NIWA undertook several studies of extreme water levels and waves based on a 45-year hindcast of hourly waves, tides and storm surges from October 1957 to September 2002, using metrological forcing from the ERA-40 re-analysis dataset produced by the ECMWF. The wave hindcast was developed as part of NIWA's Waves and Storm Surge Projection (WASSP) project (Stephens et al., 2012). Note that the report also refers to a 44-year simulation from 1958-2001 inclusive, which appears to be a subset of the more extended dataset containing only full years.

The wave model results were calibrated and validated against the Baring Head wave buoy that started operation in 1995, with results presented for 2002. The predicted and observed extreme wave heights (highest 5%) did not match well, with the results suggesting the offshore wave predictions were 1.5 m too low relative to the nearshore wave buoy measurements. The predictions were closer to the observations from gas production facilities in the South Taranaki Bight, which Johnson et al. (2007) also found for Kāpiti Coast waves). This suggests that the measured wave heights are affected by shoaling processes as they approach Baring Head. Tides were calibrated against the Queens Wharf tide gauge in Wellington Harbour. Storm surge predictions do not appear to have been calibrated or validated.

Stephens et al. (2012) present histograms of the significant wave heights predicted for 45 years at various Wellington open coast sites, including Waikanae. These plots show a strongly skewed distribution dominated by small, short-period locally generated waves, with little input from longer-period swell waves.

Coggins et al. (2016) analysed the deep-water wave conditions around New Zealand modelled by the ECMWF Re-Analysis (ERA)-Interim reanalysis to determine if there were variations and trends over time. Consistent with previous studies, they found that the west coast and southern east coast are dominated by swell wave energy from the south Indian Ocean. However, for extreme waves, there was a strong dependence on local wave generation, resulting in variations along the coastline. Most of the west coast is affected by predominant south-westerly winds. Due to sheltering by the South Island and Kāpiti Island, the Kāpiti coast is more affected by north-westerly winds. Coggins et al. (2016) also found a small increase in swell wave energy due to strengthening westerly winds at higher latitudes south of New Zealand and a small decrease in the size of locally generated extreme waves. In general, pure swell waves are associated with onshore sediment movement, and steep waves combining swell and locally generated waves are associated with offshore sediment movement (i.e. coastal erosion).

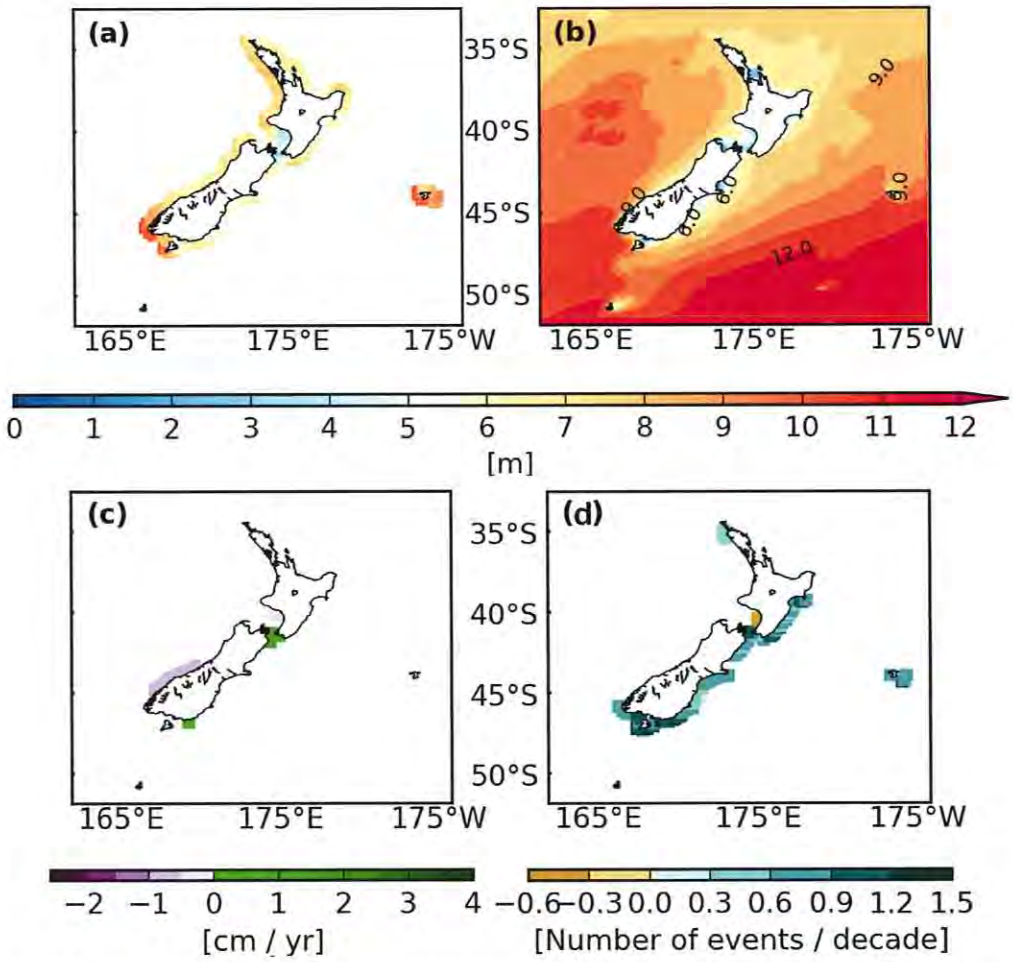

Figure 3. Significant wave height (1% AEP) (a) estimated at grid points on the 50m isobath using the Peaks-Over-Threshold (POT) Generalised Pareto Distribution approach; (b) estimated for the whole regional domain using the Annual Maxima-Generalised Extreme Value Distribution approach. Monotonic trends over hindcast, in (c) the annual average extreme Hs; (d) the number of extreme wave events. Trends were calculated using POT data on the 50m isobath. Only statistically significant values at the 95% confidence

level were plotted (Godoi et al, 2017).

Godoi (2018) undertook a PhD study into the wave climate around New Zealand, specifically, the variability in response to climate oscillations between 1958 and 2001, using the WAVEWATCH III model forced with wind and ice fields from the ERA-40 reanalysis project from ECMWF. The ERA-40 data were obtained from NIWA and is the same dataset used by Stephens et al. (2012). The PhD study included a series of published papers, such as Godoi et al. (2016), Godoi et al. (2017) and Godoi et al. (2018). Godoi et al. (2017) assessed extremely significant wave conditions around the New Zealand coast, as summarised in Figure 3.

The results of Godoi et al. (2017) confirm that Kāpiti has lower wave conditions than most of the New Zealand coast, including the south Wellington coast (especially Baring Head to Cape Palliser). Further, over the 45-year hindcast (1958-2001), the number of extreme wave events per decade and annual average extreme significant wave height declined (95% significance level).

It is also clear that the Kāpiti wave conditions differ from those at Baring Head, and therefore, Baring Head data should not be used to characterise wave processes for hazard assessments for the Kāpiti coast. Instead, as noted above, the wave conditions measured at offshore Taranaki gas production facilities are better predictors for Kāpiti.

Rapizo et al. (2021) have undertaken a detailed analysis of the Taranaki wave climate using numerical models forced by wind and ice conditions from the National Oceanic and Atmospheric Administration (NOAA) National Centers for Environmental Prediction (NCEP) Climate Forecast System Reanalysis (CFSR) for the period 2011 to 2018. The numerical models were calibrated and validated with wave measurements obtained from offshore oil and gas facilities. The model results were combined with earlier results from Godoi (2018) to characterise the wave climate and identify patterns of behaviour from 1979 to 2018.

Rapizo et al. (2021) found that the wide, shallow continental shelf in the South Taranaki Bight dissipates swell energy arriving from the southwest, resulting in smaller, shorter period swell waves than the area to the north. The swell energy decreases further towards the Kāpiti coast. The effect increases from the 90th percentile to maximum wave height. The South Taranaki Bight also displays significant variability associated with the El Niño Southern Oscillation (ENSO) and the Southern Annular Mode. During El Niño conditions with a negative SAM phase, increased south-westerly winds provide more swell wave energy into the South Taranaki Bight, contributing to larger extreme waves. For all other conditions (La Niña, neutral, or El Niño with a positive SAM phase), extreme wave energy is reduced (smaller waves). This implies that the reported wave trends depend on the proportion of time that El Niño coincided with a negative SAM within the record.

Rapizo et al. (2021) found a robust trend of a decline in the number of extreme wave events driven primarily by local wind conditions. However, there is no clear explanation as to why the frequency of local extreme wind events has declined.

2.2.2 Storm Surge and Tide

Johnson et al. (2007) found that observed storm surges were relatively small during the period of measurement (23 July 1997 to 18 December 2006), with only 5 events > 0.3 m in height. The storm surge characteristics varied with predominant wind direction, although the wind is restricted to a relatively narrow range of directions. Relative mean sea level fell by 1.8 mm.y^{-1} during the measurement period (compared to a 3.7 mm.y^{-1} rise at Queens

Wharf, Wellington), and varied by ±7.2 mm month to month. They also found that typically, the waves peaked ~6 hours before the maximum storm surge. Given the short duration of peak wave conditions, they concluded that peak storm surges do not usually coincide with the largest waves for the Kāpiti coast.

Stephens et al. (2012) determined the joint probability distribution for waves and storm tides using the highest 5% of the predicted waves. They stated that the largest waves coincide with maximum storm tide (storm surge + tide), which is inconsistent with the observations of Johnson et al. (2007). The NIWA studies use the storm tide (tide + storm surge) to determine the extreme water level, while Johnson et al. (2007) used only the storm surge. Stephens et al. (2012) note that, particularly for the Kāpiti Coast (which they consider to be the west coast from Paraparaumu to Titahi Bay), the extreme water level is strongly influenced by the tidal range, which increases northwards along the coast. They also note that the wave height is highly correlated with the extreme water level, which is understandable for the storm surge component derived from the same meteorological conditions as the waves. However, it is unclear why the offshore predictions made by WASSP should be highly correlated with the tidal height?

Lane et al. (2012) combine wave and storm tide data from Stephens et al. (2012) and sea level data from Bell and Hannah (2012) to estimate future coastal storm inundation levels and extents. They selected 8 significant storm events with AEP values close to 1% from 13 events identified within the 45-year hindcast dataset created by WASSP. Four of these events had significant erosion and/or inundation impacts on the Kāpiti Coast (as defined by Stephens et al., 2012):

- 12 September 1976 – moderate storm tide and waves
- 16 January 1980 – moderate storm tide and waves
- 6 September 1994 – large storm tide and small waves
- 7 November 1994 – small storm tide and large waves

Lane et al. (2012) noted that the Kāpiti Coast storm tide and wave interactions were different to those observed for the south coast of Wellington, with the Kāpiti Coast typically having smaller waves and larger storm tides than the Wellington coast for the same storm conditions. The storm tides for these storms were adjusted to correspond to a theoretical AEP of 1%, which resulted in a reduction in the storm-tide level of 0.03 m for the 7 November 1994 event and increases for the others of 0.02-0.20 m. Lane et al. (2012) specifically show that the storm tide level is adjusted upwards for an original AEP of 6%. They considered the 7 November 1994 storm the most severe, with an AEP <1%. Their Appendices A & B show that the 7 November 1994 storm had larger wave heights and storm tide levels on the Kāpiti Coast than the 12 September 1976 storm.

Jacobs (2021) claims that Lane et al. (2012) stated that the 12 September 1976 storm had a 0.5% AEP, which is not the case. The Jacobs (2021) interpretation is based on Figure 2.7 in their report, corresponding to Figure 2.6 in Lane et al. (2012). As noted in the caption, the significant wave heights were scaled by 1.5 based on a comparison between the model results and Baring Head. This results in larger wave heights along the coast than predicted by Johnson et al. (2007), as shown by Figure 2.6 in Jacobs (2021), where the Lane et al. (2012) values are 1.19-1.65 times larger for the 1% AEP significant wave heights. It also appears that the extreme wave statistics being compared are not the same in Figure 2.6.

However, it is unclear how Johnson et al. (2007) calculated their return period values (the 10-year return period significant wave heights in their Table 5.2 are consistently higher than the maximum significant wave height within the 10-year data set used). This suggests there may be a larger exaggeration of the wave conditions by the Wellington south coast model used by Lane et al. (2012) than they estimated.

For comparison, Gibb & Wilshere (1976) reported the following for the Kāpiti coast shortly after the September 1976 storm:

- "The meteorological conditions were not unusual and could occur frequently".
- "The cyclone caused high water levels and a storm surge which superimposed on waves of average storm height generated at beach water levels of about 2.6m above the estimated high tide. The wave run up on top of this was the major factor causing damage".
- "There was little effect at Kena Kena Point in the wave shadow of Kapiti Island or at Queen Elizabeth Park where the natural beach and foredune were very effective buffers".
- "Serious erosion at Raumati partly due to the very depressed beach allowing waves to break closer to foredune".
- "Localised scouring and erosion due to large logs rolling at dune toe ...".
- "There is no doubt that the existence of protection works at Raumati has added to the erosion there".

These observations are inconsistent with the significant wave heights of 6.53-6.55 m used by Jacobs (2021): particularly contrasting the suggestion of the worst storm on record with the observation that the waves were of "average storm height". Gibb & Wilshere (1976) also indicate that the severe erosion was localised and exacerbated by coastal structures. Jacobs (2021) justifies the larger values as being *conservative*, which appears to mean greatly exaggerated. Although the MfE (2017) guidance suggests that extreme scenarios may be used to screen the coast to identify areas of significant hazard, it then recommends that a range of (presumably more realistic) scenarios be used for the actual assessment. My concern is that extreme (*conservative*) conditions become the de facto conditions for the final hazard assessment instead of a screening tool or *stress test,* as referred to by MfE (2017).

For the Kāpiti Coast, Lane et al. (2012) selected the 6 September 1994 storm as a representative event for modelling inundation hazard. They identified that the inundation hazard due to extreme water levels, including the combined effects of storm tides and waves, was localised to tidal inlets at the mouths of the Waikanae River, Otaki River and Waitohu Stream. Smaller inlets appear to have been too small to be assessed by their model but presumably would also be impacted by the same conditions. Modelling predicted increasing extreme water elevations northwards from Paekakariki to Otaki (0.29 m increase from their Table 3-3 p.36) due to increasing storm tide elevations (their Table 3-1 p.34) and larger wave heights (increased wave setup in their Table 3-2 p.35). The coastal erosion impacts were not assessed.

Cagigal et al. (2020) developed a storm surge database and model for the entire New Zealand coastline. Their model was calibrated against 17 tide gauges around the open coast,

including a tide gauge on Kāpiti Island. The final database reconstructed storm surges for the period 1870 to 2010 inclusive. Climate model projections are then used to project future storm surge levels. A web interface allows data to be viewed and accessed for grid points around the New Zealand EEZ. Figure 4 shows the results for two locations offshore from the Kāpiti coast, indicating little change in storm surge levels along the coast. The tool would allow for the assessment of the storm surge distribution from 1870 to 2010 and assess if there are any significant differences in the future due to the changing climate. Cagigal et al. (2020) show that for the 2% AEP storm surge, the projected future distribution shows a slight decline in magnitude in the north of New Zealand (Tairua) and a slight increase in the south (Stewart Island). Kāpiti Coast District appears to have no significant projected change.

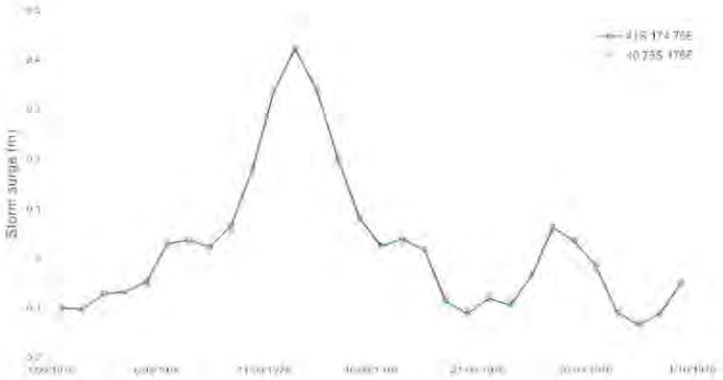

Figure 4. Hindcast storm surge for the Kāpiti coast in September 1976 extracted from the Model 20CR database using the NZ Storm Surge Data Tool (https://uoa-eresearch.github.io/storm_surge/#Model_20CR@1871-01-01).

Stephens et al. (2020) examined 220 historic extreme sea level events affecting the New Zealand coast since 1900 to determine if it was possible to identify critical storm tracks and weather types associated with these events. They sub-divided the extreme events into storm tides (85) and skew surges (135), where a storm tide was defined as the sum of the storm surge, the tide, mean sea level (MSL), and the mean sea level anomaly (MSLA) due to seasonal, interannual and inter-decadal climate variability; and the skew-surge is defined as the difference between the maximum water level and the closest high tide level (which includes contributions from the storm surge and MSLA). Skew-surge is considered a better measure of the storm surge contribution to extreme water levels when tides are present (Williams et al., 2016).

Stephens et al. (2020) found that the main driver of extreme water levels was the high tide, with most extreme events involving a very high tide (e.g. a perigean spring tide) and a moderate skew-surge. In part, this occurs because of the relatively low probability of the peak of the surge coinciding with high tide and the relatively small magnitude of storm surges in New Zealand. This means that extreme water levels are lower for Wellington (micro-tidal conditions) than Auckland (meso-tidal conditions), and extreme water levels will increase northwards along the Kāpiti coast.

Stephens et al. (2020) also identified two main Kidson weather types (Figure 5) associated with extreme water level events. The weather type associated with extreme conditions along the Kāpiti is the blocking weather system involving a low-pressure centre west of New Zealand with a blocking high-pressure centre north of the Chatham Islands (second from left,

bottom row in Figure 5). The probability of such a system varies seasonally and in response to climate oscillations such as the El Niño Southern Oscillation (ENSO), Pacific Decadal Oscillation (PDO), and Southern Annular Mode (SAM). Hence, the greatest risk of extreme coastal water levels occurs when peak tidal heights coincide with blocking weather types.

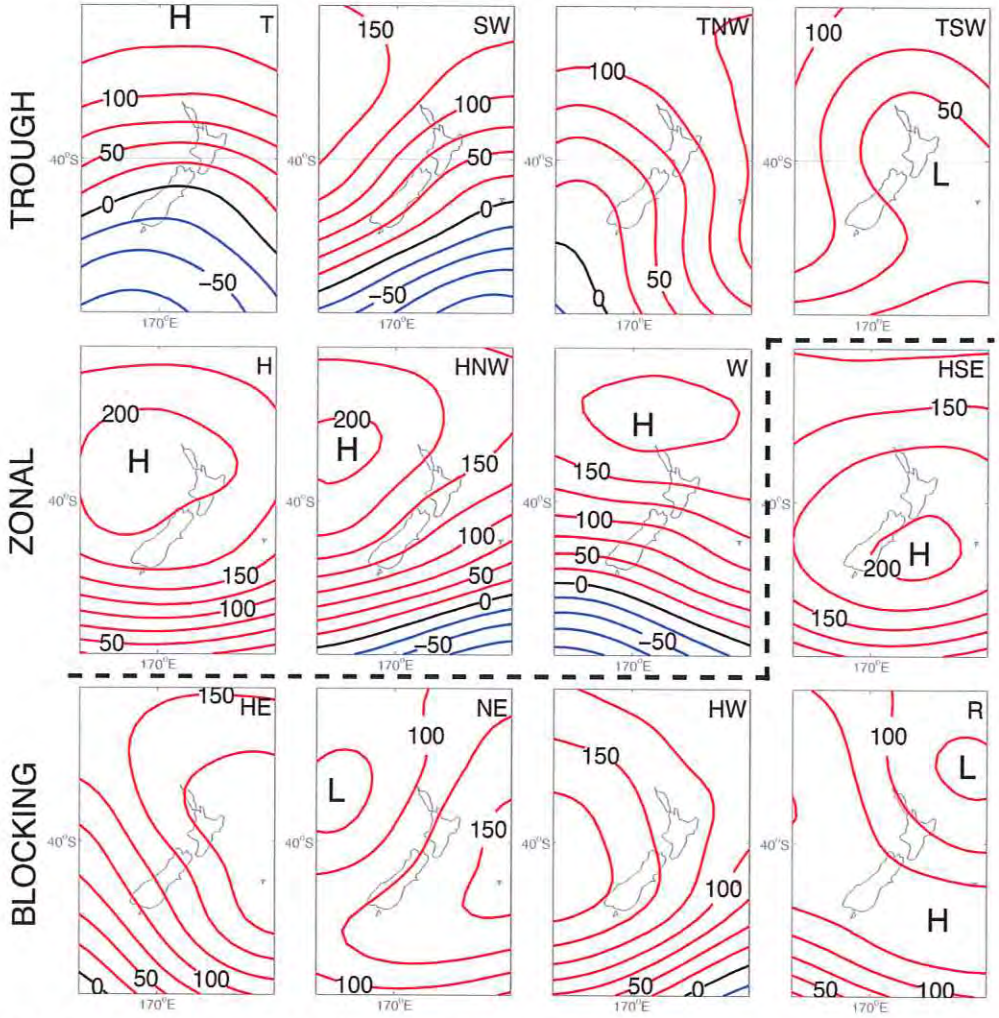

Figure 5. Kidson weather types for New Zealand (Kidson, 2000)

2.2.3 Groundwater Hazards

Inundation of the flood plain behind and swales within coastal dunes may also occur due to elevated groundwater levels for aquifers connected to the sea (MfE, 2017; Cox et al., 2020, 2023). In this case, groundwater primarily modifies existing hazards (Figure 6), although it can be argued that it may introduce new hazards to property, particularly infrastructure (Cox et al., 2023). Kāpiti Coast District has experienced transient pluvial flooding events that have been linked to groundwater, such as during and following several rainfall events in 2022 (https://www.kapiticoast.govt.nz/whats-on/news-archive/2022/impacts-of-high-groundwater). Jacobs (2021) summarises a report on climate change effects on groundwater prepared for KCDC by Sinclair Knight Merz Pty Ltd. (SKM) in 2012.

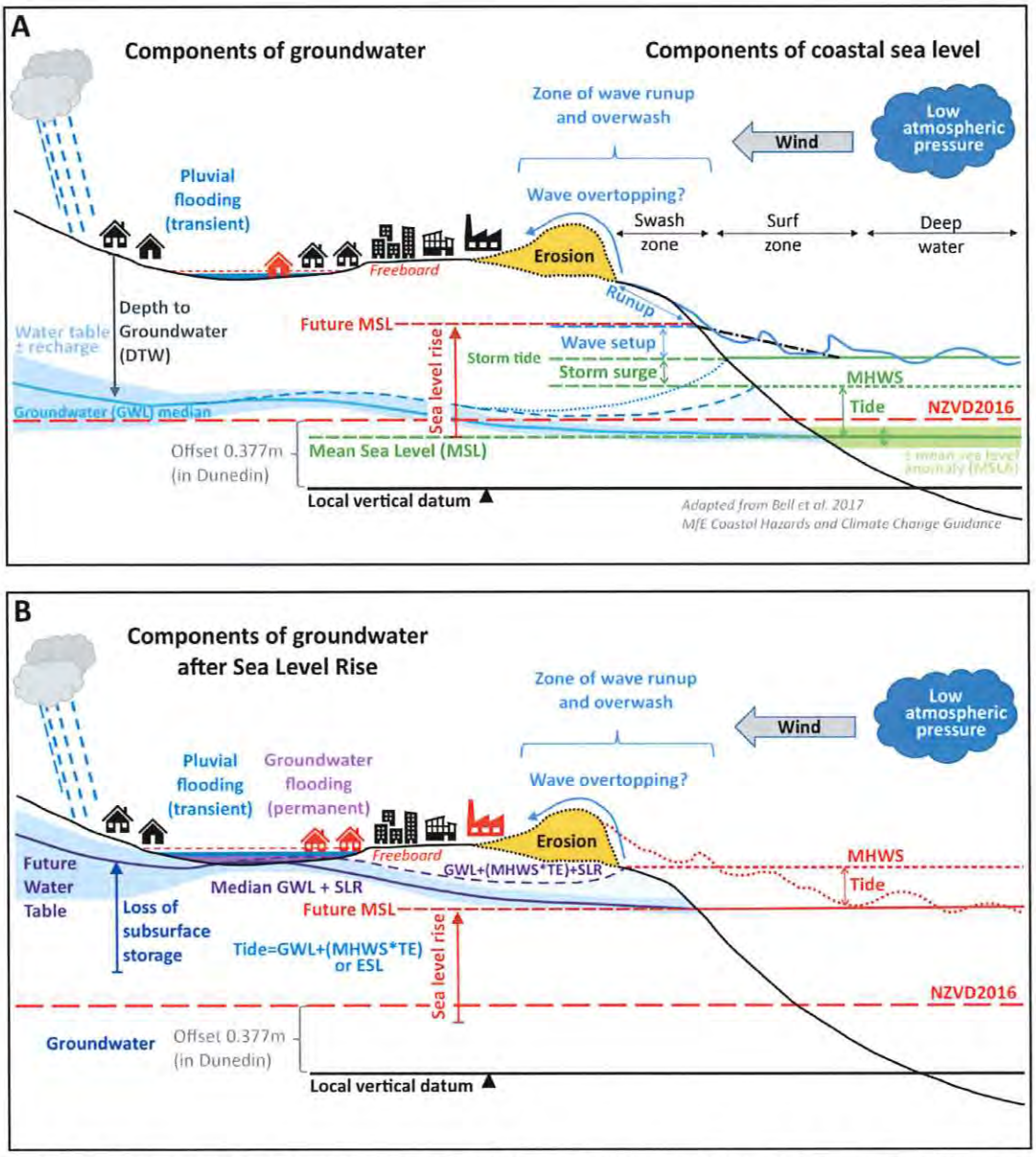

Figure 6. The influence of coastal processes on a shallow groundwater aquifer (Cox et al, 2023). (A) Interactions under present-day conditions. (B) Interactions after a relative sea level rise (excluding a storm surge component).

The most studied areas for groundwater hazards within New Zealand are Christchurch City following subsidence during the Canterbury Earthquake sequence (2010-2011) and South Dunedin (Cox et al., 2020, 2023). The area of concern in South Dunedin consists of low-lying land reclaimed from intertidal flats and coastal salt marshes in the 1800s using spoil from excavations of the hills in central Dunedin. The reclamation is separated from the open ocean to the south by coastal sand dunes >10 m high and from Port Chalmers by a ridge 2-5 m high constructed during further reclamation in the 1960s-1970s. The enclosed basin has subsequently been prone to transient pluvial flooding, with growing concern that sea level rise would increase the hazard (Figure 6).

Although it may appear that parts of Kāpiti Coast District have features in common with South Dunedin, leading to a similar hazard, the hydrogeology of South Dunedin involves a relatively simple layer-cake stratigraphy. Morrow et al. (2010) reviewed previous studies of

the hydrogeology of the Kāpiti coastal plain as part of investigating the intrusion of saline fluids into the aquifers linked to the Waikanae River. This study was undertaken after a prolonged dry period during the 2002-2003 summer, resulting in the drilling of bores to supplement the Kāpiti Coast potable water supply. Morrow et al. (2010) report that there are three aquifers within six stratigraphic units that they treat as being laterally continuous as part of a layer cake stratigraphy.

Morrow et al. (2010) suggest saline intrusion is limited to the uppermost Holocene sand wedge associated with the beach system. They note that the sand wedge varies in thickness along the coast, indicating that the stratigraphy may not be a simple layer cake. Nolan (2017) undertook coring for the coastal plain south of the Waikanae River, and McClintock et al. (2023) undertook coring in the northern plain. Their stratigraphic data suggest that the six stratigraphic units included in the review by Morrow et al. (2010) are complicated sequences of variable facies that interfere and may have limited spatial extent. This will make it difficult to model the movement of groundwater and assess the contribution to surface inundation.

A research team at the University of Canterbury reviewed available models for assessing the contribution of groundwater to surface flooding (Bosserelle et al., 2022) and concluded that no models existed that allowed this assessment to be made for any driver of rising groundwater levels. Cox et al. (2023) claim to have made some progress in developing a model but concluded that there was a range of thresholds at which rising groundwater could either become a direct hazard or modify existing hazards; there was a poor understanding of the tolerable risk associated with threshold levels and what thresholds were appropriate, and a lack of quantification of the consequences (e.g. fragility curves). They argue that this makes it unfeasible to determine the risk associated with groundwater changes in response to sea level rise (presumably increased rainfall).

2.2.4 Tsunami

The Kāpiti Coast is protected from most major tsunamis generated around the rim of the Pacific Ocean by the New Zealand landmass (de Lange & Moon, 2004; Goff & Chagué-Goff, 2015). Although it is exposed to tsunami sources in the northern Southwest Pacific region (viz. Vanuatu, Solomon Islands, Samoa), the tsunami energy is attenuated by the bathymetry of the South Taranaki Bight and focussing of tsunami waves on Taranaki and the central west coast of the South Island by waveguides such as the Norfolk Ridge and Lord Howe Rise. Hence, the tsunami hazard for the Kāpiti Coast District is predominantly due to local sources.

Goff (2002) provided the first assessment of tsunami hazards specifically for the Kāpiti Coast. This assessment suggested tsunami events of 0-5 m affecting the shoreline had an AEP of ~4% and identified several locations on the mainland where palaeotsunami deposits may occur. A palaeotsunami deposit had already been located and described from a site on Kāpiti Island by Goff et al. (2000). Subsequently, three lines of evidence were proposed by Goff & Chagué-Goff (2015) to indicate that a major tsunami event affected the South Taranaki Bight region, including the Kāpiti Coast) during the late 15th Century (1470-1510 CE). In decreasing order of reliability, these were palaeotsunami deposits, archaeological evidence, and tsunami geomorphology.

Tsunami geomorphology relies on identifying a distinctive hummocky dune field terrain attributed to the erosion of parallel dune ridges (Goff et al., 2007; Goff et al., 2009). This

type of terrain is present within Queen Elizabeth II Park and in some areas north of Pekapeka. The problem with associating this terrain with past tsunamis is that it forms in dune ridges associated with marram or European beachgrass (*Ammophila arenaria*), which was introduced to Otago in the late 1800s and became widespread following the 1903 Sand Act that encouraged planting to stabilise sand dunes around the New Zealand coast. It is unclear when it was introduced to the Kāpiti Coast District, but historical photos indicate it was common by World War I. Since Marram was introduced, there is no historical record of tsunami-eroding inland dunes in the Kāpiti Coast District.

There is good archaeological evidence of Māori communities moving inland from low-lying coastal sites to higher land nearby during the 15th Century (McFadgen, 2007; Goff et al., 2008), including from the coast between Raumati and Paraparaumu (Goff & Chagué-Goff, 2015). It is suggested that this migration was in response to the impacts of earthquakes and tsunamis (McFadgen, 2007).

Palaeotsunami deposits are generally reliable indicators of past tsunami inundation, although they can be like deposits produced by storm surges and fluvial floods. McClintock et al. (2023) provide the most detailed examination of a Kāpiti coastal palaeotsunami site from a wetland near Te Hapua Road. Previous work indicated that there have been several phases of dune growth for the coastal plain north of Paraparaumu, and some of these are linked to local seismic activity in the 13th Century, the 15th century, and 1750–1850 CE.

At the Te Hapua site, the 15th-century phase of dune building is associated with palaeotsunami deposits. The deposits include toppled trees with a dominant northeast orientation, suggesting a flow approaching from the southwest. Dating of wood samples gave dates for matai of 1250-1530 CE and rimu of 1390-1530 CE. The source of the tsunami has not yet been identified. Still, the regional distribution of deposits of similar ages suggests one of the larger offshore faults was responsible, possibly the Whakamarama Fault linked to 3 m uplift of the upper west coast of the South Island (around the Heaphy River) in the 15th Century. Interestingly, this date range immediately precedes the estimated timing of the switch from accretion to erosion for the southern Kāpiti Coast (Nolan, 2017).

Mueller et al. (2017) present the results of simulations of distant and local tsunami events that potentially could cause inundation on the Kāpiti Coast. The distant tsunami sources were predominantly from the western and northern Pacific Ocean, with some from the Puysegur subduction zone south of New Zealand. In contrast, local sources included the Hikurangi Deformation Front on the east coast of New Zealand (Wallace et al., 2014), and nearshore faults in the South Taranaki Bight. The greatest hazard is associated with the tsunami yellow zone inundation, which involves local sources with limited time for an official warning and potentially the greatest inundation. Mueller et al. (2017) identified the nearshore Fisherman Fault (seaward of Kāpiti Island) and Manaota Fault (between Kāpiti Island and the mainland) and a large subduction megathrust event in the Hikurangi Deformation Front as potentially causing yellow zone inundation. The return intervals for major seismic events on these systems are estimated as 5500 years, 21000 years, and 500 years, respectively (approximately 0.02%, 0.005%, and 0.2% AEP, respectively) (Mueller et al., 2017; Heron et al., 2019).

The assessments of tsunami hazard for Kāpiti Coast have not considered the faults further offshore. The Whakamarama Fault is possibly responsible for the 19 October 1868 Mw 7.2 Cape Farewell Earthquake, which some studies suggest was associated with a tsunami (Goff

& Chagué-Goff, 2015). NEMA (2023) recently advised the New Zealand Government of revised assessments of seismic risk that indicated that probabilities of major earthquakes in the next 50 years were 25% for the Hikurangi subduction zone (*unlikely* – Figure 1) and 75% for the Alpine Fault (*likely*). There is also an 80% chance that the Alpine Fault event will be at least Mw 8 (*likely*). This may require a revision of the tsunami risk estimates for the Kāpiti Coast District.

2.2.5 Vertical Land Movement

Although seismic hazard for Kāpiti Coast District has been well assessed for identified faults, there doesn't appear to have been any investigation into the impacts of seismic and aseismic deformation on relative sea level due to vertical land movement at the coast. Nolan (2017) reviewed the published studies relating to the tectonic setting of the Kāpiti Coast District. He noted that while the major faults are well-mapped, the differential movements associated with them are poorly understood. Paleoseismic studies cited by Nolan (2017) indicate that the southern part of the district is uplifting, while the northern area around Pekapeka is subsiding. Heron et al. (1998) attributed a terrace south of McKays Crossing to a 2 m uplift associated with the movement of the Ohariu Fault between about 1070 and 1130 years ago.

Vertical land movement is an essential component of relative sea level rise, and the Sea Level CCI project (https://climate.esa.int/en/projects/sea-level/) was established to reconcile satellite altimetric sea level data (absolute sea level) with coastal sea levels (relative sea level). This project identified that ~20% of locations have relative sea level trends that differ significantly from absolute sea level trends, predominantly areas of tectonic activity and/or with large river deltas. They calculated a global mean rate of relative sea level rise of 2.6 $mm.y^{-1}$ for the first 20 years of the 21st Century (Nicholls et al., 2021), compared to their calculated mean rate of absolute rise from satellite data for 1992-2022 of 3.4 ± 0.4 $mm.y^{-1}$. The highest rates of relative sea level rise of 7.8-9.9 $mm.y^{-1}$ occur in urban areas on river deltas affected by the extraction of groundwater and gas (Nicholls et al., 2021). Nicholls et al. (2021) argue that adaptation allows continued occupation, even with future climate impacts.

Continuous GPS data for land movement is available for 3 sites within Kāpiti Coast District (Figure 7): PAEK -Paekakariki Hill, KAPT - Kāpiti Island, and OTAK – Otaki. These indicate a complex interaction between subduction-driven subsidence, seismic rebound, and slow slip events. The data series start at different times, so comparing trends for sites in Figure 7 is misleading. However, it does suggest that the southern Kāpiti Coast District is rising, and the northern area may be sinking. Kāpiti Island does appear to be sinking, suggesting the western side of the Manaota Fault is dropping.

The limited cGPS data indicate that vertical land movements are a significant component of sea level changes for the Kāpiti Coast, given that the underlying eustatic (global) rate of sea level rise is 1.4-1.5 $mm.y^{-1}$ (Denys et al., 2020). It is also clear that the vertical land movement varies along the coast. King et al. (2021) consider the effect of vertical land movements on relative sea level around New Zealand based on paleo-sea level proxies, geological evidence and cGPS data. They note that for Wellington, the relative sea level rise rate since the 1940s is less than expected, given the underlying rate of tectonic subsidence. They state that this discrepancy is unclear but may be due to large (and/or) frequent slow

slip events (SSEs) or fluctuating inter-SEE subsidence rates. They also suggest that SSEs resulted in 0.8 mm.y^{-1} uplift for Wellington between 2000 and 2015 (before the 2016 Kaikoura Earthquake).

Hamling et al. (2022) developed an alternative approach using differences between compilations of InSAR observations of land surface elevation (which includes artificial surfaces, such as buildings) to estimate vertical land movement between 2003 and 2011. Note that this period coincides with the uplift episode for Wellington, as reported by Denys et al. (2020).

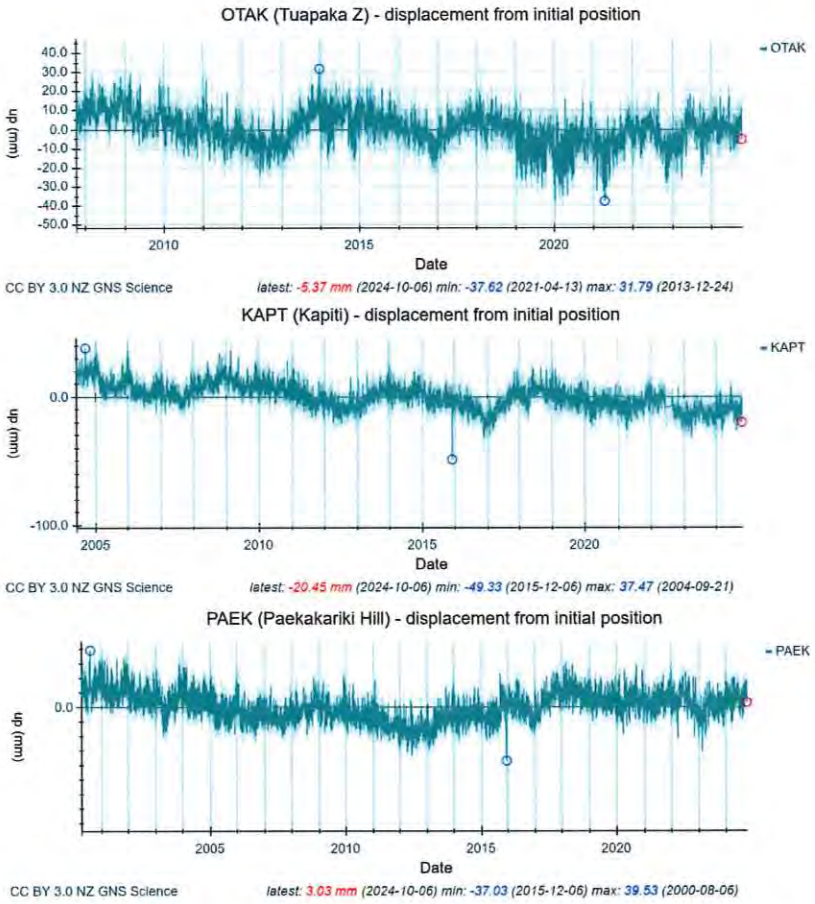

Figure 7. Continuous GPS (cGPS) vertical displacements recorded at 3 sites in Kāpiti Coast District. Plots generated by the FITS API on 7 October 2024 (https://fits.geonet.org.nz/api-docs/endpoint/plot).

Figure 8 shows the vertical deformations for New Zealand that Hamling et al. (2022) estimated and those estimated by cGPS, and the profile C-C' transect from the Wairarapa coastline to the Kāpiti Coast District. The profile data do not extend all the way to the coast for Kāpiti but show that the subsidence rate decreases towards the west coast. The coastal deformation data was extracted at 1 km resolution from the estimates shown in Figure 8, then further down-sampled to 2 km resolution for the SeaRise online tool. There were also adjustments made to the data to exclude known seismic effects around Christchurch and reduce rates of uplift that were considered too high. Comparing the cGPS data in Figure 7 and the profile in Figure 8 suggests that the InSAR estimates may be biased by the observed

subsidence of the offshore KAPT station (while the onshore stations indicate static or uplift conditions).

For the Kāpiti coastline, short-term InSAR estimates used by the SeaRise online tool (Figure 9) appear to be inconsistent with the cGPS data, supporting the conclusion that the InSAR data were not suitable for projecting long-term trends noted by Hamling et al. (2022). The interim guidance from the Ministry for the Environment (MfE, 2022) includes a disclaimer relating to using SeaRise information, as does the SeaRise tool itself. These disclaimers suggest that the information suppliers know that it is not fit for purpose despite the guidance provided.

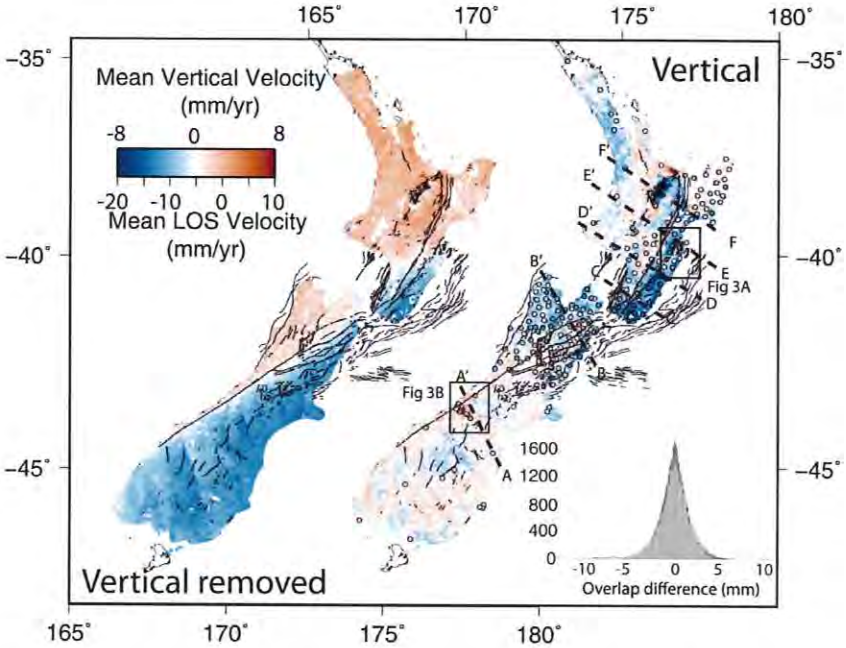

Figure 1. Best fitting LOS (left) and vertical (right) displacement rates. The figure shows a subsampled version of the full data set derived using a distance weighted sampling procedure. The histogram shows the difference in rates within all the overlap regions for the North and south Islands. The black lines show the location of mapped faults (Langridge et al., 2016). On the right-hand panel, dashed lines show the location of the profiles shown in Figure 2 and the black boxes show the regions in Figure 3. The colored dots are the vertical rates derived from GNSS covering the same observation period.

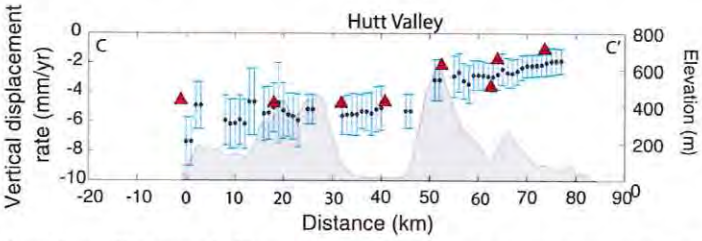

Figure 2. Profiles along six profiles shown in Figure 1. Blue dots and associated error bars are from the InSAR derived vertical velocities and the red dots are from GNSS located within 10 km of the profile. The gray polygons show the topography along each of the profiles.

Figure 8. Vertical land movement estimates for New Zealand determined by Hamling et al (2022) (upper panel and caption), and a cross-section through southern North Island (east to west) that crosses Kāpiti Coast District

The final guidance (MfE, 2024) omits the disclaimer and suggests that the InSAR estimates are the "best available science", apparently because it is the newest technology available.

The guidance then recommends that multiple lines of evidence should be used, including (but not limited to):

- RSLR with satellite-derived (InSAR) VLM rates.
- RSLR with locally monitored VLM rates (if available), which would include cGPS and geodetic surveys.
- absolute SLR projections or increments without VLM.
- local information and expert judgement.
- experience and judgements of mana whenua and others with local knowledge.

Note that the methods identified by the MfE (2024) guidance refer to sea level observations made over different periods (both in terms of duration and specific periods covered). As rates of VLM and sea level changes vary over time, it is very likely that the range of evidence will provide a range of SLR rates.

The area of most extensive ongoing accretion north of Waikanae appears to be subsiding based on paleoseismic studies (long-term) and cGPS (short-term). In contrast, the area that has been eroding for about 400 years (Nolan, 2017) is uplifting. This will be discussed further in section 3 on shoreline response to relative sea level changes.

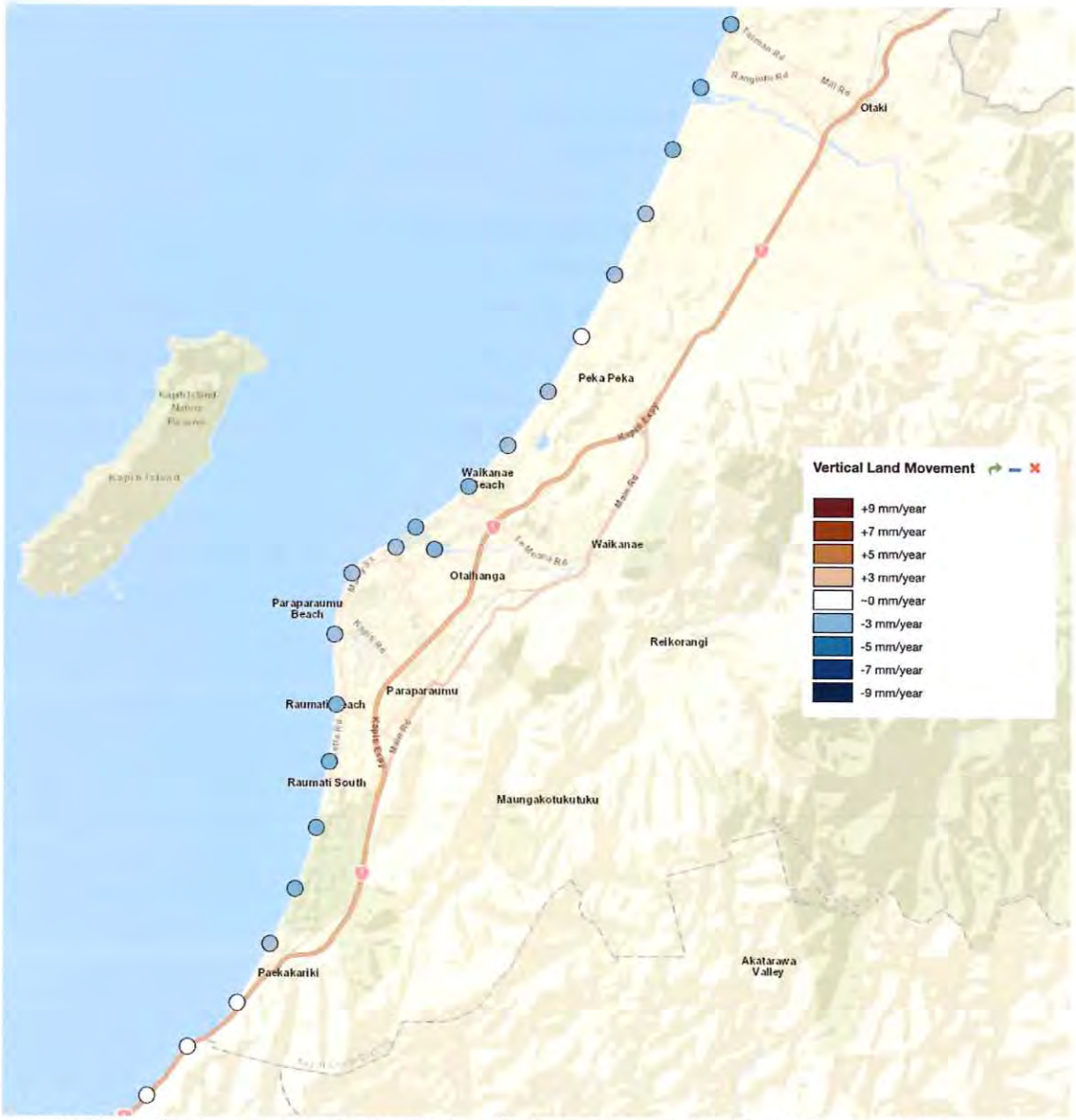

Figure 9. Vertical land movement estimates displayed by the SeaRise online tool for Kāpiti Coast District. Retrieved from https://www.searise.nz/maps-2 on 2 February 2024 (Take care to read the disclaimers before using these data).

As Hamling et al. (2022) note, the short-term rates of vertical land movement estimated from ~8 years of InSAR observations and short-term cGPS records can be completely offset by seismic deformation. For example, the 2016 Kaikoura Earthquake deformed ~110 km of the northeast South Island coast, with a complex pattern of vertical land movement ranging from 2.5 m subsidence to 6 m uplifts (Clark et al., 2017). This deformation also affected the Wellington tide gauges, causing an initial rapid subsidence of ~20 mm, followed by an uplift of ~40 mm over a more extended period after the event (Bell et al., 2018). The cGPS data for Kāpiti Coast District showed this event caused an initial movement at KAPT and PAEK (Figure 7) of 23.7 mm and 16.7 mm subsidence, respectively. This was followed by 34.1 mm and 27.0 mm uplift, respectively (Bell et al., 2018) due to post-event seismic relaxation (Ninis et al., 2023).

Bell et al. (2018) also report that some sites rose at 30 mm.y^{-1}, or ~20 times faster than the absolute rate of sea level rise (1.4-1.5 mm.y^{-1}). Deformation also occurred in response to the

2013 Seddon Earthquake, but this has not been well documented. The amount of deformation can be expected to increase with decreasing distance to the fault ruptures and increasing earthquake magnitude.

King et al. (2024) reconstructed relative sea level changes over the last ~200 years for the Pāuatahanui Inlet, Porirua Harbour, south of the Kāpiti District, using proxy sea-level indicators to estimate past sea levels. Their data indicates that the 1855 Earthquake caused ~1 ± 0.45 m (*sic.*) uplift at the Inlet. There was likely an uplift of the Kāpiti coastline, albeit by a smaller amount. The proxy data have large age and elevation uncertainties, and the authors cherry-pick values from 3 different studies estimating the rates of absolute sea level for Wellington Harbour to claim sea level rise is accelerating and a good match with the SeaRise vertical land movement estimates and hence that the short-term InSAR rates are a useful predictor of long-term rates. Given the large error ranges for their data, this claim is not justified.

Vertical land movement may also occur in response to SSEs that have generally caused an uplift for the southern North Island (Bell et al., 2018). The events recorded for up to 20 years have all been located close to the Kāpiti Coast. For the PAEK site, uplift amounted to 32.1 mm over 10 years and 41.2 m over 20 years (Figure 7). For the KAPT site, an uplift of 46.3 mm was recorded over 10 years.

2.2.6 Coastal Erosion

A series of reports have addressed coastal erosion for all or part of the Kāpiti Coast, extending back to the development of the first coastal subdivision at Raumati Beach in 1906, with severe erosion resulting in the construction of unofficial protective structures reported since the 1940s. Coddington (1972) discussed options for managing erosion for the Kāpiti Coast, including structures and renourishment. Gibb (1978a) identifies the first official protection structures constructed between 1955 and 1959.

As demonstrated by de Lange (2013), previous studies' predictions for future shoreline erosion had no skill (performed worse than chance). The studies considered by de Lange (2013) all used similar methodologies, which were developed from early work by Gibb and Healy and summarised by Healy and Dean (2000). The methodology is flawed, as recognised by Jacobs (2021), and not suitable for coasts with significant longshore sediment transport. In particular, the Bruun methodology (strictly an inundation model and not a process-based erosion model) should not be used. Equilibrium approaches such as SBeach are problematic for the reasons given in Jacobs (2021), summarised by Thieler et al. (2000), Cooper and Pilkey (2004) and Coco et al. (2020), and assessed in the PhD study by Pickett (2004) on the applicability of equilibrium methods (such as Edune) for evaluating coastal hazards. Despite recognising that the methods are flawed and, therefore, not suitable for the task, Jacobs (2021) continued to use them, citing several justifications, including MfE guidance.

de Lange (2013) showed that the Bruun method, employed to predict coastal erosion by CSL, failed to correctly predict the direction of shoreline response (erosion or accretion) to sea level changes for almost all sites modelled along the Kāpiti Coast. This indicates the method has no forecasting skill (less than tossing a coin). It was suggested to the Jacobs team that they shouldn't use any variant of the Bruun methodology for their erosion forecasting and that any methodology used should be validated by hindcasting historical shoreline changes since observed data are available for shoreline changes from 1874 and sea level changes at

Wellington since 1891. These data and their implications will be discussed further below in section 5.1.

Montaño et al. (2020) reported on a blind test of 19 different models for predicting shoreline response at Tairua Beach, New Zealand, to forcing, including storms and sea level changes. The 19 models included a mixture of shoreline process models and machine learning (statistical) techniques (Coco et al., 2020). The models produced comparable results for "normal" conditions with low forcing when little change could be expected but diverged under more extreme forcing (such as a storm), which is when most shoreline changes occur. Simulations of future changes out to 2100 CE were undertaken. Still, the divergence between models was too large, attributed to the large uncertainties associated with future forcing (i.e. forecasting the weather required as input for the models 100 years ahead is beyond present capabilities). Montaño et al. (2020) concluded that models must be calibrated; models generally performed well for the calibration period, but performance declined outside that period; machine learning methods tended to perform better, and the best overall performance was obtained from ensembles of models.

Simmons & Splinter (2022) assessed shoreline storm erosion models for beaches on the New South Wales coast, including SBEACH, XBEACH, and machine learning methods. They concluded that machine learning models performed best individually, but an ensemble of approaches provided the best overall predictive skill.

Concerning the Kāpiti Coast, it should be noted that Tairua Beach and the NSW beaches tested were embayed systems and did not involve a significant influx of sediment from rivers or longshore transport. Hence, the Kāpiti Coast will be more difficult to simulate. Nonetheless, it is likely that for short-term changes, machine learning methods will work much better than the Bruun Rule and SBEACH, and ensemble methods will be the most effective. For a longer-term (multi-decadal to centennial), uncertainties in forcing conditions preclude reliable forecasting (Montaño et al., 2020). This implies that it is not feasible to use models to assess the effects of climate change on coastal hazards 100 years from now, as required under Policy 24.

2.2.7 Effects of Changing Climate

To assess the consequences of future climatic conditions on natural hazards, Steele et al. (2019) undertook a qualitative assessment of the potential impacts of three selected natural hazards after 100 years of climate changes and sea level rise, using 24 criteria considering the effects on community, business, roads, 3 waters, lifelines infrastructure, Māori and cultural, ecology, erosion, and Civil Defence and Emergency Management. It was determined that sea level rise and its effects on coastal inundation and erosion were the main causes of increased hazards for coastal communities. This finding primarily arose from their acceptance of the Ministry for the Environment's opinion that a 1 m rise in sea level within 100 years was *virtually certain*. There was no quantitative analysis of the actual effects of sea level rise on either inundation or erosion, or consideration of the estimate's likelihood, risk, and uncertainty.

While correctly stating that climate change may modify the frequency and magnitude of natural hazards, Steele et al. (2019) did not seem to realise that climate change is not a hazard, and it doesn't create new hazards that currently do not affect the Kāpiti Coast. Climate change may result in a different level of risk in the future, and to be helpful, the

changed risk needs to be quantified, and a threshold for intolerable risk must be defined. For Kāpiti Coast District, Steele et al. (2019) identified that the greatest hazard in the future is coastal erosion affecting Raumati and Paraparaumu (the areas with the most significant historical erosion hazard, as indicated by the presence of seawalls).

As noted above for waves and storm surges, coastal hazards for Kāpiti Coast District that may be affected by changing climate already display significant interannual and decadal variability. Brown et al. (2020) concluded that for the Southwest Pacific region (including New Zealand), this natural variability will likely dominate over any responses to anthropogenic warming or other climate changes for the predictable future. This will be discussed further in section 5 in relation to the risks.

2.3 Jacobs (2022) Coastal Hazard Assessment

Jacobs (2021) notes on page 8 (paragraph. 1) that:

> *"...we have re-defined the assessment to be coastal hazard vulnerability rather than coastal hazard risk".*

The KCDC district plan defines vulnerability as:

> *"... the exposure or susceptibility of a development, building, business or community to the effects from a natural hazard event."*

Jacobs's use of vulnerability (2021, 2022) is to avoid determining the probability of the hazard affecting infrastructure, property, or people. The Jacobs (2021, 2022) report titles also refer to coastal hazard susceptibility, implying that this is explicitly addressed in addition to via the KCDC definition of vulnerability. Hazard susceptibility is generally defined as (Brabb, 1984; Domínguez-Cuesta, 2013) (my highlighting):

> "... the estimation of the ***likelihood*** of spatial occurrence of natural hazard ...".

This definition is consistent with the requirement in the NZCPS to identify areas of high risk. Vulnerability generally involves factors that may increase or decrease the susceptibility to a hazard. Therefore, despite the different terminology, there is still an implicit need to consider the likelihood. In my opinion, this means that the Jacobs (2022) report is not appropriate for assessing the level of coastal hazard risk for the Kāpiti Coast District. If likelihood is not assessed, it is not useful for characterising susceptibility and vulnerability.

Jacobs (2021, 2022) assessed coastal erosion and inundation hazards for the Kāpiti coast, assuming different scenarios of relative sea level rise (but ignoring sea level fall due to vertical land movement). The effects of other drivers of coastal erosion and inundations, such as extreme weather events and changes to sediment supply, were not specifically assessed. It was also assumed that anthropic impacts would be restricted to removing coastal protection structures as they exceeded their design life and did not consider any mitigation or adaptation measures. The assessment undertook some analysis of the consequences of the impact of 100 years of climate change combined with the natural hazards considered by mapping properties that might be affected by the scenarios considered. It was assumed that there would be no changes to infrastructure, apart from the loss of coastal protection structures, during these 100 years.

Jacobs (2021) identified many of the limitations and assumptions associated with their analysis and summarised these in sections 6.9 and 7.6 of their report for coastal erosion and

inundation, respectively. The extent of the limitations identified should raise doubt about the utility of the modelling results for planning purposes. One concerning aspect is that Jacobs's (2021) approach to uncertainty appears to select the worst-case condition as the baseline, which is justified as *conservative*. An example is the use of Stephens et al. (2012) estimated maximum wave heights for the Kāpiti coast, which were multiplied by 1.5 from modelled wave heights based on a comparison with wave conditions at Baring Head. Jacobs (2021) then treated these values as the mean for their wave height distributions and multiplied them by a further 1.5 to define a new maximum value.

Given that shoreline response is proportional to the square of the wave height, this effectively scales the impact of the modelled maximum wave height by ~500%. The historical observations for the claimed worst erosion event, September 1976, noted that the waves were not extreme compared to previous storms (Gibs & Wilshere, 1976). This will be discussed further in Section 2.3.1.

The Jacobs (2022) report essentially showed that areas of significant historical erosion would be most severely affected in the future. However, they suggest that areas not affected by historical erosion would eventually be exposed to erosion due to increasing relative sea levels. This is primarily based on inundation predicted by the Brunn Rule overtopping a planar slope approximating the present shoreline and not any process-based shoreline modelling. The underlying assumption that sea level rise always results in shoreline retreat (due to inundation and not "erosion") will be addressed in Section 3 on sequence stratigraphy.

2.3.1 September 1976 Storm

There are data used to test their modelling as described in Jacobs (2021), where they explain short-term erosion rates (storm cut) were compared to the most severe storm in the available record with ~0.5% AEP. This storm was identified as the September 1976 event, and the ranking and estimated AEP value is attributed to Lane et al. (2012). As discussed above, Lane et al. (2012) identified the 7 November 1994 storm as the most severe in their 45-year re-analysis dataset. They used the 6 September 1994 storm as their storm scenario for inundation modelling. The consequence of the Jacobs (2021,2022) hazard assessment is that the September 1976 storm scenario used is a higher probability event (> 1% AEP) than they reported.

One advantage of using the September 1976 storm is that some data about the storm characteristics and the coastal erosion impacts were reported by Gibb & Wilshrre (1976) and Gibb (1976, 1978a). Heath (1979) also published an analysis of the storm surge produced by this storm. Jacobs (2021) summarises the observed coastal erosion in their Table 6.4 (page 57). In transcribing the data from Gibb & Wilshere (1976), Jacobs (2021) presented the observations at specific locations along the coast. However, it is clear from Gibb & Wilshere that the observations are estimates of the ranges of erosion for stretches of the coast between the locations given. Further, some of the values Jacobs (2021) reported differ from those in the original data (Table 1).

Gibb (1978a) noted that in areas without coastal protection structures at Queen Elizabeth Park, the maximum erosion was around 6 m. In comparison, erosion of up to 15 m occurred in areas with structures prior to the storm. Jacobs (2021) also noted this. Gibb (1978a) also reports that daily observations of longshore currents and monthly beach profiles were made in 1974 and covered the September 1976 storm. The results from measurements of

shoreline changes at profile locations along the Kāpiti Coast between 1872 and 1977 are tabulated in Appendix 1 of Gibb (1978a) and within the New Zealand dataset tabulated in Gibb (1978b). The data for the specific locations are in the *Profile erosion* column of Table 1. Arguably, the September 1994 storm used for inundation modelling by Lane et al. (2012) has better data available to assess the impacts due to more extensive monitoring by KCDC and a larger population of potential observers.

Table 1. Observations of the ranges of coastal erosion for sections along the Kāpiti Coast for the September 1976 storm recorded by Gibb & Wilshere (1976) and the profile erosion reported by Gibb (1978a) for specific locations. Location order has been switched to correspond to Table 6.4 in Jacobs (2021).

Location	Cumulative distance north (km)	Erosion(m)	Profile erosion (m)
Pekapeka	22.0		6
		5-10	
Waimea Stream	18.1		4
		1-5	
Waikanae River mouth	15.7		2
		>1	
Paraparaumu (Kenakena Pt)	13.4		1
		1-5	
North Raumati Beach	9.6		4
		10-15	
South Raumati Beach	6.8		11
		5-10	
Queen Elizabeth II Park	5.4		1
		>1	
Surf Lifesaving Club Paekakariki	2.5		1
		1-5	
Centennial Inn Paekakariki	0		1

There are a few problems with using the September 1976 data, as summarised in Table 6.4 by Jacobs (2021). Firstly, it is not clear from Gibb & Wilshere (1976) what their erosion estimates represent: dune toe retreat, dune crest retreat, or something else. If they represent dune crest, then the effects of dune stability are included in their values. Gibb (1978a) includes some profile plots used to measure the reported erosion. The profiles were measured some unknown time after the storm, and the reported erosion extent includes the scarp collapse due to oversteepening. Hence, the last column of Table 1 in this report corresponds to the sum of short-term erosion (ST) and the dune stability factor (DS) in the Jacobs (2021) methodology.

Secondly, the higher erosion rates indicated for the northern Kāpiti Coast (Paraparaumu to Otaki) may be associated with the inlets, not the main dune systems. However, Figures 4 and 5 of Gibb (1978a) do indicate that the entire section eroded between 1974 and 1977, with the caption to Figure 4 stating that up to about 8 m of erosion affected 10 km of coast around Pekapeka (the maximum erosion measured for profiles was 6 m). From the wave modelling undertaken by Johnson et al. (2007), it appears that due to wave refraction, there are localised areas of larger wave heights, and hence increased wave setup and run-up, that can experience more severe erosion.

Thirdly, and more importantly, the effect on the sediment budget of the Kapiti Coast depends on the height of the dunes as well as the distance eroded (i.e. total volume of sediment removed). Figures 1A and 10 of Gibb (1978a) show the area at Raumati South with the greatest impact of erosion during the September 1976 storm. Figure 9 consists of beach profiles for three Raumati, Paraparaumu and Pekapeka areas. The Raumati area has high dunes mostly protected by structures, while the dunes at Paraparaumu and Pekapeka were unprotected. The profile changes show little correlation between the volume eroded and the horizontal shoreline change. Apart from the different amounts of dune erosion that occurred, some profiles indicate a significant lowering of the beach below the mean high-water mark, while others had much less change.

Finally, no data was collected for the composite beaches further north. As de Lange (2013) and Jacobs (2021) discussed, these beaches respond differently to wave erosion compared to the sandy beaches south of Pekapeka. Therefore, it is not appropriate to assume that they experienced the same erosion in 1976 as the Pekapeka to Waimea Stream section (Table 6.4 in Jacobs, 2021).

2.3.2 Sea Level Rise Response (SL)

As was the case for previous studies using a similar methodology for predicting future shoreline positions along the Kāpiti Coast, the Jacobs (2021,2022) predictions are primarily a consequence of the sea level rise response component (SL) since it has the largest magnitude. As noted above, this relies on variants of the Bruun Rule, a simple geometric relationship that predicts landward translation of the shoreline in response to a rise of sea level (i.e. inundation, or passive flooding, viz. D'Anna, 2021). Although it is conceptually linked to the migration of some form of equilibrium beach profile, which suggests erosion, this is not included in the formulation. In other words, the Bruun Rule is an *inundation* model and not a process-based shoreline erosion model (*viz*. Stive, 2004, D'Anna, 2021).

The amount of horizontal translation is solely a function of the assumed planar slope gradient and the vertical translation of sea level; effectively, the sea level rise is multiplied by a scale factor K (Figure 10). The initial Bruun Rule used the nearshore slope angle (θ) through $K = 1/tan(\theta)$ to scale the sea level rise. This was then replaced by the vertical and horizontal offsets that define the gradient, as shown in Figure 6.8 in Jacobs (2021). The Bruun Rule can only predict accretion for negative values of K, which requires negative gradients that are not generated by the various methods used. The predicted shoreline retreat is very sensitive to the assumed sea level rise and the scale factor K, particularly for low gradients (Figure 10).

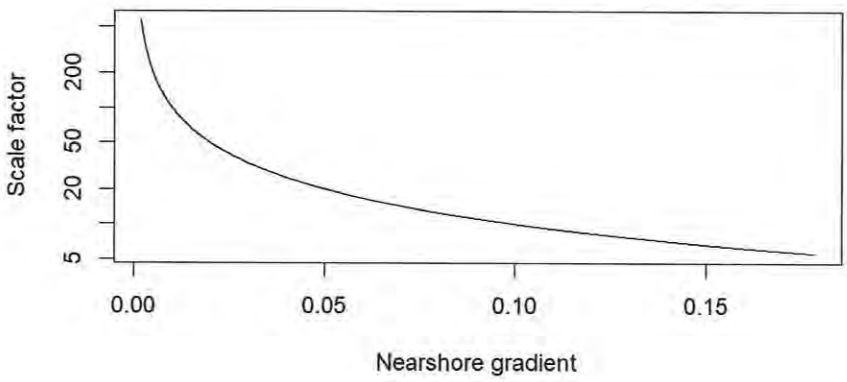

Figure 10. The original Bruun Rule can be expressed as $R = KS$ where R is the shoreline retreat, S is the sea level rise, and K is a scale factor, is a function of the nearshore slope. Here the scale factor is plotted for gradients from 0.002 to 0.178, which correspond to slope angles from 0.1° to 10°.

As indicated, the Bruun Rule can predict shoreline inundation extent 2-3 magnitudes larger than the sea level rise for very low gradients. This is only valid if *"no other sediment sources or sinks are present or if no other sediment transport gradients in cross-shore and longshore directions occur"* (Stive, 2004). For more common conditions, such as for the Kāpiti Coast, a large body of New Zealand and international observations show that the sea level response is of a similar or smaller magnitude to other shoreline processes (Stive, 2004; Pickett, 2004).

Published variations of the Bruun Rule involve either different approaches to estimating the gradient (originally the gradient of the inner continental shelf) or introducing an additional scale factor. Either approach is usually employed to increase the gradient, thereby decreasing the scale factor (Figure 10) and predicting less shoreline retreat.

Jacobs (2021) introduced a variant with a scale factor for composite and gravel beaches around the Otaki River. The variant used was developed by Todd & MacDonald (2020) for composite and mixed-sand gravel beaches on the northern Canterbury coast. The variations involve modified estimates of the gradient by adjusting the length and height scales of the slope. Somewhat surprisingly, it is claimed that these modifications are process-based, while they are solely derived from the morphology and do not incorporate any quantification of the dynamic processes involved.

Further, Table 2 in Todd & MacDonald (2020) compared the observed rate of shoreline change and predicted rates using the original Bruun Rule and their variant for five composite and mix-sand gravel beaches. Three of the beaches were observed to be accreting. The Bruun Rule and variants can only predict erosion, so 60% of their predictions incorrectly predicted the direction of the shoreline response. This demonstrates a lack of skill compared to chance (e.g. a coin toss). The Todd & MacDonald (2020) variant predicted lower erosion rates than the original Bruun Rule (due to a steeper adjusted gradient), which was closer to the observed erosion rate at one site and worse at the other. It is unclear why this approach could be considered suitable for predicting the shoreline response around the Otaki River if 80% of the predictions in Todd & MacDonald (2020) were incorrect?

For the sea rise component of the Bruun Rule, Jacobs estimated future relative sea level rise by combining an estimated VLM for the Kāpiti Coast with projected absolute sea levels, which is summarised in Figure 3.2 and Table 3.3 of Jacobs (2021). The estimated VLM rates were -1 to -3 mm.y^{-1} based on Bell & Hannah (2012), Beavan & Litchfield (2012), and Bell et al. (2018). Beavan & Litchfield (2012) don't give an overall VLM rate for Kāpiti but do report that VLM is affected by slow slip events and give estimated VLM rates for the PAEK, KAPT and OTAK cGPS sites (Figure 7) of -0.7, -2.1, and -1.3 mm.y^{-1} for record durations of 10.5, 8 and 5 y respectively. Bell & Hannah (2012) report rates of -1 to -3 mm. y^{-1} for the Wellington region, with -1 mm.y^{-1} for Kāpiti. This suggests that a rate of -1 mm.y^{-1} for VLM at the Kāpiti coast is *most likely* given the data sources cited by Jacobs (2021).

Note that there is evidence that the southern section of the Kāpiti coast is uplifting, while the northern section is subsiding. Hence, a single VLM value for the entire coast is not realistic.

The absolute sea level component used by Jacobs (2021) was derived from *Coastal Hazards and Climate Change: Guidance for Local Government* (MfE, 2017) and *the IPCC Special Report on the Ocean and Cryosphere in a Changing Climate* (IPCC, 2019). Instead of using the scenarios in those reports, Jacobs selected values for an upper and lower bound and two "intermediate" values, which were spread over the range of projections (Figure 3.2 and Table 3.3 in Jacobs, 2021) and they don't follow the median projections of any scenario. The values from MfE (2017) and IPCC (2019) have been superseded by IPCC (2021) and MfE (2022), which raises the question of whether it is sensible to undertake assessments of coastal responses to projections of sea level rise 100 years into the future when it is possible the projections will change over time? This will be considered further below in Section 6.

Jacobs (2021) undertook limited sensitivity testing of the Bruun Rule, which involved changing the dune height to consider the effect of shoreline erosion exposing higher dunes to waves. Unsurprisingly, this increased the vertical offset and hence the gradient increased, resulting in a smaller scale factor and less shoreline erosion. They also tested their projections of future shoreline response (*inundation*) against their estimated sediment budget for the Kāpiti Coast. It is unclear how this validates the Bruun Rule projections, as all it appears to do is demonstrate that the assumed planar slope eventually extends above the ground surface. For the probabilistic analysis, Jacobs (2021, 2022) increased the depth of closure which greatly reduced the gradient (increased K) and increased the shoreline inundation extent. No sensitivity analysis was undertaken of this aspect.

There was no comparison of the SL factor with to historic shoreline changes and sea level rise even though DSAS provided historic shoreline responses (referred to as LRR in Jacobs, 2022), and there is an assumed historic sea level rise of 2.74 $mm.y^{-1}$ used in their methodology (Jacobs, 2021). The DSAS LRR data are not given for all transects in Jacobs (2022). However, some values are provided on the profile plots in Appendix F of Jacobs (2022) for the 18-year beach profile measurements undertaken by Cuttriss Consultants Ltd for KCDC.

For this report, the CSL shoreline position data was updated using Google Earth satellite images (Section 4). A subset of the data for 1948-2017 corresponding to the aerial photograph coverage used by Jacobs (2021,2022) was analysed to determine the long-term trends for the CSL locations. Generalised Least Squares (GLS) regression was undertaken using R Package *nlme* to avoid any issues with serial autocorrelation. This analysis provides a linear trend and the residual standard error (RSE) to measure the goodness of fit. The RSE is defined as

$$RSE = \sqrt{\frac{\sum (y - \hat{y})^2}{df}}$$

Where y = observed value, $\hat{y}$ =predicted value, and df = degrees of freedom.

Figure 11 shows the observed change in shoreline position between 1948 and 2017 and the variability in shoreline position relative to the long-term trend (RSE). The CSL analysis used this variability as an indication of the short-term cut and fill. It is evident from Figure 11 that there is a considerable difference between the survey sites for both shoreline change and variability about the trend, some of which is due to the influence of inlets. The data also indicate that most sites accreted, with the erosion mainly concentrated within the shoreline of Queen Elizabeth II Park (Sites C3.60 to C6.57). Erosion also occurs at site C0.40, an

unprotected sand dune in Paekākāriki, and sites C9.43 and C10.28, where seawall reconstruction appears to have changed the shoreline location. Low rates of change and variability are evident for areas with seawalls for the southern Kāpiti Coast, which the changes identified being mostly due to the rectification and digitisation errors.

It is also evident from Figure 11 that the Bruun Rule predicts the wrong trend at most sites for the sea level rise between 1948 and 2017 (maximum of ~189 m inundation extent at -2.74 m.y^{-1}). For the sites within Queen Elizabeth II Park, the rates of observed shoreline change range from -0.17 to -1.08 m.y^{-1}. The highest observed rate of erosion is ~40% of the predicted rate of inundation and occurs at CS6.57 just south of the end of the South Raumati Beach seawall, where end-effects due to the seawall contribute to erosion. The next highest rate of erosion is at CS6.39 (-0.69 m.y^{-1}), and the erosion decreases steadily southwards to C3.60 north of the Wainui Stream, where the rate is -0.17 m.y^{-1}. There is an exception to this pattern at site C4.52 (Figure 11), which has the third-highest rate of erosion (-0.64 m.y^{-1}). This site also has the largest RSE value of ±9.34 m. Google Earth images suggest that pedestrian traffic between the beach and carparks at this site may be causing localised blowouts and erosion of the foredune.

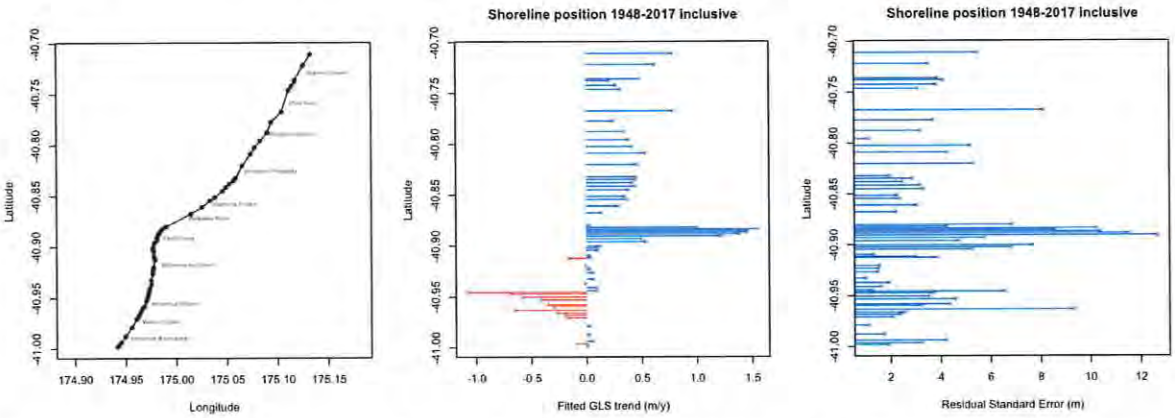

Figure 11. Generalised Least Squares analysis trend and residual standard error results for CSL sites along the Kāpiti coast, excluding site C17.31 that appears to have an undocumented datum shift.

Jacobs (2021, 2022) treats the shoreline of Queen Elizabeth II Park as a single coastal cell with similar characteristics. The historical trend of declining erosion rate southwards from Raumati to Paekākāriki, shown in Figure 11, indicates that there is a longshore change in coastal processes and/or beach characteristics. It is likely that the assumption of longshore similarity is invalid. In Table I.1 of Jacobs (2022), Queen Elizabeth II Park is subdivided into two sections: transects 126-152 in the north and transects 85-125 in the south. The boundary between the two transects is the Whareroa Stream (Jacobs, 2021): the northern division corresponds to sites C5.70 to C6.57, and the southern division corresponds to C3.60 to C5.15.

The DSAS results presented by Jacobs (2022) also show a decline in erosion rates southwards between the two cells: the lower bound, the mean and upper bound of -0.6, -0.4, and -0.1 m.y^{-1} respectively, for the north, and -0.3, -0.2, and -0.1 m.y^{-1} respectively for the south. Combining the CSL sites for the same divisions, the calculated rates (mean and 1 standard deviation) are -0.69±0.26 m.y^{-1} north and 0.32±0.16 m.y^{-1} south of the Whareroa

Stream, respectively. These are higher mean rates but less spread than assumed by Jacobs (2022).

The issues with the Bruun Rule and any variants stem from an assumption that sea level rise for an unconsolidated coast (and other types of coasts, according to some authors) will only result in erosion. Jacobs (2022) recognises that parts of the Kāpiti coast will continue to accrete for a while as sea level rises but insists that all areas will eventually erode. The following sections on the *Probabilistic approach* and *Sequence stratigraphy* will explore this assumption further.

2.3.3 Short-Term Erosion (ST)

Figure 12 shows the area experiencing the most erosion outside of Queen Elizabeth Park, as indicated by the trends in Figure 11. It also shows a sequence of aerial photographs taken of the mouth of the Waikanae River and adjacent coast, including site 370, in April 1966 (Crown 1847_4083_2), October 1973 (Crown 3686_B_2), and February 1977 (Crown 5034_B_2). Jacobs (2021) used this area to test their methodology.

For their assessment of the short-term erosion that corresponds to the erosion phase of storm cut and fill (which contributes to variability about any long-term trend), Jacobs (2021) considered two approaches: the storm erosion model of Komar et al. (1999), referred to as the geometric model; and the numerical model SBEACH.

Komar et al. (1999) developed their approach when they discovered that numerical models, including SBEACH, underpredicted the extent of dune erosion. Their approach increases the amount of erosion predicted by translating the slope of the dune face inland, which effectively incorporates the dune stability component that Jacobs (2021) adds in separately. This is illustrated by Figure B.1 in Jacobs (2021), which is identical to Figure 4 in Komar et al (1999).

After sensitivity testing, Jacobs (2021) rejected the Komar et al. (1999) method, which was developed for predicting storm cuts for the dunes of the Oregon Coast. While the Oregon dunes have also been modified by the introduction of marram (2 species), they have their own combination of morphological responses to vegetation, sediment supply and forcing by storms and relative sea-level changes (Kumler, 1969; Ruggiero et al., 2018). It is reasonable to expect that it may not be applicable to other locations, such as the Kāpiti Coast. However, Komar et al. (1999) suggested that their method (overpredicts) and numerical models such as SBEACH (underpredict). Hence, both approaches should be used to bracket the likely storm erosion.

Figure 12. Aerial photographs retrieved from https://retrolens.co.nz/ for the Waikanae River mouth and Lumsden site 370 (marked on bottom photograph).

Jacobs (2021) only used SBEACH and undertook a sensitivity analysis based on a composite profile at Lumsden site 370, just north of the Waikanae River (Figure 12), and estimated forcing conditions for the September 1976 storm. The results were compared to the Gibb & Wilshere (1976) estimates summarised in Table 1, with Jacobs (2021) assuming a range of 1-5 m applied at site 370. Gibb (1978a) reports a measured erosion of 1 m based on the Ministry of Works Department (MWD) beach profile 11 on the western side of the mouth of the Waikanae River (Table 1). He also reports the erosion for MWD profile 12, which is 188 m southwest of site 370, giving a value of 2 m, and MWD profile 13, about 475 m northeast of site 330, giving a value of 3 m. MWD profiles 14 and 15 further northeast are reported to have eroded by 4 m and 6 m, respectively.

Clearly, the extent of erosion increased northwards, given the range presented by Gibbs & Wilshere (1976), and that the value for Site 370 should have been taken as a maximum of ~2 m. This is within the range of 1-5 m simulated by Jacobs (2021) but at the lower end. Jacobs (2021) decided to use the upper limit of their range as being more consistent with the observations. Considering their choice of forcing conditions, it seems likely that the wave heights used for the sensitivity tests were significantly larger than what occurred for this site in 1976.

Figure 12 shows that this area underwent considerable natural and anthropic changes, including the development of a sub-division in the dunes at site 370 during the period leading up to the September 1976 storm. It would be difficult to exclude the possibility that these changes affected the beach/dune response to the storm conditions. Generally, it is not good practice to calibrate or validate models on data that could be contaminated by factors not allowed for in the model.

It is possible to assess the validity of the SBEACH approach by comparing the results shown in Figure B.2 of Jacobs (2021) and the measured beach profiles at site P370 (Section 4). The measured profiles were analysed to determine the median profile, the 95% confidence limits, and the extreme elevation changes (minimum and maximum) for all available surveys. Figure 13 shows the initial composite profile and predicted storm profile from Jacobs (2021) overlain on the results of the analysis of surveyed profiles. The initial profile of Jacobs (2021) has been aligned with the median profile (It wasn't possible to match the composite profile used with any specific surveyed profile). Although the initial profile extends outside the extreme elevation limits of the surveyed profile, the predicted worst-case storm profile involves less deviation from the median profile than has been observed.

The 95% confidence limits and extreme values are also not symmetrical about the media profile. Their distribution indicates that sediment has been rapidly accreted following erosion events, even if there has not been significant seaward movement of the profile. In the long term, these conditions will result in continued accretion.

The comparison indicates that the SBEACH model based on applying assumed forcing for the September 1976 storm could better predict the shore-term erosion behaviour at Site P370. It is likely that it doesn't perform well for other sites that are accreting or have a functional seawall. Overall, it is better to use the measured profile variation to estimate this component. However, this component is only important if the sea level rise component (SL) is of a similar magnitude. The projected values of SL determined by Jacobs (2022) for most sites are at least an order of magnitude larger, so the short-term erosion term falls within

the uncertainties of SL. It should be noted that if the short-term erosion component does not encroach on infrastructure or property, it can be argued that it is not an erosion hazard.

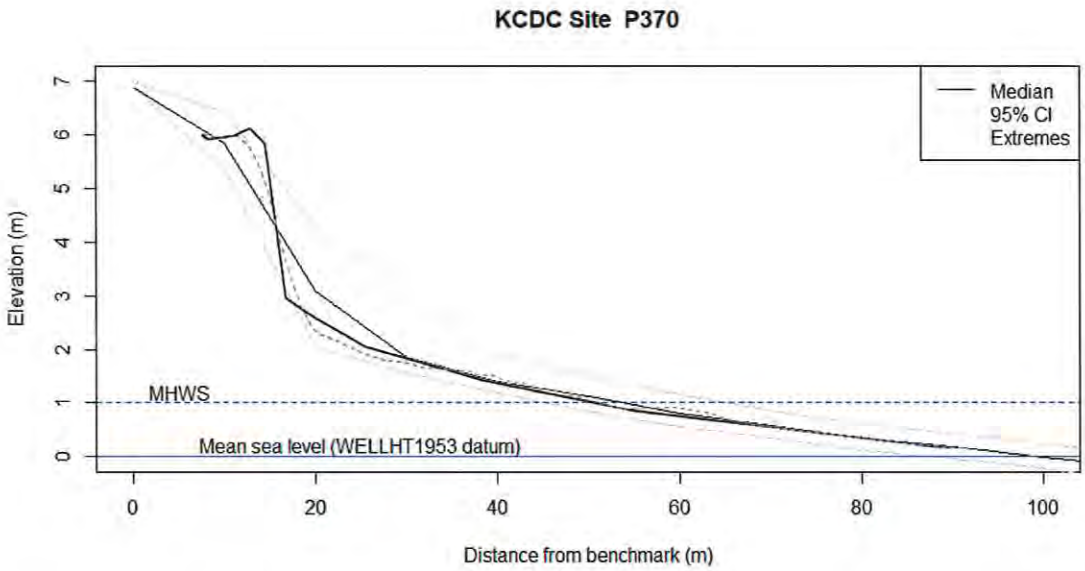

Figure 13. Comparison of the SBEACH model results shown in Figure B2 of Jacobs (2021) with the envelope of beach profile measurements at KCDC Site P370. The composite profile used by Jacobs (2021) has been aligned with the median of the surveyed profiles.

2.3.4 Dune stability factor (DS)

As a component of the calculation of the extent of erosion, Jacobs (2021) includes a dune stability factor, which they claim is suitable for the low spinifex-dominated dunes of the northern Kāpiti Coast, implying that they consider it inappropriate for the southern marram (*Ammophila arenaria*) dominated dunes. The problem with including this term is that it assumes the development of a steep scarp that persists for a reasonably long period, allowing further erosion of the scarp face. Jacobs (2021) incorporates an adjustment used by CSL to scale back the predicted erosion by allowing an offset for the formation of a talus slope at the base of the scarp as it collapses. This type of behaviour is associated with marram dunes, as marram is intolerant of salt water and forms dense root mats, which results in slabs of vegetation falling to the base of the eroding scarp, dying and rotting (unless transported away by the storm waves). The exposed scarp face collapses post-storm, particularly if there are overhanging slabs of marram vegetation.

Spinifex (kōwhangatara, *Spinifex sericeous*) dunes are more resistant to scarping (Jenks, 2018). If it occurs, spinifex is soloniferous, with much-branched, knotted, rope-like, hard, creeping culms that hang down the scarp. Spinifex is also salt and burial-tolerant, so there is an immediate source of viable vegetation to trap and colonise any sediment returning to the base of the foredune during the post-storm recovery. Observations of restored spinifex dune systems that have formed natural dune morphologies show that they recover very quickly unless there is a significant lack of available sediment (Hesp & Hilton, 2013; Jenks, 2018). It is likely that the dune stability factor is unnecessary for assessment of the longer-term coastal erosion hazard since it is part of the storm cut and fills process and, therefore, part of the measured variability in beach profiles for Spinifex-dominated foredunes). In

other words, this factor is already accounted for in the SBEACH model, and the profile variations are measured by most or all surveys. The inclusion of the term is effectively double-dipping.

2.3.5 Long-term Shoreline Trend (LT)

Jacobs (2021) used the Digital Shoreline Analysis System (DSAS) developed by the US Geological Survey to estimate the rate of change statistics from digital shoreline data (Himmelstoss et al., 2021) to assess rates of change since the 1940s from digitised aerial photographs. The version (V5) used by Jacobs was an add-on to the Esri ArcGIS desktop. The current version (V6) is a standalone product, with less capabilities. DSAS V5 could use the calculated rate of change statistics to generate predicted shorelines 10 and 20 years into the future. Since the predicted shorelines are based solely on historical trends and make no assumptions about processes and sediment budgets, they are a useful baseline for comparison of future shorelines determined by other means.

Unfortunately, Jacobs (2021) calculated their Projected Future Shoreline Position (PFSP) values for 30, 50 and 100 years into the future, which precluded such a comparison. This was a mistake as the DSAS predictions represent a naïve baseline to assess the validity of the projections made by Jacobs (2022). Various statistical methods are used to assess models' skill (viz. Murphy & Epstein, 1989; Winter, 2007), but all require something to compare the results with. If there are no observations, which is the case with a predicted future condition, then a naïve prediction that assumes no change to the system is a useful baseline for comparison. The DSAS predictions are based on the historical trends resulting from the interaction of all historical processes, including rising sea levels, climate changes, extreme weather events, and anthropic disturbances. The DSAS predictions assume that these trends will continue unchanged for 10-20 years.

DSAS determines the rates using Ordinary Least Squares (OLS) or Weighted Least Squares regression or the change between two surveys (end-point analysis). It is unclear from the discussion in Jacobs (2021) whether they used the change between the first and last survey or the average rates determined between successive pairs of surveys. The end-point approach also allows the standard deviation and/or standard error to be calculated to define the uncertainty. Ruggiero et al. (2012) explain the methodology used by DSAS and approaches for assessing the uncertainties.

Allan et al. (2003) investigated the applicability of both methods for estimating shoreline trends for the coast of Oregon, USA, for two sites: one undergoing long-term accretion and one experiencing long-term erosion. Both sites were subject to episodic storms, followed by recovery. Although the wave climate was higher energy than the South Taranaki Bight, the Oregon coast is a useful analogue for the Kāpiti coast as many climate oscillations affecting coastal processes are the same (e.g. La Niña – El Niño cycles). Allan et al. (2003) concluded that neither OLS regression nor end-point analysis provided useful information about the long-term trend as the trends were too small relative to the short-term cut and fill variations. Incorrect trends can be estimated if the data series are not long enough to average out the variability, and with enough resolution to distinguish the cut and fill phases. Clearly, the endpoint method has an insufficient resolution.

OLS regression is affected by serial autocorrelation, which means that the dependent variable (shoreline position) is a function of both the independent variable (time) and the preceding dependent variables (de Lange, 2013). One consequence is the calculated

regression coefficient (r^2) is larger than it would be if data were not serially autocorrelated. Jacobs (2021) selected the DSAS method used for different parts of the Kāpiti coastline depending on the r^2 value for the OLS regression (end-point method if $r^2 \leq 0.5$). The effect on the predicted trend is less than that for r^2. Still, it would be important if the predicted trend is extrapolated too far into the future (DSAS limits extrapolation to a maximum of 20 years).

DSAS undertakes shoreline forecasting by using a Kalman filter to forecast future shoreline positions by combining observed shoreline positions with model-derived positions (Himmelstoss et al., 2021). The filter is used to smooth the transitions between the transects used, and there are limitations on where it can be applied related to discontinuities along the coast. The DSAS Kalman filter is initialised with the linear regression rate calculated by DSAS, it then estimates the shoreline position and change rate for every 10th of a year and provides an estimate of positional uncertainty at each time step. The methodology assumes that a linear regression through past shoreline positions is a good approximation for future shoreline positions; however, this assumption may not always be valid as it may not capture all the processes that affect the shoreline position depending on the length of the time series of digitised shoreline positions. The DSAS output includes the predicted shoreline and the uncertainties.

2.3.6 Probabilistic Approach

Jacobs (2021) explains that their analysis is an improvement on previous studies due to incorporating a probabilistic approach to defining the locations of future shoreline lines (which they refer to as Projected Future Shoreline Position – PFSP). The key explanation of their procedure is in section 6.2 of Jacobs (2021), where they present the use of a Monte Carlo approach to generate a probability distribution for PFSP. An example of such a distribution is displayed in their Figure 6.7 for transect 454 (Figure 14). Their methodology involves determining the PFSP by calculating an offset due to erosion from the present shoreline, which is a linear combination of 4 components: LT = historic long-term rate of shoreline movement; SL = shoreline erosion in response to future accelerated sea level rise; ST = short term erosion; and DS = dune stability factor. As discussed above, due to using the Bruun Rule for the SL term, their PFSP is effectively the inundation extent, not erosion.

Of the four factors contributing to the PFSP, LT and SL are scaled by time: explicitly for LT and implicitly for SL due to the varying sea-level parameters over time. The remaining terms are constant throughout all time periods considered. Given that it is assumed that the rate of sea level rise will vary (accelerate) into the future, it appears contradictory to assume that LT, ST and DS are constant and do not vary with past and future changes to forcing processes due to climate changes, vertical land movement, anthropic modifications, or other factors. One consequence of this assumption is that the modelling of PFSP will inevitably predict erosion for accreting coasts when the sum of the SL, ST and DS terms exceeds the product of the LT term and elapsed time. As discussed in the sections on sequence stratigraphy and climate projections below, the assumption of constant values for LT and ST is unjustified. A constant DS term requires that the morphology of the foredune doesn't change over time. Given community efforts to restore natural dune systems and the continued growth of marram-dominated dunes, the assumption of a constant DS term is also not justified. Also, as discussed above, the DS term appears to have been incorporated into the ST term because of the methodology used, so it is not required.

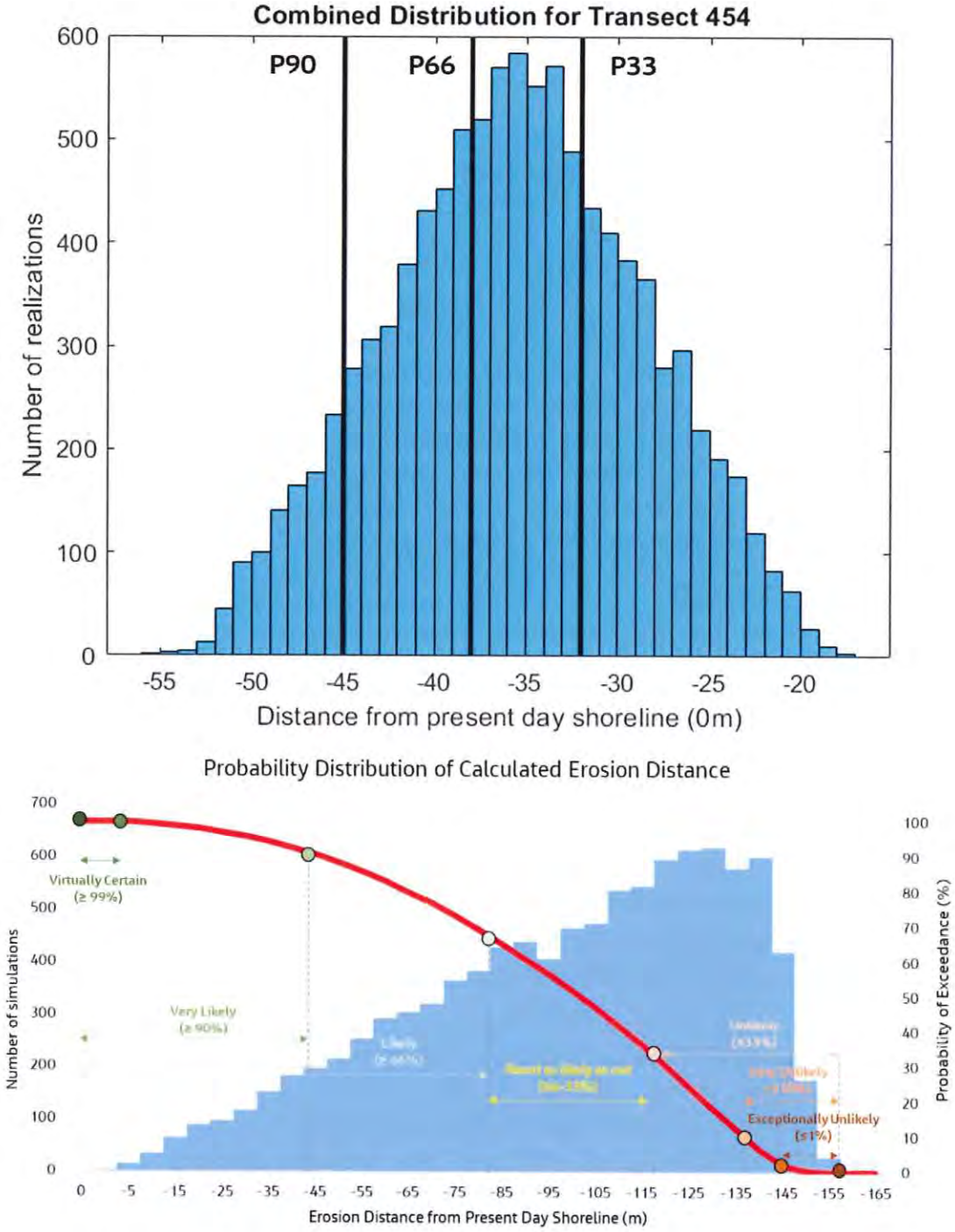

Figure 14. Examples of the PFSP probability distributions determined by the Jacobs (2021) methodology shown as (top) Figure 6.7 in Jacobs (2021) and (bottom) Figure 2.3 in Jacobs (2022). Jacobs (2021) refers to the 66-33% band of the probability of exceedance as *most likely*.

Monte Carlo simulations are useful for assessing the uncertainties in model predictions when the uncertainties in the input parameters are not well understood (Clare et al., 2022) and other methods are not available. Jacobs (2021) defined triangular probability distributions for each of the 4 terms based on the minimum, mean, and maximum values

"*obtained or assumed from the data*". The methodology used by Jacobs (2021) is different for each parameter:

- For LT, x is the estimated shoreline trend determined by the end-point method or previously calculated by CSL for transects with seawalls. The minimum, mean, and maximum are taken as $0.5x$, x, and $1.5x$, respectively. Jacobs (2010) does not explain how the probability distribution is determined for transects where an OLS regression trend was used. Given the amount of data available for the Kāpiti Coast, the 95% confidence limits for the historical trends at each site would be better limits for the distribution.
- For SL, it is unclear how the overall probability distribution was determined as Jacobs (2021) only explains how some of the maxima and minima for the parameters defining the vertical component of the gradient in the Bruun Rule were determined from observations (viz., dune height, closure depth). The horizontal distance presumably was obtained from the corresponding positions of the dune height and closure depth maxima and minima. The means appear to be taken as the mid-point between the minima and maxima to give symmetrical triangular distributions. The sea rise parameter was fixed at single values for each sea level scenario included in the assessment. Since this term dominates the calculation of PFSP, the methodology should be clarified.
- For ST, x is the maximum erosion distance determined by SBEACH simulations, which was justified by SBEACH underpredicting the September 1976 erosion. Then, the minimum, mean, and maximum are taken as $0.5x$, x, and $1.5x$, respectively. As discussed above, SBEACH did not underpredict the actual erosion. Further, there is sufficient data to provide the probability distributions of ST at survey sites or the minimum, mean, and maximum if a triangular estimated distribution is preferred.
- For DS, the minimum, mean, and maximum dune heights are determined from the beach profile data. The corresponding values for the DS probability distribution are then calculated assuming slopes of 30°, 32°, and 34°, respectively. These data are only realistic for spinifex-dominated dunes.

From the results in Jacobs (2022), it appears that the minimum, mean and maximum values are determined for all the transects in a coastal cell, but then are somehow aggregated into groups within coastal cells (Appendix I of Jacobs, 2022).

The Jacobs (2021) approach can be expressed mathematically as a linear combination of 4 triangular distributions with minimum $xmin_i$, mean x_i, and maximum $xmax_i$. Jacobs (2021, 2022) estimated all these values and assumed that the uncertainties are captured by the range from the minimum to the maximum. Hence, it can be argued that the uncertainty in these calculated terms is known. Regardless of whether the values used are true measures of uncertainty, the 4 distributions can be combined to give the maximum, mean and maximum of the PFSP as follows for n=4:

- $minimum = \sum_{i=1}^{n} xmin_i$
- $mean = \sum_{i=1}^{n} x_i$
- $maximum = \sum_{i=1}^{n} xmax_i$

This does not require Monte Carlo simulation. Examination of Figure 6.7 from Jacobs (2021) (Figure 14 top herein) and the results in Jacobs (2022) shows that the Monte Carlo simulation required more iterations than Jacobs used to converge to the mathematical solution. Otherwise, the results are the same. Note that the mathematical approach also applies to any other statistic associated with the individual distributions of the terms used (e.g. standard deviation, quartiles, and percentiles). Figure 2.3 in Jacobs (2022) shows a strongly skewed distribution (Figure 14 bottom). This arises from the methodology used to estimate the component probability distributions that produced skewed distributions for SL and DS (Appendix I of Jacobs, 2022). The degree of asymmetry varies with transects and appears to arise from the minima and maxima of dune height, and the relative distances to the inner and outer Hallermeier depths. These values affect the gradient, and DT and LT are non-linear functions of the slope or gradient.

Jacobs (2021) states that:

> " ... there is a 33% chance that the PFSP will be within the zone mapped as being the 'most likely' position and only a 10% chance that the PFSP will be landward of the P90 position".

Apart from indicating that there is a 67% probability that the *most likely* PFSP is wrong, this interpretation is dependent on the data used to determine the probability distributions for the terms used to calculate the PFSP for a site. If, as appears to be the case, the distributions are based on an aggregation of data from multiple sites from within a single coastal cell or multiple adjacent cells (it is unclear from the Jacobs reports), then there is an underlying assumption that the sites show very similar responses to forcing so that they constitute a single statistical population. If they display different responses, then the data should not be aggregated. Since it is recognised by Jacobs (2021) that sites near an inlet can be significantly affected by inlet processes, while those further away are not affected to the same extent, then it is probable that the inclusion of inlet sites in coastal cells invalidates the assumption of being a single statistical population.

While it is reasonable to assume that absolute sea level changes apply equally to the Kāpiti Coast, it is evident that vertical land movement is not uniform (Figures 7 & 9), so relative sea level changes will differ between sites, at the very least between the northern and southern parts of the coast. Extreme waves, storm surges and tides, and beach composition and morphology all vary along the coastline, as discussed above. Therefore, it is possible that many, if not all, transects along the coast have different distributions of responses to forcing. This will be considered as part of the interpretation of the beach profile data collected for KCDC by Cuttriss Consultants Ltd in Section 4.

More importantly, the PFSP distribution calculated by Jacobs is a measure of the uncertainty of the calculation of the PFSP from the terms due to their variation in whatever dataset used by Jacobs (2021, 2022); it is essentially an error analysis. This means they have only considered some of the epistemic uncertainty (imperfect knowledge of parameters) related to the methods used and have not included the aleatoric uncertainty (intrinsic randomness) related to the forcing processes. Effectively, this means that Jacobs is saying that assuming that the given scenario occurs, the shoreline response is within the estimated range. To account for aleatoric uncertainty, they should also have specified the likelihoods or probabilities of their scenarios and/or the components of their scenarios. Kroon et al. (2020)

demonstrate, by way of an example of the shoreline of the Netherlands, that assessment of both types of uncertainty is essential for predicting shoreline evolution.

Jacobs (2021) does not assess the likelihood of erosion events due to extreme weather or for the sea level projections used. For sea level projections, their approach involved combining the MfE (2017) recommendations with the updated IPCC (2019) projections, presumably from the MfE (2020) report, although this is not stated. Jacobs (2021) then chose values to cover the range of values from the projections with 2 sets of intermediate points. However, as indicated by Figure 3.2, there is no consistency in what the intermediate points represent. It is also unclear why a lower sea level is used for inundation around inlets, as the stated reason about timing doesn't make sense. Note that the shoreline position methodology is dominated by the sea level inundation term SL, so the open coast analysis uses an inundation model that overestimates inundation and higher sea level scenarios.

Since the results of the analysis are biased towards the upper bound, I will focus on those values. They represent the sum of a VLM of -3 $mm.y^{-1}$ and the maximum absolute sea level projection using RCP 8.5H+. This represents the highest 18% of the RCP 8.5 sea level projections with further adjustments, including for glacial isostasy (a component of VLM, and hence double-counted) and the effect of a warm-water anomaly east of New Zealand (temporary). These adjustments result in RCP 8.5H+ deviating from RCP 8.5 even though it should overlap the upper 18%. MfE (2024) replaced RCP 8.5H+ with the SSP5-8.5H+ projection, defined as the 83% percentile of the spread of SSP5-8.5 projections.

When it was created, the RCP 8.5 scenario was defined as being *exceptionally unlikely*, and it represented a worst-case upper-bound scenario. As shown in Figure 1, this corresponds to a probability of exceedance of <1% over the period being considered. Therefore, in relation to the Jacobs (2021) report, the RCP 8.5 scenario has a <1% probability over 100 years (Centennial Exceedance Probability (CEP)). The KCDC District Plan shows that a 1% Annual Exceedance Probability (AEP) is acceptable for hazards such as flooding and presumably inundation.

The CEP is related to the AEP, and Figure 15 shows the relationship between the different values of AEP. In particular, the 1% CEP corresponds to 0.01% AEP, or approximately a 1 in 10,000-year event. Since *exceptionally unlikely* corresponds to a probability <1% CEP, and the RCP 8.5H+ represents the most extreme 18% of RCP 8.5, the probability of the upper bound scenario being achieved in 100 years is much less than 1%. MfE (2024) uses a different definition for SSP5-8.5, which is the 83% percentile of the spread of SSP5-8.5 projections and corresponds to *unlikely* (Figure 1). More importantly, Figure 15 shows that the likelihood of experiencing at least one 1% AEP event increases quite rapidly for the first 10-20 years of a 100-period. This suggests that if the projected sea level is to be reached, it should be evident that it is rising on that trajectory within the first 20 years. This can be assessed by considering the acceleration of the measured changes in sea level and will be done in Section 5.1.

Finally, it needs to be determined what is an acceptable level of risk. At present, in Kāpiti Coast District, it is acceptable to be subject to a 1% AEP flood risk (which means there is close to a 100% probability of at least one flood event in the next 100 years), but it appears unacceptable for marine inundation to be subject to a 0.01% AEP. Note that it cannot be assumed that there will be no vertical land movement over the next 100 years, as the

probability of at least one fault zone rupturing within Kāpiti District is more likely than the upper bound projected sea level rise.

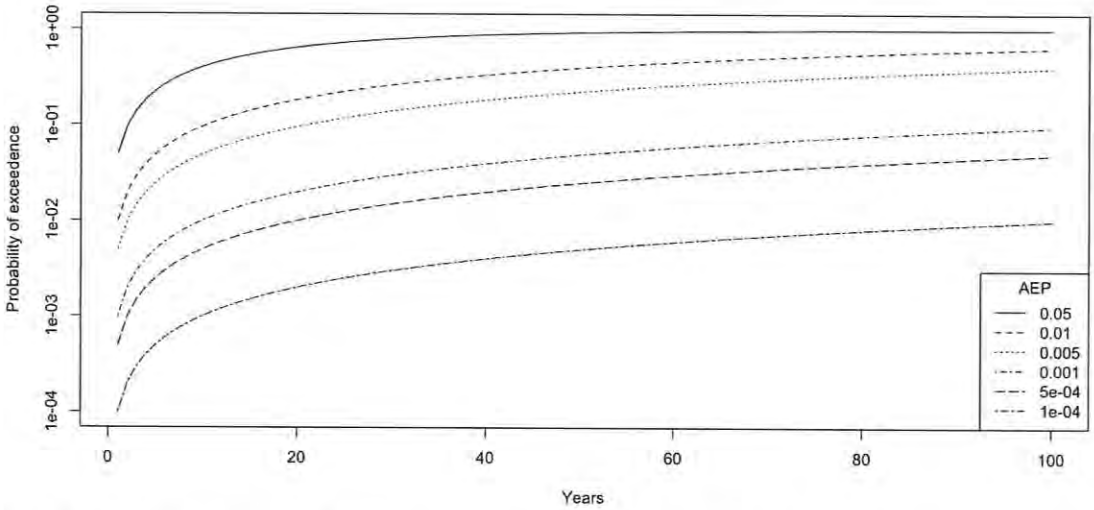

Figure 15. Plot of the probability of at least one event with the specified AEP within *n* years for 1 to 100. A 1% AEP (probability of 0.01) is commonly used for hazards such as floods in New Zealand. The 0.01% AEP (probability of 0.0001) plotted corresponds to a 10,000-year return period, which is the longest return period estimated for mapped faults in Kāpiti Coast District, and a 1% probability in 100 years.

2.3.7 Is the Coastal Hazard Susceptibility and Vulnerability Analysis Fit for Purpose?

From the outset Jacobs (2021) states that the analysis and report is focused on vulnerability. In my opinion this is inconsistent with the requirements of the NZ Coastal Policy Statement, particularly the need to identify areas of high risk. This requirement specifies that a spatial analysis of risk is necessary to identify those areas, and necessarily includes an assessment of likelihood. The assessment should also consider all hazards identified in the Coastal Policy Statement.

If the purpose of the report was to only indicate the vulnerability of coastal areas to a limited range of coast hazards, the report is also inconsistent with the definition of vulnerability used by KCDC in the District Plan. This definition also requires an assessment of likelihood.

The probabilities for the lines presented in the report are not the likelihood of being affected by the assessed coastal hazard. Instead, they represent the uncertainty in the calculated result resulting from the uncertainties in the contributing parameters for assumed scenarios, excluding any likelihood associated with the assumed future changes.

The methodology used is not an improvement on past hazard assessments and has not been verified against historical trends. It is particularly concerning that despite recognising the limitations of the methods, with most or all assumptions being violated, the analysis was performed anyway. For the results to be useful, there must be confidence that they are realistic and reasonable. This is not the case.

Hence, in my opinion, the Jacobs (2021, 2022) analysis, as reported, is not fit for purpose. However, useful information is included in the reports and collected in their preparation. If the DSAS shoreline predictions were to be included in the report or a separate report, this

would provide a useful basis for assessing coastal hazards for the Kāpiti Coast as it provides a baseline prediction for the next 20 years.

3. Sequence Stratigraphy (shoreline response to relative sea level changes)

Mao et al. (2021) assessed rates of global shoreline change for the period 1982-2019 by tracking the inferred high tide position and found that "sandy" shorelines changed at an average rate of +0.26 $m.y^{-1}$. Their plotted data shows that this reflects a greater tendency to advance than retreat despite ongoing sea level rise. Mao et al. (2021) also noted that the advancing trends were largest in areas close to rivers discharging sediment despite higher rates of sea level rise due to subsidence. So, the average rate of shoreline change in Southeast Asia was +0.64 $m.y^{-1,}$ and 67.4% of the coast advanced. Areas dominated by retreat were commonly associated with anthropic modification (causeways, ports, seawalls, etc.), which may have contributed to North America being the only continent dominated by retreat, with an average rate of shoreline change of -0.29 $m.y^{-1}$ and 66.0% of the shoreline retreating. The analysis by Mao et al. (2021) identified that the shoreline of Queen Elizabeth Park was retreating, and the rest of the Kāpiti Coast District shoreline was stable (seawalls) or accreting.

The Mao et al. (2021) analysis, like many others at a regional or local scale, indicates that sea level rise is not a good predictor of shoreline response for either inundation or erosion. This is not surprising when considering the geological record. Sequence stratigraphy is an approach used in sedimentary geology that combines the stratigraphic correlation of facies, fossils, and other rock characteristics with facies analysis to identify environments of deposition in order to recognise packages of sediments and/or rocks deposited during specific stages of cycles of relative sea level changes and/or changing sediment supply (Coe et al., 2002). These packages were initially referred to as cyclothems and were originally considered important due to their association with coal, oil, and gas, but later were linked to past climate changes. They have been extensively researched for the South Taranaki Bight, particularly in the Wanganui Basin (*viz.* Naish & Kamp, 1995).

The study of cyclothems evolved into sequence stratigraphy and provides conceptual frameworks for predicting the shoreline response to changes in relative sea level due to vertical land movement, eustatic sea level change (mostly associated with changing land-based ice volume), or a combination of both.

A key concept for sequence stratigraphy is accommodation space, which is the available volume of sediment that can be deposited (Coe et al., 2002). This is illustrated in Figure 16 where space has been created (yellow and dark grey areas) where fluvial (yellow) and marine (dark grey) sediment can be deposited (accretion). If no space is available, the sediment is transported out of the area (stable, no change). Also, if the processes transporting sediment can move more sediment than is being delivered, then erosion can occur. A rise in relative sea level creates more accommodation space, and a drop reduces it (Figure 17). Beyond the interpretation of old rocks and sediments, this concept has been found to apply to their modern equivalents. This includes a wide range of coastal depositional environments, including beaches (*viz.* Jackson & Cooper, 2009), estuaries (*viz.* Heap & Nichol,1997), and coral reefs (*viz.* McLean & Kench, 2015).

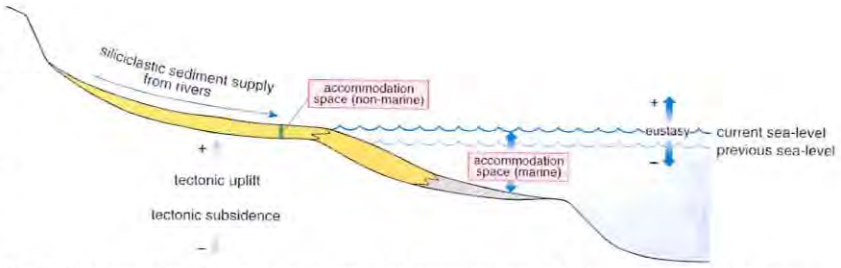

Figure 16. Schematic diagram illustrating accommodation space and the components of relative sea level changes. Increased sea level causes increased accommodation space, and then increased sedimentation if sufficient sediment is available (Coe *et al*, 2002). Decreased sea level causes erosion due to the loss of accommodation space, with any excess sediment bypassing the affected region.

The scenario illustrated in Figure 17 is the simplest response, assuming sufficient sediment is delivered to the system. However, this is not always the case. Figure 18 illustrates all possible combinations of changing relative sea level and sediment availability, with eight possible situations forming a cyclic response to changes in sea level (a cyclothem). Not all eight will arise, and hence, cyclothems typically contain subsets of these responses.

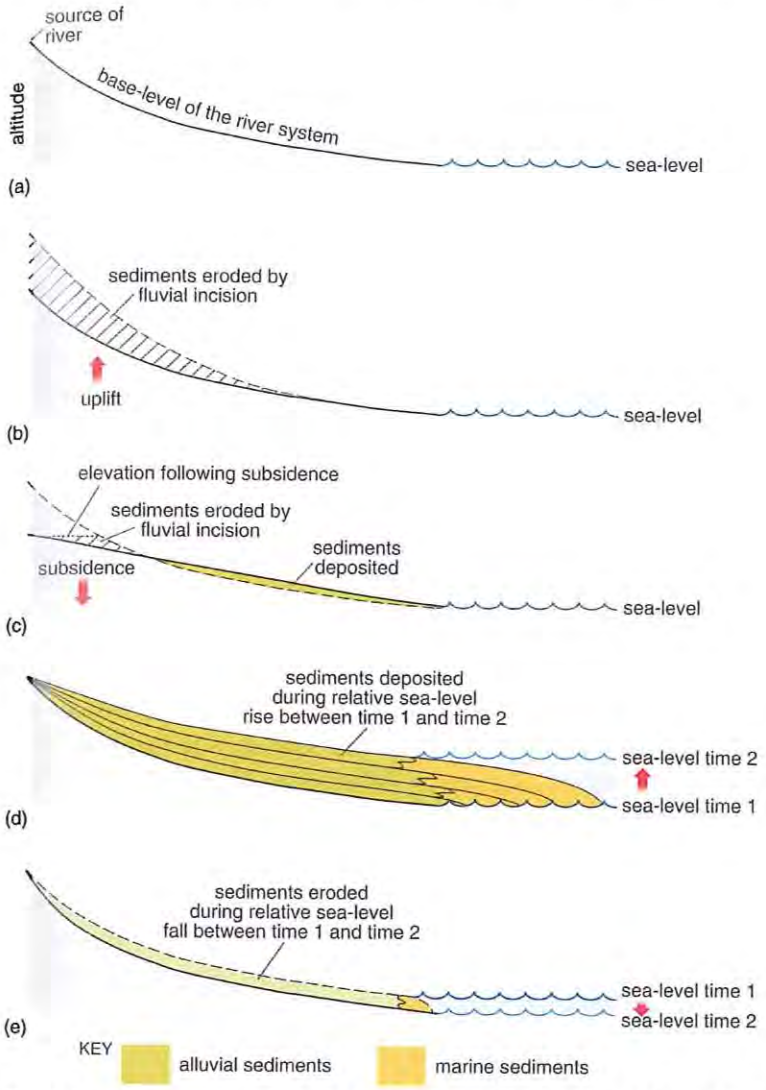

Figure 4.2 (a) The equilibrium profile of an alluvial system. In order to maintain the equilibrium profile, erosion or deposition of alluvial sediments will take place if there is a relative sea-level change and/or tectonic movement in the source area. (b) Erosion of sediments due to uplift of the source area. (c) Erosion and deposition of sediments along the alluvial profile due to subsidence of the source area. (d) Deposition of sediments due to a relative sea-level rise. (e) Erosion of sediments due to a relative sea-level fall.

Figure 17. Sediment deposition and erosion responses to changing fluvial base levels due to relative sea level changes (Coe *et al*, 2002). Sea level rise causes deposition (seaward expansion of flood plains) and sea level fall cases erosion.

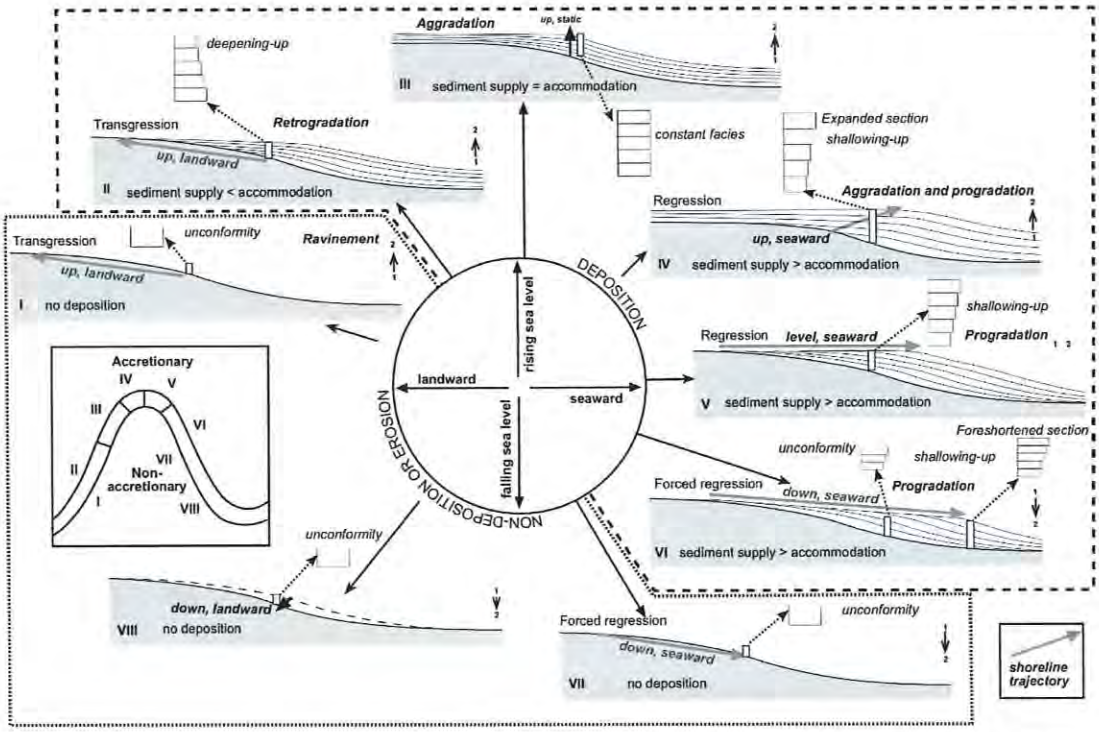

Fig. 23.3 The various possible patterns of sedimentation that can result from different relative amounts of sediment supply and relative sea-level change are summarised in this diagram. The responses to the different combinations are expressed in terms of vertical sedimentary successions, as seen in successions of strata in outcrop or boreholes, or as geometries seen in regional cross-sections or seismic reflection profiles expressed in terms of shoreline trajectories. Eight main scenarios (I–VIII) are recognised.

Figure 18. Summary of the sediment deposition and erosion consequences of different combinations of sediment supply and changes in relative sea level, resulting from the balance between available sediment volume and accommodation space (Nichols, 2009).

In terms of Figure 18, the situation for the Kāpiti coast corresponds to types II, III and IV depending on the sediment availability. North of Paraparaumu during the Holocene, there has been sufficient sediment supply to fill any accommodation space created, and the shoreline has accreted (Type IV). South of Paraparaumu, the sediment supply has reduced as the cuspate foreland has grown, so over time, this area has changed from Type IV to Type III and then possibly Type II (*viz.* Nolan, 2017) as the relative sea level has risen.

Jacobs (2021,2022) justify their assumption of reducing sediment supply as sea level rises with an outdated paradigm that claims that there was a rapid progradation of the shoreline due to a high influx of sediment at the end of post-glacial marine transgression (~120 m of sea level rise for the South Taranaki Bight). Since then, this paradigm assumes that sediment supply to the coast has decreased to essentially nothing in modern times (or the near future). Jacobs (2021,2022) suggests the initial high sediment supply was due to a sudden post-glacial outpouring from the catchments supplemented by onshore sediment movement from the submerged flood plains.

It should be noted again the Bruun Rule is an inundation model with a simple planar slope approximating the shoreline relief. What Jacobs (2022) has determined is the point in the future when the sea level on the imaginary slope is higher than the actual topography. Jacobs (2021) recognises that this approach is not suitable for assessing coastal inundation and uses a more appropriate methodology for their inundation assessment.

Considering their assumed paradigm of declining sediment availability during interglacials, it is now recognised that for New Zealand:

- Glacial conditions were colder, drier, and windier than present (Bostock et al, 2013; Lorrey et al, 2012), with the dominant palaeoenvironments and vegetation in the catchments of the South Taranaki Bight being shrubland-grassland with some beech forest and rare patches of conifers (Lorrey et al, 2012).
- Under these conditions, erosion rates in the catchments were high, generating a high sediment flux to the oceans (Carter et al., 2002). These conditions were associated with braided river systems.
- As conditions warmed from 15-9.5 ka, and vegetation cover increased, the sediment supply reduced. Offshore depocenters became increasingly mud dominated as coarser sediment was trapped closer to shore. Rivers start becoming entrenched into their flood plains as the base level rose and gradients decreased (Figure 17).
- Offshore sediment cores did not show any significant change in sediment supply beyond the continental shelf when sea level reached approximately present-day levels around 7.5-7 ka.
- Accretion of the shoreline around present-day sea level commences. Sedimentation occurs at a relatively steady rate (*viz*. Oliver et al., 2014), but as the prograding (accreting) shoreline moves into deeper water, the horizontal advance per unit volume of sediment added decreases.
- Ongoing pulses of sedimentation are associated with volcanic activity, earthquakes, and extreme storms (Carter et al., 2002).

Studies of the evolution of specific beach systems around New Zealand and Australia indicate that they have followed a trajectory of punctuated accretion (viz. Dougherty & Dickson, 2012; Dougherty, 2014; Oliver et al., 2014). In other words, there is an overall trend for accretion with episodic phases of retreat.

There is no evidence to support the assumption of declining sediment supply. In the future, it is possible that the rate of sea level rise may exceed the capacity for sediment supply to fill the increased accommodation space. For New Zealand, there are historical examples of abrupt relative sea level changes of up to 8 m due to seismic displacement, such as the Kaikoura Earthquake (2016). Although there have been examples of temporary erosion immediately after the event, in general, there has been progradation possibly aided by the temporary increase in sediment supply due to the earthquake. It is difficult to see how the much slower long-term rate of projected absolute sea level rise would exceed the rate of sediment supply for the Kāpiti Coast, although future climate changes may have some influence, as discussed below in Section 5.

4. Observations of Shoreline Change for the Kāpiti Coast District

The CSL database of shoreline changes used by de Lange (2013) was updated using Google Earth imagery to provide a quality control check on the DSAS analysis by Jacobs (2022), although it is recognised that there are significant uncertainties with the shoreline positions due to different types of measurements and criteria for defining the shoreline. These data cover a maximum period from 1870 to 2022 (up to 152 years). For the extension to the CSL database using Google Earth, the shoreline was taken as either the toe of the foredune, the

base of a dune scarp, or the base of a seawall. Distances from the CSL benchmarks were measured with the Google Earth Ruler tool. The resulting data were used to determine the overall pattern of long-term trends from the earliest data in the CSL database. For this analysis, the database was transferred to the statistical package R (https://www.r-project.org/) and analysed using routines written in R. These are available if required.

A more reliable set of shoreline-change data is provided by the Cuttriss Consultants Ltd surveys undertaken periodically for KCDC and used by John Lumsden to analyse shoreline changes. These data cover the period from June 2000 to November 2023 (approximately 23.5 years); their locations are indicated in Figure 19. The measured beach profiles were interpolated to a uniform 10 m cross-shore spacing and transferred to a database in R, which then was analysed using routines written in R. These are also available if required.

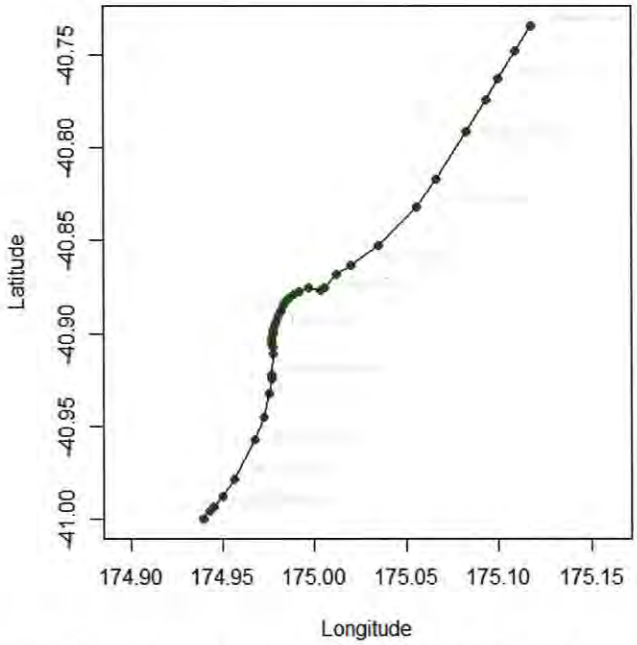

Figure 19. Locations of beach profiles surveyed by Cuttriss Consultants Ltd for KCDC. Also shown are the locations of rivers and streams.

Figure 20 shows the mean rate of change of the shoreline position ($m.y^{-1}$) for the extended CSL database. The pattern of shoreline changes is the same as when analysed by de Lange (2013), so it is reasonable to assume that the shorter Cuttriss Consultants Ltd database was not collected during a period when the shoreline behaviour was significantly different from the long-term historical trend.

The data displayed in Figure 20 show that most of the Kāpiti Coast shorelines are advancing or stable, with retreat predominantly occurring at Queen Elizabeth Park and around the Waikanae River mouth. The greatest observed shoreline changes occur at the Waikanae River mouth (retreat) and immediately south of the Otaki River mouth (advance), followed by the apex of the cuspate foreland (advance). These changes are consistent with the longer-term trends for the Holocene determined by Nolan (2017). It is generally accepted that the absolute (eustatic) sea level has been rising since 1870, and the measured relative sea level data for Wellington also indicate that it is possible that the relative sea level has been rising for the Kāpiti Coast since at least 1901. Therefore, it is reasonable to assume

that the long-term trends displayed in Figure 20 include any impacts of sea level rise. Since climate change is considered to have been occurring since ~1750 CE, the effects of climate change are also incorporated in the observations.

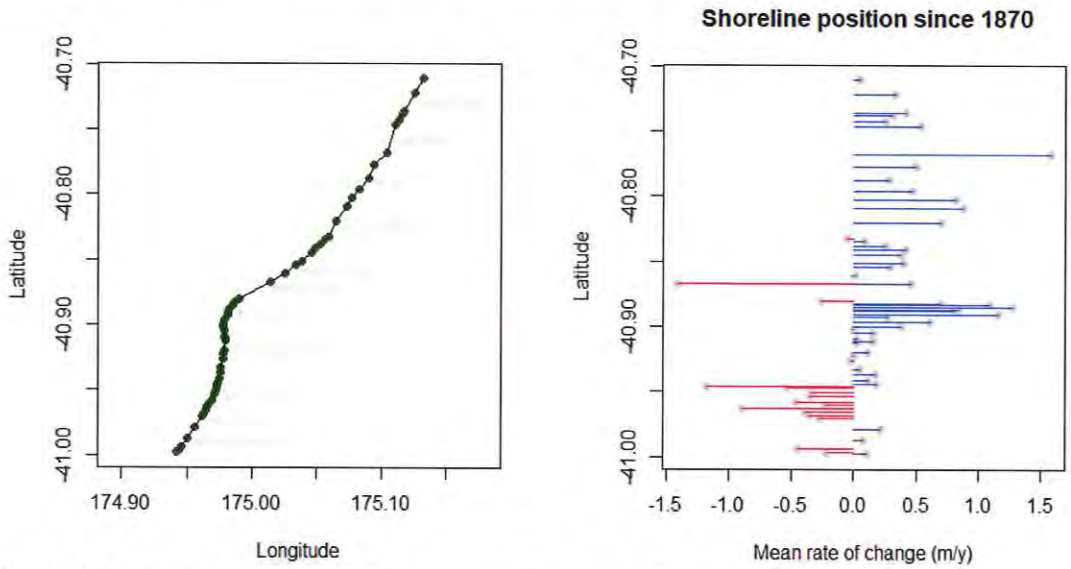

Figure 20. Summary of mean rates of shoreline position change for CSL sites since 1870.

Figure 21 shows the mean rate of change for the location of MHWS between June 2000 and November 2023. The pattern is the same as for the CSL data (Figure 20), allowing for the absence of beach profile sites in Queen Elizabeth Park. Therefore, it is reasonable to infer that there has not been any significant qualitative change in trends since 1870. Combining Figures 20 and 21 highlight that the areas vulnerable to coastal erosion are Queen Elizabeth Park and locations close to the Waikanae River.

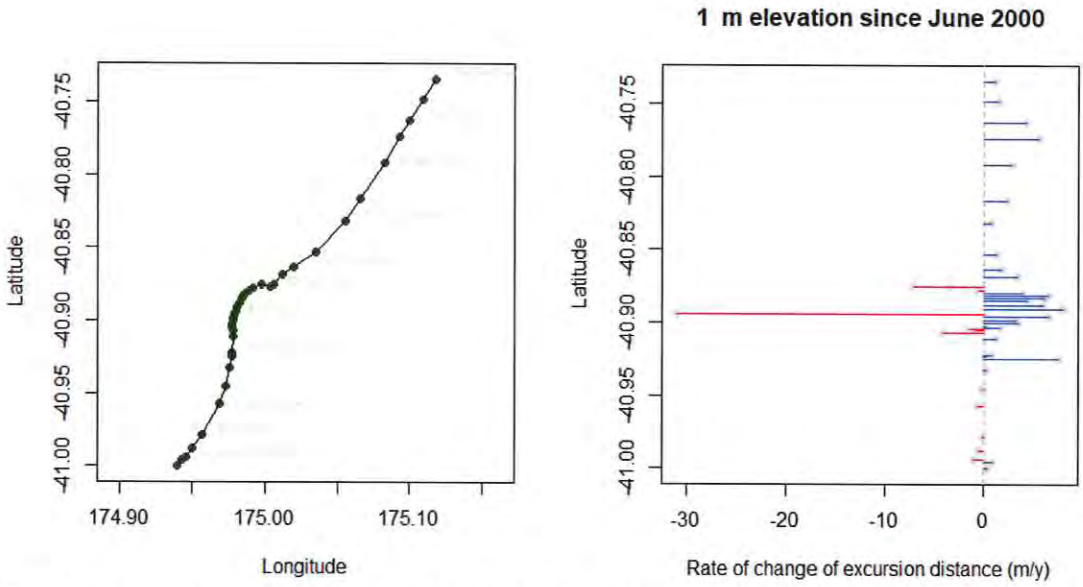

Figure 21. Summary of mean rates of MHWS position change for KCDC sites between June 2000 and November 2023.

Erosion adjacent to the Waikanae River is primarily in response to major floods breaching the spit across the river mouth (Figure 12). Spit breaching disrupts the longshore movement of sediment and provides a localised region of increased accommodation space that will accumulate sediment until the spit is reformed. This will temporarily reduce sediment transport to the south. The influence of the Waikanae River is evident in Figure 22, which shows the mean position of MLWS, MSL and MHWS for all the Cuttriss sites over the period June 2000 to November 2023. This figure shows that there is significant offshore movement of the MLWS position at P360) associated with a spit breaching event, followed by onshore movement as sediment accumulates. Some of this sediment is derived from continuing river erosion of the spit as the channel migrates southward, which is reflected in the landward movement of the MHWS position at P340.

Figure 23 displays the envelopes of beach profiles measured for sites P370, P360, P340 and P350 located along the section of coast from the Waikanae River mouth to the apex of the cuspate foreland at Kenakena Point (Figure 24). Site P370 is like most locations further north, with variations in the location of the base of the foredune, zones of increased variation associated with the formation and migration of offshore bars, and the formation and migration of a sand berm on the intertidal beach, in response to beach cut and fill cycles.

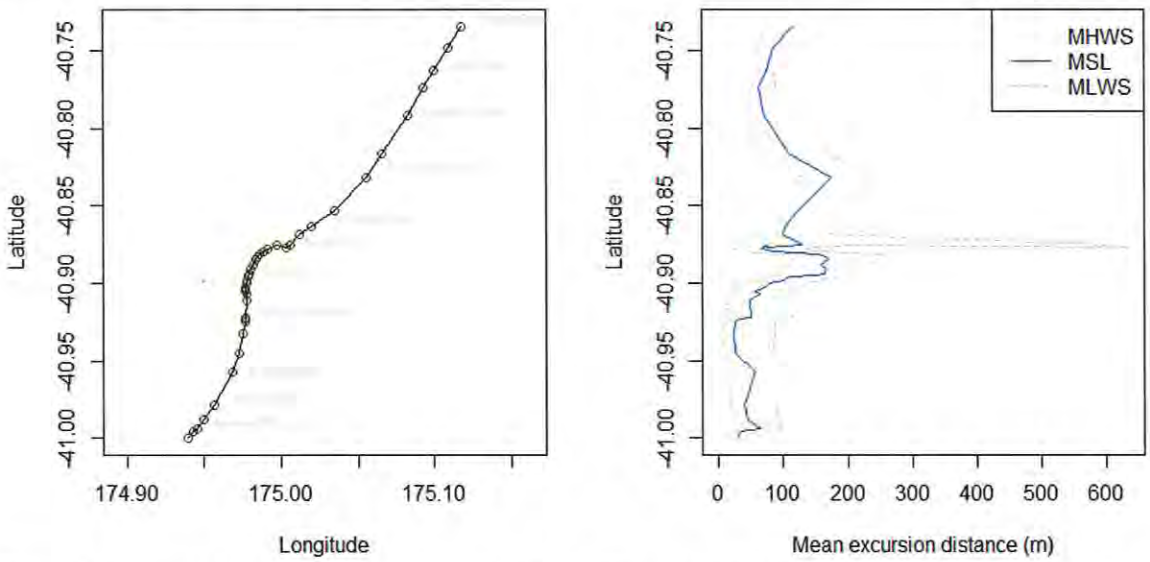

Figure 22. Summary of mean excursion distances for MLWS, MSL and MHWS for KCDC sites between June 2000 and November 2023.

Site P360 is located at the Waikanae River mouth and shows the loss of the sand spit due to spit breaching followed by the southward migration of the river, which is associated with accretion offshore followed by erosion as the sediment moves back onshore and alongshore. Figure 24 shows that overall, the Waikanae River doesn't contribute much sediment to the offshore area as no delta is present. However, sediment transported offshore by a spit breach may be contributing to the offshore shoaling area on either side of Kenakena Point (circular green patches with maximum elevations of 0.9 m above the chart datum). The link between spit breaching and large changes in the locations of MSL and MLWS on the beach profile is clear.

Profiles P350 and P340 are south of the Waikanae River and are affected by disruptions to longshore sediment transport by spit breaching at the Waikanae River. These profiles are

similar, so only site P340 is included. The effects of spit breaching are evidenced by the extent of movement at elevations from MSL to -1.5 m (indicated by the horizontal width of the profile envelope). Although the beach above MSL experienced episodes of erosion, overall, it is undergoing long-term accretion as indicated by the asymmetric distribution of the extremes and 95% confidence limits (larger gap from the median on the seaward side of the profile envelope). This pattern is evident for all the profiles in Figure 23 but is clearer for P340.

Profile P330 is located at the apex of the cuspate foreland (Kenakena Point). This profile has undergone accretion between June 2000 and November 2023, which is most evident in the growth of the foredune. The other obvious feature of this location is the rapid increase in depth, around 470 m offshore from the start of the profile. This is also clear in Figure 24, which also shows the rapid drop from the beach system into the Rauoterangi Channel. The narrow width means that there is a high likelihood that sediment moved offshore during storm erosion will drop below the closure depth (offshore extent of the beach) and be unable to be transported back to the shoreline. This was previously suggested as a cause of erosion further south by Gibb (1978a).

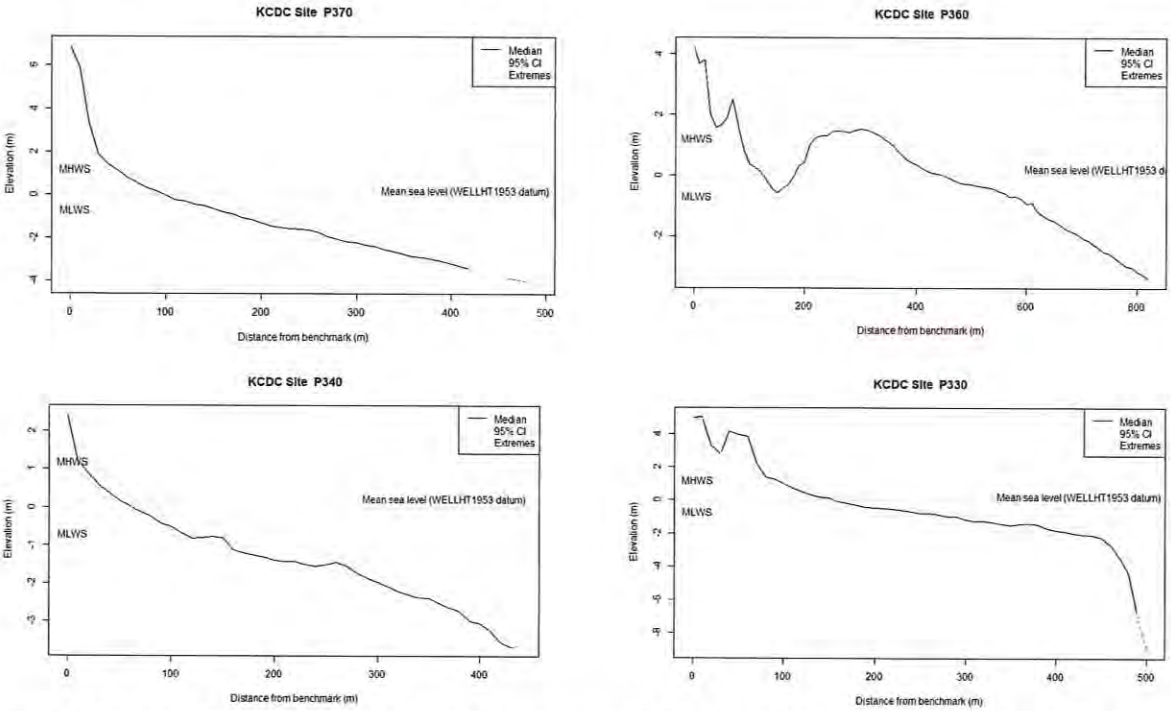

Figure 23. Beach profile envelopes for a north to south sequence of KCDC sites (P370, P360, P340, & P330) near the Waikanae River mouth. The median, minimum and maximum profiles, and 95% confidence limits are shown for all available surveys between June 2000 and November 2023. The locations of these sites are shown in Figure 24.

The rates of change in Figures 20 and 21 were calculated as the ratios of movement to elapsed time between successive surveys. The trends for the changing positions of the shoreline, MHWS, MSL, MLWS and 3 m depth contour were also determined using ordinary least squares (OLS), generalised least squares (GLS) and singular spectrum analysis (SSA) methods. GLS fits a linear trend to data and is intended for data that may be correlated and/or have unequal variances. The time series of changing coastal positions are serially autocorrelated as the next position is dependent on the current position and may also involve changing variances over time to natural climate variability and climate change. OLS

was used by Jacobs (2021, 2022) and does not account for these issues. The base R routines were used for OLS analysis, and the non-linear mixed effects R package *nmle* was used for GLS analysis. Since Jacobs (2021, 2022) also used the end-point method (linear trend between the first and last survey points), the end-point rate (EPR) was also calculated.

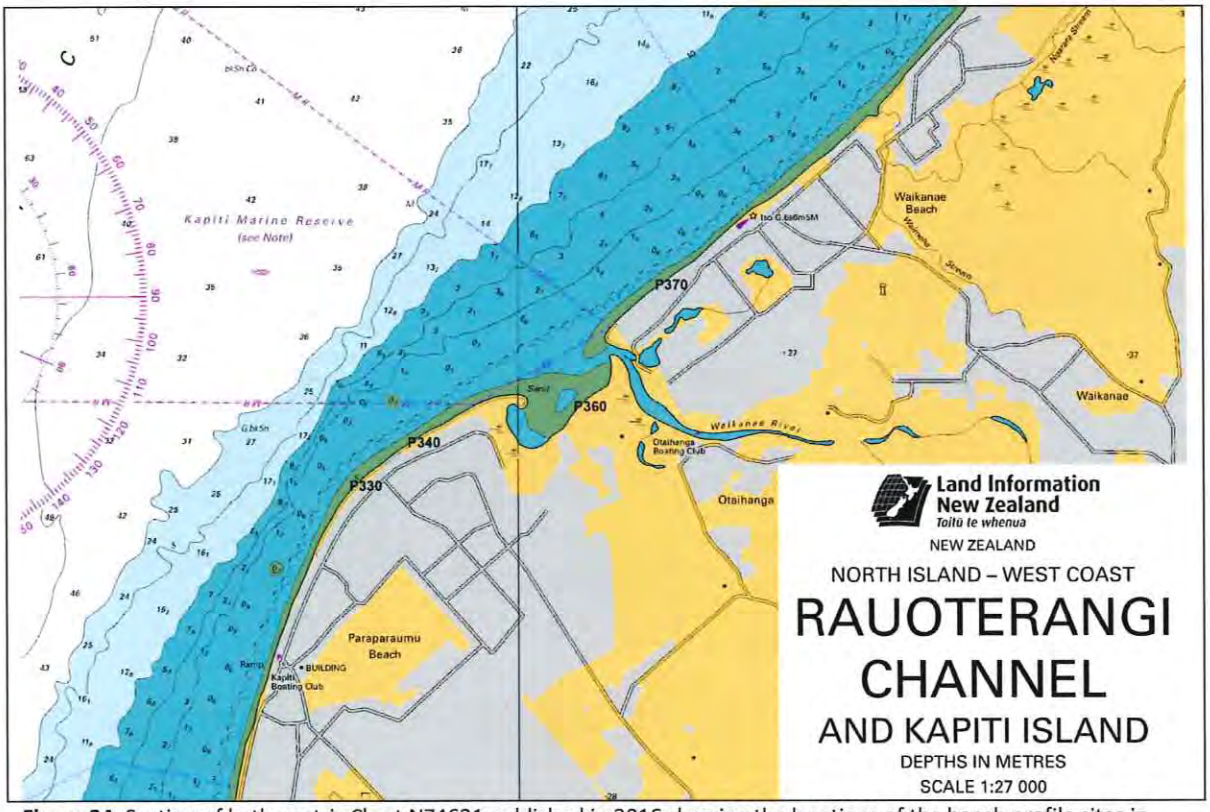

Figure 24. Section of bathymetric Chart NZ4631 published in 2016 showing the locations of the beach profile sites in Figure 23.

SSA is a non-linear technique used to decompose a time series into a set of periodic constituents, identify the dominant constituents, and use these to forecast future values. It is often used for time series data that may involve a climate influence. The R package *Rssa* was used for this analysis.

Figure 25 compares the trends predicted by OLS and GLS for the positions of MSL and the 3 m depth contours for all sites with sufficient data. Although the pattern of advancing and retreating along the Kāpiti Coast is very similar for both methods, the estimated rates differ. This means that predicting future positions will depend on the methodology used to establish the underlying trend. Figure 26 shows the trends calculated by Jacobs (2022) using the end-point method and OLS (referred to as EPR and LRR in their report). Although the pattern along the Kāpiti Coast is similar, the values differ, with no predictable relationship between the two.

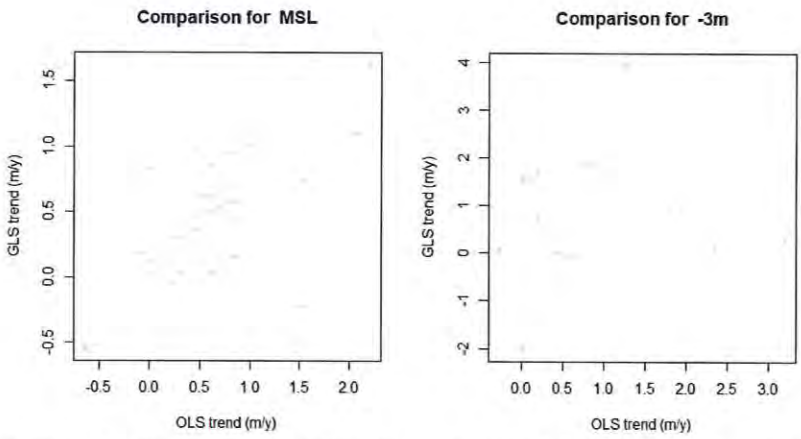

Figure 25. Comparisons of the trends from June 2000 to November 2023 for the MSL (left) and 3 m depth (right) positions using OLS and GLS methods.

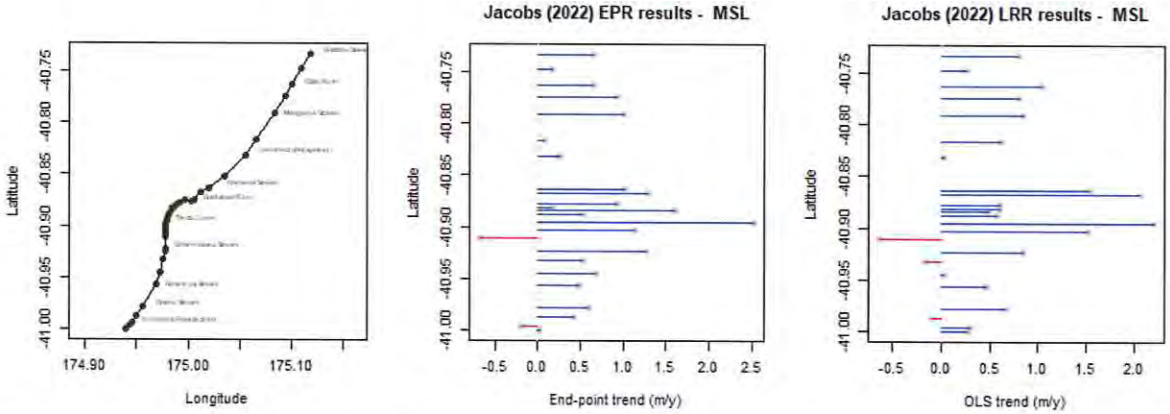

Figure 26. Comparisons of the trends for MSL determined by the end-point method (centre) and OLS method (right) by Jacobs (2022).

Since the shoreline position time series is serially autocorrelated and may be non-stationary due to climate change, GLS is more appropriate than OLS or the end-point method. However, the differences between predictions based on OLS and GLS trends only become more significant than the uncertainties at greater than 15-25 years in the future.

Figure 27 shows the fitted GLS trends for the MSL and 3 m depth positions for all available beach profiles between June 2000 and November 2023. The Residual Standard Error (RSE) is a measure of how well the trend fits the data, with smaller values indicating a better fit. It provides an estimate of the fit with the same units as the observations. The alternative commonly used for OLS is the coefficient of determination (r^2), which is a measure of the proportion of the variance of the observations explained by the fitted statistical model (a straight line in the case of OLS). It does not have units, so it is harder to assess in terms of the uncertainty of the trend.

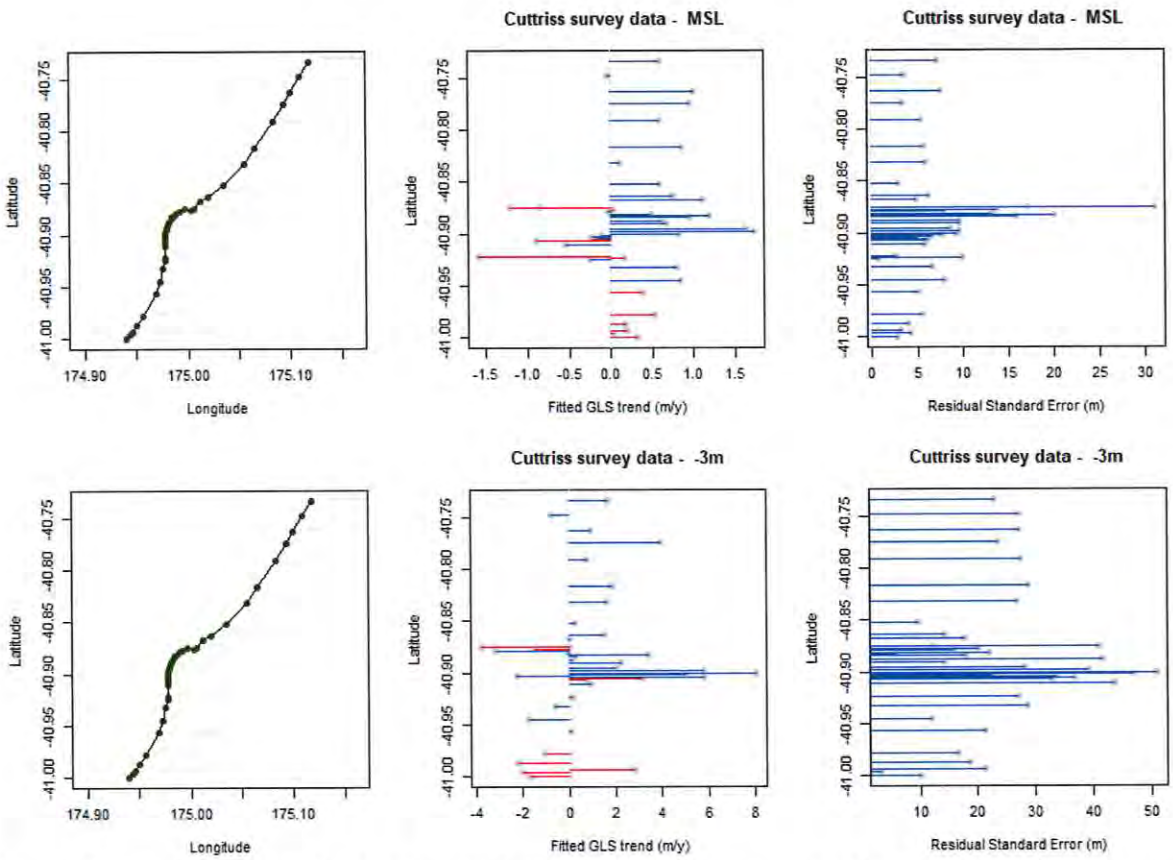

Figure 27. Fitted GLS trends and Residual Standard Errors for MSL and 3 m positions for KCDC site beach profiles between June 2000 and November 2023.

Figure 28 shows the MSL excursion distances for the sites close to the Waikanae River mouth shown as profile envelopes in Figure 23. The GSL trend is also plotted for each site, and there is considerable scatter about the trend for most profiles. Further, some sites show a time-dependent variation in the residuals (vertical distance between the observations and the trend line), such as P340. For these sites, this is caused by the spit breaching and subsequent recovery. This behaviour also means that linear trends are not reliable predictors of future shoreline position.

John Lumsden, and subsequently Cuttriss Consultants Ltd, calculated unit beach volumes (profile area above a specific elevation multiplied by a 1 m unit width to derive a volume). This is a useful measure of the volume of sand available for transport at the specified location, and by determining volumes for different elevations it can provide a quantified estimate of the distribution of sand in the system. Generally, sediment in the surf zone is more mobile than in the rest of the system, and longshore sediment transport predominantly occurs within the surf zone.

Figure 29 shows the mean unit beach volumes above MLWS, MSL and MHWS for all KCDC sites between June 2000 and November 2023. The pattern along the Kāpiti coast is like the excursion distances in Figure 22. However, there are differences for the area south of the apex of the cuspate foreland (Kenakena Point). These are due to the seawalls protecting the high dunes formed by Marram around the start of the 20th Century and contributing to the loss of the subaerial beach.

Analysis of the trends for beach volume changes did not reveal any differences to the behaviour discussed above for excursion distances, so it will not be repeated here.

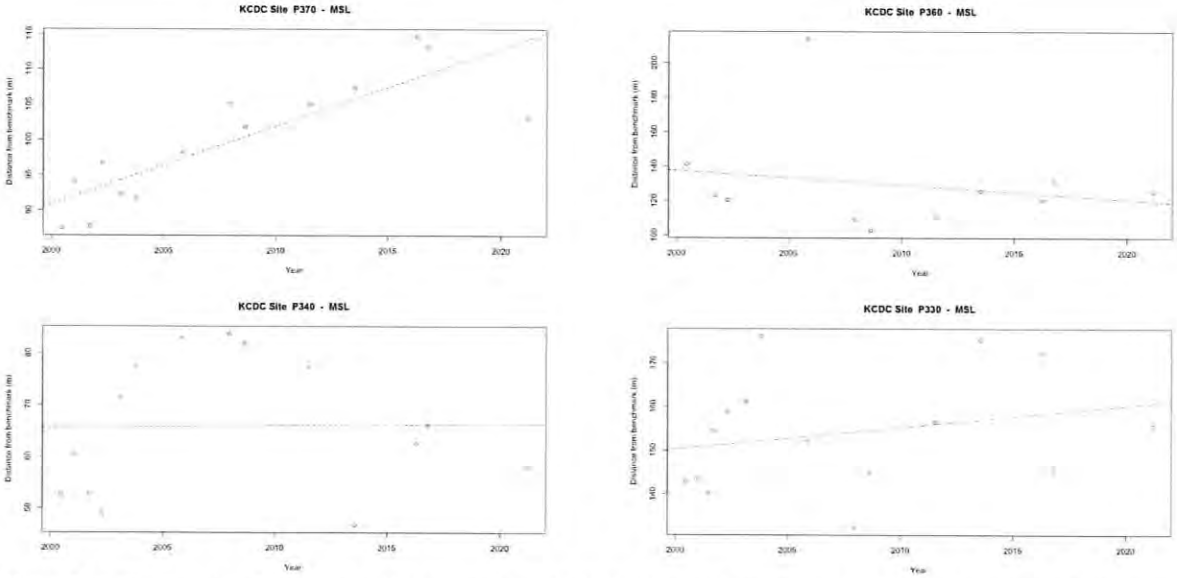

Figure 28. MSL excursion distances for KCDC sites P330, P340, P360 and P370 near the Waikanae River mouth between June 2000 and November 2023. The overall trend estimated by GLS is shown as a dashed line. The beach profile envelopes for these sites are shown in Figure 23 and their locations in Figure 24.

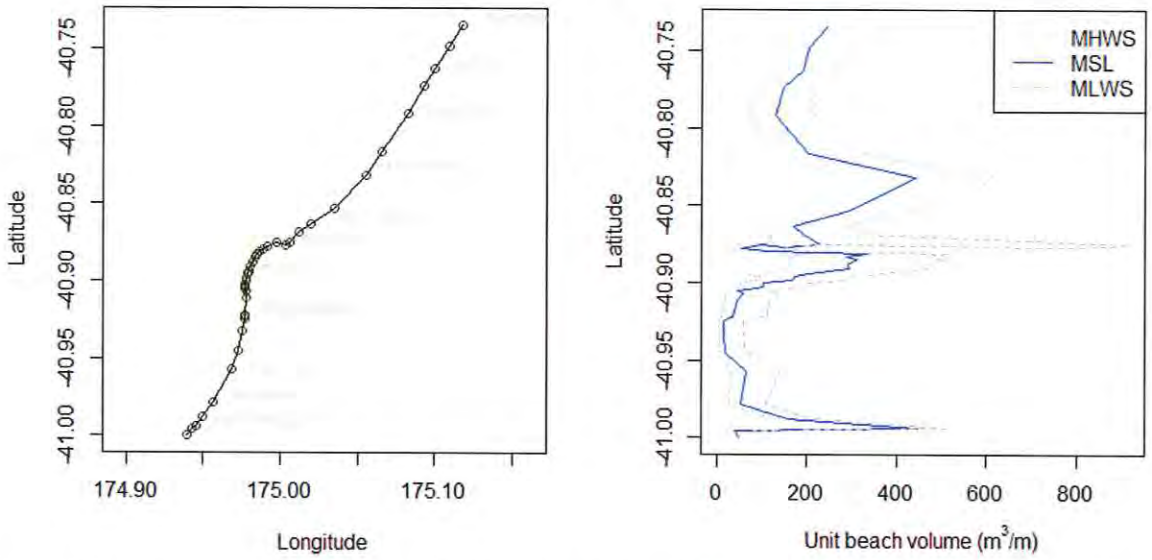

Figure 29. Mean volume per unit beach width ($m^3.m^{-1}$) above MLWS, MSL, and MHWS determined from the Cuttriss survey data for June 2000 to November 2023.

5. Future Shoreline Responses Changing Relative Sea Level and Climate.

With respect to historic and future shoreline changes for the Kāpiti Coast District, the main drivers are sediment supply, extreme weather events, and relative sea levels. Previous studies, including Jacobs (2021, 2022), have focussed on relative sea levels as the primary driver of their projections of future vulnerability. While this is reasonable for coastal inundation, coastal erosion is a consequence of severe weather events, which include flooding contributing to spit breaching, as discussed in Section 4.

Table 12.12 | Emergence of CIDs in different time periods, as assessed in this section. The colour corresponds to the confidence of the region with the highest confidence: white cells indicate where evidence is lacking or the signal is not present, leading to overall *low confidence* of an emerging signal.

Climatic Impact-driver Type	Climatic Impact-driver Category	Already Emerged in Historical Period	Emerging by 2050 at Least for RCP8.5/SSP5-8.5	Emerging Between 2050 and 2100 for at Least RC8.5/SSP5-8.5
Heat and Cold	Mean air temperature	1		
	Extreme heat	2	3	
	Cold spell	4	5	
	Frost			
Wet and Dry	Mean precipitation		6 / 7	
	River flood			
	Heavy precipitation and pluvial flood			8
	Landslide			
	Aridity			
	Hydrological drought			
	Agricultural and ecological drought			
	Fire weather			
Wind	Mean wind speed			
	Severe wind storm			
	Tropical cyclone			
	Sand and dust storm			
Snow and Ice	Snow, glacier and ice sheet		9	10
	Permafrost			
	Lake, river and sea ice	11		
	Heavy snowfall and ice storm			
	Hail			
	Snow avalanche			
Coastal	Relative sea level		12	
	Coastal flood			
	Coastal erosion			
Open Ocean	Mean ocean temperature			
	Marine heatwave			
	Ocean acidity			
	Ocean salinity	13		
	Dissolved oxygen	14		
Other	Air pollution weather			
	Atmospheric CO_2 at surface			
	Radiation at surface			

High confidence of decrease	Medium confidence of decrease	Low confidence in direction of change	Medium confidence of increase	High confidence of increase
~80%	~50%	< 10%	~50%	~80%

Figure 30. Table 12.12 from Ranasinghe et al (2021) – Chapter 12 IPCC AR6 WGI report

1. *High confidence* except over a few regions (Central North America and North-western South America) where there is *low agreement* across observation datasets.
2. *High confidence* in tropical regions where observations allow trend estimation and in most regions in the mid-latitudes, *medium confidence* elsewhere. 3. *High confidence* in all land regions.
4. Emergence in Australia, Africa and most of Northern South America where observations allow trend estimation.
5. Emergence in other regions.
6. Increase in most northern mid-latitudes, Siberia, Arctic regions by mid-century, others later in the century.
7. Decrease in the Mediterranean area, Southern Africa, South-west Australia.
8. Northern Europe, Northern Asia and East Asia under RCP8.5 and not in low-end scenarios.
9. Europe, Eastern and Western North America (snow).
10. Arctic (snow).
11. Arctic sea ice only.
12. Everywhere except West Antarctica under RCP8.5.
13. With varying area fraction depending on basin.
14. Pacific and Southern oceans then many other regions by 2050.

Ranasinghe et al. (2021) assessed the available information on climate change for the purpose of risk assessment (Chapter 12 IPCC AR6 WGI report). This included consideration

of a variety of climate impact drivers if they already had a quantifiable impact and estimated when quantifiable impacts could be detected, assuming the worst case RCP8.5/SSP5-8.5 scenario (Figure 30). Two time periods were considered: by 2050 CE and between 2050-2100 CE. Considering drivers of hazards related to vulnerability along the Kāpiti Coast (discussed in Section 2.1), they report no quantifiable evidence of climate change impacts that have emerged globally at the time of writing. By 2050 CE, they predict that there may be evidence of accelerated relative sea level rise (medium confidence (50% chance) and no other changes affecting New Zealand. For the remainder of the 21st Century, they predict acceleration of sea level rise (medium confidence) and an increase in mean precipitation (high confidence 80% chance).This suggests that the aspects of climate change that should be considered for a vulnerability or hazard assessment by KCDC are relative sea level rise and an increase in mean rainfall. Extreme weather responses to climate change impacts are not predicted to be an issue according to Ranasinghe et al (2021). Future changes to relative sea level will be considered first for Kāpiti Coast, although, as discussed above, sediment supply appears to be the main factor associated with the evolution of the cuspate foreland and shoreline.

5.1 Historic Sea Level Change

The best method for determining long-term local sea level changes at the coast is the deployment of tide gauges and co-located GNSS networks, while remote sensing satellite systems are more useful for assessing contemporary global and regional patterns (Abedisi et al., 2021). Tide gauges measure relative sea level, which includes any effects due to vertical land movement (VLM). Co-located GNSS data allows the determination of VLM at the site and, hence, the estimation of the underlying absolute sea level. The longest relative sea level time series available are typically from tide gauges with limited VLM observations. This is true for New Zealand, and the long-term records from New Zealand are a significant component of estimated sea level rise for the Southern Hemisphere, where there are limited records available (Figure 31). These tide gauge data are the best available for assessing historical sea level changes for the Kāpiti Coast.

Relative sea level has been measured at ports around the New Zealand coast since the 1890s. The data for some ports are available online from organisations interested in global sea levels. Unfortunately, although the data in the repositories are all ultimately derived from the same source, the record lengths available may differ, and the data may be adjusted in different ways so that analyses of sea level changes can give different results depending on the specific dataset used. For this discussion, the dataset maintained by Toitū Te Whenua (Land Information New Zealand (LINZ)) for annual mean relative sea level measured at 7 ports around New Zealand is used as provided online at https://www.linz.govt.nz/products-services/data/types-linz-data/sea-level-data/sea-level-data-downloads. These data are a combination of older measurements made by ports and present-day tide gauge installations managed by LINZ that are linked to cGPS stations to determine vertical land movements. Usually, 2 tide gauges in close proximity are operated by LINZ to maximise data recovery. LINZ also provides documentation summarising all the adjustments made to the raw data obtained. The documentation for the data used for this analysis was last updated between 14-18 November 2022 for all sites except Moturiki, which was updated on 16 February 2023.

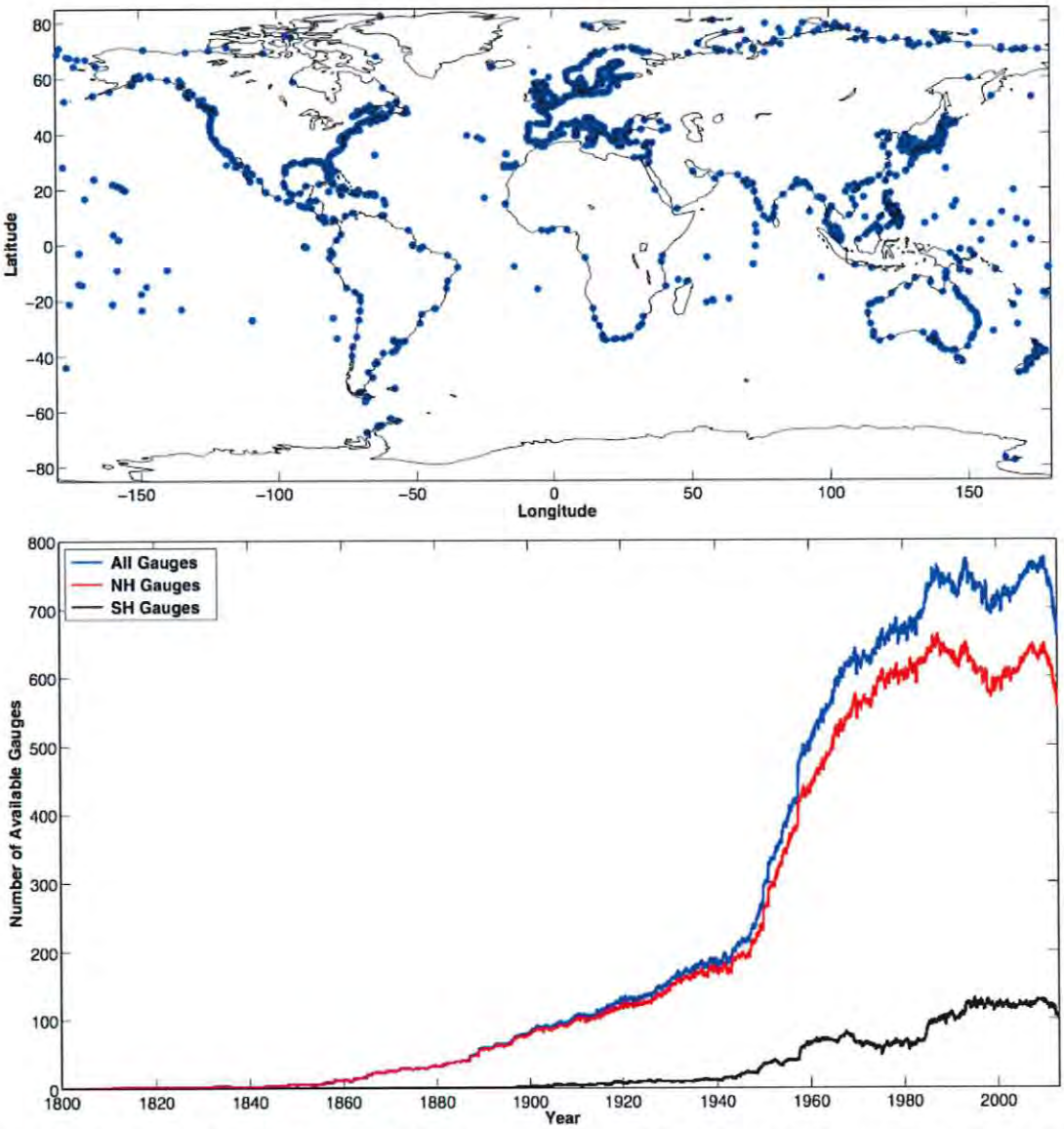

Figure 31. (Top) Spatial distribution of the 1420 tide gauges in the PSMSL RLR dataset. (Bottom) Number of available tide gauges in the PSMSL RLR dataset through time globally (blue), in the Northern Hemisphere (red), and in the Southern Hemisphere (black). Figure from Hamlington (2022).

Figure 32 shows the time series of annual mean relative sea levels analysed. There are different datums used for each site, and the data have not been adjusted to a common datum. Considering the interannual variations in sea level displayed in Figure 31, it is evident that the east coast sites, including Wellington, show a consistent pattern, although their underlying trends vary. The two shorter west coast sites (Port Taranaki and Nelson) display also show a consistent pattern that differs from that on the east coast. The same difference between the west and east coasts is evident in satellite data, with sea levels in the Tasman Sea west of New Zealand behaving differently at interannual to decadal scales to the Pacific Ocean east of New Zealand (de Lange, 2010). NIWA previously collected sea level data from a gauge located on Kāpiti Island, but these data are not readily available. Published reports that include analyses of the Kāpiti tide gauge data indicate that the sea level trends can differ from those at Wellington (*viz.* Johnson et al., 2007). Therefore, it is

possible that sea level data for Wellington are not a reliable indicator of short-term relative sea level (inter-annual to inter-decadal scales) for the Kāpiti Coast.

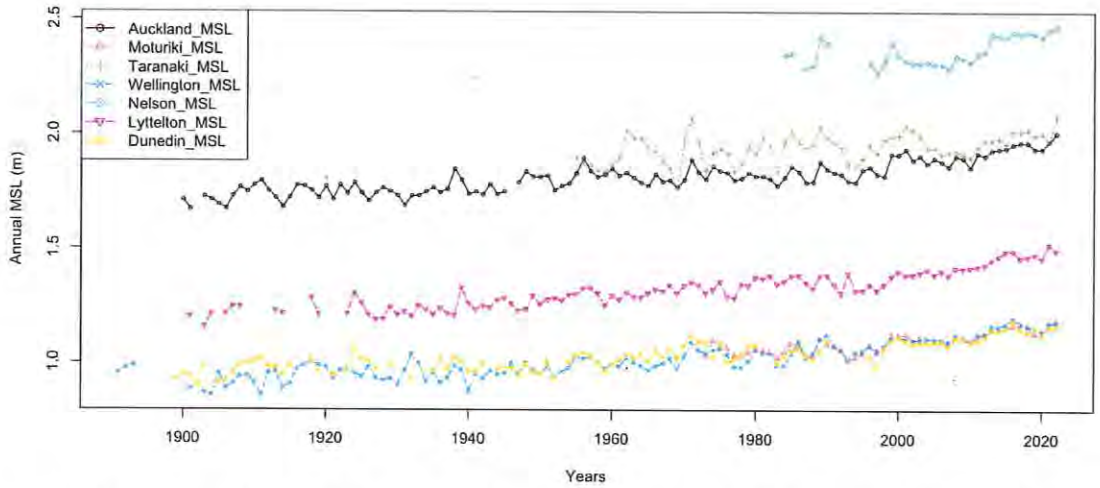

Figure 32. Time series of annual mean relative sea level for sites recorded by LINZ, which are predominantly located on the east coast of New Zealand. Data downloaded from https://www.linz.govt.nz/products-services/data/types-linz-data/sea-level-data/sea-level-data-downloads.

However, for long-term trends (>60 years), the behaviour of all ports in Figure 32 appears to be very similar. Given that Auckland and Wellington have long records available, these two ports will be used to assess relative sea level changes as an indication of what may have occurred for Kāpiti. Figure 33 shows the results of an analysis of the Auckland and Wellington relative sea level data plotted in Figure 32 using the R package *msltrend* developed by Watson (2016). This package uses Singular Spectrum Analysis (SSA) to determine the various constituents contributing to the observed sea level and can determine the instantaneous velocity and acceleration in sea level changes (Figure 33). The constituents determined by SSA can be used to forecast future sea levels. The reliability of the forecasts decreases with increasing time. For the Auckland and Wellington data, the forecasts appear to be reliable for 10-20 years into the future.

Figure 33 indicates that the overall behaviour of the two ports is similar, with both instantaneous velocity and acceleration showing the same broadscale patterns, albeit with different magnitudes and small-scale variations. This indicates that the difference in sea level trends between the two ports is primarily due to vertical land movement. This is most evident for the periods 1900-1930 (subsidence) and 2010-2020 (uplift) for Wellington. This analysis indicates that the rate of relative sea level rise increased at both ports since around 1980 to ~2.2 $mm.y^{-1}$ at Auckland and 3.0 $mm.y^{-1}$ at Wellington. Currently, it is not possible to determine if this is a change in the long-term trend or due to a combination of longer-period tidal constituents and medium-term sea level oscillations (up to 60 years duration). The acceleration results indicate that sea level rise is slowing at both ports, suggesting it is associated with longer period constituents, which peaked around 2016, and sea level oscillations.

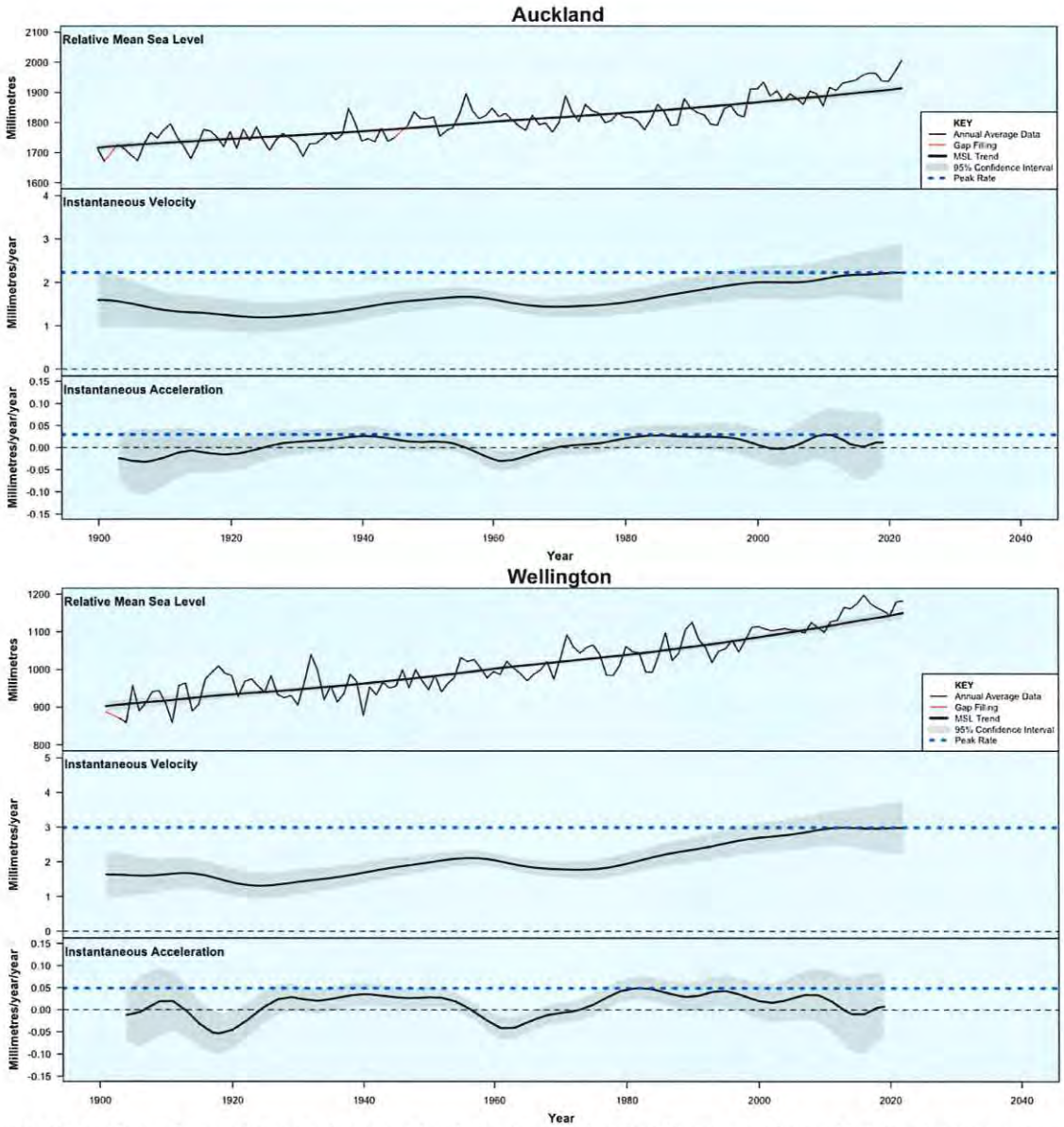

Figure 33. Analysis of annual mean relative sea levels for Auckland and Wellington performed by Singular Spectrum Analysis (SSA) using the R package *msltrend* developed by Watson (2016).

It is possible to assess if the observed sea level rise is consistent with climate change projections. Figure 33 shows the observed relative sea level at Wellington combined with the projected sea level rise by 2100 CE as predicted by the SeaRise online tool using the SSP5-8.5 scenario as recommended by MfE (2024) as a stress test. This approach uses 3.09 $mm.y^{-1}$ of subsidence at the tide gauge location (Queens Wharf) and the median projected scenario results (p50) to predict 1130 mm of relative sea level rise by 2100 CE. The R package *msltrend* was used to combine the SeaRise predicted sea level with the observed data and determine the instantaneous velocities and accelerations required to achieve that scenario (Figure 34).

Comparing the predicted instantaneous acceleration for 2005-2022 with that observed (Figure 33), it is clear that the required peak acceleration of 0.21 $mm.y^{-2}$ is much higher than the observed acceleration that had a peak value of 0.05 $mm.y^{-2}$ in 1982. Further, the required acceleration in 2019 was 0.07 $mm.y^{-2}$, while the observed acceleration was <0.01

mm.y^{-2}. The observed sea level changes at Wellington are not consistent with the SeaRise predictions, and lower observed acceleration indicates that the deviation between the SeaRise predictions and observations will continue to increase in the future.

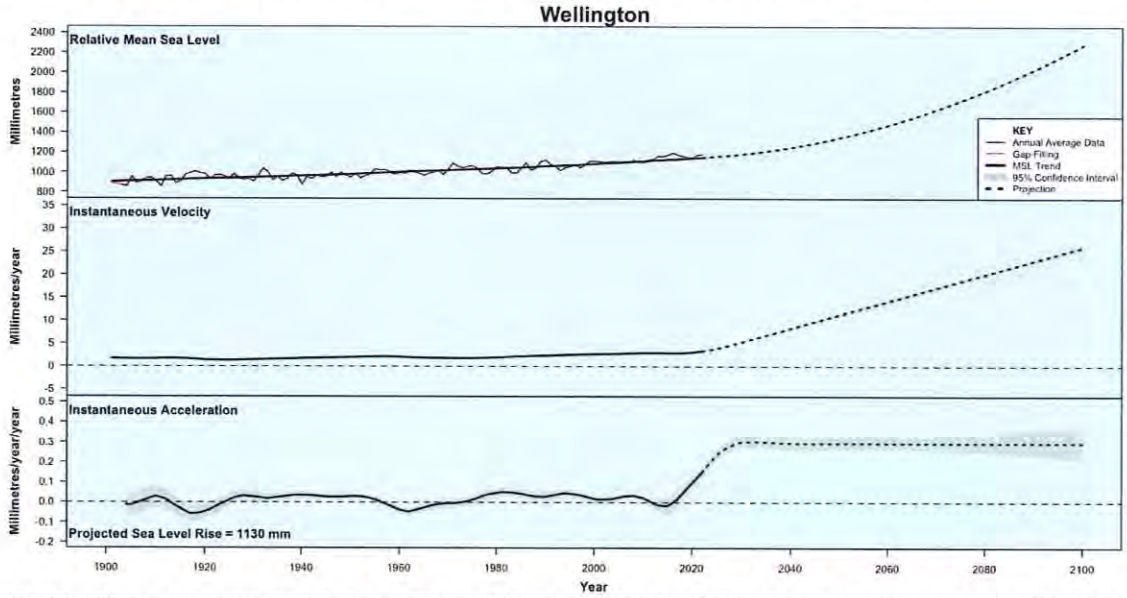

Figure 34. SSA analysis using the R package *msltrend* (Watson, 2016) for observed mean relative sea level at Wellington combined with a projected future relative sea level rise of 1130 mm by 2100 CE as determined by the SeaRise online tool for scenario SSP5-8.5 (p50) with -3.09 mm.y^{-1} vertical land movement.

Absent any evidence of sustained acceleration in the long-term trend of absolute sea level for New Zealand as determined by the analysis of Denys et al. (2020) and the *msltrend* analyses above for Wellington (Figures 33 & 34), the baseline scenario for future sea level along the Kāpiti Coast should be a continuation of the historical trend. Table 2 summarises the relative and absolute sea level trends for New Zealand ports from Denys et al. (2020).

Table 2. Summary of relative and absolute sea level trends, and record durations for port tide gauges analysed by Denys et al (2020) (Tables 2 & 6 therein). Also included is the average trend for New Zealand.

Site	Relative sea level (mm.y^{-1})	Absolute sea level (mm.y^{-1})	Record duration (y)
Auckland	+1.57 ± 0.15	+1.41 ± 0.18	113
New Plymouth	+1.46 ± 0.54	+1.42 ± 0.54	60
Wellington	+2.18 ± 0.17	+1.56 ± 0.36	115
Lyttelton	+1.91 ± 0.13	+1.64 ± 0.26	97
Dunedin	+1.35 ± 0.15	+1.21 ± 0.35	96
New Zealand average	+1.69 ± 0.28	+1.45 ± 0.36	

Denys et al. (2020) undertook a detailed analysis of a range of processes affecting vertical land movement, including major earthquakes, slow-slip events, glacial-isostasy, solid earth deformation, and local effects (consolidation, compaction, groundwater extraction, etc.). They identified 27 major earthquakes between 1855 and 2013 that affected the tide gauge sites in Table 2 through vertical and/or horizontal land movement. This included 9 events between August 2003 and August 2013, during the cGPS monitoring period used to determine underlying tectonic VLM and earthquake VLM for their analysis. The analysis of VLM using satellite InSAR data by Hamling et al. (2022) covered the period 2003-2011, which included 7 earthquakes affecting tide gauge sites in the South Island (Denys et al., 2020). The Wellington site was impacted by 2 earthquakes in 2013, immediately after the InSAR data period.

Considering the North Island sites in Table 2, the absolute sea level trends range from 1.41 ± 0.18 $mm.y^{-1}$ to +1.56 ± 0.36 $mm.y^{-1}$. The New Plymouth dataset is barely long enough to determine a long-term trend and perhaps should be ignored in preference for the longer datasets from Wellington and Auckland. However, it is the only site recording the trend for the west coast of New Zealand, which shows a different pattern of sea level changes to the east coast, as discussed above. Considering the rates at Auckland, New Plymouth and Wellington, in my opinion, the overall New Zealand average trend of 1.45 ± 0.36 $mm.y^{-1}$ is a reasonable *likely* estimate for the rate of absolute sea level rise for Kāpiti Coast until evidence of a sustained acceleration or deceleration is found from continued monitoring at existing port tide gauges and linked cGPS stations.

5.2 Future Sea Level Change

At a local scale, relative sea level is more important than absolute sea level. Historic relative sea level time series can be extrapolated to provide predictions with confidence limits using statistical models. Methods used include SSA, as shown in the previous section, for analysing historical sea level trends, Autoregressive Integrated Moving Average (ARIMA), Support Vector Regression (SVR), and Long Short-Term Memory (LTSM) Recurrent Neural Networks (RNN). Studies comparing forecasts with observations indicate predictive skill improves moving from statistical models (e.g. ARIMA) to machine learning (e.g. SVR) to deep learning (e.g. LTSM) (*viz.* Balogun & Abedisi, 2021). The difficulty with these approaches is that the forecast is limited to a relatively short period into the future, especially if the underlying process is not stationary (e.g. varies with changing climatic conditions). Apart from the effects of future climate changes, it is now recognised that the annual sea level cycle, which is driven mostly by seasonal changes, is non-stationary for many portions of the global coastline, including all of New Zealand (Bell & Goring, 1998; Barroso et al., 2024). This non-stationary variation accounts for a portion of the interannual fluctuations evident in Figures 32, 33 and 35. While this is accounted for in statistical models, it is not included in the process models used to project sea levels from projected future climate change.

Figure 35 shows a hindcast of the predicted sea level for 2012-2022 at Wellington based on an ARIMA AR(4) statistical model fitted to the observed relative sea levels for 1902-2011. This model predicts a fall in sea level due to a deceleration in the rate of sea level rise that began ~1980 (Figure 33). It failed to account for the change to more La Niña weather patterns that occurred ~1998, or the effects of earthquakes in 2013 and 2016, or the effects of slow slip events. It has included the effects of climate change as all the data used to develop the model were influenced by climate change (1902-2011). Despite the change to more frequent La Niña conditions, which increased MSL around New Zealand, especially north of Christchurch (de Lange, 2001), the observed sea level fell within the 95% confidence limits until the tide gauges were displaced by the effects of VLM.

The behaviour shown in Figure 35 illustrates some of the difficulties for forecasting future sea level:

- The uncertainties increase with time as shown by the increasing separation of the 95% confidence limits between 2002 and 2050. Also, the initial separation of the limits in 2002 is smaller than the interannual to decadal-scale variability evident in the observed sea levels from 1902-2001. This indicates that the estimated confidence limits are under-predicting the uncertainty.

- It is not possible to reliably predict episodic vertical land movement associated with earthquakes, slow slip events, or other processes.
- It is very difficult to account for unknown time-varying processes that affect absolute sea level.

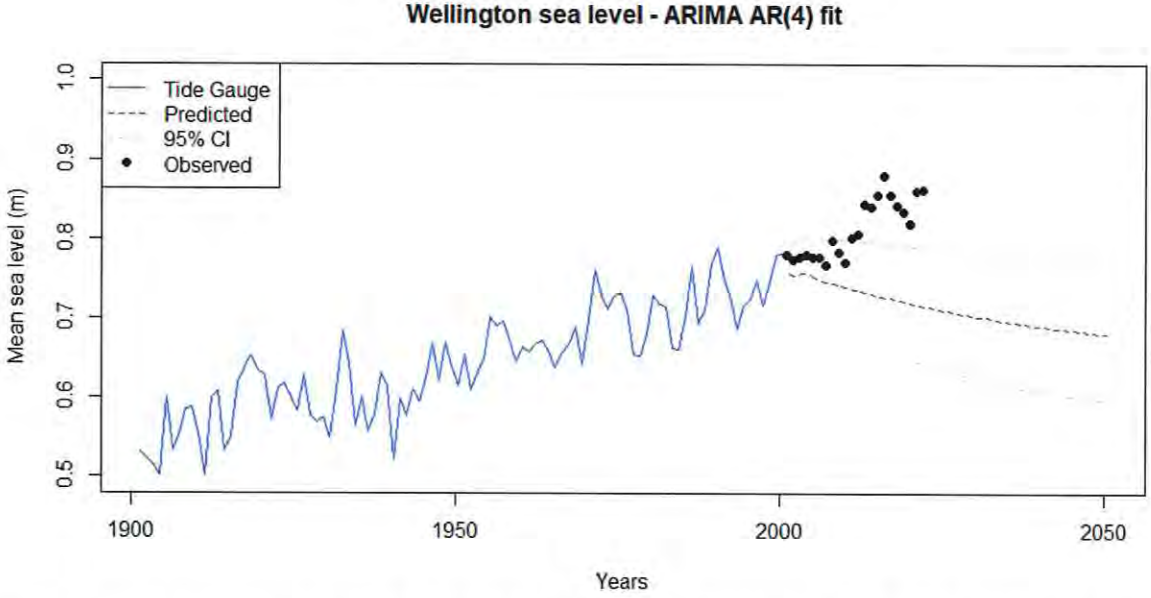

Figure 35. Forecast relative sea levels for Wellington from 2002-2052 derived from a ARIMA AR(4) model fitted to the measured relative sea levels from 1902-2001. The observed sea levels for the first decade of the forecast are also plotted.

The last two issues relate to the projections of future sea levels that MfE (2024) recommends. Before 2022, MfE publications providing guidance on coastal hazards to local government bodies (MfE, 2004; 2008; 2017) noted the rate of relative sea-level change around New Zealand was consistent with the global average rate of absolute sea-level change and did not specifically consider VLM. With the interim guidance on sea levels published in 2017 (MfE, 2017), it was indicated that for any specific location around the coast the VLM at that location should be combined with the absolute sea level projections to assess future sea level.

The 2017 guidance recommended using the online SeaRise tool (https://www.searise.nz/maps-2) to undertake this analysis, despite the disclaimer that required acceptance for access to the tool stating that it was not suitable for planning purposes. The disclaimer for planners on the website for 26 May 2024 had two sections that stated:

> *"The Antarctic Research Centre at Te Herenga Waka: Victoria University of Wellington (ARC), the Institute of Geological and Nuclear Sciences Limited (GNS Science), and the National Institute of Water & Atmospheric Limited (NIWA) have provided data on vertical land movement for this web map. The data was collected across the period from 2003 to 2011. It is an estimate only and subject to uncertainty. We make no representations or warranties as to the data and shall not be liable to any person who uses or relies on the data or this web map on any ground for any loss, damage or expense arising from such use or reliance.*

By clicking the 'Accept' button, you acknowledge you have read and accepted the terms of this disclaimer.

By using the Takiwā Data Analytics Platform, including viewing data on that platform, you agree to this disclaimer. Takiwā Data Analytics Platform is a SaaS tool that enables customers to visualise and present data in different formats and views. The data used on Takiwā Data Analytics Platform (which may contain opinions, representations, and advice) is supplied by customers or other third parties (including publicly available information). Where analysed data is made available on the Takiwā Data Analytics Platform, that analysis (and the determination of the algorithms, assumptions, and other methods used to conduct that analysis) is undertaken by customers or other third parties and not by Takiwā. You agree that Takiwā has no responsibility or liability for such data or for how that data has been analysed (including where the data or the analysis is incorrect, inaccurate, incomplete, or unsuitable for your purposes). To the maximum extent permitted by law, Takiwā disclaims all warranties, conditions, guarantees, and/or representations relating to such data and how that data has been analysed. Any reliance that you place on such data is at your own risk.

By clicking the 'Accept' button, you acknowledge you have read and accepted the terms of this disclaimer."

The guidance published in 2024 (MfE, 2024) amended the interim guidance to recommend that multiple lines of evidence be considered for relative sea level at any location, including the online SeaRise tool. The VLM and absolute sea-level components for future relative sea levels along the Kāpiti coast will be discussed separately below.

5.2.1 Future Vertical Land Movement

The prehistoric and historic VLM trends for Kāpiti Coast District were discussed in section 2.2.5 above and include the SeaRise locations where VLM trends and sea level projections are available (Figure 9). The VLM data used by SeaRise was estimated from InSAR and GNSS (cGPS) data between 2003 and 2011 and calculated as averages of 2 km spacings along the coast. It represents a subset of the original gridded data set developed by Hamling et al. (2020), from which coastal data were extracted at 1 km spacings. The 1 km data were then converted to 2 km spacings, and these are used by the SeaRise tool. The GNS server link provided by Hamling et al. (2020) gives access to the full gridded data for New Zealand and both the 1 km and 2 km datasets. The data for the Kāpiti coast were extracted from the 1 km and 2 km datasets, and they are plotted in Figure 36. It is unclear what the legend provided by the SeaRise tool represents (Figure 9), so the VLM data were binned into - 5 to - 3 $mm.y^{-1}$, -3 to -1 $mm.y^{-1}$, -1 to 0 $mm.y^{-1}$, 0 to 1 mm. y^{-1}, 1 to 3 $mm.y^{-1}$, and 3 to 5 $mm.y^{-1}$.

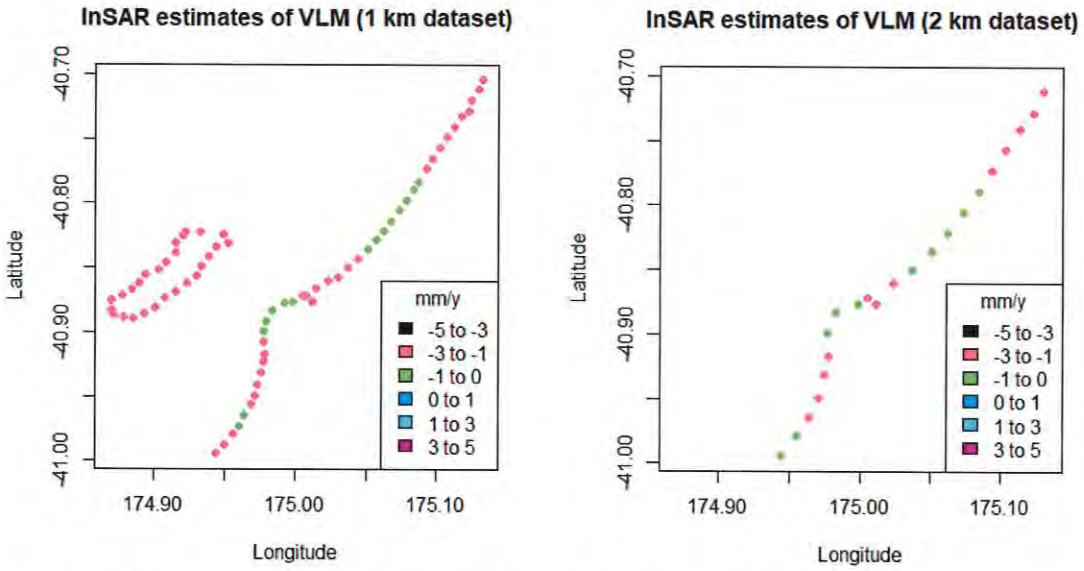

Figure 36. InSAR estimates of vertical land movement (VLM) for the Kāpiti Coast as determined by Hamling et al (2020) at 1 km (left) and 2 km (right) resolution. The 2 km dataset is used by the SeaRise online tool. Data were obtained from https://doi.org/10.21420/E1C1-MQ19.

Comparing the 1 km (left) and 2 km (right) rates of VLM in Figure 36, the most obvious difference is the omission of Kāpiti Island from the 2 km dataset. Although some islands are missing from the 1 km dataset, and so there were no data available for the SeaRise tool (https://www.searise.nz/faqs-1), the exclusion of Kāpiti Island is unexplained. The VLM rates for Kāpiti Island are very consistent and range from -1.275 to -1.300 mm.y^{-1} with a median of -1.293 mm.y^{-1}. Figure 7 shows a maximum rate between 2005 and 2023 of -3.86 mm.y^{-1} for the KAPT cGPS data, but the rate of VLM is highly variable at different time scales (Figure 7). Kāpiti Island VLM estimates are less likely to be affected by anthropic factors than the mainland coastline.

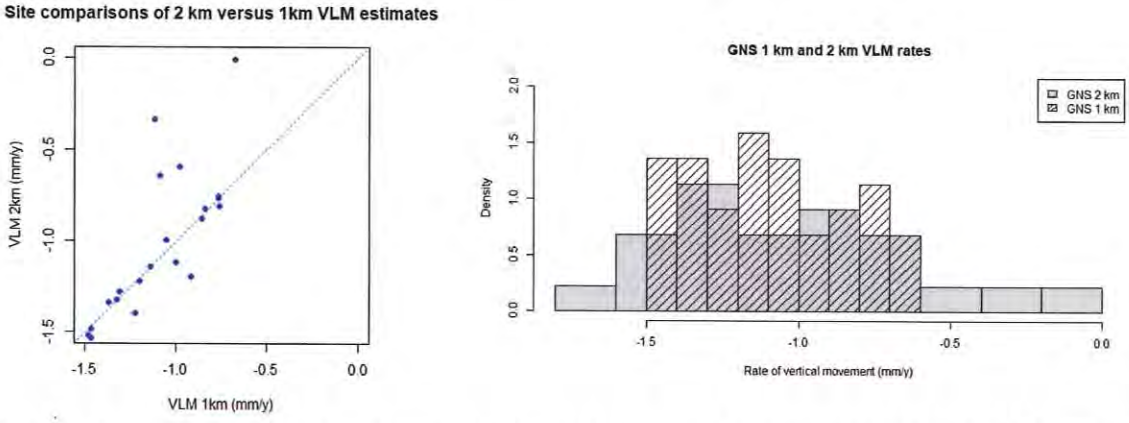

Figure 37. Comparison of the VLM rates estimated from InSAR observations for the Kāpiti Coast from the 1 km and 2 km GNS databases: (left) comparisons for SeaRise coastal sites at 2 km resolution, (right) comparisons of the distributions of the 1 km (cross-hatched) and 2 km (shaded) databases (shown as density, which is the proportion of the total sample, to allow for different numbers of data points (Figure 36).

The 1 km dataset also includes estimates of the uncertainty of the VLM rates, which is given as the standard deviation (1 sigma error) derived from the InSAR data used to estimate the mean rate between 2003 and 2011; the number of observations, a data quality factor, and the search radius used to select InSAR and GNSS data for estimating VLM at each coastal location. This information is not included in the 2 km dataset and is not visible on the SeaRise tool. Figure 38 shows the 1-km dataset estimates of the VLM rates for the Kāpiti Coast with the 1-sigma error. For most locations, the error range is quite large, and for 34% of the sites, the error range includes zero VLM. Taking the 2-sigma error range, all but the southernmost 3 sites include zero VLM. The southernmost 3 sites, including the PAEK GNSS station (Figure 7) within their search radius, have the lowest number of observations for the data plotted and poor-quality factors. Although their 1-sigma errors are very small, they are probably not reliable estimates (PAEK data indicates uplift, while the InSAR + GNSS analysis estimates subsidence).

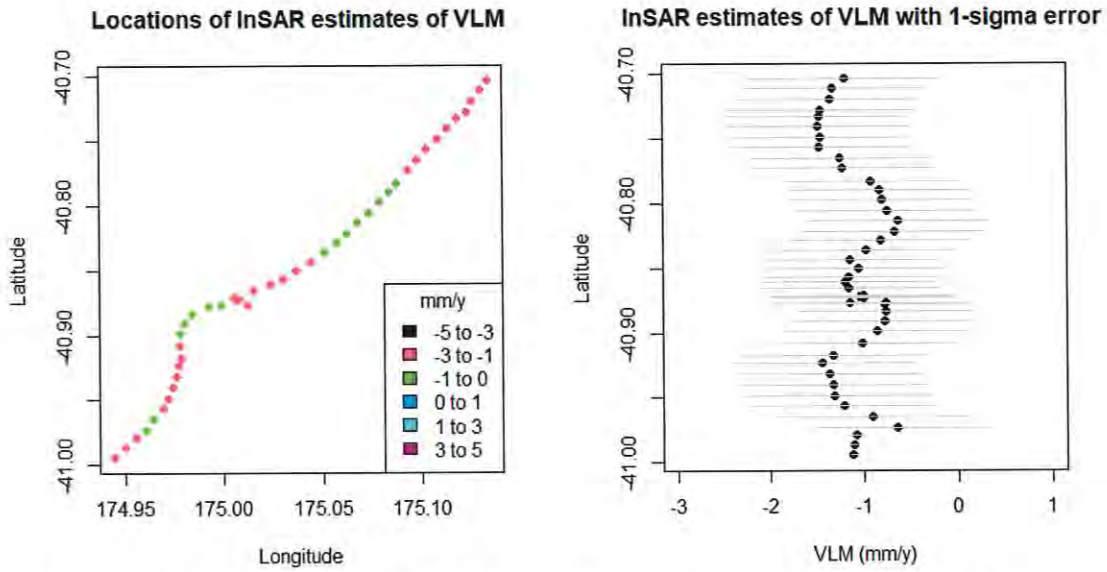

Figure 38. InSAR estimates of VLM for Kāpiti Coast from the 1 km GNS database, with the 1-sigma error.

Hamling et al. (2020) identified limitations in using their estimates to predict long-term VLM. In particular, they noted that:

> *"A major challenge for estimating the long-term VLM for New Zealand is its dynamic tectonic and volcanic setting. While the Envisat data presented here [their paper] spans a time period where New Zealand was relatively unaffected by earthquakes, areas of coastline are not stable through time. ... the majority of the east coast margin is currently experiencing subsidence of ~5 mm/yr but is largely a result of coupling along the plate interface. Assuming that in the future, there will be a rupture along the margin, this pattern of subsidence will likely be reversed, as was seen during the Kaikōura earthquake in 2016. There, the coastline was subsiding at rates of ~2–3 mm/yr but was uplifted by 3–10 m by the co-seismic deformation (Hamling et al., 2017), causing long-term changes to the coast."*

More recently, Naish et al. (2024) provided a long list of caveats that should be considered when extrapolating short-term InSAR estimates of VLM for long-term projections of relative

sea levels. Unfortunately, after demonstrating why they shouldn't use the data for their analysis, they proceeded to do so anyway.

Similarly, in my opinion, the limitations and caveats identified are valid, and the disclaimers on the SeaRise website should not be ignored. Overall, the VLM estimates used by SeaRise are a snapshot that illustrates the short-term variability of VLM around the New Zealand coast but is of little practical value for forecasting long-term trends.

The difficulty for the Kāpiti Coast is that there is little reliable information on past long-term trends, and the occurrence of episodic seismic events and slow slip events is unpredictable. In Section 6, an alternative approach is suggested to deal with this issue.

5.2.2 Future Absolute Sea Level

It has been recognised for several decades that predicting future relative sea levels is difficult due to non-stationary distributions for the underlying processes (Stewart et al, 1990). Prediction of future extreme sea levels, including storm surges and other processes, requires assessing the effects of non-stationarity (*viz.* Bardsley et al. 1990; Hunter, 2010), which is not done by the methodology recommended by MfE guidance (MfE, 2017). Prediction is further complicated by the uncertainties associated with the forecasting of future climatic conditions that may contribute to changes in absolute sea level.

The unknown time-varying processes that alter the processes affecting absolute sea level are also the principal reason that shoreline change models cannot reliably predict more than 20-30 years into the future (Coco et al., 2020) and is recognised as an issue for weather and climate prediction (Parker, 2010). While ensemble modelling allows forecasting the short to medium future with a reasonable degree of certainty for shoreline change and weather, it is not a useful approach for climate forecasting (Parker, 2010) that is necessary to forecast future absolute sea levels.

Recognition of this problem by climate modellers resulted in the adoption of scenarios and pathways to facilitate projecting future climate (e.g. Wigley & Taper, 1992; IPCC, 2000; Ward et al., 2011; Pirani et al., 2024). Mathews et al. (2021) define a scenario as used by the IPCC AR6 as:

> *"A plausible description of how the future may develop based on a coherent and internally consistent set of assumptions about key driving forces (e.g., rate of technological change, prices) and relationships. Note that scenarios are neither predictions nor forecasts, but are used to provide a view of the implications of developments and actions".*

They also define pathways as:

> *"The temporal evolution of natural and/or human systems towards a future state. Pathway concepts range from sets of quantitative and qualitative scenarios or narratives of potential futures to solution-oriented decision-making processes to achieve desirable societal goals. Pathway approaches typically focus on biophysical, techno-economic, and/or socio-behavioural trajectories and involve various dynamics, goals, and actors across different scales".*

Although these were defined in the IPCC glossary, the IPCC working groups used them interchangeably and did not use them consistently (Meinshausen, 2024; Pirani, 2024).

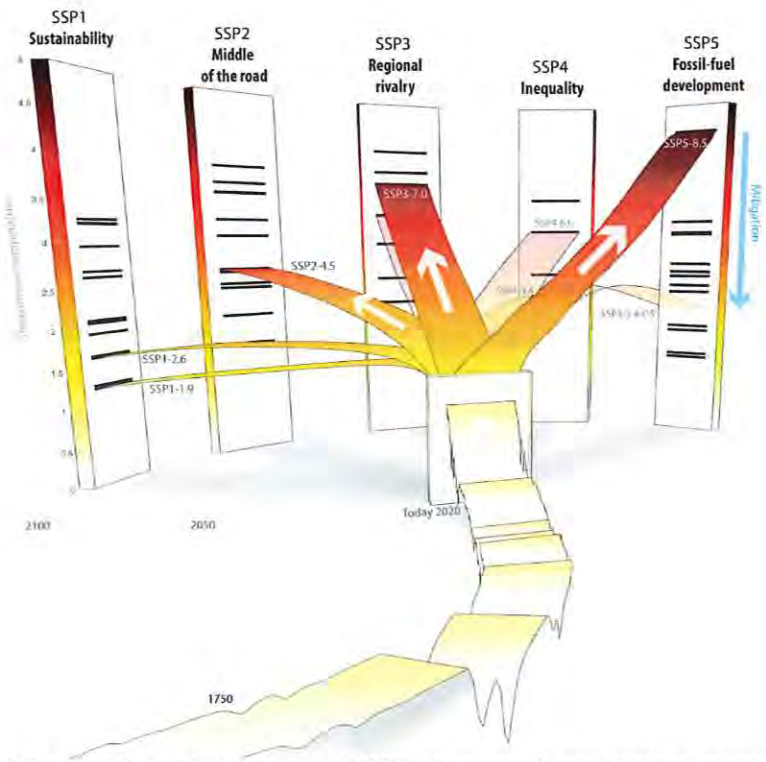

Figure 39. Figure 1 from Meinshausen et al (2020) illustrating the temperature ranges associated with the 5 families of socio-economic scenarios used by IPCC AR6. See text for further explanation.

Strictly as defined above, the scenarios and pathways have no likelihood and no uncertainties. However, as is evident from the IPCC AR6 reports and the underpinning literature, authors do express opinions about the relative likelihoods and recognise that there are uncertainties, particularly for some types of pathways, such as the *framing climate pathways* in the AR5 and AR6 reports (Meinshausen et al., 2020; Meinshausen et al., 2024). Essentially, the scenario reflects a specific objective or condition (e.g. 8.5 $W.m^{-2}$ of additional radiative forcing), and the pathways represent different combinations of factors that may produce the scenario outcome (Meinshausen et al., 2024). In practice, the likelihood of a projected climate outcome can be assessed as the combination of how plausible the scenario is, and the number of pathways that produce the outcome. The uncertainty is difficult to define as the necessary data are generally not available.

Figure 39 shows the five socio-economic SSP families used for climate projections by IPCC AR6. Shown are illustrative temperature levels relative to pre-industrial levels with historical temperatures (front band), current (2020) temperatures (small block in the middle), and the branching of the respective scenarios over the 21st century for the five different socio-economic scenarios. The small black horizontal bars on the 2100 pillars for each SSP indicate illustrative temperature levels for the range of SSP scenarios that were available at the time of creating the benchmark SSP scenarios. The labelled opaquer bands over the 21st century from 2020 indicate the five SSP scenarios SSP1-1.9, SSP1-2.6, SSP2-4.5, SSP3-7.0, and SSP5-8.5 that are used as priority scenarios in IPCC AR6. The more transparent bands indicate the remaining "Tier 2" SSP scenarios, namely SSP3-7.0-LowNTCF, SSP4-3.4, SSP4-6.0, and SSP5-3.4-OS.

The blue indicative arrow on the right side indicates the effect of mitigation action on SSP5, which reduces temperature levels in 2100 and throughout the 21st century – depending on the respective reference scenario and level of mitigation. The lowest level of the blue arrow corresponds to the SSP5-3.4-OS scenario, which involves an overshoot pathway where the radiative forcing target is exceeded for a period before dropping to the target before 2100 CE (Mathews et al., 2021). This scenario assumes net-zero is achieved by 2080 and that bio-sequestration of CO_2 continues (Melnikova et al., 2021), while the upper SSP5-8.5 scenario assumes no policy implementation and no sequestration of CO2 by biological carbon sinks. These SSP5 scenarios are intended to bracket plausible future trends.

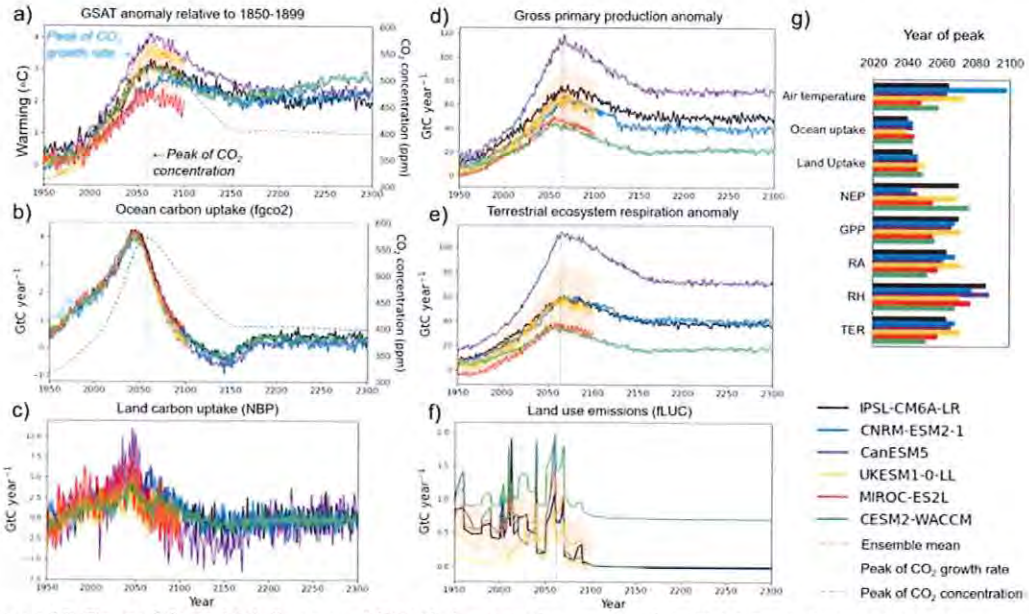

Figure 40. Figure 2 from Melnikova et al (2021) showing the results of six CMIP Earth System Models projecting future conditions for the SSP5-3.4-OS Overshoot Pathway.

Figure 41 shows the spread of CMIP6 model projected mean global surface temperature anomalies for the opaque pathways in Figure 39 as plotted by Hausfather et al. (2022), where 95% uncertainty ranges correspond to 95% of the model projections (dashed thin lines = all CMIP6 models, solid thin lines = excluding "too hot" CMIP models). Also shown in Figure 41 are the ranges of IPCC AR6 best estimates (solid thick lines), referred to as "assessed global warming" in the AR6 WG1 report (IPCC, 2021).

Assessed global warming combines model projections with other lines of evidence and effectively selected CMIP6 models that had an equilibrium climate sensitivity (ECS) that fell within the AR6 *likely* range of 2.5-4.0°C, which was largely based on the review of Sherwood et al. (2020). About 20% of CMIP6 models fall outside the *very likely* AR6 ECS range of 2.0-5.0°C, with most (18%) being above 5°C. Further, 27% of the CMIP6 models are hotter than the highest ECS CMIP5 model (Figure 42). As noted by Hausfather et al. (2020), although the IPCC AR6 WG1 authors effectively moved to a limited set of the CMIP6 temperature projections for some analyses, this was not done by most authors that used the projections to assess other aspects of climate change, including sea level projections even though it was

recognised that excluding high ECS models may substantially alter sea level projections (Hermans et al., 2021).

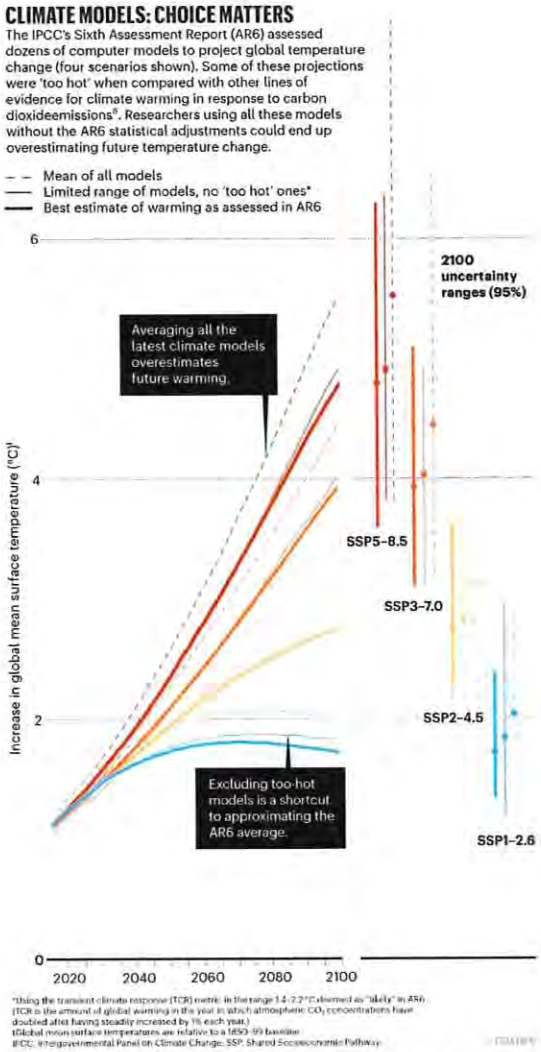

Figure 41. Figure from Hausfather et al (2022) showing the spread of model projections of future global surface temperature increases. See text for details.

For the next round of climate modelling (CMIP7) intended to inform the 7th series of IPCC Assessment Reports (AR7), it has been recommended that new scenarios and pathways be adopted (van Vuuren et al., 2023). Although the details, particularly the timing, have not been finalised, there is agreement that the highest emission scenario will have a lower peak radiative forcing than SSP5-8.5 (van Vuuren et al., 2023; Meinshausen et al., 2024). Currently, this appears to be an overshoot scenario with a peak value of 7.0 $W.m^{-2}$, like SSP3-7.0 (Figures 39 & 41), but with radiative forcing declining after the peak is reached.

The use of the highest projected values, as was done for the RCP8.5 H+ sea level scenario included in the 2017 guidance for local government (MfE, 2017), is of concern as it biases analyses towards *very unlikely to exceptionally unlikely* conditions.

Figure 43 shows the sea level rise projections recommended by the Ministry for the Environment (MfE, 2024), which includes a redefined SSP5-8.5H+ projection taken as the 83% percentile of the spread of SSP5-8.5 projections. This is a different definition from that

used previously for RCP-8.5H+ sea level projections, which was the mean of the highest 18% of projections. Figure 43 includes the time of onset and the latest that specified sea levels may be reached for absolute sea level increases of 0.4 m and 1.0 m. MfE (2024) also provides a table of the median time of onset for the scenarios in Figure 43 at 0.1 m increments from 0.2 m to 2.0 m. The time ranges for reaching a specified absolute sea level rise in Figure 43 highlight the large uncertainty associated with sea level projections.

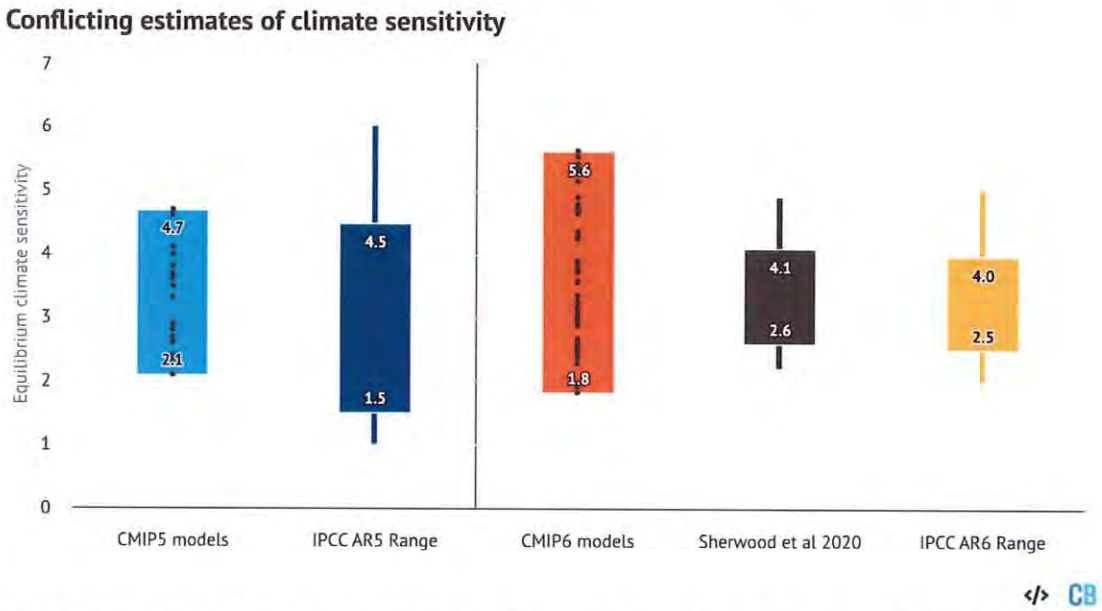

Figure 42. Range of equilibrium climate sensitivity from the previous generation of climate models (CMIP5), the IPCC 5th Assessment Report (AR5), the newest climate models (CMIP6), Sherwood et al 2020, and the IPCC 6th Assessment Report (AR6). For Sherwood et al, AR5 and AR6 the *likely* climate sensitivity (66% range) is shown by the thick bars while the *very likely* sensitivity (90% range) is shown by the thin bars.
https://www.theclimatebrink.com/p/revisiting-the-hot-model-problem.

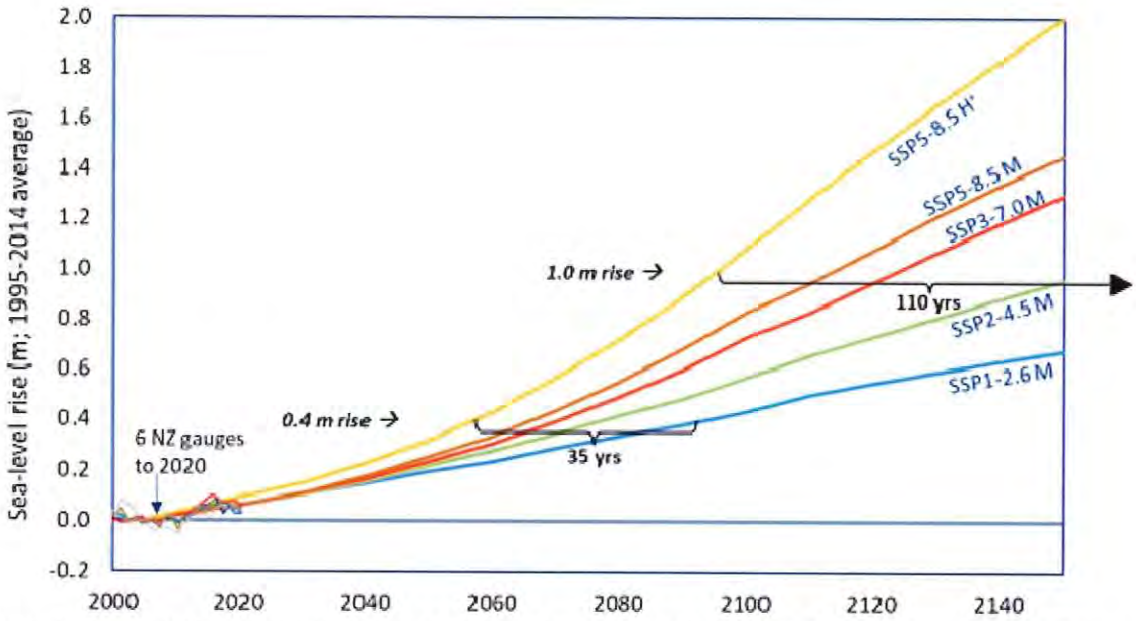

Figure 43. Figure 10 from *Coastal hazards and climate change guidance* (MfE, 2024) showing the recommended sea-level rise (SLR) projections (excluding vertical land movement) based on shared socio-economic pathways scenarios

(SSP) for central New Zealand.

Apart from the impact of the different emission scenarios, there are differences between the Atmosphere-Ocean General Circulation Models (AOGCMs) that are used to estimate future sea levels for each scenario. Couldrey et al. (2021) undertook a comparison of sea level projections made by CMIP5 AOGCMs that were forced by identical climate change forcings, including heat, momentum (wind stress), and freshwater inflows. They found that the spread in projected sea levels was comparable to the spread associated with the global temperature projections for different emissions scenarios used to drive the AOGCMs (e.g. Figure 41). In other words, the AOGCMs increase the uncertainties for sea level projections.

Another consequence of the shift to *assessed global temperatures* was a move in IPCC AR6 to focus on the consequences of specified levels of temperature increase rather than predicting the timing at which values were exceeded. MfE (2024) discusses the use of time of onset for sea level rise in the latest guidance document. In my opinion, this is a more practical approach when dealing with forecasting future conditions with high levels of uncertainty. This will be discussed further in section 6. Overall, the CMIP6 projections of global mean absolute sea level did not significantly change from the CMIP5 projections but involved a faster acceleration late in the 21st Century and a longer duration of committed sea level rise. This is possibly due to a lower response due to thermal expansion and a greater component due to the melting of ice caps (Slangen et al., 2022). The potential contribution of increased melting and/or destabilisation of major ice caps, particularly the West Antarctic Ice Sheet (WAIS) and Greenland Ice Sheet, resulted in additional sea level scenarios involving low-likelihood high-impact ice sheet process including SSP1-2.6 Low Confidence and SSP5-8.5 Low Confidence (Figure 44).

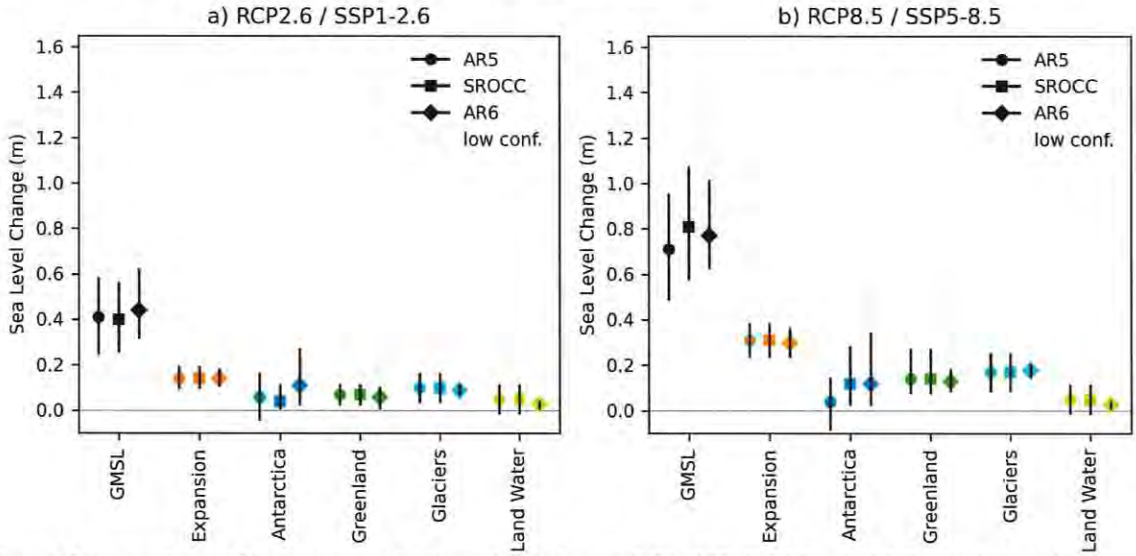

Figure 44. Comparison of 21st century projections of global mean SLC in AR5, SROCC and AR6. Total GMSL and individual contributions, between 1995 and 2014 and 2100 (m), median values and likely ranges of medium confidence projections, for (a) RCP2.6/SSP1–2.6 and (b) RCP8.5/SSP5–8.5. AR6 low confidence projections for SSP1–2.6 and SSP5–8.5 in grey for Greenland, Antarctica and GMSL. Figure 1 from Slangen et al (2022).

NASA provide an online tool for displaying and downloading the CMPI6 global absolute sea level projections for PSMSL tidal stations that are adjusted for regional variations (https://sealevel.nasa.gov/ipcc-ar6-sea-level-projection-tool). The data provided by this tool

appear to be utilised by the SeaRise online tool, and a comparison between the NASA and the SeaRise absolute sea level projections for Wellington (Figure 45) suggests they are identical.

The NASA tool only provides projection data for PSMSL tidal stations, which means Wellington, Nelson and Port Taranaki, for assessing future Kāpiti Coast sea levels. There is little difference between the projected absolute sea levels for these 3 stations. Figure 45 shows the median projections for the five SSP scenarios in Figure 39 and the two low-confidence scenarios accounting for the extreme melting of ice sheets for the Wellington tide gauge. The likely range of each median projection is indicated by shading. It does not include the SSP5-8.5H+ scenario recommended by MfE (2024), but this lies above the likely range of SSP5-8.5 projections.

In my opinion, the NASA tool provides a more useful way of presenting the projections that are not available from SeaRise. These are plots of the time that specified increases in sea level may be reached under the different scenarios (time of onset) and can be generated at 0.1 m intervals from 0.1-5.0 m above the 1995-2014 average MSL. These plots provide more information than Table 6 in MfE (2024).

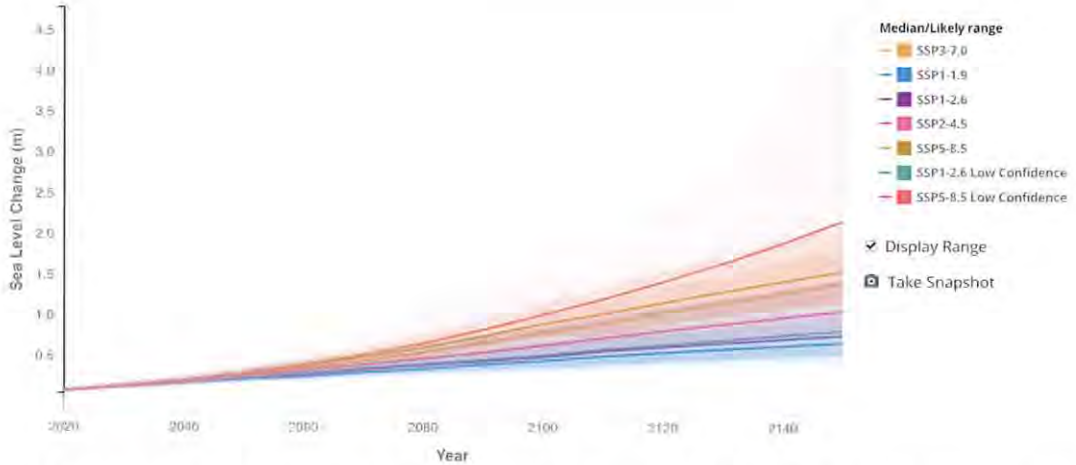

Figure 45. Sea level change for Wellington from SSP scenarios resulting from medium confidence processes, and two low-confidence scenarios. Shaded ranges show the 17th-83rd percentile ranges. Projections are relative to a 1995-2014 baseline. Plot generated by the NASA sea level projection tool.
https://sealevel.nasa.gov/ipcc-ar6-sea-level-projection-tool?psmsl_id=500&data_layer=scenario

Figure 46 shows the time of onset plots at Wellington for rises of 0.5 and 1.0 m. In my opinion, these show more clearly the uncertainties associated with the scenarios than the time series of sea levels in Figure 45. If specific sea level rises are associated with unacceptable levels of hazard, the choice of scenario may span a significant period (see time ranges for SSP1-2.6 Low Confidence, for example), which can lead to over- or under-design and implementation of responses if an adaptative approach is used. Further, the time of onset is more useful if a scenario-neutral approach is used, as suggested by MfE (2017) and Factsheet 2 on *Sea-level rise scenarios* provided by the SeaRise website. This approach will be discussed in Section 6.

Both Figures 45 and 46 demonstrate the very large uncertainties in the magnitude and timing of future absolute sea level changes and how rapidly those uncertainties increase at longer time scales. Also, as indicated in Figure 34, all the scenarios shown in Figures 44 and 45 require faster rates of absolute sea level rise since the baseline period of 1995-2014 than has been observed (Note that Figure 34 is relative sea level, while the others are absolute sea level, so VLM makes the rates of sea level rise appear closer together).

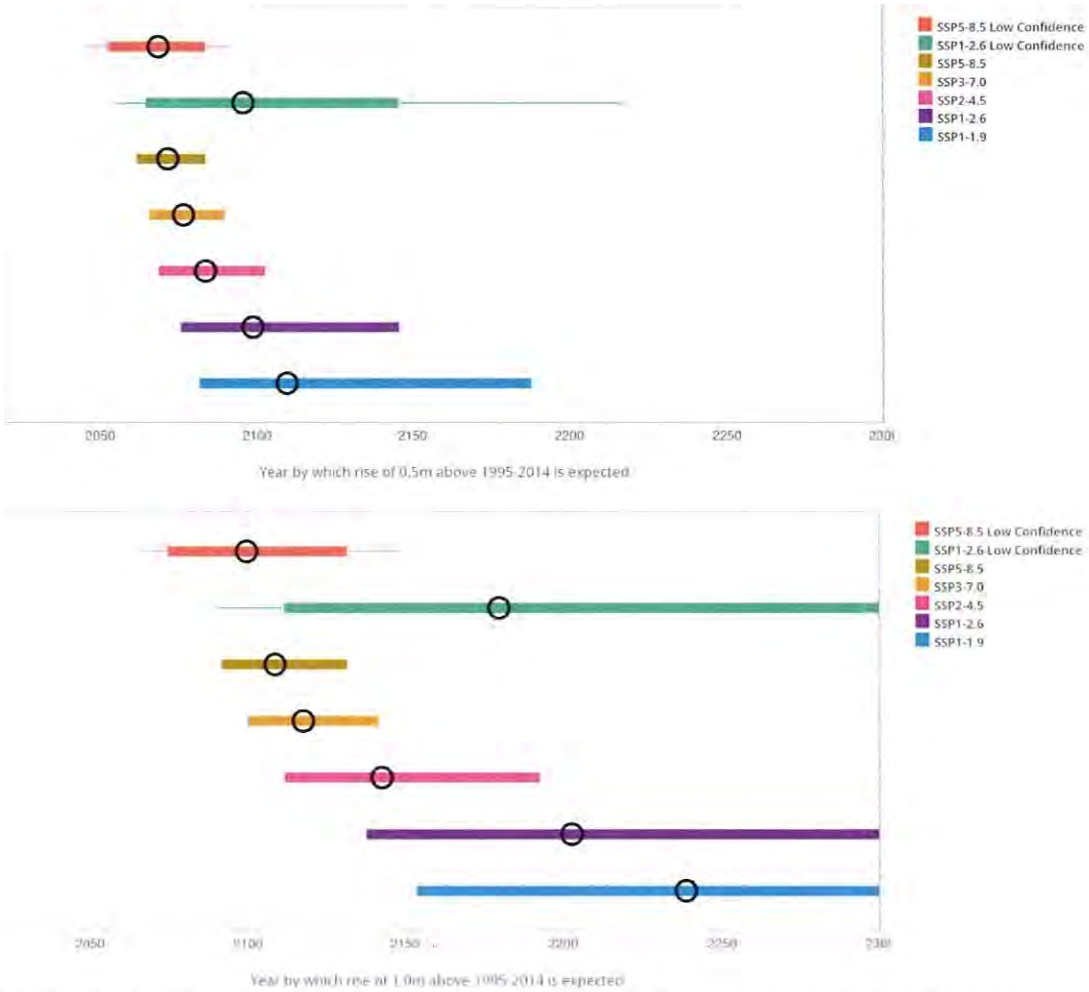

Figure 46. Projected time of onset for absolute sea level rises of 0.5 and 1.0 m above the 1995-2014 baseline at Wellington.

https://sealevel.nasa.gov/ipcc-ar6-sea-level-projection-tool?psmsl_id=500&data_layer=scenario

Kopp et al. (2023) present a methodology for developing probabilistic estimates of absolute, relative and extreme sea level change. While the method works reasonably well over short timeframes, it doesn't cope with the uncertainties associated with ice sheet melt. While the uncertainties related to ice sheet responses affect the magnitude of projected sea level to a greater extent for the larger emission scenarios (e.g. RCP 8.5), they have the greatest impact on the timing of low emission scenarios (e.g. RCP2.6).

Interestingly, whilst MfE guidance (MfE, 2008; 2017; 2024) suggests using the extreme magnitude sea level projections as a "stress test", which is intended to test policies and strategies, Turner et al. (2023) suggest that low emission scenarios (SSP1-2.6 and SSP2-4.5) are better for planning purposes as they can be used to avoid "lock-ins' in terms of

risk and adaption need for sea-level rise. A "lock-in" was defined by AR6 WGII as:

> *"a situation in which the future development of a system, including infrastructure, technologies, investments, institutions and behavioural norms, is determined or constrained ("locked in") by historical developments".*

Use of the lower emission *likely* scenarios would be consistent with the requirements of the NZCPS. However, in my opinion, it is not currently possible to reliably predict absolute sea level 100 years into the future as required due to the uncertainties involved in the emission scenarios and the modelling uncertainties. At shorter timescales, the differences between the scenarios are not great, so it would not be as important to select the "correct" scenario. The alternative scenario-neutral approach discussed in Section 6 is independent of the scenarios and is not affected by scenario choice.

5.3 Historic Climate Change and Projected Future Climate

This section reviews assessments for the Greater Wellington Region of past climate change, and projections of future climate, with respect to the drivers of coastal hazard, which are all associated with extreme weather (predominantly atmospheric pressure, winds and rainfall). Projected absolute sea level implicitly incorporates changing atmospheric and sea surface temperatures, so these will not be discussed here.

Chappell (2014) presents a summary of the current climate conditions for the Greater Wellington Region, including the Kāpiti Coast District. The climate of this region varies considerably spatially and temporally, which makes trends that may be due to climate change very difficult to detect. Variability in this region is strongly influenced by Cook Strait, which provides a sea level opening in the main ranges associated with the plate boundary running through New Zealand that modifies overall wind flows and the rugged topography. The Tararua and Rimutaka Ranges contribute to higher variability of temperature and rainfall for the eastern areas compared to the western, while Cook Strait contributes to stronger winds for the southern area compared to the northern area. This means that the Kāpiti Coast tends to have weaker winds and less variation in rainfall and temperature than the rest of the Greater Wellington Region. It also tends to be relatively sunny, contributing to the title "Golden Coast".

5.3.1 Historic Climate Change

There are very few published quantitative studies summarising historic climate change for the Greater Wellington Region. Woolley et al. (2020) provide an analysis of historical data for extreme winds, rainfall, MSL pressure, and dew point temperature. Chappell (2014) provides a summary of the weather and climate of the Wellington Region that updates earlier summaries but doesn't assess long-term trends. Some trends have been determined by StatsNZ and are available on their website (https://www.stats.govt.nz/information-releases/new-zealands-environmental-reporting-series-our-atmosphere-and-climate-2023/). Figure 47 shows the trends for the annual average of the daily maximum wind gust for 17 stations, including Wellington, between 1980 and 2022. Most stations show a decreasing trend.

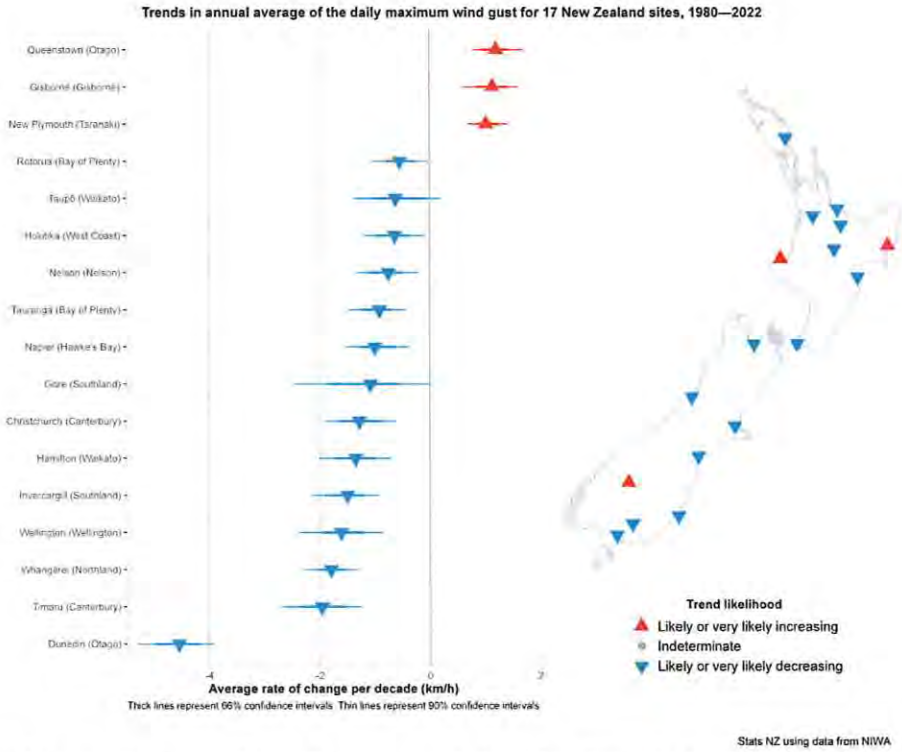

Figure 47. Trends in annual average of the daily maximum wind gust for 17 New Zealand sites, 1980-2022. https://www.stats.govt.nz/indicators/extreme-wind/

StatsNZ also provide data on trends for extreme rainfall defined as the maximum daily rainfall, and wet days where the rainfall exceeds the 95% percentile of the daily rainfall distribution. For the period 2013-2022, Wellington had an average daily maximum rainfall of 67.6 mm, and on average, 25.4% of the annual rainfall occurred on very wet days. Wellington showed no trend in extreme rainfall over the period 1960-2022). As noted above, Chappell (2014) showed that there are spatial differences in rainfall for the Greater Wellington Region. Unfortunately, Chappell (2014) uses different definitions for extreme rainfall, so the data they present cannot be readily compared to the StatsNZ results. Figure 48 compares the distribution of monthly total rainfall between Paraparaumu and Wellington Airports. The data suggest that Paraparaumu is more affected by atmospheric river events than Wellington (Prince et al., 2021; Reid et al., 2021), resulting in episodic intense rainfall events during the tropical cyclone season from September to April.

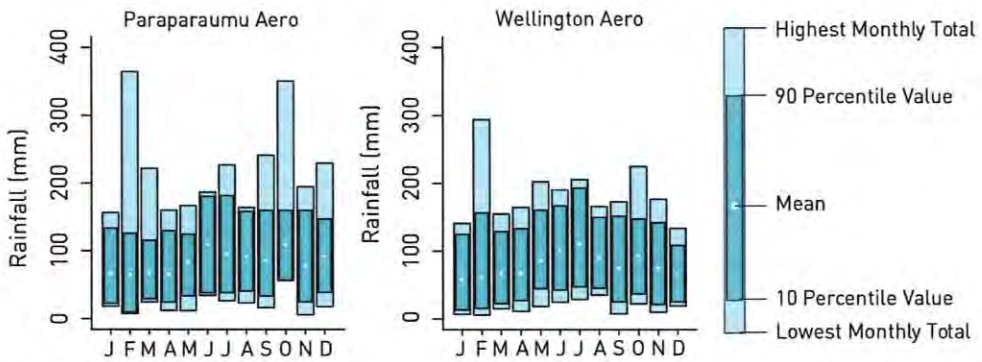

Figure 48. Monthly variation in rainfall for Kāpiti Coast (Paraparaumu Aero) and Wellington (Wellington Aero) for the period 1981-2010. (part of Figure 11, Chappell (2014)).

Pearce et al. (2017) include the summary information from Chappell (2014) and provide some analysis of long-term trends. For rainfall, they report a slight decrease in total annual rainfall at Kelburn of 6 mm/decade over 1928-2016, which was not significant (r^2=0.0063), and a slight increase at Bagshot Station near Masterton of 17 mm/decade over 1922-2009, which was not significant (r^2=0.0619). Pearce et al. (2017) also provide an analysis of extreme rainfall expressed as maximum daily rainfall and days exceeding 20 mm. At Kelburn for 1928-2016, the trend for maximum daily rainfall was a decrease of 0.8 mm/decade (r^2=0.0095), and days exceeding 20 mm increased by ~2 days per century (r^2 = 0.0085). At Bagshot Station for 1924-2009, the trend for maximum daily rainfall was a decrease of 2.1 mm/decade (r^2=0.0469), and days exceeding 20 mm decreased by ~2 days per century (r^2 = 0.0118). It seems reasonable to conclude that there has been no significant change in extreme rainfall for the Greater Wellington Region since the 1920s associated with climate change.

Pearce et al. (2017) did not analyse historical trends for extreme winds or storms. Woolley et al. (2020) undertook additional analyses for the Greater Wellington Regional Council that considered extreme winds, extreme rainfall, and extreme sea-level atmospheric pressure. They included different stations for their analysis compared to Pearce et al (2017): Kelburn (splicing Kelburn, Buckle St, & Thorndon), Wellington Aero, Paraparaumu Aero/EWS, Masterton (splicing Essex St, Waingawa, Te Ore Orde, Masterton, Cadet Farm, WRC Masterton Office, and Wairarapa College), Masterton Aero, and East Taratahi (near Masterton). The Masterton record for wind only extended from 1995-2019 and required splicing data from two stations. Therefore, the Masterton record will not be discussed here.

The extreme wind analysis by Woolley et al. (2020) mostly presents the results of Turner et al. (2019), who developed a methodology for combining wind data for different stations close to Cook Strait. The analysis by Turner et al. (2019) considered homogenised data for 1972-2017 and for Wellington found a slight increase in the magnitude of the annual average maximum daily gust (0.063 $m.s^{-1}$ per decade) with a slight decrease in the number of days of extreme wind gusts of 1.2 days per decade (90th percentile), 0.9 days per decade (95th percentile), and 0.2 days/decade (99th percentile). The annual trends were predominantly due to trends in Spring, with the remained seasons showing no measurable trends. The trend found for the magnitude of the maximum daily gust is in the opposite direction to the analysis presented for Wellington over 1980-2022 by StatsNZ (Figure 46). In my opinion, based on the published studies, there is no significant trend in extreme winds for Wellington, and this is probably also the case for the Kāpiti Coast District.

Woolley et al. (2020) undertook an analysis of historical rainfall for composite rainfall records at Kelburn, Wellington Airport, Paraparaumu Airport and Masterton using different criteria for extreme rainfall to the other studies referred to above. The criteria used were specified by the Greater Wellington Regional and are summarised in Table 3. The analysis was undertaken by the High-Intensity Rainfall Design System (HIRDS) and should be based solely on observations. HIRDS provides analyses for other locations, but these are more likely to be based on estimated rainfall.

Kelburn had the longest record covering the decades from the 1870s to the 2010s, while Paraparaumu's record started in the 1950s. Paraparaumu recorded the highest average annual number of rain events exceeding 5 mm within 10 minutes. Kelburn recorded the highest average number of events for all other criteria. Paraparaumu ranked second for intensities from 10mm/30min to 50mm/12 hours, third for 60mm/day, and fourth for all

higher thresholds. All four stations displayed large interdecadal variations that made identifying any trends difficult. The only possible trends recognised were for short-duration intensities (10-60 minutes) at Kelburn. Looking at the metadata available on NIWA's climate database for the Kelburn rainfall data suggests that the apparent trend may be due to changes to instrumentation and the data collected (Sub-daily measurements started in 1940). In particular, the observations show a large step change around the 1980s that produces the apparent trend.

Table 3. Annual rainfall thresholds analysed for Wellington Region sites from the High Intensity Rainfall Design System (HIRDS) available online at https://hirds.niwa.co.nz/.

Annual rainfall thresholds
Number of events >5mm in 10 min
Number of events >10 mm in 30 min
Number of events >15mm in 1 hour
Number of events >40mm in 6 hours
Number of events >50mm in 12 hours
Number of events >60mm in 24 hours
Number of events >100mm in 48, 72, and 120 hours

Atmospheric pressure has been recorded from six sites around central Wellington since 1862, making it one of the longest metrological observation datasets for New Zealand. Since extreme storms are also typically associated with extremely low atmospheric pressure over a relatively wide area, these data provide some insight into the frequency and magnitude of extreme storms since 1862. The recorded data were corrected to a standard temperature (0°C) and mean sea level elevation and combined into a one-time series for several international research initiatives by Woolley et al. (2020). They analysed this time series to determine the distribution of atmospheric pressure and trends over time. Pressures above the 90% percentile, and below the 10% percentile were considered as representing extreme pressures, with those below the 10% percentile representing storms.

Woolley et al. (2020) found no long-term trend for the annual mean MSL pressure but a weak trend of decreasing annual maximum MSL pressures (not statistically significant) and a statistically significant trend of increasing minimum MSL pressure (~2 hPa per century). Note that 1 hPa pressure drop results in ~10 mm sea level rise), and increasing minimum pressure suggests decreasing storm intensity. Wolley et al. (2020) suggest that, overall, these trends should not be considered meaningful as they may reflect changes in location and instrumentation over time.

Woolley et al. (2020) also reported seasonal variations, with most high-pressure extremes occurring during the Summer, while low-pressure extremes occurred year-round. Variability was also associated with climate oscillations at interannual (ENSO) and decadal (PDO) timescales. The amplitude associated with pressure changes at these temporal scales is significant (comparable to the amplitude of the seasonal cycle) and obscures long-term or time-dependent statistical trends.

A negative correlation was found between the percentage of observations below the 10% percentile and the Southern Oscillation Index (SOI) (Woolley et al., 2020). This indicates that during El Niño, there tends to be a greater-than-average occurrence of extreme low-pressure events in Wellington. Conversely, during La Niña, there tends to be a lower-than-average occurrence of low-pressure events in Wellington. Similarly, for 90% percentile exceedance, there tends to be a higher-than-average occurrence of high-pressure events in Wellington during La Niña and a lower-than-average occurrence of pressure events during El Niño. This pattern appears to also hold for Paraparaumu Airport.

Since the PDO is associated with increased/decreased frequency of El Niño events (Jiang et al., 2013; Heidemann et al., 2024), it is not surprising that Woolley et al. (2020) found a strong correlation between the PDO and pressure extremes (after smoothing). Their results showed that during the positive phase of the PDO, the proportion of observations falling below the 10% percentile tends to be higher than average, while the converse occurs in the negative phase of the PDO. A somewhat negative correlation occurs for the observations above the 90% percentile and there tends to be a lower-than-average proportion of observations exceeding this threshold during positive phases of the PDO and vice versa.

None of the reports to the Greater Wellington Regional Council provided an analysis of the frequency and magnitude of storms, although they consistently identified Cyclone Giselle (Wahine Storm) in 1968 as a notably severe storm. Woolley et al (2020) also indicated that storms producing strong southerly winds were particularly damaging to Wellington. They identified Cyclone Giselle, and two more storms in 1974 and 2013 as being strong examples of these events.

Dunn (2010) examined coastal storm activity for the east coast of the North Island from East Cape to Wellington and compiled a database of all historical storms associated with coastal impacts/damage between 1930 and 2005. Data were obtained from meteorological observations from 1962-2005 and news reports of storms from 1930-1962. The southern area around Wellington experienced an average of 9 "coastal" storms per year, with significant variability (2-19 storms per year) and no detectable long-term trend. Years with 14 or more storms included 1966, 1974, 1976, 1977, 1989 and 1992. There was no obvious relationship between the number of storms and the occurrence of very strong storms. The coastal storms were predominantly associated with southerly winds, and there was no significant correlation with tropical cyclones transitioning to extra-tropical storms (now called Cyclones) affecting the southern North Island.

Withers et al. (2009) examined temperature trends for 19 stations in New Zealand, involving 57-time series of annual minima, means and maxima to test if the predicted changes due to climate change were evident. They found *"a surprising diversity of behaviour"*, including 1/3 of stations exhibiting decreasing trends. Their analysis indicated an overall tendency for decreasing variability associated with less extreme temperatures (minimum and maximum). The observations were inconsistent with the expected effects of climate change. Griffiths et al. (2014) similarly examined extreme rainfall trends for New Zealand from 1961 to 2012 at 28 stations, including Paraparaumu, and found no trends associated with climate change.

Overall, there is no detectable pattern of change in the historical data that can be linked to climate change reported in the literature for the Kāpiti Coast District.

5.3.2 Prehistoric Climate Change

Some studies have assessed prehistoric extreme weather patterns for the lower North Island and for source regions of tropical cyclones that may impact the Kāpiti Coast. Grant (1981) examined patterns of tropical cyclone activity and coastal impacts for New Zealand and eastern Australia and identified decadal-scale patterns. Specifically, Grant (1981) identified an increase in the frequency of tropical cyclones in the 1950s that continued into the 1960s and 1970s. This was associated with an increase in rainfall and frequency of river floods compared to the period 1920-1950. Grant (1981) also linked the pattern of changing storm frequency with coastal changes involving accretion and erosion for the upper North Island. Salinger and Mullan (1999) found the same pattern of rainfall changes as Grant (1991) and separated them into three periods: 1930-1950, 1951-1975, and 1976-1994. These periods are now recognised as phases of the PDO (e.g. Salinger et al., 2001).

Grant undertook a series of studies investigating floodplain deposits around the North Island (Grant, 1985), which included the Tararua and Ruahine Ranges. A detailed study of the Ruahine Ranges documented periods of extreme weather since 1770 (Grant, 1991), which covers the period of anthropic climate change as defined by legislation for New Zealand. Phases of increased sedimentation on the floodplains were linked to disturbance of upper catchment vegetation by increased rainfall and windiness, while phases of soil development were linked to periods of lower rainfall and calmer winds. Dating of the paleosols and woody debris in the flood deposits was used to define 8 periods of increased sedimentation (and probably greater storminess) since the Taupo Eruption ~1800 years ago. Although Grant (1985) attempted to link the periods of increased storminess to solar activity, the resolution of the dating was not ideal, and the correlation was poor. Some of the phases of sedimentation could also be linked to volcanic eruptions, major earthquakes and anthropic forest disturbance.

A series of studies investigated climate, volcanic eruption and seismic impacts on a single catchment using landslide and flood deposits within Lake Tutira, Hawke's Bay, which formed about ~7200 years ago when a landslide dammed a valley (Edin & Frogatt, 1996; Eden & Page, 1998Orpin et al., 2010; Gomez et al. 2015). The volcanic tephra intercalated in the sediment cores provided additional constraints on dating and a well-documented history of anthropic changes, resulting in a detailed record of prehistoric and historic extreme events for the mid-to late-Holocene.

Eden and Page (1998) examined the youngest part of the sediment sequence in Lake Tutira, and based on changes in sediment characteristics they identified 340 events to produce a 2250-year storm chronology. They were able to identify specific historical storm events and isolate anthropic effects on sediment input to the lake.

Page et al. (2009) extended the analysis to the full thickness of the Lake Tutira sediments and identified 1400 layers of storm deposits since the lake formed. They recognised 25 periods when storm magnitudes and frequencies increased for decades to centuries. Periods of major storm activity occurred at 500–700, 1100–1250, 1850–2100, 2850–3200, 3600–4000, 4300–4500, 4700–4900, 5700–5900, and 6850–6900 cal. yr BP (Figure 49). The youngest periods are consistent with the Matawhero and pre-Kaharoa phases of storminess identified by Grant (1985). The most intense period of storm activity occurred about 2000 years ago, before human arrival in New Zealand, when the average major storm recurrence interval was 1.9 years (Figure 49), compared with the current 5-year average recurrence

interval. This period is consistent with paleoclimate proxy records from other locations in New Zealand and around the Southern Hemisphere. However, not all stormy periods at Lake Tutira correlate with other locations. Page et al. (2009) also noted that there was no trend of increasing storminess, which had been expected due to the intensification of ENSO events affecting tropical and sub-tropical regions over the last 4000 years, and possibly evidenced by marine sediment cores offshore from New Zealand.

Gomez et al. (2011) investigated the relationship between storminess within the Lake Tutira Catchment and the ENSO and SAM climate oscillations after it was determined that these oscillations have a major impact on New Zealand precipitation (Ummenhofer & England, 2007; Ummenhofer et al., 2009). They found that the variability in storm frequency and magnitude at Lake Tutira (Figure 49) was associated with the frequency of La Niña events, with increased storminess occurring when La Niña occurred during positive SAM periods. Therefore, storminess was correlated with interactions between ENSO and SAM at millennial timescales that involved changing phase relationships between the two oscillations. Specifically, ENSO influence on New Zealand strengthens (frequency of La Niña increases) when ENSO is in phase with SAM and weakens when it is out of phase. A similar relationship appears to occur between the ENSO and PDO oscillations at centennial timescales but was not assessed by Gomez et al. (2011).

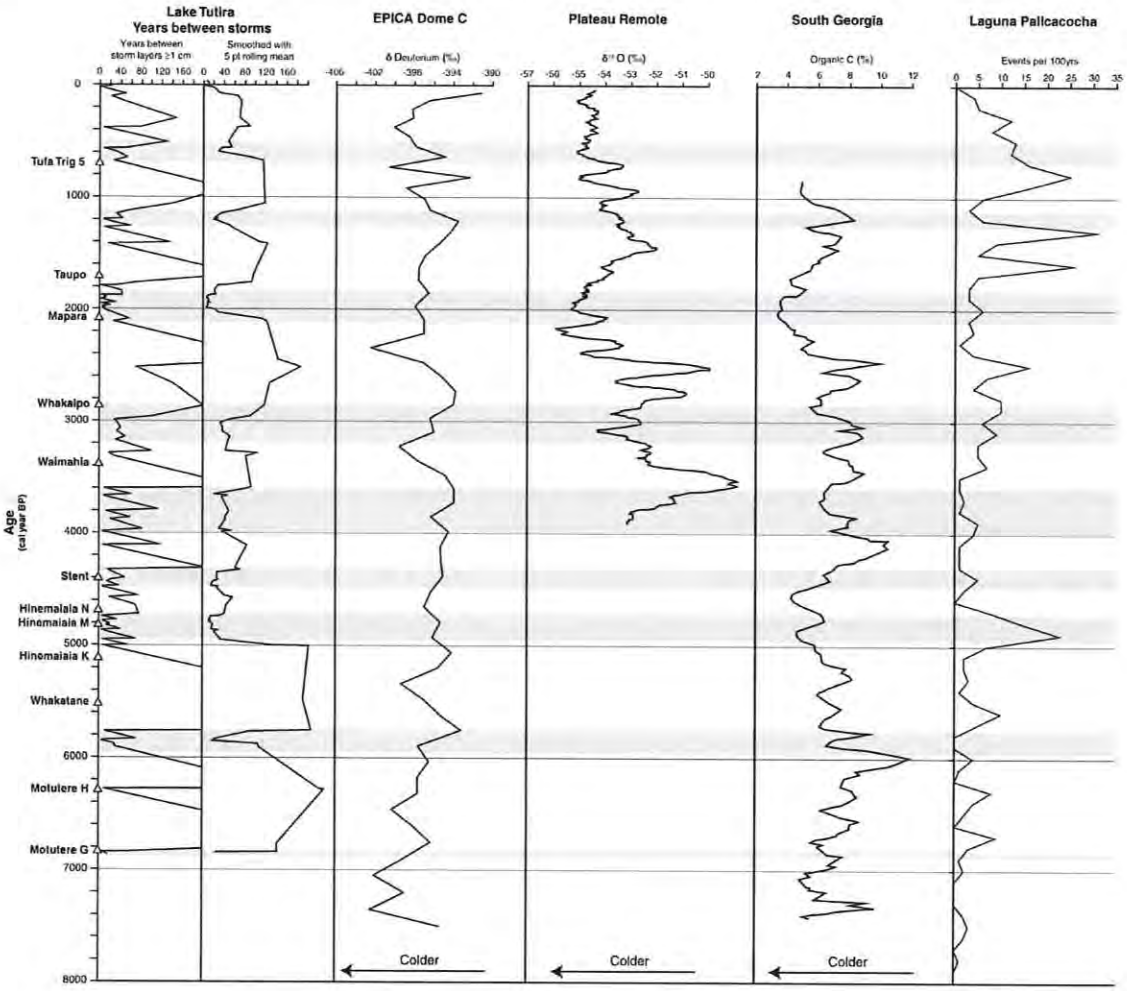

Figure 49. Regional paleoclimate proxy records for the mid to late Holocene (left to right): Lake Tutira storm frequency represented by sediment layers≥1 cm; δ deuterium record (‰) from EPICA Dome C ice core, Antarctica; $\delta^{18}O$ record (‰) from Plateau Remote ice core, Antarctica; organic carbon (%) from lake sediment core, South Georgia; and time series for ENSO events from Laguna Pallcacocha sediments, Ecuador. Tephras (Δ) are marked on vertical axis. Major stormy periods are marked by grey shading. Figure 6 from Page et al (2009).

Gomez et al. (2011) suggested that the phase relationship between ENSO and SAM was modulated by solar insolation changes linked to the precession component of the Earth's orbit around the Sun. They did not find any relationship with climate change and noted that the prediction of future storminess required the prediction of ENSO and SAM phase interactions.

Poverty Bay and the Waipaoa River Catchment were the focus of an international study examining the effects of climatic changes, natural disturbances (e.g. earthquakes and volcanic eruptions), and anthropic factors on sedimentation from the source to sink (MARGINS *Source-to-Sink* program, Carter et al. (2010)). Sediment deposits from the floodplains, lakes, continental shelf, and deeper continental margin sites were used to develop chronologies of major depositional events. Gomez et al. (2007) and Upton et al. (2013) linked the terrestrial and marine deposits in Poverty Bay and Lake Tutira to assess the climate forcing of these depositional events, which were assumed to be produced by severe storms.

Gomez et al. (2007) distinguished two types of storm deposits. One was consistent with the deposits in Lake Tutira and was associated with landsliding linked to ENSO variability. These deposits implied a variation in storm frequency and magnitude that they attributed to changing solar insolation due to the precession orbital component. The other deposits were attributed to infrequent extreme storms, with two events identified in their 2400-year record. Three other similar deposits in the sequence were attributed to major earthquakes. Gomez et al. (2007) noted that the largest historical storm event for the Waipaoa Catchment before the study did not produce an identifiable deposit in the marine core analysed. Their data also indicated that there was a period of intense storm activity ~2000 years ago.

Upton et al. (2013) used numerical modelling to develop a 5500-year reconstruction of sediment discharge for the Waipaoa Catchment to compare with the chronology developed from sediment cores. They used the impact of the 1988 Cyclone Bola event to calibrate and validate their model. Their results indicated that most variations in sediment discharge were associated with centennial and millennial-scale fluctuations in precipitation associated with storms. Their interpretation was that precipitation was a major control on sediment production, but the effect of precipitation was modified by vegetation. Hence, the model predicted the highest erosion rates in the catchment during glacial conditions with reduced forest cover (increased tussock grasslands) and the lowest erosion rates during interglacial conditions with increased forest cover. The model also predicted a greater frequency of major storms before human occupation of New Zealand, with a peak in storminess ~2000 years ago. This peak in storminess was inferred to be associated with an increase in tropical cyclones passing over the lower North Island.

Coastal deposits and speleothems from Queensland, Australia, have been used to investigate the frequency and magnitude of tropical cyclones forming in the Coral Sea and north of the Tasman Sea (Nott & Hayne, 2001; Nott et al., 2007). These studies have

resulted in a ~6000-year chronology of intense paleo-cyclones that has been used to assess tropical cyclone risk for Australia (Mortlock et al., 2023). The source region for tropical cyclones affecting Queensland is also the source for many tropical cyclones affecting New Zealand, particularly the west coast, including Kāpiti Coast District (Lorrey et al., 2014; Chappell, 2014).

The frequency and magnitude of tropical cyclones affecting Australia varies in response to climate oscillations, with the dominant ones being the Indian Ocean Dipole (IOD) and ENSO, which are modulated by the PDO. Based on the limited historical record (1909 to present, but only considered reliable since 1981), positive (negative) PDO, El Niño (La Niña) and positive (negative) IOD are all associated with a reduction (increase) in tropical cyclone frequency along the east coast of Australia (Mortlock et al., 2023). At longer timescales, other processes have been suggested as intensifying or weakening tropical cyclone generation, including volcanic eruptions and solar activity (Mortlock et al., 2023).

The ~6000-year record was used to assess prehistoric (before 1909) tropical cyclone frequency and magnitude. This analysis indicates that the modern instrumental period has experienced a below-average incidence of tropical cyclones, and during peak activity, landfalling Category 5 tropical cyclones were almost 5 times more frequent for northeast Australia. This corresponds to a change from a Category 5 AEP of ~1.1% to ~5.0%. One of the periods in increased frequency of Category 5 tropical cyclones occurred ~2000 years ago and may be associated with the increased storminess for the lower North Island discussed above. However, this also requires that the storms generated track over New Zealand, and the Australian data are based on landfalling tropical cyclones on the northeast coast of Australia. It is unlikely that those landfalling tropical cyclones would have continued to track over New Zealand.

5.3.3 Future Climate Change

As stated by Chappell (2014) the climate of the Greater Wellington Region is characterised by large spatial and temporal variability, and this is largely driven by climate oscillations operating at different timescales (Sections 5.3.1 and 5.3.2). The oscillations that have been identified as affecting climate for New Zealand include ENSO and IOD that occur on 3-7 cycles, PDO at centennial timescales, and SAM at millennial timescales.

Although the ENSO and IOD cycles are shorter than the 30-year definition of a climate normal, the number, intensity, and pattern of extremes of cycles varies at longer timescales. For example, IOD and ENSO may not completely cycle and produce 2 or 3 consecutive extremes of the same phase, so a 30-year period can experience a higher proportion of one extreme, resulting in a climate shift. The IOD had 3 consecutive positive phases from 2006-2007, and ENSO had 3 consecutive La Niña phases from 2020-2022. It is uncertain if there is a trend in the occurrence of ENSO and IOD cycles linked to historic climate change or whether the longer timescale oscillations (PDO and SAM) are modulating the shorter cycles.

Analyses of climate model projections for the Southwest Pacific have consistently noted that the behaviour of key features such as the Intertropical Convergence Zone (ITCZ), South Pacific Convergence Zone (SPCZ), and meridional and (north-south) zonal (east-west) airflow over New Zealand (Figure 50) are poorly simulated (*viz*. Francis and Renwick, 1998; Brown et al., 2020). Cai et al. (2023) undertook an assessment of climate modelling approaches to determine if the models could simulate climate change impacts on ENSO by focusing on sea surface temperatures for 1901-1960 and 1961-2020. They identified an increased

magnitude of ENSO extremes after 1960 that they attributed to climate change and found that ¾ of the models predicted this change. In contrast, Heidemann et al. (2024) examined sea surface temperature data from 1920-2022 and found that the observed changes in ENSO frequency and magnitude could be explained by the PDO oscillation.

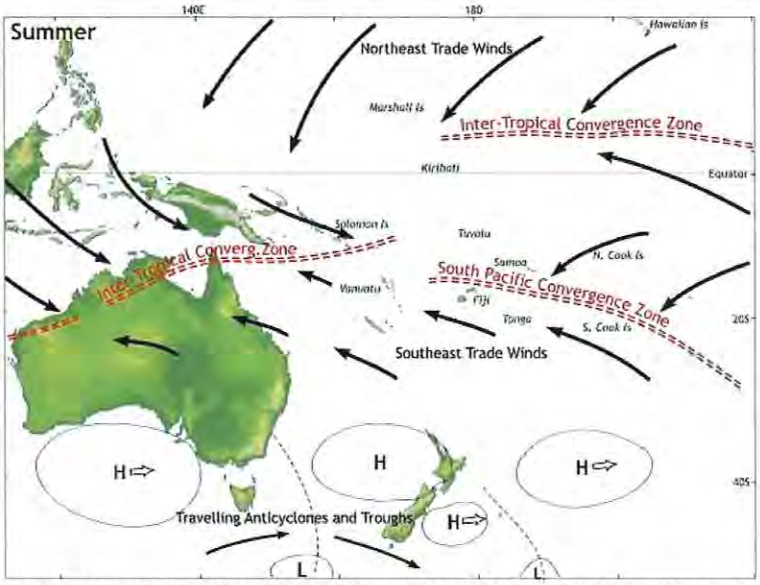

Figure 50. Typical low-level flows during the Summer, and main atmospheric circulation features (https://blog.metservice.com/node/987).

At present, it does not appear possible for GCMs to correctly predict the behaviour of the major atmospheric features affecting New Zealand weather (and hence climate) for more than a few months into the future.

The GCM results are at too coarse a resolution to provide useful regional projections for New Zealand (Renwick et al., 1999), so different approaches have been used to downscale the GCM projections to regional projections. These include empirical relationships (*viz.* Carey-Smith et al., 2018), statistical downscaling (*viz.* Renwick et al., 2009) and nested regional climate models (*viz.* Renwick et al., 1998; Drost et al., 2007). Although it was found that, depending on the GCM model selected for downscaling, regional projections improved with increasing resolution, the effects of local topography were very difficult to simulate, and at some point, increasing resolution caused increasing biases towards higher temperatures and/or rainfall (*viz.* Drost et al., 2006).

Pearce et al. (2017) and Pearce et al. (2019) present projections of the future climate for the Greater Wellington Region under the RCP2.6, RCP4.5, RCP6.0 and RCP8.5 scenarios using statistical downscaling from 41 CMIP5 GCMs, and nested regional models (dynamical downscaling) involving 6 CMIP5 GCMs. They also used the High-Intensity Rainfall Design System (HIRDS) tool developed by NIWA, which uses an empirical relationship to predict future rainfall from an interpolated grid of historical rainfall extreme value distributions (Carey-Smith et al., 2018). The relationship assumes a linear relationship between mean annual temperature and extreme rainfall applies for future climate change, as given by the Clausius-Clapeyron relation (~7% increase per 1°K increase in temperature). This approach was justified by a study comparing different GCM projections of rainfall changes in response

to increasing temperatures. There does not appear to have been a comparison with observed responses.

Other studies (Salinger & Griffiths, 2001; Griffiths, 2007,2013; Griffiths et al., 2014) have not found any consistent trend between historic extreme rainfall and temperature in New Zealand. Griffiths (2007) specifically compared the warmer 1950-2004 period to colder earlier data and found small changes linked to variations in the frequency of westerly winds but not temperature. These variations in wind patterns are associated with ENSO, SAM and PDO (Griffiths, 2011). Harrington & Renwick (2014) found similar small changes when comparing 1950-1979 to 1980-2009. There is also a strong correlation between mean annual rainfall and the frequency/magnitude of extreme rainfall events, so an increase in mean rainfall in the future may be associated with a higher frequency/magnitude of extreme rainfall. However, historic mean annual rainfall shows interannual to multi-decadal variations but no long-term trends.

Considering the projected climate changes to extreme weather that may affect coastal processes for the Kāpiti Coast, Pearce et al. (2017) Pearce et al. (2019) and provide the following summaries:

- **Extreme rainfall** – Rare, large extreme events are *likely* to increase in intensity due to more moisture being held in a warmer atmosphere (Clausius-Clapeyron assumption), with up to 25% increase in magnitude for Wellington and the southern coast under RCP8.5 in 2090. However, there was significant variation in the models considered, with most projecting less than ±5% change. Kāpiti Coast District may experience a larger increase in mean rainfall than Wellington in the winter.
- **Atmospheric pressure** – Mean sea level pressure is projected to increase in summer, causing more northeasterly winds and anticyclonic conditions, and decrease in winter, resulting in stronger westerly winds. This implies a reduction in storms affecting the Kāpiti Coast District.
- **Extreme winds** - Most of the Wellington Region is *likely* to experience stronger extreme winds, although the magnitude of these changes is small, with a maximum of 4% increase projected for the eastern Wairarapa hill country at 2090 under RCP8.5.
- **Storms** - Storms may become more intense, but there is significant uncertainty surrounding projections of tropical and extra-tropical storms into the future.

Macara et al. (2022) updated the analysis of Pearce et al. (2017) for the areas west of the Tararua and Rimutaka Ranges, using the same CMIP5 GCM projections. The downscaling of CMIP5 projections was expected to be completed at some time in 2024. The 2022 update mostly included 5 more years of observations and didn't cover all of the extreme weather indicators above, but it did change the projections for heavy rainfall and 1% AEP extreme rainfall based on modelling historic rainfall (HIRDS):

- **Heavy rainfall** - Heavy rainfall events (99th percentile of daily rainfall totals) are generally projected to become more severe in the future. By 2040, the magnitude of heavy rainfall events is projected to change by -1% to +12% (RCP8.5). By 2090, heavy rainfall event magnitude is projected to increase by 1-12% (RCP2.6) or 2-30% (RCP8.5)

- **Extreme rainfall** – Rare, extreme rainfall events are also expected to increase in both frequency (between two-fold and three-fold increases for various durations) and magnitude (up to 40% increase) based on the Clausius-Clapeyron assumption.

Overall, the projections of Pearce et al. (2017) and Macara et al. (2022) are consistent with Figure 30 (Table 12.12 from the AR6 WGI report), which shows that the projected changes are smaller than the natural variability occurring at present, although some events under the implausible RCP8.5 may exceed natural variability by 2090. It should also be noted that in both the historic and prehistoric records discussed above, there are no statistically significant long-term trends associated with climate change for indicators of extreme weather.

6. Implications for Managing Coastal Erosion Hazard.

As discussed in Section 2.3, the methodology employed by Jacobs (2021, 2022) is not an improvement on previous studies that have assessed coastal hazards for the Kāpiti Coast since the 1970s. While some of the problems raised in Section 2.3 relate to specific aspects of the Jacobs approach, such as using an inundation model (Bruun Rule) to predict shoreline erosion, the predominant issue is the requirement for prediction and determination of the likelihood of inundation and shoreline erosion 100 years or more into the future. The consensus view in the literature is that it is not possible to reliably predict either the driving forces for coastal hazards or their consequences more than 10-20 years ahead. It is also difficult to assess the likelihood as the underlying processes are non-stationary, involving a combination of oscillations at different timescales and a long-term trend (climate change), which alters the likelihood over time (*viz.* de Lange & Gibb, 2000).

Studies of the predictive reliability of different approaches for forecasting shoreline response (*viz.* Coco et al., 2020) demonstrate that the highest predictive skill is provided by an ensemble of models using a statistical approach. However, due to deep uncertainty about future processes driving coastal hazards, they cannot reliably forecast more than a couple of decades into the future. A simpler approach that is useful over this shorter time frame, although the confidence limits increase rapidly beyond 10-15 years, is extrapolation of historical trends. Since historical data have been influenced by climate change, the effects of climate change are incorporated, albeit without any correction for future non-stationary effects (e.g. accelerating climate change). The historical data also reflects the impacts of anthropic factors such as land use changes, inlet modifications, sand extraction and seawalls. The DSAS software used by Jacobs (2021, 2022) to assess historical erosion rates can undertake this type of prediction with reasonable success out to 20 years (*viz.* Islam & Crawford, 2022; Abd-Elhamid et al., 2023).

The approach taken by Jacobs (2021, 2022) to deal with uncertainty has been to be "conservative", which means that they have almost certainly predicted more shoreline inundation and retreat that will occur. This has been confounded by presenting an error analysis for their calculations as a probability of specific inundation or retreat occurring. The concern is that this restricts potential management options for addressing coastal hazards, which normally involve three categories of responses (O'Donnell, 2022): protect, accommodate (adapt), or retreat. Undeveloped shorelines also have the option of avoidance.

Retreat options are often viewed as a last resort when protection or accommodation options are not viable due to cost, the speed of shoreline change, or excessive vulnerability

(O'Donnell, 2022). MfE (2024) states the opinion that *"only avoidance and retreat strategies provide permanent reduction of risk"*. However, there are many examples worldwide that show that there are viable long-term alternatives to retreat for existing infrastructure, such as:

- Oosterschelde and Maeslant Barrier in the Netherlands.
- Thames Barrier in the United Kingdom
- Modulo Sperimentale Elettromeccanico (MoSE) in Italy.

It has been recognised that many options for managing coastal hazards have failed due to political and legal issues (O'Donnell, 2022), and retreat options have been particularly difficult to implement due to social, cultural and economic issues, particularly for those relocated (Tubridy et al., 2022). The adverse consequences of retreat options are generally most severe when they are imposed by a top-down management approach (Tubridy et al., 2022), and they are most effective when community-led (O'Donnell, 2022; Tubrity et al., 2022). MfE (2024) highlights the importance of community involvement and an adaptive approach to coastal hazards.

Considering the whole range of approaches, most studies have found that an incremental implementation, which may involve more than one type of approach, is the most effective strategy (O'Donnell, 2022). Even if a retreat option is a final solution, many studies have identified that a staged implementation based on the cost-benefits of different options is a very effective strategy given the uncertainty and changing infrastructure (*viz*. Turner et al., 2007; Oulsen, 2019; Cutler et al., 2020; Eaves, 2022). This approach is consistent with the dynamic adaptive pathways planning (DAPP) approach recommended by MfE (2024).

In my opinion, to develop an adaptive management approach for the Kāpiti Coast District, a different method of assessing coastal hazard risk is required than that used by Jacobs (2021, 2022). MfE (2024) provides a range of coastal management case studies, which demonstrate that there are viable alternatives to the methodology used for Kāpiti Coast District for the last half-century. One methodology used to various degrees by several case studies is a scenario-neutral approach, which can be adopted within an adaptive management framework to inform community-led decisions. This is outlined in the next section.

6.1 Alternative Scenario Neutral Approach

Essentially, the risk assessment for the Kāpiti Coast can be separated into two components: the vulnerability to specific levels of hazard and the likelihood of that level occurring. The vulnerability assessment needs to concentrate on two hazards: coastal inundation over different durations and erosion of the shoreline. While this was the stated purpose of the Jacobs (2021, 2022) report, their report does identify the vulnerability for specific levels of inundation and erosion hazards. The likelihood assessment component is difficult for the reasons discussed above, but by utilising an adaptive approach, it is possible to assess risk over shorter time frames and adjust the response if risk changes due to climate change or other factors in the future. The development of levels of hazard for vulnerability assessment can be informed by projections of conditions 100 years or more into the future if required.

6.1.2 Vulnerability Assessment

Considering inundation first, this may occur in response to a range of different processes, including relative sea level rise, extreme water levels due to storm surges and high tides,

tsunamis, and extreme rainfall. For a vulnerability assessment, it is not necessary to treat these separately, although it may be useful to distinguish salt water from freshwater inundation and short-term inundation (e.g. storms and extreme rainfall) from "permanent" inundation (relative sea level rise) for the purpose of identifying impacts.

The procedure to follow for a scenario-neutral approach to vulnerability assessment of inundation is:

1. Define a range of elevations that include all reasonable estimates of future water levels from any cause – such as relative sea level, storm surge, tsunami, and combinations of these. For example, water levels from 0.5 to 5 m in 0.5 m increments will cover the projected relative sea levels for the Kāpiti Coast, shown in Figure 45. Since it is more likely that the Kāpiti Coast will be affected by VLM associated with a major earthquake than the collapse of the West Antarctic Ice Cap over the next 100 years, it may be useful to also consider the effects of relative sea-level fall. For example, a drop of sea level will result in erosion of riverbeds as they adjust to a lower base level, which may have adverse effects for upstream infrastructure.
2. Identify the areas below each of the specified elevations, for example, with a Geographic Information System (GIS).
3. Assess the characteristics of each area in terms of the effects of inundation (what are the specific vulnerabilities in terms of damage, injury, and death).

Appendices A.1 to A.4 of MfE (2024) illustrate variations of this approach used by case studies of coastal inundation hazards around New Zealand. Note that the Jacobs (2021, 2022) PFSP lines are really inundation extents due to the influence of the Bruun Rule, which predicts inundation assuming a planar slope as a component of their coastal erosion calculation.

Similarly, the procedure to follow for a scenario-neutral approach to vulnerability assessment of coastal erosion is:

1. Define a range of distances that include all reasonable estimates of future coastal erosion from any cause. For example, distances from 25 m to 1500 m in 25 m increments are ~6 times the maximum historical erosion distance since 1870 (Figure 20). If accretion may result in adverse effects such as increased flooding of the lowlands, then also include a range of accretion rates. Note that the maximum accretion rate is slightly higher than the maximum erosion rate for the Kāpiti Coast (Figure 20).
2. Identify the areas seaward/landward of each of the specified erosion/accretion distances; for example, with a Geographic Information System (GIS).
3. Assess the characteristics of each area in terms of the effects of coastal erosion (what are the specific vulnerabilities in terms of damage, injury, and death).

Having identified the vulnerabilities, the specific inundation levels and erosion/accretion distances can be used as the trigger points within an adaptation framework to develop community-led responses to changing levels of risk in the future, as recommended by MfE (2024). As part of the development of responses, there should be consideration of the time required to implement any response once a trigger point is reached, as this will constrain

how much warning time is required. In my experience, responses supported by the community can usually be implemented within 10-20 years.

6.1.3 Likelihood Assessment

The likelihood component of the risk assessment is now the probability that the specified elevation or distance will be exceeded within a specified time frame. Since it is not possible to reliably determine this beyond short time scales, it is suggested that the focus should be on short time frames consistent with planned response implementation, where statistical methods can provide reliable predictions. As discussed above, none of the processes driving inundation or coastal erosion show any evidence of an accelerating trend at present. In the case of relative sea level, a large acceleration should already have been observed (Figure 34) if the sea level is to reach the higher projections included in MfE (2024).

For planning purposes, it is possibly more useful to consider the time of onset, i.e. the time at which sea level or coastal erosion reaches critical levels or distances. Predicting the time of onset is best achieved by extrapolating historical trends for time frames of 10-20 years, but can be informed by projections (e.g. Figure 46).

6.1.4 Monitoring

Monitoring of sea level and extreme weather can identify any changes to historical trends that may be occurring, and hence provide the necessary information for revising adaptation responses. Extreme weather events appear to be well observed and tracked by organisations such as MetService, NIWA, and StatsNZ, so there shouldn't need to be any additional monitoring required.

A problem for the Kāpiti Coast is that the relative sea level trends may differ from those at the standard ports (Wellington, Nelson and New Plymouth) due to differences in vertical land movements. In my opinion, it would be useful to acquire existing data for the Kapiti Island tide gauge (held by NIWA?) and reinstate a permanent tide gauge on Kāpiti Island near the cGPS station there. Kapiti Island is preferable to most of the mainland Kāpiti Coast due to the rocky shoreline that avoids problems with erosion and accretion affecting the gauge. Data from Kāpiti Island will provide a better indicator of the trends of relative sea level for the region than more distant existing gauges, and the cGPS station will provide data on the VLM, allowing calculation of the absolute sea level (RSL - VLM = ASL).

A cGPS station located near the mouth of the Waikanae River would be useful to provide data for the vertical movement in the central area of the Kāpiti Coast. Using data from Kāpiti Island, the relative sea level can be determined for the rest of the mainland coast using the cGPS data.

6.1.5 Prediction

Sea level trends can be determined for the Kāpiti Coast from observations (ideally from a local site) and used to predict the time of onset for specified future sea levels. At longer time scales, methods such as the NASA tool discussed above (Figure 46) can give an indication of the time of onset based on sea level projections.

As discussed above, the DSAS tool used by Jacobs (2021, 2022) to determine historical rates of shoreline movement can also be used to predict shoreline position 10 and 20 years into the future. By periodically updating the DSAS database with shoreline locations over time, these predictions can be updated as needed. Comparing the predicted shorelines with the

critical distances identified previously will provide information on the likely time of onset for coastal erosion impacts.

Climate change projections may inform the development of a response plan under an adaptation framework if the intended response requires more than 20 years to implement. While NZCPS Section 24 requires considering the *likely* effects of climate change over the next 100 years, as discussed above, it is not possible to produce reliable predictions that far into the future, and scenario projections strictly have no probability or likelihood. In my opinion, if it is deemed essential to estimate onset times beyond 20 years, it would be more useful to follow the practice used for other hazards as was used for lifeline vulnerability assessments for major urban areas in New Zealand (viz. CAE, 1991; de Lange & Hull, 1994). This involves defining a Maximum Credible Event (MCE) and a Design Level Event (DLE). For the Wellington region, the MCE earthquake had a probability of ~10% in 50 years, and the DLE corresponded to a 50% probability in 50 years. The important criterion was credibility, or plausibility, given the assumptions and uncertainties.

As noted by IPCC AR6 and discussed above, the extreme scenarios used for the CMIP6 modelling of climate change are not plausible. Considering Figure 46 above, for plausible scenarios, the uncertainties for onset times are large, which makes selecting a single value for the future problematic. However, with an adaptive approach, in my opinion, it is not necessary to identify the onset time beyond the next few decades, provided that the review step in the approach is undertaken regularly at, say, 10–15-year intervals. This would be sufficient to detect changing risks as a consequence of climate change and implement the community-preferred response.

7. References

Abd-Elhamid, H. F., Zeleňáková, M., Barańczuk, J., Gergelova, M. B., & Mahdy, M. (2023). Historical Trend Analysis and Forecasting of Shoreline Change at the Nile Delta Using RS Data and GIS with the DSAS Tool. *Remote Sensing*, 15(7).

Adebisi, N., Balogun, A.-L., Min, T. H., & Tella, A. (2021). Advances in estimating Sea Level Rise: A review of tide gauge, satellite altimetry and spatial data science approaches. *Ocean & Coastal Management*, 208, 105632.

Allan, J. C., Komar, P. D., & Priest, G. R. (2003). Shoreline variability on the high-energy Oregon Coast and its usefulness in erosion-hazard assessments. *Journal of Coastal Research*, Special Issue 38, 83-105.

Arias, P.A., N. Bellouin, E. Coppola, R.G. Jones, G. Krinner, J. Marotzke, V. Naik, M.D. Palmer, G.-K. Plattner, J. Rogelj, M. Rojas, J. Sillmann, T. Storelvmo, P.W. Thorne, B. Trewin, K. Achuta Rao, B. Adhikary, R.P. Allan, K. Armour, G. Bala, R. Barimalala, S. Berger, J.G. Canadell, C. Cassou, A. Cherchi, W. Collins, W.D. Collins, S.L. Connors, S. Corti, F. Cruz, F.J. Dentener, C. Dereczynski, A. Di Luca, A. Diongue Niang, F.J. Doblas-Reyes, A. Dosio, H. Douville, F. Engelbrecht, V. Eyring, E. Fischer, P. Forster, B. Fox-Kemper, J.S. Fuglestvedt, J.C. Fyfe, N.P. Gillett, L. Goldfarb, I. Gorodetskaya, J.M. Gutierrez, R. Hamdi, E. Hawkins, H.T. Hewitt, P. Hope, A.S. Islam, C. Jones, D.S. Kaufman, R.E. Kopp, Y. Kosaka, J. Kossin, S. Krakovska, J.-Y. Lee, J. Li, T. Mauritsen, T.K. Maycock, M. Meinshausen, S.-K. Min, P.M.S. Monteiro, T. Ngo-Duc, F. Otto, I. Pinto, A. Pirani, K. Raghavan, R. Ranasinghe, A.C. Ruane, L. Ruiz, J.-B. Sallée, B.H. Samset, S. Sathyendranath, S.I. Seneviratne, A.A. Sörensson, S. Szopa, I. Takayabu, A.-M. Tréguier, B. van den Hurk, R. Vautard, K. von Schuckmann, S. Zaehle, X. Zhang, and K. Zickfeld, 2021: *Technical Summary*. In *Climate Change 2021: The Physical Science Basis*. Contribution of Working Group I to the Sixth Assessment Report of the Intergovernmental Panel on Climate Change. Cambridge University Press, Cambridge, United Kingdom and New York, NY, USA, pp. 33–144.

Auckland Council, 2014. *Natural Hazard Risk Communications Toolbox*, Auckland Regional Council & GNS, 48 p.

Balogun, A.-L., & Adebisi, N. (2021). Sea level prediction using ARIMA, SVR and LSTM neural network: assessing the impact of ensemble Ocean-Atmospheric processes on models' accuracy. *Geomatics, Natural Hazards and Risk*, 12(1), 653-674.

Bardsley, W. E., Mitchell, W. M., & Lennon, G. W. (1990). Estimating future sea level extremes under conditions of sea level rise. *Coastal Engineering*, 14(3), 295-303.

Barroso, A., Wahl, T., Li, S., Enriquez, A., Morim, J., Dangendorf, S., Piecuch, C., & Thompson, P. (2024). Observed Spatiotemporal Variability in the Annual Sea Level Cycle Along the Global Coast. *Journal of Geophysical Research: Oceans*, 129(4), e2023JC020300.

Beavan, R. J., & Litchfield, N. J. (2012). Vertical land movement around the New Zealand coastline: implications for sea-level rise. *GNS Science Report* 2012/29. GSN, Wellington. 41 p.

Bell, R. G., & Goring, D. G. (1998). Seasonal variability of sea level and sea-surface temperature on the north-east coast of New Zealand. *Estuarine, Coastal and Shelf Science*, 46(2), 307-318.

Bell, R.G., & Hannah, J. (2012). *Sea-level variability and trends, Wellington Region*. Report prepared for Greater Wellington Regional Council and Vision NZ Ltd, NIWA Client Report HAM2012-043. 74 pp.

Bell, R.G., Denys, P., & Hannah, J. (2018). *Update on relative sea-level rise and vertical land movement*, Wellington Region. Report prepared for Greater Wellington Regional Council and Vision NZ Ltd, NIWA Client Report 2019007HN. 36 pp.

Bodeker, G., Cullen, N., Katurji, M., McDonald, A., Morgenstern, O., Noone, D., Renwick, J., Revell, L. and Tait, A. (2022). *Aotearoa New Zealand climate change projections guidance: Interpreting the latest IPCC WG1 report findings.* Prepared for the Ministry for the Environment, Report number CR 501, 51p.

Bosserelle, A.L., Morgan, L.K., & Hughes, M.W. (2022). Groundwater Rise and Associated Flooding in Coastal Settlements Due To Sea-Level Rise: A Review of Processes and Methods. *Earth's Future*, 10(7), e2021EF002580.

Bostock, H.C., Barrows, (T.T., Carter, L., Chase, Z., Cortese, G., Dunbar, G. B., Ellwood, M., Hayward, B., Howard, W., Neil, H. L., Noble, T. L., Mackintosh, A., Moss, P. T., Moy, A. D., White, D., Williams, M. J. M., & Armand, L. K. (2013). A review of the Australian-New Zealand sector of the Southern Ocean over the last 30 ka (Aus-INTIMATE project). *Quaternary Science Reviews*, 74, 35-57.

Brabb, E.E., 1984. Innovative approaches to landslide hazard and risk mapping. In *Proceedings of the Fourth International Symposium on Landslides*, Toronto, Vol. 1, pp 307–324.

Brown, J. R., Lengaigne, M., Lintner, B. R., Widlansky, M. J., van der Wiel, K., Dutheil, C., Linsley, B.K., Mathews, A.J., Renwick, J. (2020). South Pacific Convergence Zone dynamics, variability and impacts in a changing climate. *Nature Reviews Earth & Environment*, 1(10): 530-543.

Cagigal, L., Rueda, A., Castanedo, S., Cid, A., Perez, J., Stephens, S.A., Coco, G., & Méndez, F J. (2020). Historical and future storm surge around New Zealand: From the 19th century to the end of the 21st century. *International Journal of Climatology*, 40(3), 1512-1525.

CAE, 1991. Lifelines in earthquakes: Wellington Case Study, Project Report. Centre for Advanced Engineering, University of Canterbury, August 1991. 225 pp.

Cai, W., Ng, B., Geng, T., Jia, F., Wu, L., Wang, G., . . . McPhaden, M. J. (2023). Anthropogenic impacts on twentieth-century ENSO variability changes. *Nature Reviews Earth & Environment*, 4(6), 407-418.

Carey-Smith, T., Henderson, R., & Singh, S. (2018). *High Intensity Rainfall Design System, Version 4*, Prepared for Envirolink. NIWA Client Report 2018022CH, NIWA, Wellington. 73 pp.

Carter, L., Manighetti, B., Elliot, M., Trustrum, N., & Gomez, B. (2002). Source, sea level and circulation effects on the sediment flux to the deep ocean over the past 15 ka off eastern New Zealand. Global and Planetary Change, 33(3), 339-355.

Carter, L., Orpin, A. R., & Kuehl, S. A. (2010). From mountain source to ocean sink – the passage of sediment across an active margin, Waipaoa Sedimentary System, New Zealand. *Marine Geology*, 270(1), 1-10.

Chappell, P. R. (2014). The climate and weather of Wellington, 2nd Edition. NIWA Science and Technology Series, Number 65. NIWA, Wellington: 39 pp.

Clare, M.C.A., Piggott, M.D., & Cotter, C.J. (2022). Assessing erosion and flood risk in the coastal zone through the application of multilevel Monte Carlo methods. *Coastal Engineering* 174: 104118.

Clark, K.J., Nissen, E.K., Howarth, J.D., Hamling, I.J., Mountjoy, J.J., Ries, W.F., Jones, K., Goldstien, S., Cochran, U.A., Villamor, P., Hreinsdóttir, S., Litchfield, N.J., Mueller, C., Berryman, K. R.Strong, D.T. (2017). Highly variable coastal deformation in the 2016 MW7.8 Kaikōura earthquake reflects rupture complexity along a transpressional plate boundary. *Earth and Planetary Science Letters*, 474, 334-344.

Coco, G., Bryan, K., Montaño, J., & Cagigal, L. (2020). Modelling coastal evolution for rising sea levels, *Coastal systems and sea level rise: What to look for in the future*, Special Publication 4, December 2020, New Zealand Coastal Society, 21-24.

Coe, A. L., Bosence, D. W. J., Church, K. D., Flint, S. S., Howell, J. A., & Wilson, R. C. L. (2002). *The sedimentary record of sea-level change* (A. L. Coe Ed.). Cambridge, UK: The Open University and Cambridge University Press.

Cooper, J. A. G., & Pilkey, O. H. (2004). Sea-level rise and shoreline retreat: time to abandon the Bruun Rule. *Global and Planetary Change*, 43(3-4), 157-171.

Couldrey, M. P., Gregory, J. M., Boeira Dias, F., Dobrohotoff, P., Domingues, C. M., Garuba, O., . . . Zanna, L. (2021). What causes the spread of model projections of ocean dynamic sea-level change in response to greenhouse gas forcing? *Climate Dynamics*, 56(1), 155-187.

Cox, S.C., Ettema, M.H.J., Mager, S.M., Glassey, P.J., Hornblow, S., & Yeo, S. (2020). *Dunedin groundwater monitoring and spatial observations*. GNS Science report 2020/11, GNS Science, Lower Hutt. 86 pp.

Cox, S.C., Ettema, M.H.J., Chambers, L.A., Easterbrook-Clarke, L.H., & Stevenson, N.I. (2023). Dunedin groundwater monitoring, spatial observations and forecast conditions under sea-level rise. GNS Science report 2023/43, GNS Science, Lower Hutt. 103 pp.

D'Anna, M., Idier, D., Castelle, B., Vitousek, S., & Le Cozannet, G. (2021). Reinterpreting the Bruun Rule in the Context of Equilibrium Shoreline Models. *Journal of Marine Science and Engineering*, 9(9), 22 pp.

de Lange, W.P. (2001). Interdecadal Pacific Oscillation (IPO): a mechanism for forcing decadal scale coastal change on the northeast coast of New Zealand. *Journal of Coastal Research, Special Issue 34*, 657-664.

de Lange, W.P. (2010). *Abrupt sea level changes in response to Pacific Decadal Oscillation phase shifts*. Presented at the New Zealand Coastal Society Conference: Te Tara o Te Ika a Maui, Whitianga, November 2010.

de Lange, W.P. (2013). *Kāpiti Coast Coastal Hazard Assessment*. Report prepared for Coastal Ratepayers United. December 2013.

de Lange, W.P., & Gibb, J.G. (2000). Is the annual exceedence probability (AEP) an appropriate tool for quantifying extreme coastal water level hazard? *International Coastal Symposium 2000*, Rotorua. p. 122.

de Lange, W. P., & Hull, A. G. (1994). Tsunami hazard for the Auckland Region. Earth Sciences Department, University of Waikato, and Institute of Geological and Nuclear Sciences Limited, November 1994, 37 pp.

de Lange, W.P., & Moon, V.G. (2004). Estimating earthquake and landslide tsunami hazard for the New Zealand coast. *Bulletin of the New Zealand National Society for Earthquake Engineering*, 37(2), 62-69. reference

de Vilder, S.J., Kelly, S.D., Buxton, R.B., Allan, S., & Glassey, P.J. (2024). *Landslide planning guidance reducing landslide risk through land-use planning*. GNS Science miscellaneous series, 144. GNS Science, Lower Hutt (NZ). 77 pp.

Denys, P.H., Beavan, R.J., Hannah, J., Pearson, C.F., Palmer, N., Denham, M., & Hreinsdottir, S. (2020). Sea Level Rise in New Zealand: The Effect of Vertical Land Motion on Century-Long Tide Gauge Records in a Tectonically Active Region. *Journal of Geophysical Research: Solid Earth*, 125(1), e2019JB018055.

Domínguez-Cuesta, M.J. (2013). Susceptibility. In: Bobrowsky, P.T. (eds) *Encyclopedia of Natural Hazards*. Encyclopedia of Earth Sciences Series. Springer, Dordrecht.

Dougherty, A.J., & Dickson, M.E. (2012). Sea level and storm control on the evolution of a chenier plain, Firth of Thames, New Zealand. *Marine Geology*, 307-310, 58-72.

Dougherty, A.J. (2014). Extracting a record of Holocene storm erosion and deposition preserved in the morphostratigraphy of a prograded coastal barrier. *Continental Shelf Research*, 86, 116-131.

Drost, F., Renwick, J., Bhaskaran, B., Oliver, H., & McGregor, J. (2007). Simulation of New Zealand's climate using a high-resolution nested regional climate model. *International Journal of Climatology*, 27(9), 1153-1169.

Dunn, A.S. (2010). *Coastal Storm Activity along the Eastern North Island of New Zealand - East Cape to Wellington*. PhD Thesis, University of Waikato, Hamilton, New Zealand. 217 pp.

Eden, D. N., & Froggatt, P. C. (1996). A 6500-year-old history of tephra deposition recorded in the sediments of Lake Tutira, eastern North Island, New Zealand. *Quaternary International*, 34-36, 55-64.

Eden, D.N., & Page, M J. (1998). Palaeoclimatic implications of a storm erosion record from late Holocene lake sediments, North Island, New Zealand. *Palaeogeography, Palaeoclimatology, Palaeoecology*, 139(1-2), 37-58.

Francis, R., & Renwick, J.A. (1998). A regression-based assessment of the predictability of New Zealand climate anomalies. *Theoretical and Applied Climatology*, 60(1-4): 21-36.

Gibb, J.G. (1976). Coastal erosion along Wellington's west coast. *Soil and Water* 13(3): 6-7.

Gibb, J.G. (1978a). The problem of coastal erosion along the 'Golden Coast' Western Wellington, New Zealand. *Water & Soil Technical Publication No 10*, 20 pp.

Gibb, J.G. (1978b) Rates of coastal erosion and accretion in New Zealand, *New Zealand Journal of Marine and Freshwater Research*, 12:4, 429-456.

Gibb, J.G. (2012). *Local relative Holocene sea-level changes for Porirua Harbour area, Greater Wellington Region*. Report prepared for Greater Wellington Regional Council, June 2012, Coastal Management Consultancy Ltd, Report CR 2012/1. 12 pp.

Gibb, J.G., & Wilshere, D.S. (1976). *Coastal Erosion – Kāpiti Coastline. Notes of storm Saturday 11-Monday 13 September 1978*. 9 pp.

Godoi, V.A. (2018). *A detailed characterisation of the wave climate around New Zealand and its variability*. PhD Thesis. The University of Waikato, Hamilton, New Zealand. 169 pp.

Godoi, V. A., Bryan, K. R., & Gorman, R. M. (2016). Regional influence of climate patterns on the wave climate of the southwestern Pacific: The New Zealand region. *Journal of Geophysical Research: Oceans, 121*(6), 4056-4076.

Godoi, V.A., Bryan, K R., Stephens, S.A., & Gorman, R.M. (2017). Extreme waves in New Zealand waters. *Ocean Modelling, 117*, 97-110.

Godoi, V.A., Bryan, K.R., & Gorman, R.M. (2018). Storm wave clustering around New Zealand and its connection to climatic patterns. *International Journal of Climatology, 38*(S1), e401-e417.

Goff, J. (2002). *Kāpiti District Council: Tsunami hazard and risk*. GeoEnvironmenal Consultants Client Report GEO2002/20017. 41 pp.

Goff, J., & Chagué-Goff, C. (2015). Three large tsunamis on the non-subduction, western side of New Zealand over the past 700 years. *Marine Geology*, 363, 243-260.

Goff, J. R., Lane, E., & Arnold, J. (2009). The tsunami geomorphology of coastal dunes. *Natural Hazards Earth System Science* 9(3), 847-854.

Goff, J., McFadgen, B., Wells, A., & Hicks, M. (2008). Seismic signals in coastal dune systems. *Earth-Science Reviews*, 89(1), 73-77.

Goff, J. R., Rouse, H. L., Jones, S. L., Hayward, B. W., Cochran, U., McLea, W., Dickinson, W. W., & Morley, M. S. (2000). Evidence for an earthquake and tsunami about 3100–3400 yr ago, and other catastrophic saltwater inundations recorded in a coastal lagoon, New Zealand. *Marine Geology* 170(1): 231-249.

Gomez, B., Carter, L., & Trustrum, N. A. (2007). A 2400 yr record of natural events and anthropogenic impacts in intercorrelated terrestrial and marine sediment cores: Waipaoa sedimentary system, New Zealand. *Geological Society of America Bulletin*, 119(11-12), 1415-1432.

Gomez, B., Corral, Á., Orpin, A. R., Page, M. J., Pouderoux, H., & Upton, P. (2015). Lake Tutira paleoseismic record confirms random, moderate to major and/or great Hawke's Bay (New Zealand) earthquakes. *Geology*, 43(2), 103-106.

Gorman, R.M., Bryan, K.R., & Laing, A.K. (2003a). Wave hindcast for the New Zealand region: nearshore validation and coastal wave climate. *New Zealand Journal of Marine and Freshwater Research*, 37(3): 567-588.

Gorman, R.M., Bryan, K.R., & Laing, A.K. (2003b). Wave hindcast for the New Zealand region: deep-water wave climate. *New Zealand Journal of Marine and Freshwater Research*, 37(3): 589-612.

Grant, P.J. (1981). Recently increased tropical cyclone activity and inferences concerning coastal erosion and inland hydrological regimes in New Zealand and Eastern Australia. *Climatic Change*, 3(3), 317-332.

Grant, P.J. (1985). Major periods of erosion and alluvial sedimentation in New Zealand during the Late Holocene. *Journal of the Royal Society of New Zealand*, 15(1), 67-121.

Grant, P. J. (1991). Disturbance in the forests of the Ruahine Range since 1770. *Journal of the Royal Society of New Zealand*, 21(4), 385-404.

Griffiths, G. A., McKerchar, A. I., & Pearson, C. P. (2014). Towards prediction of extreme rainfalls in New Zealand. *Journal of Hydrology (New Zealand)*, 53(1), 41-52.

Griffiths, G. M. (2007). Changes in New Zealand daily rainfall extremes 1930 - 2004. *Weather and Climate*, 27, 3-44.

Griffiths, G. (2011). Drivers of extreme daily rainfalls in New Zealand. *Weather and Climate*, 31, 24-49.

Griffiths, G. (2013). New Zealand six main centre extreme rainfall trends 1962-2011. *Weather and Climate*, 33, 76-88.

Guillén, J., Simarro, G., Calvete, D., Ribas, F., Fernández-Mora, A., Orfila, A., Falqués, A., de Swart, R., Sancho-García, A., & Durán, R. (2024). Sediment leakage on the beach and upper shoreface due to extreme storms. *Marine Geology* 468, 107207.

Hague, B.S., & Talke, S.A. (2024). The Influence of Future Changes in Tidal Range, Storm Surge, and Mean Sea Level on the Emergence of Chronic Flooding. *Earth's Future*, 12(2), e2023EF003993.

Hamling, I.J., Hreinsdóttir, S., Clark, K., Elliott, J., Liang, C., Fielding, E., & Stirling, M. (2017). Complex multi-fault rupture during the 2016 Mw 7.8 Kaikōura earthquake, New Zealand. *Science*, 356(6334), eaam7194

Hamling, I.J., Wright, T.J., Hreinsdóttir, S., & Wallace, L.M. (2022). A Snapshot of New Zealand's Dynamic Deformation Field from Envisat InSAR and GNSS Observations Between 2003 and 2011. *Geophysical Research Letters*, 49(2), e2021GL096465.

Hamlington, Benjamin &, Thompson, Phil & National Center for Atmospheric Research Staff (Eds). Last modified 2022-09-09 "The Climate Data Guide: Tide gauge sea level data." Retrieved from https://climatedataguide.ucar.edu/climate-data/tide-gauge-sea-level-data on 2024-05-21.

Harrington, L., & Renwick, J. (2014). Secular changes in New Zealand rainfall characteristics 1950-2009. *Weather and Climate,* 34, 50-59.

Healy, T. R., & Dean, R. G. (2000). Methodology for delineation of coastal hazard zones and development setback for open duned coasts. In J. B. Herbich (Ed.), Handbook of coastal engineering, pp. 19.11-19.30).

Heath, R.A. (1979) Significance of storm surges on the New Zealand coast, *New Zealand Journal of Geology and Geophysics* 22(2): 259-266

Heidemann, H., Cowan, T., Power, S. B., & Henley, B. J. (2024). Statistical relationships between the Interdecadal Pacific Oscillation and El Niño–Southern Oscillation. *Climate Dynamics*, 62(3), 2499-2515.

Hermans, T. H. J., Gregory, J. M., Palmer, M. D., Ringer, M. A., Katsman, C. A., & Slangen, A. B. A. (2021). Projecting Global Mean Sea-Level Change Using CMIP6 Models. *Geophysical Research Letters*, 48(5), e2020GL092064.

Heron, D.W., Lukovic, B., Wang, X., & Power, W.L. (2019). *Evacuation time estimates for local source tsunami for Porirua and Kapiti suburbs*, GNS Science report; 2019/79. Lower Hutt, GNS Science. 192 p

Heron, D.W., van Dissen, R., & Sawa, M. (1998). Late Quaternary movement on the Ohariu Fault, Tongue Point to MacKays Crossing, North Island, New Zealand. *New Zealand Journal of Geology and Geophysics*, 41:4, 419-439

Himmelstoss, E.A., Henderson, R.E., Kratzmann, M.G., and Farris, A.S. (2021). *Digital Shoreline Analysis System (DSAS) version 5.1 user guide,* U.S. Geological Survey Open-File Report 2021–1091, 104 pp.

Hunter, J. (2010). Estimating sea-level extremes under conditions of uncertain sea-level rise. *Climatic Change*, 99(3), 331-350.

IPCC (2000). *IPCC Special Report on Emission Scenarios*, Cambridge University Press, Cambridge, UK.

IPCC (2019). *IPCC Special Report on the Ocean and Cryosphere in a Changing Climate*. Cambridge University Press, Cambridge, UK and New York, NY, USA, 755 pp.

IPCC (2021). *Climate Change 2021: The Physical Science Basis. Contribution of Working Group I to the Sixth Assessment Report of the Intergovernmental Panel on Climate Change*. Cambridge University Press.

Islam, M. S., & Crawford, T. W. (2022). Assessment of Spatio-Temporal Empirical Forecasting Performance of Future Shoreline Positions. *Remote Sensing*, 14(24).

Jackson, D., & Cooper, J. (2009). Geological control on beach form: accommodation space and contemporary dynamics. *Journal of Coastal Research*, 69-72.

Jacobs (2021). *Kāpiti Coast Coastal Hazard Susceptibility and Vulnerability Assessment Volume 1: Methodology*. Report for Kāpiti Coast District Council. IS355300-NC-RPT-003|1, 177 pp.

Jacobs (2022). *Kāpiti Coast Coastal Hazards Susceptibility and Vulnerability Assessment Volume 2: Results*. Report for Kāpiti Coast District Council. IS355300-NC-RPT-004|2, 188 pp. + appendices

Jenks, G. K. (2018). Restoring the natural functional capacity of coastal dune ecosystems: Utilising research records for New Zealand littoral refurbishment as a proxy for analogous global responses. *Journal of Coastal Conservation* 22(4), 623-665.

Jiang, N., Griffiths, G., & Lorrey, A. (2013). Influence of large-scale climate modes on daily synoptic weather types over New Zealand. *International Journal of Climatology*, 33(2), 499-519.

Johnson, D., Goring, D., McCoomb, P., Beamsley, B., Zynfogel, R. (2007). *Design wave and water levels for the Kāpiti Coast*. Report prepared for the Kāpiti Coast District Council, MetOcean Solutions Ltd, New Plymouth. 30 pp.

Jones, N. (2022). Rare 'triple' La Niña climate event looks likely. *Nature*, 607(21), 10.1038.

King, D. J., Newnham, R. M., Gehrels, W. R., & Clark, K. J. (2021). Late Holocene sea-level changes and vertical land movements in New Zealand. *New Zealand Journal of Geology and Geophysics*, 64(1), 21-36.

King, D.J., Newnham, R.M., Rees, A.B.H., Clark, K.J., Garrett, E., Gehrels, W.R., . . . Levy, R.H. (2024). A ~200-year relative sea-level reconstruction from the Wellington region (New Zealand) reveals insights into vertical land movement trends. *Marine Geology, 467*, 107199.

Komar, P.D., McDougal, W.G., Marra, J.J., and Ruggiero, P., 1991. The rational analysis of setback distances: Applications to the Oregon Coast. *Shore & Beach* 67(1): 41-49.

Kopp, R. E., Oppenheimer, M., O'Reilly, J. L., Drijfhout, S. S., Edwards, T. L., Fox-Kemper, B., . . . Xiao, C. (2023). Communicating future sea-level rise uncertainty and ambiguity to assessment users. *Nature Climate Change*, 13(7), 648-660.

Kroon, A., de Schipper, M. A., van Gelder, P. H. A. J. M., & Aarninkhof, S. G. J. (2020). Ranking uncertainty: Wave climate variability versus model uncertainty in probabilistic assessment of coastline change. *Coastal Engineering*, 158, 103673.

Kumler, M. (1969). Plant succession on the sand dunes of the Oregon coast. *Ecology*, 50(4), 695-704.

Laing, A.K., Bell, R.G., Goring, D.G., Gorman, R.M., Reid, S.J., & Renwick, J.A. (2000). *Kāpiti Coast erosion hazard investigations: waves, tides, storm surge and sea-level rise*. Report for J. Lumsden, Coastal Engineering Consultants & Kāpiti Coast District Council. NIWA Client Report WLG2000/59. 57 pp.

Lane, E., Gorman, R., Plew, D., & Stephens, S. (2012). *Assessing the storm inundation hazard for coastal margins around the Wellington Region*. Report prepared for Greater Wellington Regional Council, NIWA Client Report CHC2012-073. 148 pp.

Lorrey, A. M., Griffiths, G., Fauchereau, N., Diamond, H. J., Chappell, P. R., & Renwick, J. (2014). An ex-tropical cyclone climatology for Auckland, New Zealand. *International Journal of Climatology*, 34(4), 1157-1168.

Lorrey, A. M., Vandergoes, M., Almond, P., Renwick, J., Stephens, T., Bostock, H., Mackintosh, A., Newnham, R., Williams, P. W., Ackerley, D., Neil, H., & Fowler, A. M. (2012). Palaeocirculation across New Zealand during the last glacial maximum at ~21 ka. *Quaternary Science Reviews*, 36, 189-213.

Macara, G., Woolley, J.-M., Sood, A., & Stuart, S. (2022). *Climate change projections for west of Wellington's Tararua and Remutaka Ranges*. Report prepared for Greater Wellington Regional Council, NIWA Client Report 2022069WN. 134 pp.

Mao, Y., Harris, D. L., Xie, Z., & Phinn, S. (2021). Efficient measurement of large-scale decadal shoreline change with increased accuracy in tide-dominated coastal environments with Google Earth Engine. *ISPRS Journal of Photogrammetry and Remote Sensing*, 181, 385-399.

Matthews JBR, Möller V, van Diemen R, Fuglestvedt JS, Masson-Delmotte V, Méndez C, et al. (2021): Annex VII: Glossary. In: *Climate Change 2021: The Physical Science Basis. Contribution of Working Group I to the Sixth Assessment Report of the Intergovernmental Panel on Climate Change*. Cambridge, United Kingdom and New York, NY, USA: Cambridge University Press (2021). 2215–56.

McLean, R., & Kench, P. (2015). Destruction or persistence of coral atoll islands in the face of 20th and 21st century sea-level rise? *WIREs Climate Change, 6*(5), 445-463.

McClintock, J., Goff, J., & McFadgen, B. (2023). Reconstructing a palaeotsunami: Geomorphological and cultural change associated with a catastrophic 15th century event, Kāpiti Coast, Aotearoa/New Zealand. *The Holocene*, 34(4), 377-386.

McFadgen, B.G. (2007). *Hostile Shores: Catastrophic Events in Pre-Historic New Zealand and Their Impact on Māori Coastal Communities*. Auckland University Press, Auckland, 298 pp.

Meinshausen, M., Nicholls, Z. R. J., Lewis, J., Gidden, M. J., Vogel, E., Freund, M., Beyerle, U., Gessner, C., Nauels, A., Bauer, N., Canadell, J.G., Daniel, J.S., John, A., Krummel, P.B., Luderer, G., Meinshausen, N., Montzka, S.A., Rayner, P.J., Reimann, S., Smith, S.J., van den Berg, M., Velders, G.J.M., Volmer., M.K., & Wang, R.H.J. (2020). The shared socio-economic pathway (SSP) greenhouse gas concentrations and their extensions to 2500. *Geoscientific Model Development*, 13(8), 3571-3605.

Meinshausen, M., Schleussner, C F., Beyer, K., Bodeker, G., Boucher, O., Canadell, J.G., Daniel, J.S., Diongue-Niang, A., Driouech, F., Fischer, E., Forster, P., Grose, M., Hansen, G., Hausfather, Z., Ilyina, T., Kikstra, J.S., Kimutai, J., King, A.D., Lee, J.-Y., Lennard, C., Lissner, T., Nauels, A., Peters, G.P., Pirani, A., Plattner, G.K., Pörtner, H., Rogelj, J., Rojas, M., Roy, J., Samset, B.H., Sanderson, B. M., Séférian, R., Seneviratne, S., Smith, C. J., Szopa, S., Thomas, A., Urge-Vorsatz, D., Velders, G.J.M., Yokohata, T., Ziehn, T., & Nicholls, Z. (2024). A perspective on the next generation of Earth system model scenarios: towards representative emission pathways (REPs). *Geoscientific Model Development*, 17(11): 4533-4559.

Melnikova, I., Boucher, O., Cadule, P., Ciais, P., Gasser, T., Quilcaille, Y., . . . Tanaka, K. (2021). Carbon Cycle Response to Temperature Overshoot Beyond 2°C: An Analysis of CMIP6 Models. *Earth's Future*, 9(5), e2020EF001967.

MfE (2004). *Coastal Hazards and Climate Change: A guidance manual for Local Government.* Ministry for the Environment, Wellington. 145 pp.

MfE (2008). *Coastal Hazards and Climate Change: A guidance manual for Local Government (2nd Edition).* Ministry for the Environment, Wellington. 129 pp.

MfE (2017). *Coastal Hazards and Climate Change: Guidance for Local Government.* Ministry for the Environment, Wellington. 279 pp

MfE (2020). *National Climate Change Risk Assessment for Aotearoa New Zealand: Main report – Arotakenga Tūraru mō te Huringa Āhuarangi o Āotearoa: Pūrongo whakatōpū*. Wellington: Ministry for the Environment

MfE (2022). *Interim guidance of the use of new sea-level rise projections.* Ministry for the Environment, Wellington. 35 pp.

MfE (2024). *Coastal hazards and climate change guidance*. Ministry for the Environment, Wellington. 200 pp.

Montaño, J., Coco, G., Antolínez, J.A.A., Beuzen, T., Bryan, K.R., Cagigal, L., Castell, B., Favidson, M.K., Goldstein, E.B., Ibaceta, R., Idier, D., Ludka, B.C., Masoud-Ansari, S., Méndez, F.J., Murray, A.B., Plant, N.G., Ratliff, K.M., Robinet, A., Rueda, A., Sénéchal, N., Simmons, J.A., Splinter, K.D., Stephens, S., Towend, I., Vitousek, S., Vos, K. (2020). Blind testing of shoreline evolution models. *Scientific Reports*, 10(1), 2137.

Morrow, F.J., Ingham, M.R., & McConchie, J.A. (2010). Monitoring of tidal influences on the saline interface using resistivity traversing and cross-borehole resistivity tomography. *Journal of Hydrology*, 389(1), 69-77.

Mortlock, T. R., Nott, J., Crompton, R., & Koschatzky, V. (2023). A long-term view of tropical cyclone risk in Australia. *Natural Hazards*, 118(1), 571-588.

Mueller, C., Power, W.L., Wang, X., & Lukovic, B. (2017). *Hydrodynamic inundation modelling and delineation of tsunami evacuation zones for Porirua and Kapiti Coast*. GNS Science consultancy report 2017/200, GNS Science, Lower Hutt (NZ). 37 pp.

Murphy, A.H., & Epstein, E.S. (1989). Skill scores and correlation coefficients in model verification. *Monthly Weather Review*, 117, 575-581.

Naish, T., & Kamp, P.J. (1995). Pliocene-Pleistocene marine cyclothems, Wanganui Basin, New Zealand: A lithostratigraphic framework. *New Zealand Journal of Geology and Geophysics*, 38(2), 223-243.

Naish, T., Levy, R., Hamling, I., Hreinsdóttir, S., Kumar, P., Garner, G. G., Kopp, R. E., Golledge, N., Bell, R., Paulik, R., Lawrence, J., Denys, P., Gillies, T., Bengtson, S., Howell, A., Clark, K., King, D., Litchfield, N., & Newnham, R. (2024). The Significance of Interseismic Vertical Land Movement at Convergent Plate Boundaries in Probabilistic Sea-Level Projections for AR6 Scenarios: The New Zealand Case. *Earth's Future*, 12(6), e2023EF004165.

NEMA (2023). *Briefing to the Incoming Minister for Emergency Management and Recovery. National Emergency Management Agency*, Wellington. 20 pp.

Nichols, G. (2009). *Sedimentology and stratigraphy* (2nd ed.). Chichester, UK: Willey-Blackwell.

Nicholls, R.J., Lincke, D., Hinkel, J., Brown, S., Vafeidis, A.T., Meyssignac, B., . . . Fang, J. (2021). A global analysis of subsidence, relative sea-level change and coastal flood exposure. *Nature Climate Change*, 11(4), 338-342.

Ninis, D., Howell, A., Little, T., & Litchfield, N. (2023). Causes of permanent vertical deformation at subduction margins: Evidence from late Pleistocene marine terraces of the southern Hikurangi margin, Aotearoa New Zealand. *Frontiers in Earth Science, 11*.

Nolan, R.M. (2017). Late Holocene sedimentation on the southern Kāpiti Coast. MSc thesis, Victoria University of Wellington. 162 pp.

Nott, J., Haig, J., Neil, H., & Gillieson, D. (2007). Greater frequency variability of landfalling tropical cyclones at centennial compared to seasonal and decadal scales. *Earth and Planetary Science Letters*, 255(3-4), 367-372.

Nott, J., & Hayne, M. (2001). High frequency of 'super-cyclones' along the Great Barrier Reef over the past 5,000 years. *Nature*, 413(6855), 508-512.

O'Donnell, T. (2022). Managed retreat and planned retreat: a systematic literature review. Philosophical Transactions of the Royal Society B, 377(1854), 20210129.

Oliver, T.S.N., Dougherty, A.J., Gliganic, L.A., & Woodroffe, C.D. (2014). Towards more robust chronologies of coastal progradation: Optically stimulated luminescence ages for the coastal plain at Moruya, south-eastern Australia. *The Holocene*, 25(3), 536-546.

Orpin, A.R., Carter, L., Page, M.J., Cochran, U.A., Trustrum, N.A., Gomez, B., Palmer, A.S., Mildenhall, D.C., Rogers, K M., Brackley, H.L., & Northcote, L. (2010). Holocene sedimentary record from Lake Tutira: A template for upland watershed erosion proximal to the Waipaoa Sedimentary System, northeastern New Zealand. *Marine Geology,* 270(1), 11-29.

Parker, W.S. (2010). Predicting weather and climate: Uncertainty, ensembles and probability. *Studies in History and Philosophy of Science Part B: Studies in History and Philosophy of Modern Physics*, 41(3), 263-272.

Pearce, P., Fedaeff, N., Mullan, B., Sood, A., Bell, R., Tait, A., Collins, D., & Zammit, C. (2017). *Climate change and variability - Wellington Region*, Report prepared for Greater Wellington Regional Council. NIWA Client Report 2017066AK, NIWA, Auckland. 192 pp.

Pearce, P., Fedaeff, N., Mullan, B., Rosier, S., Carey-Smith, T., & Sood, A. (2019). *Wellington Region climate change extremes and implications*, Report prepared for Greater Wellington Regional Council. NIWA Client Report 2019134AK, NIWA, Auckland. 132 pp

Pickett, V. (2004). *The application of equilibrium beach profile theory to coastal hazard identification in the Bay of Plenty*. PhD Thesis, The University of Waikato, Hamilton, New Zealand.

Pirani, A., Fuglestvedt, J.S., Byers, E., O'Neill, B., Riahi, K., Lee, J.-Y., Marotkze, J., Rose, S.K., Schaeffer, R., & Tebaldi, C. (2024). Scenarios in IPCC assessments: lessons from AR6 and opportunities for AR7, *npj Climate Action*, 3:1.

Prince, H. D., Cullen, N. J., Gibson, P. B., Conway, J., & Kingston, D. G. (2021). A Climatology of Atmospheric Rivers in New Zealand. Journal of Climate, 34(11), 4383-4402.

Ramsay, D.L., Gibberd, B., Dahm, J., & Bell, R. (2012). Defining coastal hazard zones and setback lines. A guide to good practice. NIWA Hamilton, New Zealand. 91 pp

Ranasinghe, R., Ruane, A.C., Vautard, R., Arnell, N., Coppola E., Cruz, F.A., Dessai, S., Islam, A.S., Rahimi, M., Ruiz Carrascal, D., Sillmann, J., Sylla, M.B.,Tebaldi ,C., Wang, W., & Zaaboul, R. (2021). Climate Change Information for Regional Impact and for Risk Assessment. In *Climate Change 2021: The Physical Science Basis. Contribution of Working Group I to the Sixth Assessment Report of the Intergovernmental Panel on Climate Change* [Masson-Delmotte, V., et al (eds.)]. Cambridge University Press, Cambridge, United Kingdom and New York, NY, USA, pp. 1767–1926.

Reid, K. J., Rosier, S. M., Harrington, L. J., King, A. D., & Lane, T. P. (2021). Extreme rainfall in New Zealand and its association with Atmospheric Rivers. *Environmental Research Letters*, 16(4), 044012.

Renwick, J.A. (2011). Kidson's synoptic weather types and surface climate variability over New Zealand. *Weather and Climate*, 31: 3-23.

Renwick, J. A., Katzfey, J. J., Nguyen, K. C., & McGregor, J. L. (1998). Regional model simulations of New Zealand climate. *Journal of Geophysical Research: Atmospheres*, 103(D6), 5973-5982.

Renwick, J. A., Katzfey, J. J., McGregor, J. L., & Nguyen, K. C. (1999). On Regional Model Simulations of Climate Change Over New Zealand. *Weather and Climate*, 19, 3-13. doi:10.2307/44279923

Renwick, J. A., Mullan, A. B., & Porteous, A. (2009). Statistical Downscaling of New Zealand Climate. Weather and Climate, 29, 24-44. doi:10.2307/26169704

Ruggiero, P., Hacker, S., Seabloom, E., & Zarnetske, P. (2018). The Role of Vegetation in Determining Dune Morphology, Exposure to Sea-Level Rise, and Storm-Induced Coastal Hazards: A U.S. Pacific Northwest Perspective. In L. J. Moore & A. B. Murray (Eds.), *Barrier Dynamics and Response to Changing Climate* (pp. 337-361). Cham: Springer International Publishing.

Ruggiero, P., Kratzmann, M.G., Himmelstoss, E.A., Reid, D., Allan, J., & Kaminsky, G. (2013). *National assessment of shoreline change—Historical shoreline change along the Pacific Northwest coast*. U.S. Geological Survey Open-File Report 2012–1007, 62 p.

Salinger, M. J., & Mullan, A. B. (1999). New Zealand Climate: Temperature and precipitation variations and their links with atmospheric circulation 1930-1994. *International Journal of Climatology*, 19(10), 1049-1071.

Salinger, M., & Griffiths, G. (2001). Trends in New Zealand daily temperature and rainfall extremes. *International Journal of Climatology: A Journal of the Royal Meteorological Society*, 21(12), 1437-1452.

Salinger, M. J., Renwick, J. A., & Mullan, A. B. (2001). Interdecadal Pacific Oscillation and South Pacific Climate. *International Journal of Climatology*, 21(14), 1705-1721.

Saunders, W.S.A, Beban, J.G, & Kivington, M. (2013). *Risk-based land use planning for natural hazard risk reduction*. GNS Science miscellaneous series, 67. GNS Science, Lower Hutt (NZ). 97 pp

Sherwood, S. C., Webb, M. J., Annan, J. D., Armour, K. C., Forster, P. M., Hargreaves, J. C., . . . Zelinka, M. D. (2020). An Assessment of Earth's Climate Sensitivity Using Multiple Lines of Evidence. *Reviews of Geophysics*, 58(4), e2019RG000678.

Simmons, J.A., & Splinter, K.D. (2022). A multi-model ensemble approach to coastal storm erosion prediction. Environmental modelling & software, 150, 105356.

Slangen, A. B. A., Palmer, M. D., Camargo, C. M. L., Church, J. A., Edwards, T. L., Hermans, T. H. J., . . . van de Wal, R. S. W. (2023). The evolution of 21st century sea-level projections from IPCC AR5 to AR6 and beyond. *Cambridge Prisms: Coastal Futures*, 1, e7.

Steele, C., Williams, N., & Dawe, I., 2019. *Greater Wellington: Preparing coastal communities for climate change - Assessing coastal vulnerability to climate change, sea level rise and natural hazards*. Report to Wellington Regional Council, Mitchell Daysch Ltd, 97 pp.

Stephens, S., Gorman, R., & Lane, E. (2012). *Joint probability of storm tide and waves on the open coast of Wellington*. Report prepared for Greater Wellington Regional Council, NIWA Client Report HAM2011-095. 47 pp.

Stephens, S.A., Bell, R.G., & Haigh, I.D. (2020). Spatial and temporal analysis of extreme storm-tide and skew-surge events around the coastline of New Zealand. *Natural Hazards and Earth System Science* 20(3): 783-796.

Stewart, R.W., Kjerfve, B., Milliman, J., & Dwivedi, S.N. (1990). *Relative sea-level change: a critical evaluation, Unesco (COMAR) Working Group on Mean Sea-Level Rise and its influence in the coastal zone.* Unesco/IOC Paris: 22 pp.

Thieler, E.R., Pilkey Jr, O.H., Young, R.S., Bush, D.M., & Chai, F. (2000). The use of mathematical models to predict beach behavior for US coastal engineering: a critical review. *Journal of Coastal Research*, 48-70.

Todd, D., & MacDonald, K. (2020). Estimating the erosional effects of sea level rise on gravel beaches: Case study of the Canterbury coast, *Coastal systems and sea level rise: What to look for in the future*, Special Publication 4, December 2020, New Zealand Coastal Society, 31-37.

Turner, F. E., Malagon Santos, V., Edwards, T. L., Slangen, A. B. A., Nicholls, R. J., Le Cozannet, G., . . . Adhikari, M. (2023). Illustrative Multi-Centennial Projections of Global Mean Sea-Level Rise and Their Application. Earth's Future, 11(12), e2023EF003550.

Turner, R., Safaei Pirooz, A. A., Flay, R. G. J., Moore, S., & Revell, M. (2019). Use of High-Resolution Numerical Models and Statistical Approaches to Understand New Zealand Historical Wind Speed and Gust Climatologies. *Journal of Applied Meteorology and Climatology*, 58(6), 1195-1218.

Ummenhofer, C.C., & England, M.H. (2007). Interannual extremes in New Zealand precipitation linked to modes of Southern Hemisphere climate variability. *Journal of Climate*, 20(21), 5418-5440.

Ummenhofer, C.C., Sen Gupta, A., & England, M. H. (2009). Causes of Late Twentieth-Century Trends in New Zealand Precipitation. *Journal of Climate*, 22(1), 3-19.

Upton, P., Kettner, A. J., Gomez, B., Orpin, A. R., Litchfield, N., & Page, M. J. (2013). Simulating post-LGM riverine fluxes to the coastal zone: The Waipaoa River System, New Zealand. *Computers & Geosciences*, 53, 48-57.

van Vuuren, D., Tebaldi, C., O'Neill, B.C., ScenarioMIP SSC and workshop participants (2023*). Pathways to next generation scenarios for CMIP7: ScenarioMIP workshop report*. doi:10.5281/zenodo.8186116.

Wallace, L.M., Cochran, U.A., Power, W.L., & Clark, K.J. (2014). Earthquake and tsunami potential of the Hikurangi subduction thrust, New Zealand: Insights from paleoseismology, GPS, and tsunami modeling. *Oceanography* 27(2):104–117.

Ward, J.D., Werner, A.D., Nel, W.P., & Beecham, S. (2011). The influence of constrained fossil fuel emissions scenarios on climate and water resource projections. *Hydrology and Earth System Science Discussions*, 8(2), 2627-2665.

Watson, P.J. (2016). Identifying the best performing time series analytics for sea level research. In *Time series analysis and forecasting: Selected contributions from the ITISE conference*. 261-278.

Wigley, T.M.L., & Taper, S.C.B. (1992). Implications for climate and sea level of revised IPCC emissions scenarios. *Nature*, 357, 293-357.

Williams, J., Horsburgh, K.J., Williams, J.A., & Proctor, R.N.F. (2016). Tide and skew surge independence: New insights for flood risk. *Geophysical Research Letters* 43(12): 6410-6417.

Winter, C. (2007). On the evaluation of sediment transport models in tidal environments. *Sedimentary Geology*, 202(3), 562-571.

Woolley, J.-M., Turner, R., Rampal, N., Carey-Smith, T., Yang, E., & Pearce, P. (2020). *Historic climate extremes analysis for the Wellington Region*. Report prepared for Greater Wellington Regional Council, NIWA Client Report 2020089AK. 77 pp.

8. Appendix 1: Technical Terms

PALEOTSUNAMI DEPOSITS

When a tsunami strikes a coastline, it generally has localised, significant, catastrophic effects. These deposits may be left onshore during the inundation phase or affect offshore deposits in the backwash phase.

In the geologic record, paleotsunami onshore deposits are hard to distinguish from normal storm deposits, although the extent of the inundation is usually more extensive than that of storm deposits. Overtopping debris into a coastal lagoon (northern end of Kapiti Island) and inland mobilisation of significant coastal pumice deposits are two examples found in New Zealand.

ANTHROPOGENIC INFLUENCES AND EFFECTS OF ANTHROPIC ACTIVITIES

The term describes changes (generally environmental) caused or influenced by human activity. An example would be "the existence of roads or cities where once there were forests". In climate change circles, it is commonly used to describe the effects of fossil fuel usage.

The term Anthropocene has been proposed as the current geological epoch but rejected mainly due to the difficulty in defining a "start date": the rise of agriculture (12,000 years BP), the start of the Industrial Revolution (circa 1780), and the first atomic test (Trinity July 1945) are all possibilities.

BRUUN RULE

Per Bruun originally published the rule in 1962 in an American engineering journal. It is used to estimate shoreline recession in response to sea level rise. The rule is a simple, two-dimensional mass conversion equation (explicitly it is a passive flooding equation). It generally predicts coastal recession to be ten to 50 times the sea level rise, dependent on the beach slope.

It remains in use today, but Bruun himself recognised early the problems when applied to a three-dimensional situation. Various modifications have been made, but the coupled effects of sediment supplies (longshore drift), wave energy, tidal currents, wind action, sediment types and grain size, and depth of closure remain challenges in using the rule for accurate modelling.

SBEACH EQUILIBRIUM MODEL (STORM INDUCED BEACH CHANGE)

SBEACH is a numerical model for simulating storm-induced beach change. It is used to predict likely storm-cut volumes and horizontal movement of the dune toe.

DSAS ESTIMATES

The US Geological Survey developed the **D**igital **S**horeline **A**nalysis **S**ystem (DSAS) to estimate the rate of change in the statistics from digital shoreline data. Since the advent of aerial photography in the 1940s, most areas now have an extensive database of digitised aerial imagery that DSAS can use to calculate rate of change statistics and therefore generate predicted shorelines 10 and 20 years into the future. Since the predicted shorelines are based solely on historical trends and make no assumptions about processes and sediment budgets, they are a useful baseline for comparison of future shorelines determined by other means.

MONTE CARLO APPROACH

The Monte Carlo method is a statistical simulation. Its primary developer was physicist Stanislaw Ulam, who developed it when working on nuclear weapons projects at the Los Alamos National Laboratory in 1946. The name comes from the Monaco casino, where Stanislaw was inspired by his uncle's gambling habits. Monte Carlo methods are a broad class of computational algorithms that rely on repeated random sampling to obtain numerical results.

The underlying concept is to use randomness repeatedly to solve problems that might be deterministic in principle. For example, you can manually compute the probability of a particular outcome in, say, rolling dice.

HOLOCENE TREND OF ACCRETION OF THE KAPITI CUSPATE FORELAND

The Paraparaumu Beach headland is one of the best examples of a cuspate foreland growing in the lee of an island. Wave refraction around Kapiti Island forms an area of low wave energy.
The Holocene is defined as the time since the end of the last major ice age. Sea level peaked about midway through the Holocene. The Kapiti Coast has been accreting ever since. The beach line north of the cuspate has been accreting at about half a metre per year seaward for the last 5,000 years.

BARING HEAD DATA (WAVES) SHOULD NOT BE USED FOR KAPITI COAST

When looking at waves affecting the Kapiti Coast, Baring Head data should not be used. There is good data available from oil platforms in the Taranaki Bight.

Puysegur Subduction Zone as a Tsunami Origin

South of Fiordland, the Indian Plate is subducting under the Pacific Plate in the Puysegur zone. This is opposite to the orientation of subduction to the north of New Zealand in the Kermadec zone. Massive sea floor collapse/earthquake movements in the Puysegur area are a probable source for tsunamis on the Kapiti Coast.

9. Appendix 2: Kāpiti Coast: Example DSAS Analysis of Future Shoreline Locations

9.1. Introduction

The movement of shorelines on sedimentary coasts is a consequence of many processes and/or factors, which include:

- Weather affects the wave climate and wind-forced circulation and determines the balance between fair weather (generally associated with accretion) and storm conditions (generally associated with erosion).
- Sediment supply determines whether there is a sediment surplus or deficit at any specific location.
- Relative sea level changes, which determines the available accommodation space that controls if surplus sediment is deposited or bypasses, or where sediment is eroded from if there is a deficit.
- Anthropic factors, such as beach renourishment/mining, structures that limit shoreline movement, and changes to vegetation.

An important feature of sedimentary coasts, compared to other types, is that the shoreline can advance (accrete) or retreat (erode). The main factors controlling this behaviour are sediment supply and accommodation space (sea level).

The US Geological Survey (USGS) developed the Digital Shoreline Analysis System (DSAS) for estimating the rate of change statistics from digital shoreline data (Himmelstoss *et al.*, 2021) to assess rates of change since the 1940s from digitised aerial photographs. DSAS can use the calculated rate of change statistics to generate predicted shorelines 10 and 20 years into the future. Since the predicted shorelines are based solely on historical trends and make no assumptions about processes and sediment budgets, they are a useful baseline for comparison of future shorelines determined by other means. DSAS was used to develop the New Zealand National Coastal Change Dataset (Dickson *et al.*, 2022), which is available online at https://coastalchange.nz/.

9.2. DSAS Analysis

DSAS version 6 was used for the analysis presented here. This is a standalone application provided by the USGS with a standard workflow (Figure A2.1). The largest source of error in the analysis is the first step, which is preparing the input data. The error occurs when shorelines are digitised from different types of images due to different interpretations of where the shoreline occurs. A standard approach is to use a single operator to undertake the digitisation (e.g. Dickson et al., 2022). The analysis used the shorelines digitised from aerial photographs by Jacobs and the shorelines digitised from aerial photographs and high-resolution satellite images for the New Zealand Coastal Change Dataset (NZCCD). Both sets of data included uncertainty estimates for the shoreline positions, and a default value of ±10 m was used in the analysis if the uncertainty estimate for any shoreline was missing. The NZCCD shorelines were digitised by a single operator, while it is unclear what procedure Jacobs followed.

DSAS generates a series of transects along the coast perpendicular to a baseline defined by the user (Figure A2.2). This baseline can either be landward (onshore) or seaward (offshore)

of the shorelines being analysed. For this analysis the onshore baseline defined by Jacobs was used. One kilometre long transects were generated every 10 m of the Kāpiti coastline, with a 250 m smoothing to reduce the influence of small features on the orientations of the transects.

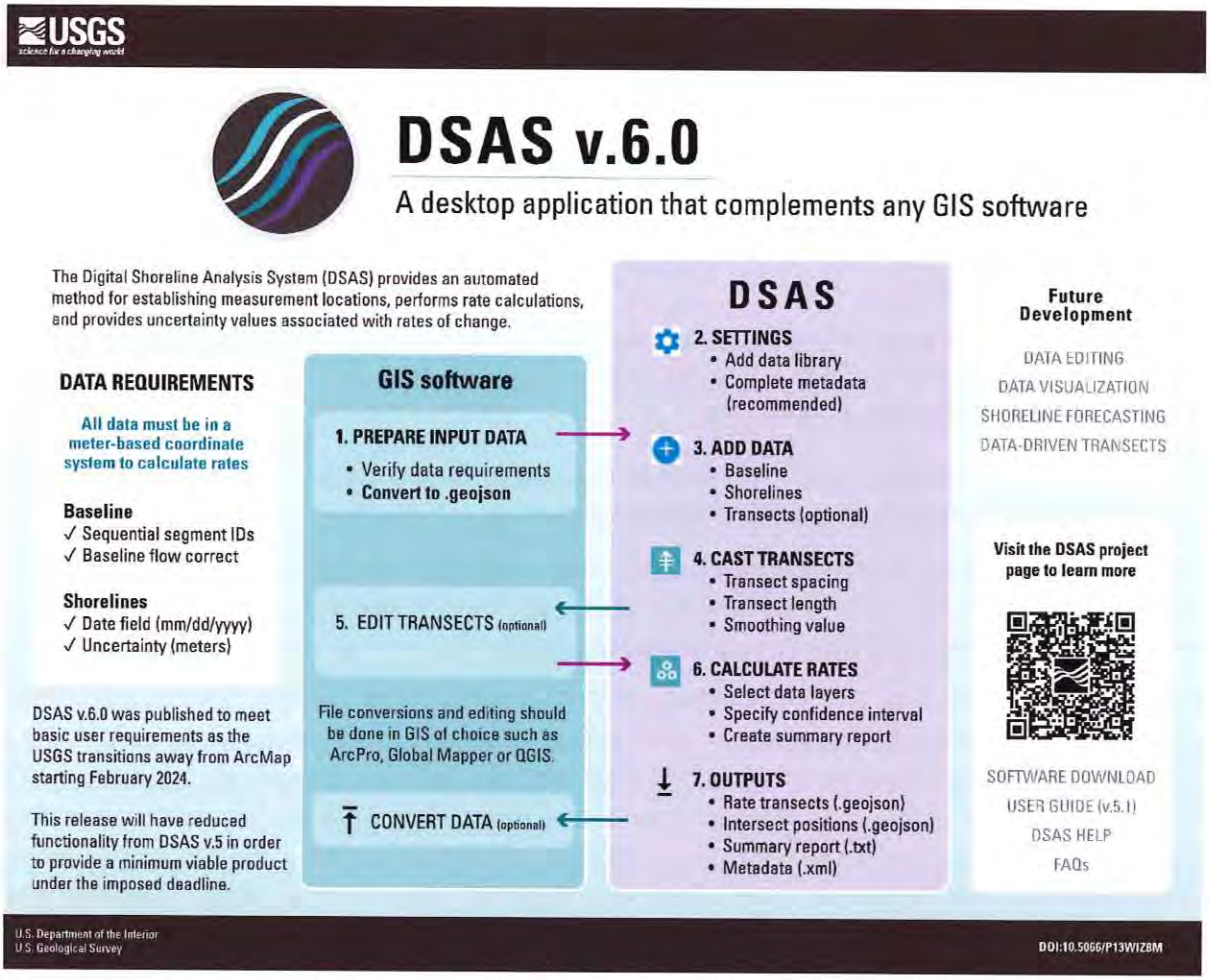

Figure A2.1. Summary of the data requirements and workflow for DSAS V.6.

DSAS measures the distance between the baseline and each shoreline intersection along a transect and combines date information and positional uncertainty for each shoreline to generate a range of measures of the shoreline changes. The standard measures generated are (Himmelstoss *et al.*, 2021):

- Distance measurements:
  - Shoreline Change Envelope (SCE) – maximum distance between shorelines intersected by the transect. This value is always positive.
  - Net Shoreline Movement (NSM) – distance between the oldest and youngest shoreline intersected by the transect. This measure does not detect changes in the direction of shoreline change (accretion to erosion, or vice versa), the magnitude of changes between shorelines (accelerating or decelerating trends), or cyclical movements (which are common along the Kāpiti coast)
- Statistics
  - End Point Rate (EPR) – NSM divided by the time elapsed between the oldest and youngest shorelines. It inherits the limitations of NSM,

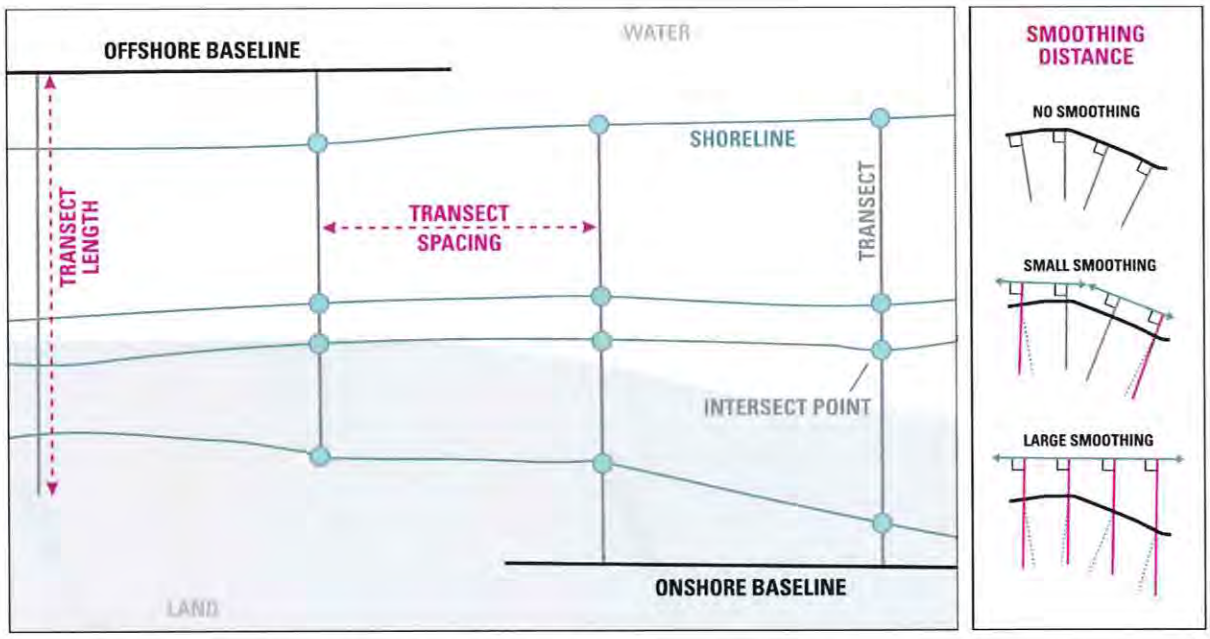

Figure A2.2. Definitions of the components of a DSAS analysis of shoreline positions.

- Uncertainty of the End Point Rate (EPRunc) – calculated from the uncertainties of the endpoint positions (u_A and u_B) and the elapsed time between the youngest ($date_B$) and oldest ($date_A$) as given by

$$EPRunc = \frac{\sqrt{(u_A^2 + u_B^2)}}{(date_B - date_A)}$$

This results in the uncertainty becoming smaller as the elapsed time increases.

- Linear Regression Rate (LRR) – ordinary least squares regression of the location of all shoreline intersections for a transect. At least 3 intersections are required to determine LRR. LRR tends to produce lower rates of change than EPR, which some authors suggest is a limitation (Himmelstoss *et al.*, 2021).
  - Standard Error (LSE) – root mean square of the residuals between the measured shoreline locations (y) and the predicted locations (y'). The equation used is

$$LSE\ or\ WSE = \sqrt{\frac{\sum (y - y')^2}{n - 2}}$$

  - Confidence Interval (LCI) – at the specified confidence level LCI is the LSI multiplied by the two-tailed test statistic. For example, given a 95% confidence limit there is a 5% probability that the rate of change lies outside the range LRR±LCI. This then applies to shoreline predictions that multiply the rate of change by a duration.
  - R-squared (LR2) – defines the proportion of the variation in shoreline position that is explained by the fitted linear relationship. This means that the smaller the residuals (and LSE), the better the relationship (LR2 closer to 1.0).
- Weighted Linear Regression Rate (WLR) – a higher weighting is placed on shoreline intersections with the lowest uncertainty (u) using a weight given by $w = 1/u^2$.
  - Standard Error (WSE) – corresponds to LSE.
  - Confidence Interval (WCI) – corresponds to LCI
  - R-squared (WR2) – corresponds to LR2

The results of all calculations are output to a rates file (.geojson) accompanied by an intersects file (.geojson) and associated metadata (.xml). A summary report (.txt) can also be output.

9.3. DSAS Analysis Results

Figure A2.3 shows the distribution of LRR estimates of the rates of shoreline change along the Kāpiti coast for the Jacobs and NZCCD shoreline datasets. The overall pattern is the same for both datasets, but there are small differences. The differences mostly occur around inlets, which is mostly due to the NZCCD dataset avoiding areas affected by migrating inlets.

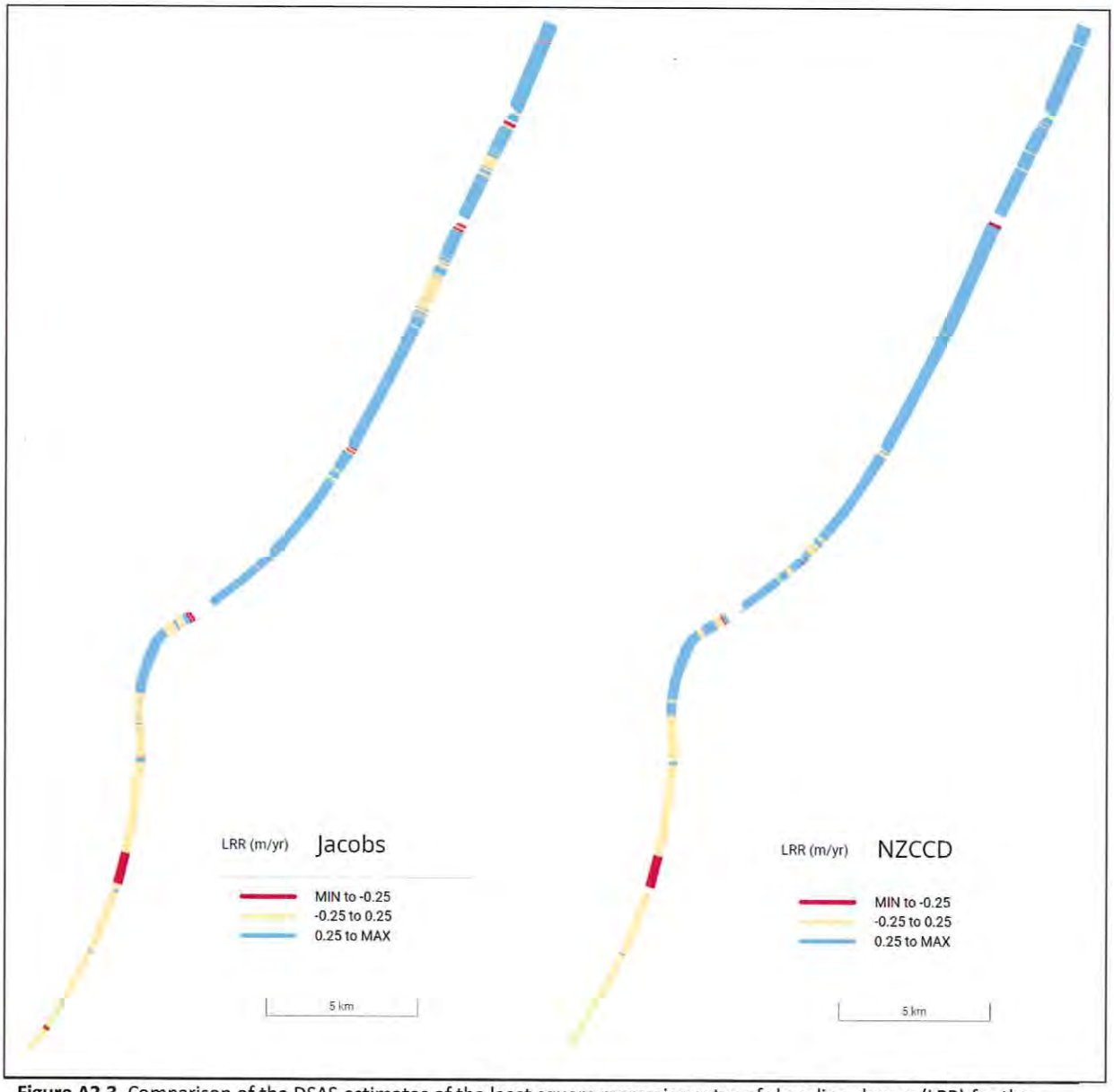

Figure A2.3. Comparison of the DSAS estimates of the least square regression rates of shoreline change (LRR) for the Kāpiti coast using the Jacobs (1948-2017) and NZCCD (1939-2021) datasets.

Table A2.1 summarises the results of the DSAS analyses, excluding the weighted linear regression results as they were identical to the ordinary linear regression results. For parameters relating specifically to eroding or accreting transects, the proportion of

transects with significant changes is indicated by percentages in parentheses. A significant change is one where the uncertainty range does not include no change (zero). This means that the total of the percentages will normally not be 100%, with the differenced being the proportion of transects with no significant change (within the -0.25-0.25 m/y band in Figure A2.3).

Table A2.1. Summary of the results generated by DSAS for 10 m transects along the Kāpiti coast using the Jacobs and NZCCD shoreline datasets. Percentages in parentheses indicate the proportions of significant rates associated with erosion and accretion.

Parameter	Jacobs (1948-2017)	NZCCD (1939-2021)
Number of transects	3809	3758
Shoreline Change Envelope - Average	42.65 m	43.74 m
Shoreline Change Envelope - Range	1.32-326.55 m	0.86-332.04 m
Net Shoreline Movement - Average	30.68 m	28.96 m
Net Shoreline Movement – Average erosion	-13.57 m (14.2%)	-13.06 m (23.8%)
Net Shoreline Movement – Average accretion	38.02 m (85.8%)	42.07 (76.2%)
End Point Rate and uncertainty - Average	0.43 ± 0.01 m/y	0.49 ± 0.01 m/y
End Point Rate – Average erosion	-0.27 m/y (10.4%)	-0.22 m/y (12.2%)
End Point Rate – Average accretion	0.54 m/y (80.6%)	0.71 m/y (68%)
Linear Regression Rate and 95% Confidence Interval - Average	0.43 ± 0.03 m/y	0.42 ± 0.05 m/y
Linear Regression Rate – Average erosion	-0.23 m/y (7.8%)	-0.17 mm/y (3.2%)
Linear Regression Rate – Average accretion	0.51 m/y (69.5%)	0.56 mm/y (50.4%)

The DSAS results are consistent with the trends shown by the shoreline surveys undertaken by Cuttriss Consultants Ltd for the Kāpiti Coast District Council (de Lange, 2024). The overall pattern is one of accretion for the northern 2/3 of the coast (north of approximately the Marine Parade – Rua Road intersection), and predominantly stable for the southern 1/3 due to the presence of seawalls. Most erosion occurs around inlets and the unprotected areas of the southern section of the coast, particularly along the shoreline of Queen Elizabeth Park (red areas in Figure A2.3).

In terms of the current erosion hazard, the present areas with significant erosion trends may be considered high risk depending on the impacts of erosion. Areas that are stable due to the presence of a seawall represent areas of potential high risk if the seawall fails or is removed in the future. Areas that are currently accreting at a significant rate are not exposed to an erosion risk unless there are structures close enough to the shoreline to be affected by storm erosion (Short-Term erosion component of the Jacobs report).

As discussed by de Lange (2024), it is possible to evaluate the validity of the Bruun Rule for predicting coastal erosion on the Kāpiti coast using the observed shoreline changes over the last 70-80 years (Table A2.1). Briefly, the Bruun Rule can be expressed as

$$R = KS$$

Where *R* is the shoreline response (strictly an inundation limit), *S* is the sea level rise, and *K* is a constant derived from the slope at the shoreline in various ways depending on the version of the Bruun Rule employed. While this relationship is mostly used to determine the distance for a change in elevation, R and S can also be expressed as rates of change (effectively by dividing both sides of the equation by a duration). Hence, the average LRR for a transect and the average rate of sea level rise (2.74 mm/y in Jacobs, 2021) can be used to determine K for each transect.The rates determined by DSAS for the Jacobs dataset were used to predict the constant K (after multiplying the rates by -1 to adjust for the convention used in the Bruun Rule, where the landward movement of the waterline is positive). The results showed 82.1% of transects were associated with $K \leq 0$, which is not permissible for the Bruun Rule as it implies the seabed is above sea level and increasing in height with distance offshore. The positive *K* all occurred at 627 transects with negative rates of shoreline change (erosion), although 330 were not significant (rate was less than uncertainty). The *K* values were converted to a nearshore slope (θ in radians) using the original definition of

$$K = \frac{1}{tan\theta}$$

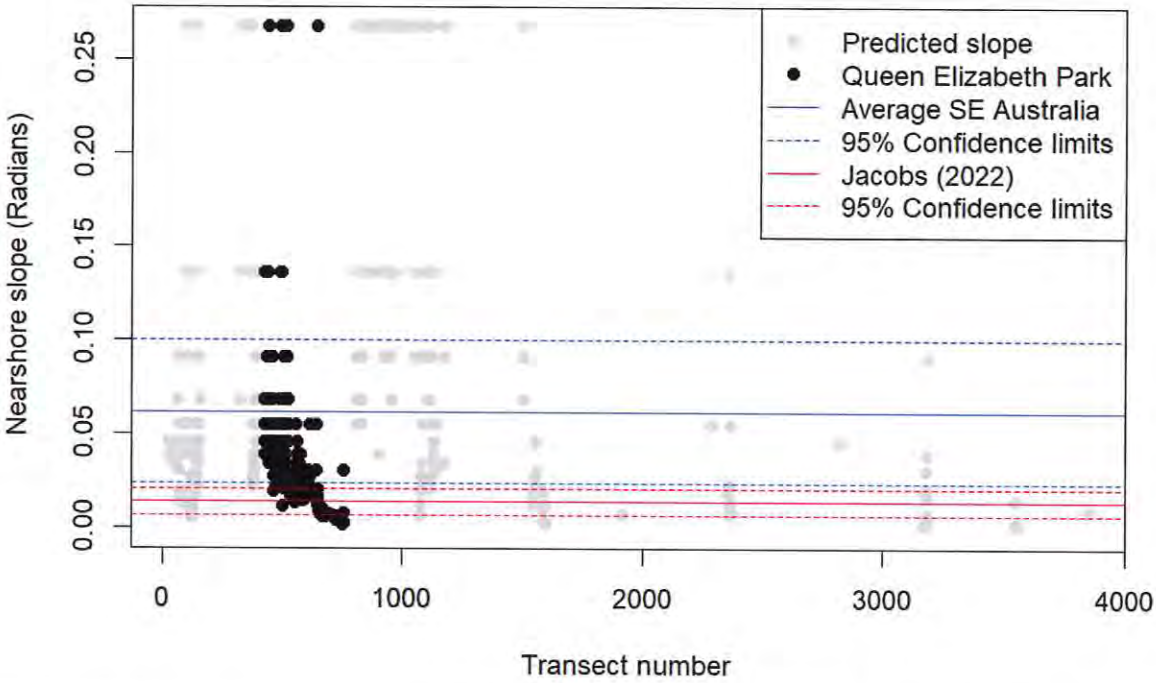

Figure A2.4. Nearshore slopes estimated from the DSAS LRR values for shoreline change and an assumed relative sea level rise rate of 2.74 mm.y^{-1}. The solid blue line is the average beach slope for 13624 transects along the southeast Australian coast from Fraser Island (Qld) to Lakes Entrance (Vic), and the dashed blue lines are the corresponding 95% (2σ) confidence limits. The solid red line is the average nearshore slope for the Kāpiti coast beach profiles determined by Jacobs (2022), and the dashed red lines are the corresponding 95% confidence limits.

Figure A2.4 shows the slopes determined for transects with erosional rates of shoreline change and the 95% confidence range and mean of beach slopes determined for beaches on

the southeast coast of Australia (Vos *et al.*, 2020) as a comparison. 45% of the transects (282) lie within the range of values defined by the 95% confidence range. Jacobs (2021), in Table 2.4, gives beach slopes for sandy beaches from 0.023 to 0.100 that are consistent with the southeast Australian data. They also provide slopes for mixed sand/gravel beaches of 0.384-0.411 that are above the values predicted (Figure A2.4).

However, the method used by Jacobs (2021) determined the slope between the top of the dune and the closure depth, which usually differs from the beach slope (typically, the beach slope is steeper, as noted by Jacobs, 2021). A scale factor based on the proportion of sand was also applied to mixed sand/gravel beaches to complicate comparisons. Jacobs (2022) determined the nearshore slopes for beach profiles sites monitored by Cuttriss Consultants Ltd, and applied them to groups of transects within coastal cells. Hence, it was not possible to compare the results for individual transects.

However, the distribution of nearshore slopes could be derived from the data presented in Jacobs (2022). Considering the upper and lower bounds used by Jacobs (2022), the nearshore slopes varied from 0.0042 to 0.0552 radians (corresponding to K values from 239 to 18). This encompasses all of the data plotted in Figure 4. The reported range is a consequence of some outlying values, such as the stretch of mixed-sand gravel beach south of the Otaki River. Most of the data (95%) lies between 0.0070 and 0.021 radians (K values of 48 to 143), with a mean of 0.0140 radians (K = 71.5). These values are plotted on Figure A2.4 in red.

The transects north from transect 1153 are all associated with inlets. The cluster between transects 1478 and 1569 also includes part of the sand extraction zone used for a beach renourishment trial undertaken in 1994 (Lumsden, 1998). This section of the coast will be discussed further below.

Although the data plotted in Figure A.4 indicate that there may be a reasonable relationship between sea level rise and shoreline response, they represent a small proportion of the coast. Most of the transects (90%) plotted occur south of transect 1153, located at the northern boundary of 36 Tainui Street and have an average trend of -0.02 m/y and a range of -0.01 to -1.35 m/y (90% from 0 to -0.10 m/y). Apart from Queen Elizabeth Park (black dots in Figure 4), most of the remaining transects have a seawall that affects the beach slope and rates of shoreline change. Considering the Queen Elizabeth Park transects with nearshore slopes that are consistent with observed erosion rates, only 86 transects may produce realistic results using the Bruun Rule (2.3% of the transects overall). Note that this may represent random chance, and not a reliable relationship.

9.4. Prediction of Future Shoreline Positions

DSAS was first released in 1992 as a tool for MapGrafix and ArcInfo GIS software. It has undergone continual development since then, with the inclusion of additional capabilities. Version 5.1 included the ability to forecast future shoreline positions based on the rates determined from historical data. The forecast was derived using a Kalman Filter to model the measured shoreline positions along a transect, and then extrapolating the model by 10 and 20 years. This approach was preferred overusing a linear regression model, as the Kalman Filter could simulate time-varying rates of shoreline movement.

In April 2024, DSAS moved to a standalone application (V6) due to the expected loss of ArcGIS software from the market. This version lacks all of the capabilities of Version 5 and

cannot forecast future shorelines. For the purpose of this report, a script was written in R that extracts the shoreline trend data generated by DSAS Version 6, and estimates the intersections of future shoreline positions along the transects. For the Kāpiti coast, the ordinary linear regression (LRR) rate was used so that only transects with at least historic shorelines were used. Note that the LRR values are consistent with the LR values determined by Jacobs, but they were not aggregated into coastal cells.

Future shorelines were determined for 10, 20, 35, 50 and 100 years from the last surveyed coastline (2017). Figure A2.5 shows an example of the predicted shoreline positions for an accreting section of the coastline extending from the Kapiti Boating Club to 135 Manly St, Paraparaumu. This example shows the influence of stormwater discharges across the beach, such as at the beach access by Nathan Avenue. The sharp curvature of the shorelines determined from the dune toe for these areas results in distortion of the trends relative to straighter sections further away. The NZCCD shorelines are smoothed and do not produce the sharp changes evident in Figure A2.5. Hence, it should be noted that the level of detail in the digitised shorelines affects the predictions. This section of coastline was also the location of sand extraction for a beach renourishment trial in 1994 (from 71 to 131 Manly St).

Figure A2.6 is an example from a region of the coast at the northern end of Queen Elizabeth Park that is currently eroding and represents the area with the highest erosion rates without the presence of a major inlet. In this case, erosion is highest immediately south of the end of the Raumati seawall and probably includes seawall end effects (e.g. Kraus, 1988; Kraus and McDougal, 1996). North of Queen Elizabeth Park, the properties seaward of The Esplanade are stabilised by the seawall. However, if the seawall is removed or fails, this area is likely to undergo rapid erosion due to the growing embayment immediately south of the seawall.

Figure A2.7 shows the coast between about 151 Manly St, Paraparaumu, and the mouth of the Waikanae River. Although the rates of shoreline change are similar along this stretch of coastline, there are large changes in the uncertainty as defined by the 95% confidence limits. The increasing uncertainty between 213 Manly St (Taheke St intersection) and the Waikanae River is due to the recent (last 30 years) shoreline changes caused by the migration of the river mouth and disruption of the longshore sediment transport while the spit reforms across the river mouth. However, the very large uncertainties immediately west of 213 Manly St are not obviously linked to the river processes.

Figure A2.8 shows the shoreline data used to derive the rates of shoreline change and confidence limits. From this image, it is clear that the uncertainties are driven primarily by the rapid change in the position of the 1948 shoreline in the vicinity of Taheke St. Looking at the aerial photographs available on Retrolens (http://retrolens.nz/) and the NZCCD shorelines, the maximum westward longshore movement of the Waikanae River occurred around 1952 when it reached the present location of Watson Drive. This was followed by rapid accretion (and sand stabilisation with vegetation), such that all of the current development lies landward of the 1956 shoreline.

The predicted future shorelines do not include:

- A component accounting for storm-induced cut and fill. If this was to be included, it should be based on site-specific measured distributions of historical storm erosion and recovery. Due to the presence of Kāpiti Island, the shape of the shoreline, and the type of beach, the impact of storms varies along the coastline, as reviewed by de Lange

(2024). Over the longer term, any imbalance between erosion losses and recovery gains produces the trends estimated by DASS. Given the values reported for the Kāpiti coast (de Lange, 2024), the impact on the predicted shorelines is too small to see at the scale of typical hazard maps.

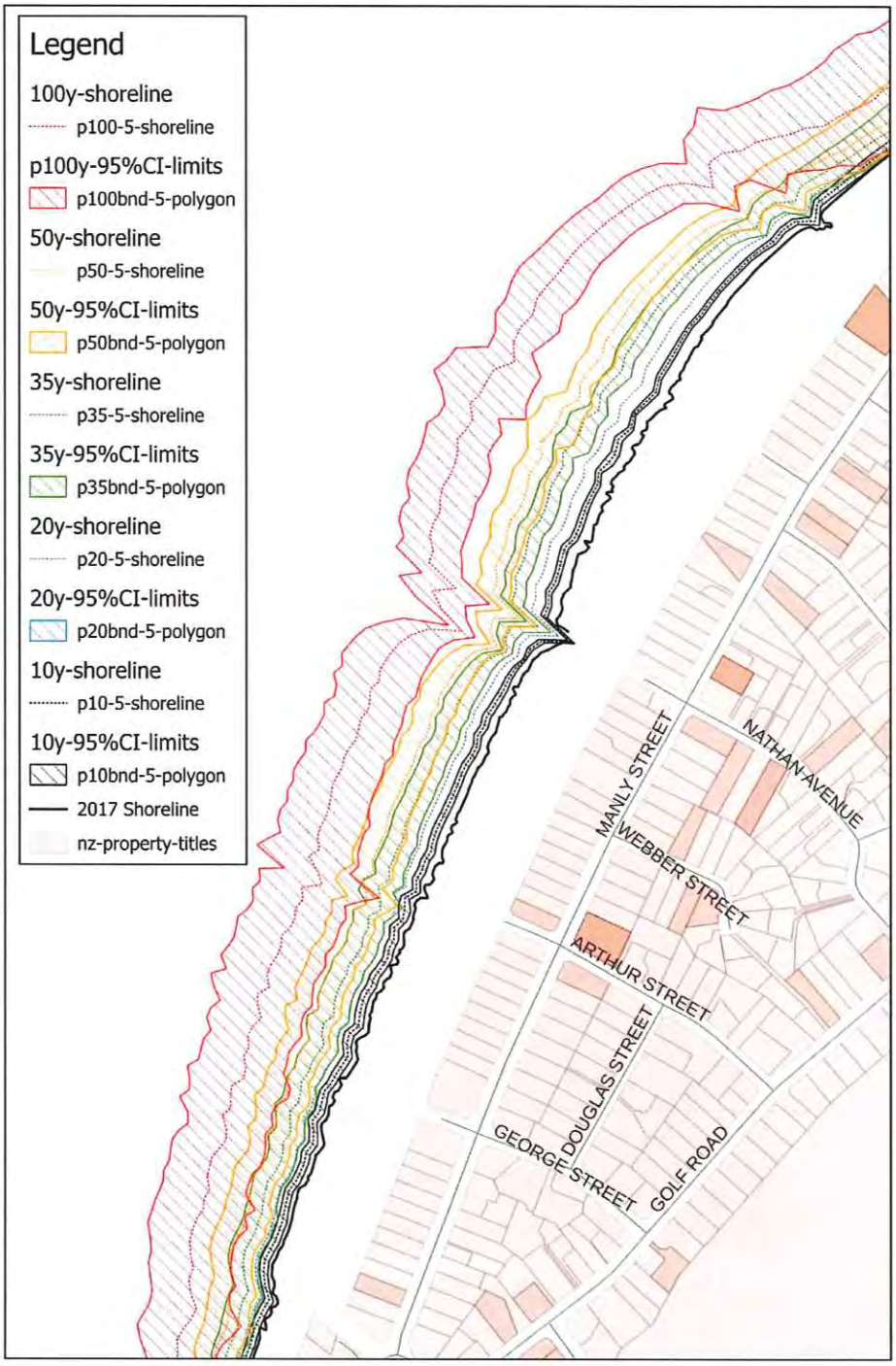

Figure A2.5. Predicted shoreline positions for an accreting section of the Kāpiti coast relative to the 2017 shoreline. The mean positions are defined by dotted lines, and the two-tailed 95% confidence limits are defined by the cross-hatched polygons.

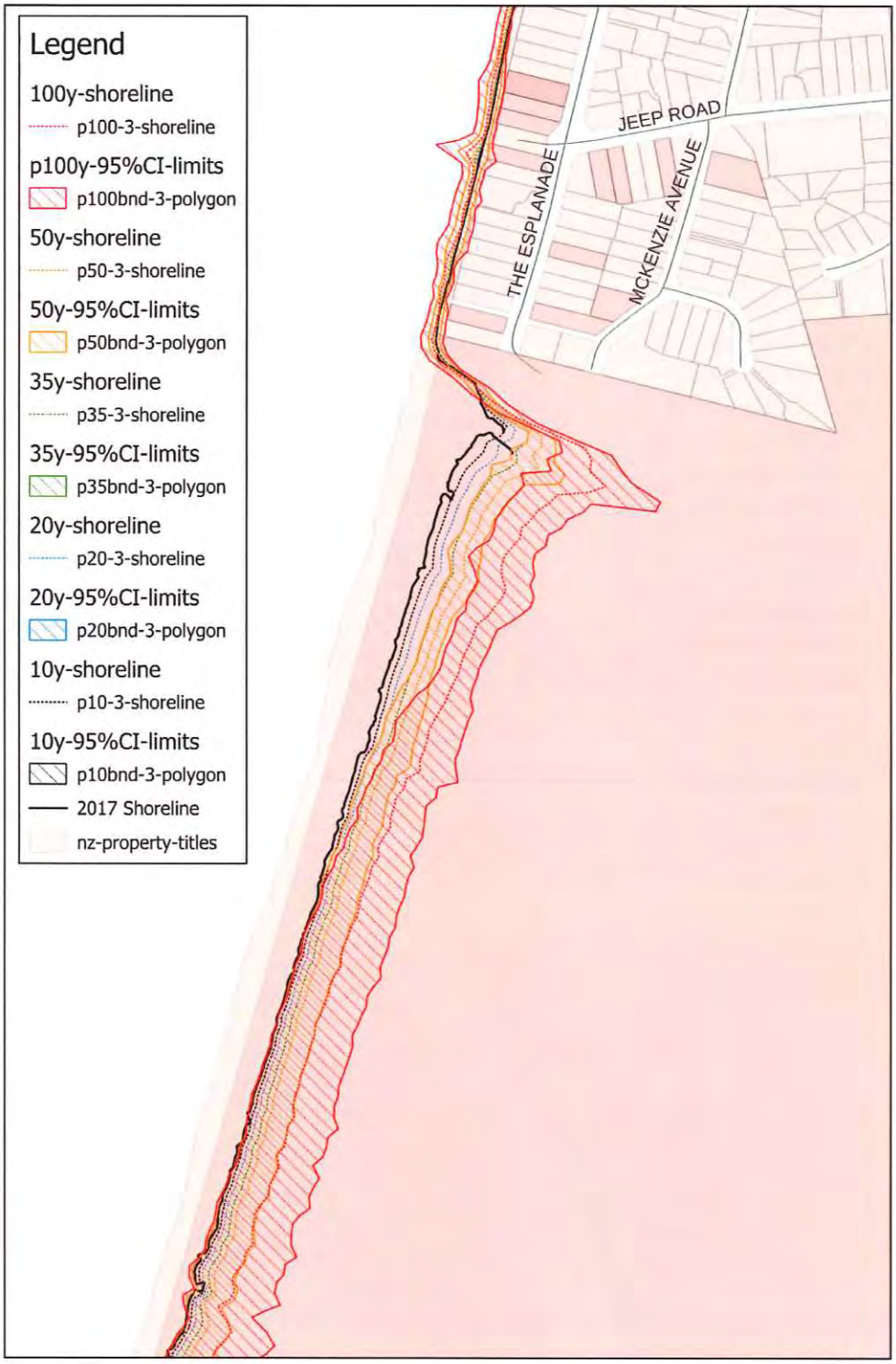

Figure A2.6. Predicted shoreline positions for an eroding section of the Kāpiti coast relative to the 2017 shoreline. The mean positions are defined by dotted lines, and the two-tailed 95% confidence limits are defined by the cross-hatched polygons.

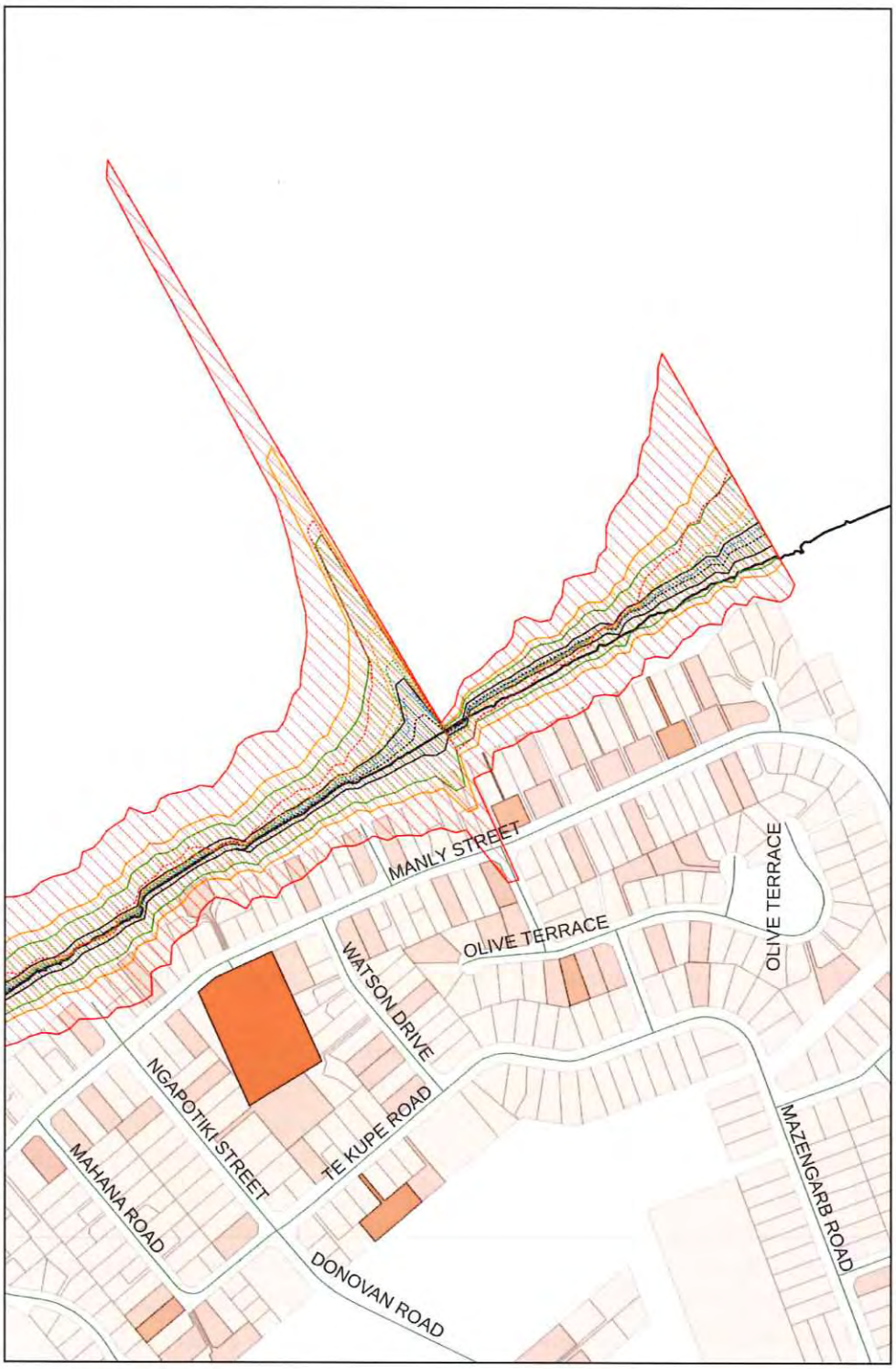

Figure A2.7. Predicted shoreline positions for a section of the Kāpiti coast adjacent to the Waikanae River. Shorelines are relative to the 2017 shoreline. The mean positions are defined by dotted lines, and the two-tailed 95% confidence limits are defined by the cross-hatched polygons.

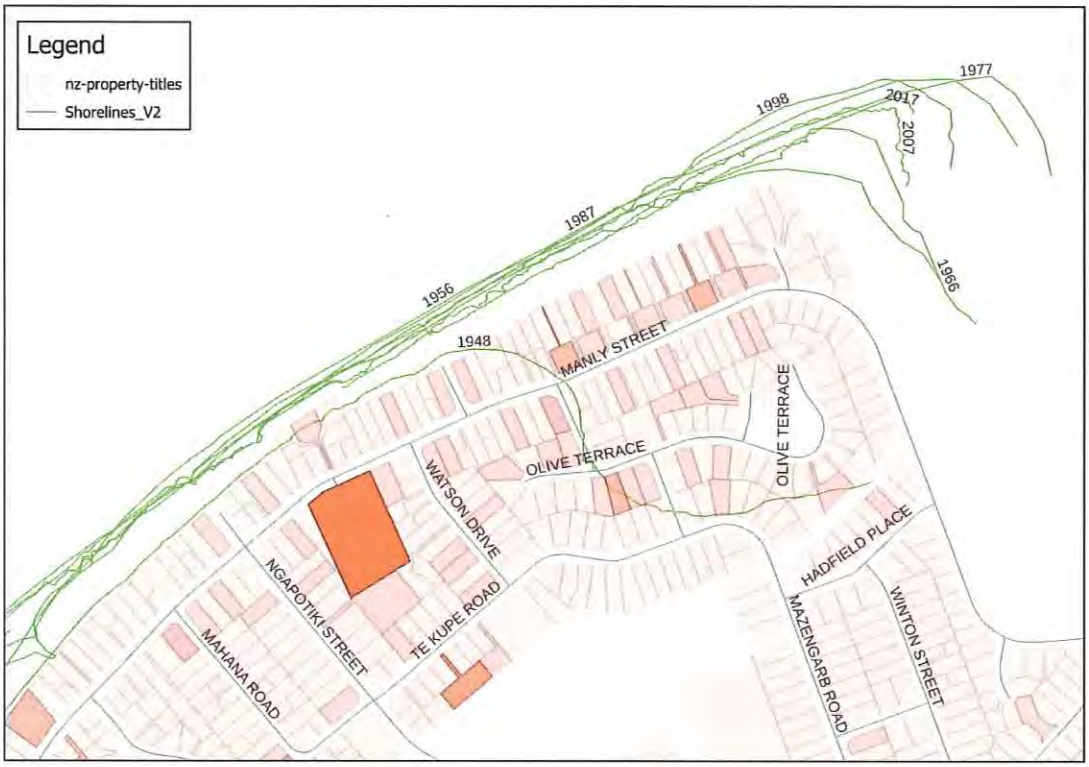

Figure A2.8. Shorelines provided by KCDC and used for the DSAS analysis. The area shown in Figure A2.7 is the central area of this map.

- A component accounting for the slope of dunes. The uncertainties for the shorelines used are larger than any correction to the shoreline position for the dune slope, and the magnitude of this component is typically smaller than storm-induced cut. Hence, it is too small to discern at the scale of typical hazard maps. Note that with a two-tailed confidence limit, there is a 2.5% probability of the future shoreline being landward of the predicted confidence limits.
- A component accounting for changing climate particularly changes in storminess, wave climate and sea level. The rates of shoreline change determined by DSAS incorporate the effects of all the processes impacted on the shoreline as listed in the Introduction. Since climate has been changing throughout the period covered by the DSAS analysis, the effects on those processes have also been integrated into the results. The key question is whether future climate changes will have a significantly different effect, or not. As discussed in de Lange (2024), the IPCC AR6 WG1 report (Chapter 12) concluded that the predicted changes relevant to processes affecting coastal hazards would not be distinguishable from normal variability until late this century at the earliest.

De Lange (2004) also noted that it is recognised that it is not possible to reliably predict changing climate or shoreline responses more than a couple of decades ahead (typically 10-20 years as performed by DSAS version 5.1). All the climate change-related projections for the Kāpiti Coast District reviewed by de Lange (2004) showed little change (less than the observed variability) before 2050 CE. Figures A2.9, A2.10 and A2.11 show the 35-year (2052 CE) shoreline predictions and the 2050 CE projections used for KCDC hazard areas.

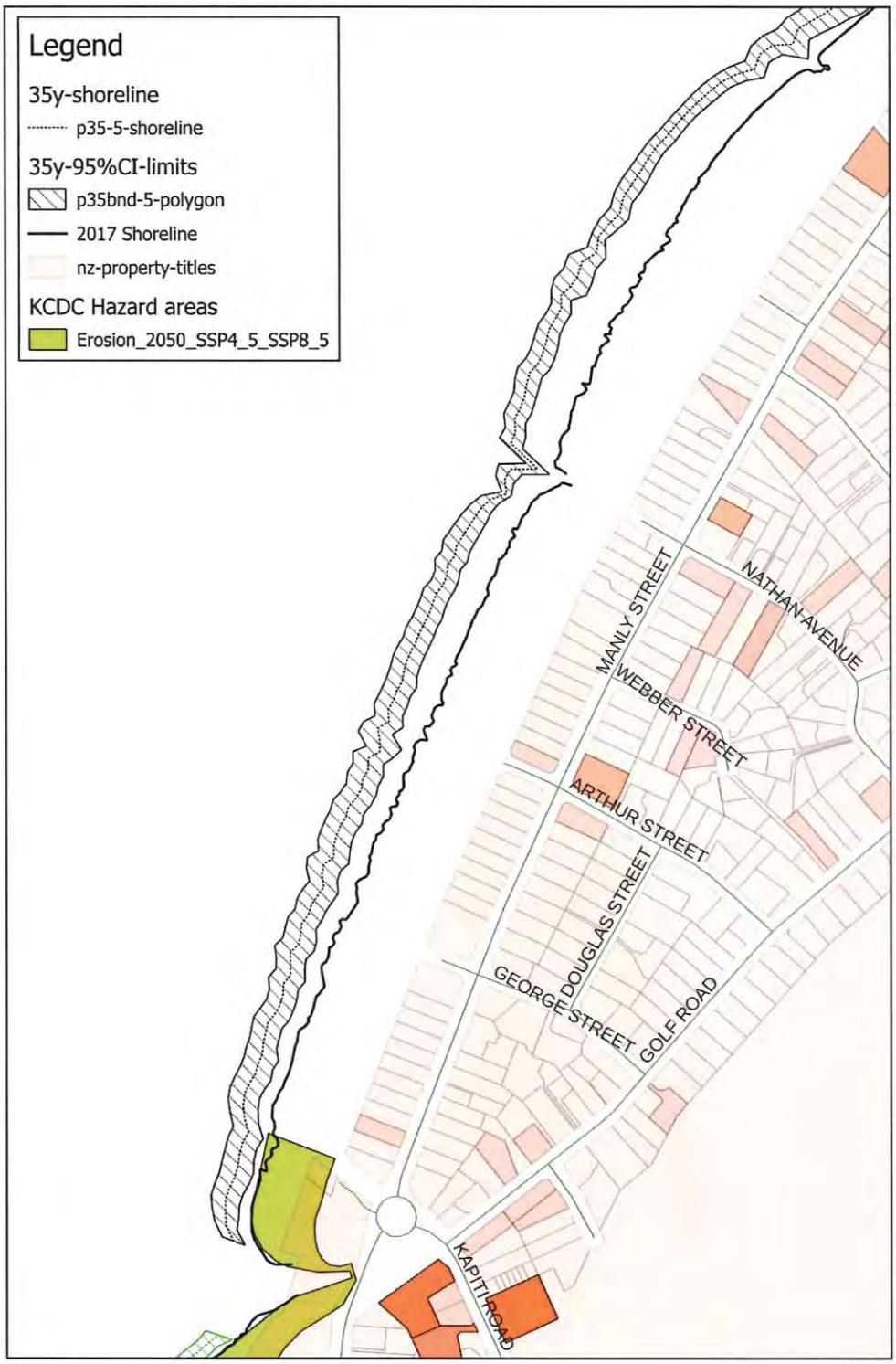

Figure A2.9. The 35-year shoreline (2052 CE) for an accreting section of the Kāpiti coast predicted by extrapolation of the linear regression rate of shoreline change (LRR) determined by DSAS, and the 2050 CE hazard areas provided by KCDC. The mapped area corresponds to Figure A2.5.

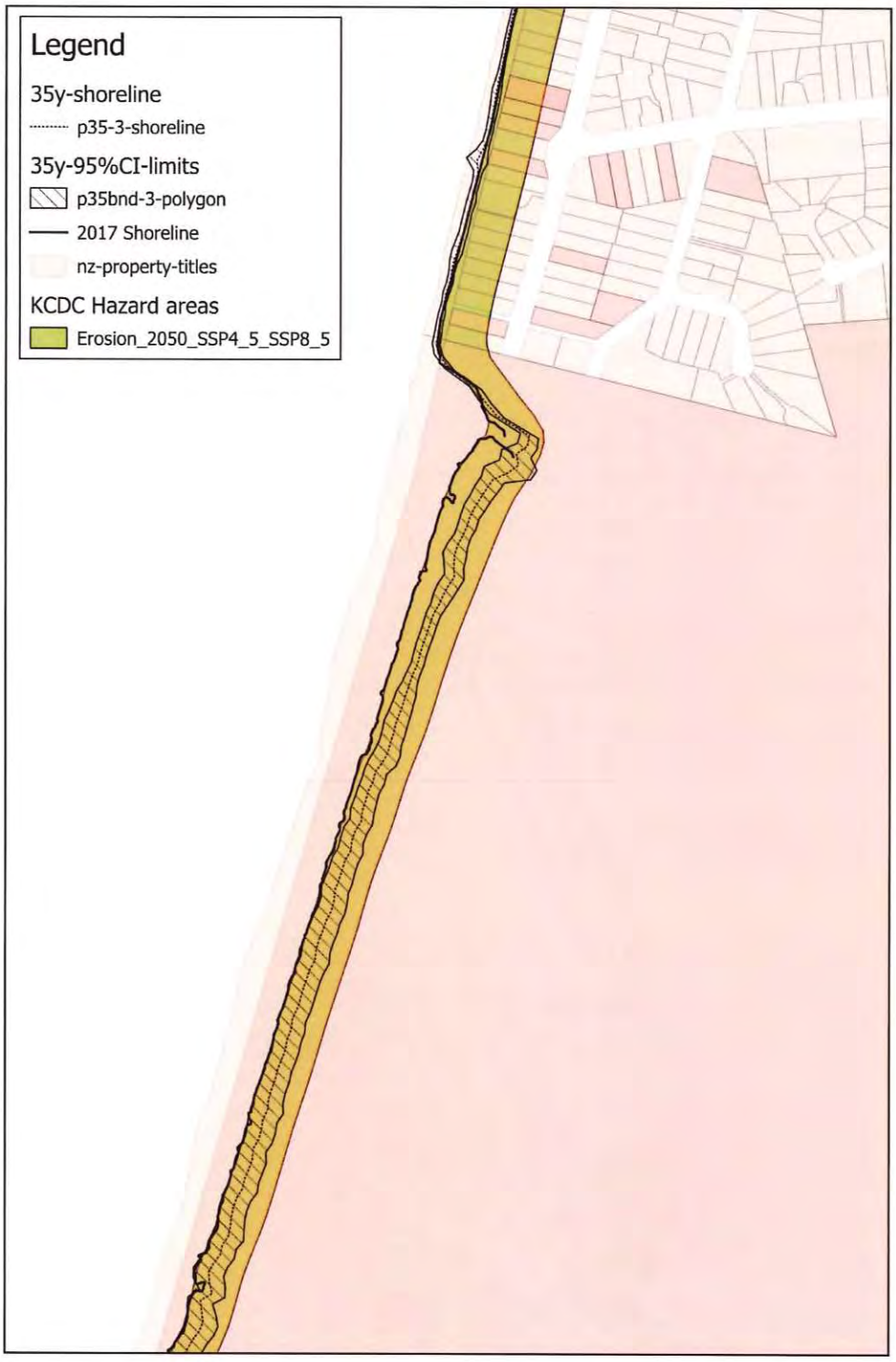

Figure A2.10. The 35-year shoreline (2052 CE) predicted for an eroding section of the Kāpiti coast by extrapolation of the linear regression rate of shoreline change (LRR) determined by DSAS, and the 2050 CE hazard areas provided by KCDC. The mapped area corresponds to Figure A2.6.

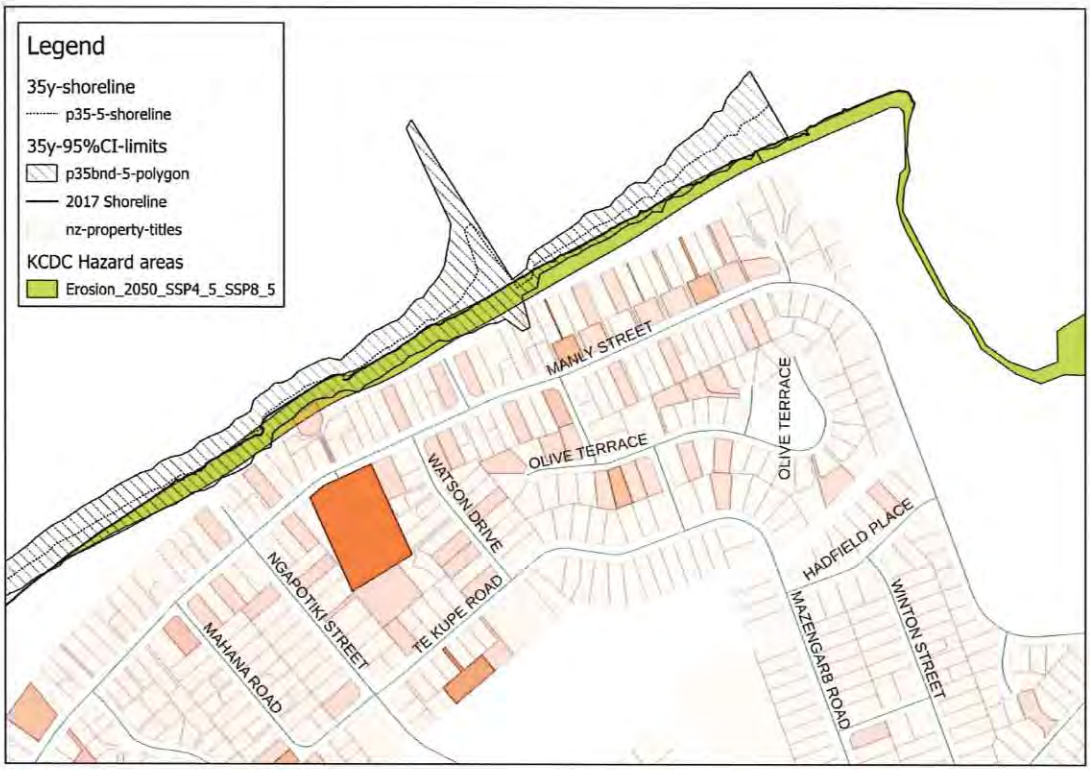

Figure A2.11. The 35-year shoreline (2052 CE) for a section of the Kāpiti coast adjacent to the Waikanae River predicted by extrapolation of the linear regression rate of shoreline change (LRR) determined by DSAS, and the 2050 CE hazard areas provided by KCDC. The area mapped corresponds to Figures A2.7 and A2.8.

The 2050 CE Hazard areas combine the projections for scenarios SSP4.5 and SSP8.5 as there is little difference between them. For the entire coastline, the widest hazard areas occur at inlets, with the surprising exceptions of the Otaki and Waikanae Rivers. This appears to be a consequence of the different methodologies used for assessing the hazard areas for inlets (Section 6, Jacobs, 2021). The DSAS analysis did not provide reliable estimates of shoreline trends for the inlets, apart from the smallest features, so they are no included in the predicted future shorelines.

Considering Figure A2.9, there is no erosion hazard area for most of the accreting coast, except close to the inlet at the southern end of the section shown. This occurred because the "erosion" determined by the Bruun Rule and other components, was less than the "accretion" determined from the long-term trend. For the rest of the coast currently accreting, the sum of "erosion" terms exceeded the "accretion" resulting in a narrow hazard area. The width of this area is predominantly determined by the Bruun Rule.

For the eroding coast in Figure A2.10, the predicted shorelines from the DSAS analysis overlap the KCDC hazard area for Queen Elizabeth Park but progressively move towards the seaward margin towards the south (a trend that continues to the southern boundary of the Park. The 95% confidence limit area is smaller than the hazard area. The difference is predominantly due to the Bruun Rule.

Finally, in Figure A2.11, the KCDC hazard area appears very close to the location where the 35-year confidence limit polygon crosses over to the landward side of the 2017 shoreline. The KCDC hazard area widens through the zone where the DSAS analysis results were

affected by the 1948 shoreline (discussed above) and then narrows as it merges with the hazard area determined for the Waikanae River inlet using a different methodology.

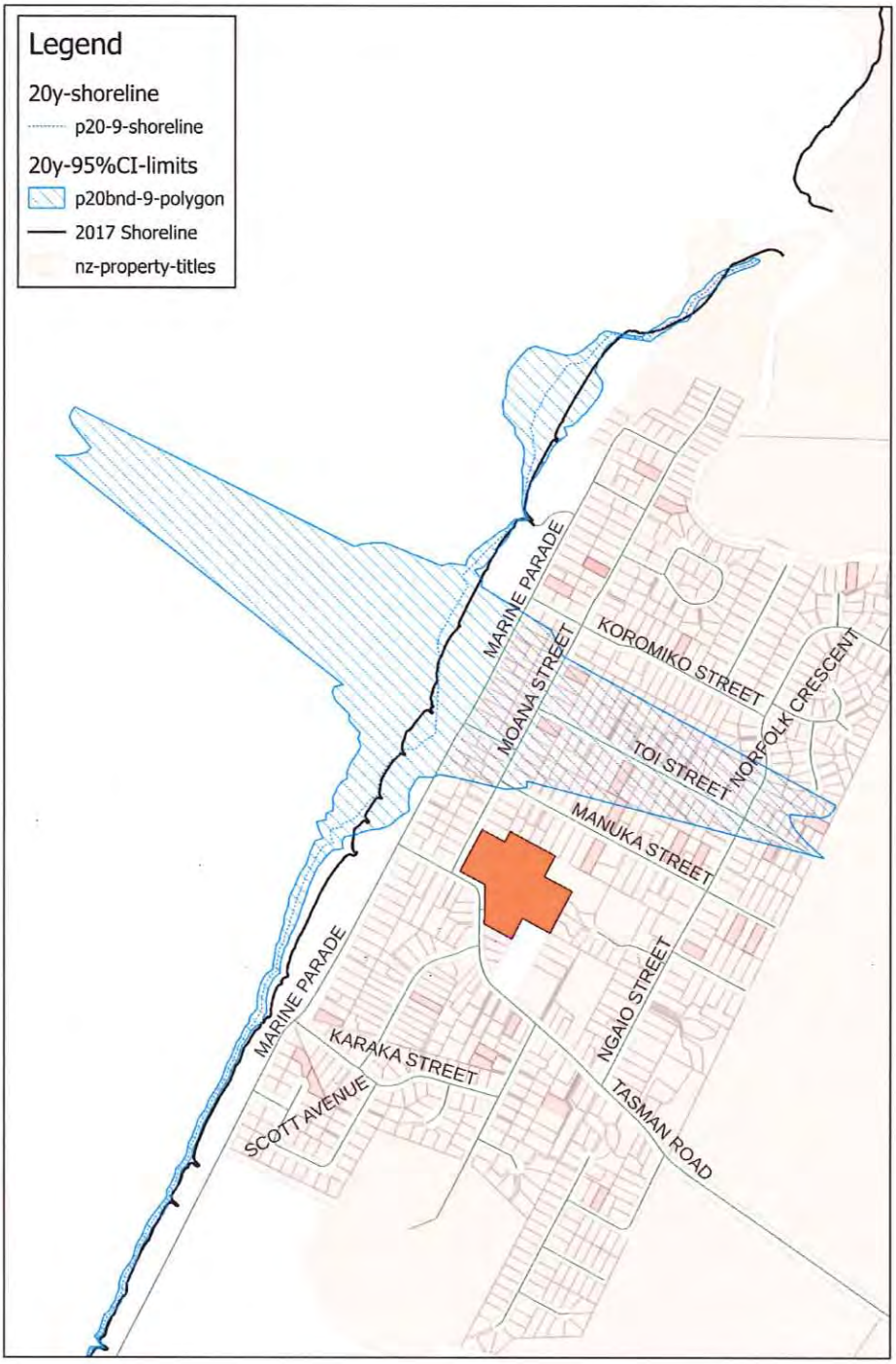

Figure A2.12. The 20-year shoreline (2037 CE) for a section of the Kāpiti coast at Otaki Beach predicted by extrapolation of the linear regression rate of shoreline change (LRR) determined by DSAS. The shoreline is relative to the 2017 shoreline. The mean position is defined by the dotted blue line, and the two-tailed 95% confidence limits are defined by the cross-hatched polygon.

Overall, the DSAS predictions tended to produce a narrower hazard area than the KCDC hazard areas. This was expected due to not using the Bruun Rule. However, there are exceptions. Most of these occur close to inlets as illustrated by Figure A2.7, but some are not closely linked with inlets. Figure A2.12 illustrates the 20-year predicted shoreline and

95% confidence limits for Otaki Beach. This stretch of coast has very large uncertainties for the predicted rates of shoreline change, possibly due to the oscillations in shoreline position associated with the southwards movement of pulses of sediment from rivers further north. The predicted shoreline (dotted line) shows zones of erosion and accretion about the 2017 shoreline consistent with migrating pulses.The hazard area due to inundation was not mapped, as the projected water level changes by 2050 CE were too small to show up for a bath-tub inundation model. Most of the shoreline is too high and steep.

9.5. Shoreline Maps

Maps of the predicted future shorelines were prepared using QGIS (version 3.34.10-Prizen) and exported as a series of A3-sized PDF images at 1:7500 scale. The maps include the 10-year (2027 CE) and 20-year (2037 CE) predictions relative to the 2017 shoreline. The purpose of the maps was primarily to demonstrate that DSAS can be used to regularly produce updated predictions for an adaptative management approach as outlined in de Lange, 2024).

As discussed above, the QGIS project includes predicted shorelines for 2052 CE, 2067 CE, and 2117 CE. However, as explained by de Lange (2024), these cannot be considered reliable predictions, which is reflected in the increasing width of the 95% confidence limits with increasing duration. Hence, they have not been included in the maps produced.

Further, it is clear from the analysis that the DSAS estimates of rates of shoreline change are affected by the characteristics of the digitised shorelines. This is discussed at length by Himmelstoss *et al.* (2021). For short-term predictions, these issues may not be important for most of the Kāpiti coast. However, there are some areas where the DSAS estimates do not appear to be very reliable at any time scale. This is particularly noticeable for Otaki Beach (Map 2 of the series), as illustrated in Figure A2.12.

9.6. References

Dickson, M., Ford, M., Ryan, E., Tuck, M., Sengupta, M., & Lawrence, J. (2022). The use of historic and contemporary coastal-change data for adaptation decision making. In *Coastal adaptation: Adapting to coastal change and hazard risk in Aotearoa New Zealand, Special Publication 5* (pp. 55-59). New Zealand Coastal Society.

Himmelstoss, E.A., Henderson, R.E., Kratzmann, M.G., & Farris, A.S. (2021). *Digital Shoreline Analysis System (DSAS) version 5.1 user guide,* U.S. Geological Survey Open-File Report 2021–1091, 104 pp.

Jacobs (2021). *Kāpiti Coast Coastal Hazard Susceptibility and Vulnerability Assessment Volume 1: Methodology*. Report for Kāpiti Coast District Council. IS355300-NC-RPT-003|1, 177 pp.

Jacobs (2022). *Kāpiti Coast Coastal Hazards Susceptibility and Vulnerability Assessment Volume 2: Results*. Report for Kāpiti Coast District Council. IS355300-NC-RPT-004|2, 188 pp. + appendices

Kraus, N. C. (1988). The effects of seawalls on the beach: an extended literature review. *Journal of Coastal Research*, Special Issue 4, 1-28.

Kraus, N. C., & McDougal, W. G. (1996). The effects of seawalls on the beach: Part I, an updated literature review. *Journal of Coastal Research*, 12(3), 691-701.

Lumsden, J. (1998). Coastal Management at Paraparaumu: Post-renourishment trial monitoring, Report No. 3. Report to Kapiti Coast District Council. 11 pp.

Vos, K., Harley, M.D., Splinter, K.D., Walker, A., & Turner, I.L. (2020). Beach Slopes from Satellite-Derived Shorelines. *Geophysical Research Letters*, 47(14), e2020GL088365.